Dengue virus diverts the mosquito phospholipid metabolism for replication

Thomas Vial

THÈSE

En vue de l'obtention du

DOCTORAT DE L'UNIVERSITÉ DE TOULOUSE

Délivré par l'Université Toulouse 3 - Paul Sabatier

Présentée et soutenue par

Thomas VIAL

Le 29 Juin 2020

Le virus de la dengue détourne le métabolisme des phospholipides du moustique pour sa réplication

Ecole doctorale : **BSB - Biologie, Santé, Biotechnologies**

Spécialité : **MICROBIOLOGIE**

Unité de recherche :
PHARMA-DEV -Laboratoire Pharmacochimie et Pharmacologie pour le Développement

Thèse dirigée par
Eric DEHARO

Jury

M. Louis Lambrechts, Rapporteur
M. Jean-Luc Imler, Rapporteur
Mme Isabelle Morlais, Examinatrice
M. Jean-Charles Portais, Examinateur
M. Eric Deharo, Directeur de thèse
M. Julien Pompon, Co-directeur de thèse
M. Guillaume Marti, Invité

Dengue virus diverts the mosquito phospholipid metabolism for effective infection

Thomas Vial

École Doctorale BSB – Biologie, Santé, Biotechnologies
Université Toulouse 3 - Paul Sabatier

ACKNOWLEDGMENTS

These four years spent on this project have been intense, first by being based in Laos and travelling to Singapore and Toulouse to initiate the project, and then full time in Singapore. I would like to thank here all the people who contributed in any way to the realization of this thesis work in the best conditions.

First of all, I would like to thank Eric Deharo, my thesis director, who allowed me to be part of this incredible experience in Laos four years ago, by opening the doors of the IRD to me and get back to research work. Thank you for your confidence on all these different projects and especially for proposing me this research project by sending me to Singapore. You pushed me to enroll a thesis, which was not necessarily in my plans at the beginning.

I would also like to thank the person who supported and accompanied me tirelessly throughout this research project, my thesis co-director Julien Pompon. Thank you welcoming me at Duke-NUS and for allowing me to turn those valuable preliminary data into a thesis project. I do not count the precious advices, rereading, Skype meeting to lead to the big picture and to get the right message. Your availability and your support on the analysis and writing of the papers and the manuscript were essential.

I particularly thank Mariano Garcia-Blanco for having done me the honor of joining his laboratory and for having taken advantage of his always brilliant remarks and advice. Thanks also to Linfa Wang for his welcome to the EID department.

Of course, I warmly thank the members of the MGB lab team. Thanks to Shi-Chia, Mayra and KC for bringing me their experience and advices. Thanks to Vanessa and Ben for their technical support and especially to Wei Lian for helping me a lot, especially at the end of the thesis for many experiments. Thanks to Menchie for training me in insectary and for providing me with a lot of mosquitoes. I can't count the hours spent sorting female mosquitoes, dissecting midgut or testicles in the heat and humidity.

I would like to thank Guillaume Marti for training and coaching me on the metabolomics part and for welcoming me during my stays in Toulouse. These numerous samples and long hours of mass spectrometry provided a considerable amount of data. I would like to thank Nicolas Fabre for his welcome at Pharmadev and the members of UMR-152 whom I was able to meet briefly. Thanks to Franck for helped me during my stays in the lab and for received my numerous shipments of samples from Singapore.

Thanks to the members of the thesis committee, Mariano, Eng Eong Ooi and Jean-Paul Kovalic, for helping me to share my results at important moments and to oriented me on the project.

Finally, I would like to thank my family and friends who gave me their support despite the distance. First of all, my parents and my sister, who encouraged me from the beginning, when I left France. My friends and the many discussions on WhatsApp that kept me connected. Finally, I would like to thank my wife, Melanie, the first to support me, without whom it would have been difficult to move forward in the same way and with whom I look forward to sharing the next adventures.

ABSTRACT

More than half of the world population is at risk of dengue virus (DENV) infection because of the global distribution of its mosquito vectors. There is neither effective vaccine nor therapeutics. The only available strategy relies on insecticides, against which mosquitoes are developing resistance. Viruses utilize the host metabolome for replication and dissemination. This is particularly true for envelope viruses like DENV that relies on host lipid membranes to complete their life-cycle. To reach an optimal metabolic environment, viruses subvert the host metabolome. Understanding DENV-mosquito metabolic interactions will reveal novel strategies to stop DENV transmission. Here, we characterized how DENV hijacks the *Aedes aegypti* mosquito lipidome to identify targets for novel transmission-blocking interventions. To describe metabolic changes throughout the mosquito DENV cycle, we deployed a Liquid chromatography–high resolution mass spectrometry (LC-HRMS) workflow at different stages of vector infection. We revealed a major phospholipid reconfiguration throughout the DENV mosquito cycle, in cells, midguts, and whole mosquitoes. To decipher how DENV reconfigures phospholipids, we phylogenetically characterized acylglycerolphosphate acyltransferase (AGPAT) enzyme isoforms and identified those (i.e., AGPAT1) that catalyze a central rate-limiting step in phospholipid biogenesis. We found that DENV infection decreased AGPAT1 expression, which depletion enhances infection by maintaining high aminophospholipid (aminoPL) concentrations, especially phosphatidylcholine (PC) and phosphatidylethanolamine (PE), during DENV mosquito cycle. By demonstrating that DENV-mediated *AGPAT1* downregulation provides a proviral environment, these results reveal the first metabolic host factor in mosquitoes and emphasize the role of aminophospholipids in DENV cellular cycle. We then undertook to precise how DENV influences aminoPL biosynthesis and what stage of DENV cellular cycle requires aminoPL reconfiguration. *De novo* biosynthesis of PC and PE is known as the Kennedy pathway, where a diacylglycerol (DAG) incorporates either a choline or an ethanolamine group. AminoPL remodeling by deacylation/reacylation then ensures membrane dynamism that participates in membrane rearrangements. Using isotopic labelling through ethanolamine or choline supplementation, we showed that DENV modulates PC and PE biosynthesis by interacting with membrane remodeling. Further supporting the importance of the Kennedy pathway in DENV infection, ethanolamine supplementation reduced virus titer in mosquito cells by altering composition of specific PC and PE. While ethanolamine-mediated aminoPL disruption did not alter attachment, internalization or translation, it reduced replication and resulted in a lower ratio of infectious particles, likely because of deficient replication. These results strongly support the importance of aminoPLs in DENV infection of mosquitoes and reveal the importance of aminoPL composition in replication. PC and PE are the most abundant phospholipid species in eukaryotic cells and contribute to cell membrane architecture, especially in the endoplasmic reticulum, where replication takes place. Disruption of aminoPL reconfiguration may represent a novel strategy to interfere with DENV subversion of mosquito metabolome.

RESUME

Plus de la moitié de la population mondiale est exposée au risque d'infection par le virus de la dengue (DENV) en raison de la distribution mondiale de ses moustiques vecteurs. Il n'existe ni vaccin ni traitement efficace. La seule stratégie disponible repose sur les insecticides, contre lesquels les moustiques développent une résistance. Les virus utilisent le métabolome de l'hôte pour la réplication et la dissémination. C'est particulièrement vrai pour les virus enveloppés comme le DENV qui dépend des membranes lipidiques de l'hôte pour compléter son cycle de vie. Pour atteindre un environnement métabolique optimal, les virus perturbent le métabolome de l'hôte. La compréhension de ces altérations chez les moustiques vecteurs pourrait révéler de nouvelles stratégies pour bloquer la transmission du DENV. Ici, nous avons caractérisé comment le DENV détourne le lipidome du moustique *Aedes aegypti*. Pour décrire les changements métaboliques tout au long du cycle du DENV chez le moustique, nous avons débeloppé une méthode de chromatographie liquide et de spectrométrie de masse à haute résolution (LC-HRMS) à différents stades de l'infection chez le vecteur. Nous avons révélé une reconfiguration majeure des phospholipides tout au long du cycle du DENV chez le moustique, dans les cellules, l'intestin moyen et le moustique entier. Pour déchiffrer la façon dont le virus reconfigure les phospholipides, nous avons caractérisé phylogénétiquement les isoformes de l'enzyme acylglycerol-phosphate acyltransférase (AGPAT) et identifié celles qui catalysent une étape limitante dans la biogenèse des phospholipides. Nous avons constaté que l'infection par le DENV diminuait l'expression de AGPAT1, dont la déplétion renforce l'infection en maintenant des concentrations élevées d'aminophospholipides (aminoPL), en particulier la phosphatidylcholine (PC) et la phosphatidyléthanolamine (PE), pendant le cycle du DENV chez le moustique. En démontrant que la sous-régulation de AGPAT1, causé par le virus, fournit un environnement proviral, nous révèlons le premier facteur métabolique hôte chez les moustiques et soulignent le rôle des aminophospholipides dans le cycle cellulaire viral. Nous avons ensuite cherché à confirmer que le virus influence la biosynthèse des aminoPL et déterminer à quel stade du cycle viral la reconfiguration des aminoPL est nécessaire. La biosynthèse de novo de PC et de PE est connue sous le nom de voie de Kennedy, où un diacylglycérol (DAG) incorpore soit un groupe choline, soit un groupe éthanolamine. Le remodelage des AminoPL par déacylation/réacylation assure ensuite un dynamisme des membranes qui participe aux réarrangements membranaires. En utilisant un marquage isotopique avec une supplémentation en éthanolamine ou en choline, nous avons montré que le virus module la biosynthèse des PC et des PE en interagissant avec le remodelage membranaire. Soulignant l'importance de la voie de Kennedy dans l'infection par le DENV, la supplémentation en éthanolamine a réduit le titre du virus dans les cellules de moustiques en modifiant la composition de PC et PE. Bien que la supplémentation en éthanolamine n'ait pas modifié l'attachement, l'internalisation ou la traduction, elle réduit la réplication et entraîne un ratio plus faible de particules infectieuses, probablement en raison d'une réplication déficiente. Ces résultats confirment l'importance des aminoPL dans l'infection des moustiques par le DENV et révèlent l'importance de la composition des aminoPL dans la réplication. Les PC et PE sont les espèces de phospholipides les plus abondantes dans les cellules eucaryotes et contribuent à l'architecture de la membrane cellulaire, en particulier dans le réticulum endoplasmique, où la réplication a lieu. L'inhibition de la reconfiguration des aminoPL par la supplémentation en éthanolamine pourrait représenter une nouvelle stratégie pour interférer avec la perturbation du métabolome des moustiques par le virus de la dengue.

Popular thesis summary

Dengue is endemic in tropical and subtropical regions, and has now encroached onto temperate regions because of the geographic expansion of its vector, *Aedes aegypti*. In the absence of effective treatment and vaccine, the only intervention is vector mosquito containment. Here, we explore the changes induced by dengue virus (DENV) in mosquito metabolite content, to uncover targets for blocking transmission. DENV relies on host metabolism to proliferate, particularly the membrane lipids that compose the architecture of the host cell. We described metabolic changes incurred by DENV throughout the mosquito cycle. Membrane lipids, called phospholipids, were highly reconfigured through reduction of an enzyme involved in their biogenesis to produce a pro-viral environment. Furthermore, we showed that the production chain of the two main phospholipid species is altered by DENV to promote viral replication. Our work comprehensively describes metabolic changes associated with DENV infection, reveal how DENV subdues the host membrane, emphasize the importance of phospholipids and identify their role in replication in mosquitoes.

Résumé de thèse vulgarisé

La dengue est endémique dans les régions tropicales, et empiète désormais sur les régions tempérées en raison de l'expansion géographique de son vecteur, *Aedes aegypti*. En l'absence de traitement et de vaccin efficaces, le confinement des moustiques est le seul moyen de contrôle. Ici, nous explorons les changements induits par le virus de la dengue au niveau du métabolisme des moustiques tout au long de leur cycle de vie, afin de découvrir des cibles pour bloquer la transmission. Le virus s'appuie sur le métabolisme de l'hôte pour proliférer, en particulier les lipides membranaires qui composent l'architecture de la cellule hôte. Les lipides membranaires, appelés phospholipides, sont fortement reconfigurés, à travers la réduction d'une enzyme impliquée dans leur biogenèse pour produire un environnement pro-viral. Nous avons montré que la chaîne de production des deux principales espèces de phospholipides est modifiée par le virus pour favoriser sa réplication. Nos travaux décrivent les changements métaboliques membranaires causés par le virus de la dengue et identifient leur rôle dans la réplication chez les moustiques.

TABLE OF CONTENTS

LIST OF FIGURES AND TABLES

CHAPTER 1 – Introduction to host-virus metabolic interactions in dengue virus

CHAPTER 2 – Dengue virus reduces AGPAT1 expression to alter phospholipids and enhance infection in *Aedes aegypti*

Chapter 3 – DENV activates phospholipid remodeling for replication

LIST OF SYMBOLS AND ABBREVIATIONS

AA	Amino acid
ABC	ATP-binding cassette
AC	Acylcarnitine
ACC	Acetyl-CoA carboxylase
ADE	Antibody-dependent enhancement
AGPAT	Acyl-sn-glycerol-3-phosphate O-acyltransferases
AminoPL	Aminophospholipids
AMPK	Adenosine monophosphate-activated protein kinase
APLS	Amphipathic lipid packing sensor
ARA	Acid arachidonic
ATP	Adenosine triphosphate
AUP1	Ancient ubiquitous protein 1
BMP	Bis(monoacylglycerol)phosphate
Bti	*Bacillus thuringiensis israelensis*
C	Capsid protein
CDC	Center for disease control and prevention
CDP	Cytidine diphosphate
CDS	CDP-diacylglycerol synthase
Cho	Choline
CI	Cytoplasmic Incompatibility
CK/EK	Choline kinase/Ethanolamine kinase
CL	Cardiolipin
CLS	Cardiolipin synthase
CM	Convoluted membranes
CoA	Coenzyme A
CPT	DAG:CDP-choline cholinephosphotranferase
CT	CTP:phosphocholine cytidyltransferase
CTP	Cytidine triphosphate
CYD	Chimeric yellow fever dengue
DAG	Diacylglycerol
DC	Dendritic cells
DENV	Dengue virus
DF	Dengue fever
DHF	Dengue hemorrhagic fever

DHA	Docosahexaenoic acid
DSS	Dengue shock syndrome
dsRNA	Double-stranded RNA
E	Envelope protein
ECDC	European centre for disease prevention and control
EK	Ethanolamine kinase
EPA	Ecosapentaenoic acid
EPT	DAG:CDP-ethanolamine ethanolaminephosphotranferase
ER	Endoplasmic reticulum
ET	CTP:ethanolamine cytidyltransferase
Etn	Ethanolamine
FA	Fatty acid
FAS	Fatty acid synthase
G3P	Glycerol-3-phosphate
GABA	Gamma-Aminobutyric acid
GAG	Glycosaminoglycans
GAPDH	Glyceraldehyde-3-phosphate dehydrogenase
GC	Gas chromatography
GL	Glycerolipid
GPAT	Glycerol-3-phosphate acyltransferase
GST	Glutathione transferases
HCV	Hepatitis C virus
HILIC	Hydrophilic interaction liquid chromatography
HSP	Heat-shock protein
IFN	Interferon
IL	Interleukin
ITM	Insecticide-treated materials
ITN	Insecticide-treated bed nets
JEV	Japanese encephalitis virus
LA	Linoleic acid
LC	Liquid chromatography
LD	Lipid droplet
LLIN	Long-lasting insecticides-nets
LPLAT	Lysophospholipid acyltransferase
LPCATs	Lysophosphatidylcholine acyltransferase
LysoPA	Lysophosphatidic acid

LysoPC	Lysophosphatidylcholine
LysoPE	Lysophosphatidylethanolamine
LysoPI	Lysophosphatidylinositol
LysoPG	Lysophosphatidylglycerol
LysoPL	Lysophospholipid
M/prM	Membrane/premembrane protein
MAM	Mitochondria-associated membranes
MS	Mass spectrometry
MBOAT	Membrane-bound O-acyltransferase
MR	Mannose receptor
MSI	Metabolomics standards initiative
MUFA	Monounsaturated fatty acids
NS	Non structural
NIAID	National institute of allergy and infectious diseases
NHP	Non-human primate
NADH	Nicotinamide adenine dinucleotide
NDGA	Nordihydroguaiaretic acid
NMR	Nuclear magnetic resonance
ORF	Open reading frame
PA	Phosphatidic acid
PAF	Platelet-activating factor
PC	Phosphatidylcholine
PCA	Principal component analysis
PE	Phosphatidylethanolamine
PE-Cer,	Ceramide Phosphoethanolamine
PEMT	PE methyltransferase
PFU	Plaque-forming unit
PI	Phosphatidylinositol
PIP	Phosphoinositide
PIS	PI synthase
PL	Phospholipid
PLA	Phospholipase A
PLB	Phospholipase B
PLC	Phospholipase C
PLD	Phospholipase D
PLS	Partial least squares

PG	Phosphatidylglycerol
PGP	Phosphatidylglycerol phosphate
PGPS	PGP synthase
PS	Phosphatidylserine
PSD	PS decarboxylase
PSS	PS synthase
PUFA	Poly-unsaturated fatty acids
RIDL	Release of insects carrying dominant lethals
RC	Replication complex
RNA	Ribonucleic acid
RNP	Ribonucleoprotein
dsRNA	Double-stranded RNA
RNAi	RNA interference
SIT	Sterile Insect Technique
SL	Sphingolipid
SM	Sphingomyelin
SMS	Sphingomyelin synthase
SREBP	Sterol regulatory element-binding proteins
T	Tubular structures
TBEV	Tick-borne encephalitis virus
TAG	Triacylglycerol
TCA	Tricarboxylic acid
TIC	Total ion current
TLR	Toll-like receptor
TNF- α	Tumor necrosis factor-α
UTR	Untranslated regions
Ve	Double-membrane vesicle
VIP	Variable influence on projection
VP	Vesicle packet
WHO	World Health Organization
WNV	West Nile virus
YFV	Yellow Fever virus
ZKV	Zika virus
(+)ssRNA	Positive single strand RNA
(-)ssRNA	Negative single strand RNA

CHAPTER 1 – Introduction to host-virus metabolic interactions in dengue virus

1. Dengue: a disease in expansion without efficient control

1.1. Dengue

1.1.1. A global burden

Dengue is an arthropod-borne viral disease (arbovirose) that currently infects about 400 million people every year throughout the tropical and subtropical world [1]. Dengue virus (DENV) is the most widespread arbovirus. It emerged in the second part of the 20th century [2], and ever since its incidence has increased 30-fold, according to WHO. Asia is the continent the most affected by dengue as it bears 70% of total infection. For instance, India represents 34% of the total infection. Africa is estimated to contribute 16% of global infections. However, African dengue burden is probably underestimated because of poor surveillance and presence of other diseases presenting similar symptoms. Americas represents 14% of infections, with majority of cases in Brazil and Mexico. The annual global cost incurred by dengue is estimated at US$ 8.9 billion, according to a study conducted in 2013 in 142 countries with active DENV transmission [3]. The average cost per dengue case is US$152, although actual cost varies according to clinical outcome. Estimated hospital admission for dengue costs US$70 but rises to US$84,730 for fatal cases. Dengue economic burden is higher than for other major infectious diseases, such as cholera, viral gastroenteritis, Chagas or rabies, because of the lack of available treatment and insufficient systematic diagnosis. Other factors associated to dengue outbreaks worsen the cost. The healthcare system can be congested during epidemic episode, resulting in difficulties

to provide accurate diagnosis. Loss of productivity, ability to work, impact on tourism also increase the economic burden [4].

DENV is transmitted by the bite of an infected female mosquito of the genus *Aedes*. Because of the *Aedes* geographical distribution more than 40% of the global population is at risk to contract dengue [5], encompassing 128 countries [6]. *Aedes* distribution now extends in all continents, including North America and Europe [5] in addition to the usual subtropical regions. Consequences are an expanding distribution of DENV (Fig 1).

1.1.2. From asymptomatic to severe dengue

About 75% of people infected with DENV remain asymptomatic (not registered in hospital). The other 25% represents around 100 million patients that experience a range of different symptoms from flu-like illness to vascular leakage, hemorrhages, organ failure and shock [1].

1.1.2.1 Clinical phase

The incubation period is usually 5-10 days and up to 14 days, followed by sudden onset of symptoms divided in 3 phases: febrile, critical and recovery.

The febrile phase starts with high fever during 3-7 days, vomiting and multiple symptoms (rash, headache, bone pain, retro-orbital pain, flush, hematuria, minor bleeding). The liver can be enlarged and sensitive. A decrease in total white cells can suggest dengue at this stage. The early febrile phase can be difficult to distinguish from other febrile diseases. Moreover, those symptoms can not differentiate an outcome into severe and non-severe dengue.

The critical phase begins when the fever decreases and complications start to develop. Most patients improve in this phase, but some can undergo vascular leak

syndrome. Increased vascular permeability can result in plasma leakage, intravascular volume depletion and lead to dengue shock syndrome (DSS) [7]. In the latter case, fluid overload induces respiratory distress. Vascular leak syndrome usually resolves within 1 or 3 days. Patients can also suffer from severe bleeding, especially during prolonged shock. Although uncommon, organ impairment can occur and includes hepatitis, encephalitis and myocarditis.

The recovery phase lasts 1-2 weeks with good supportive care. Fluids are reabsorbed, then hematocrit, white blood cells and platelets stabilize. Some patients may experience rash and remain tired for several days.

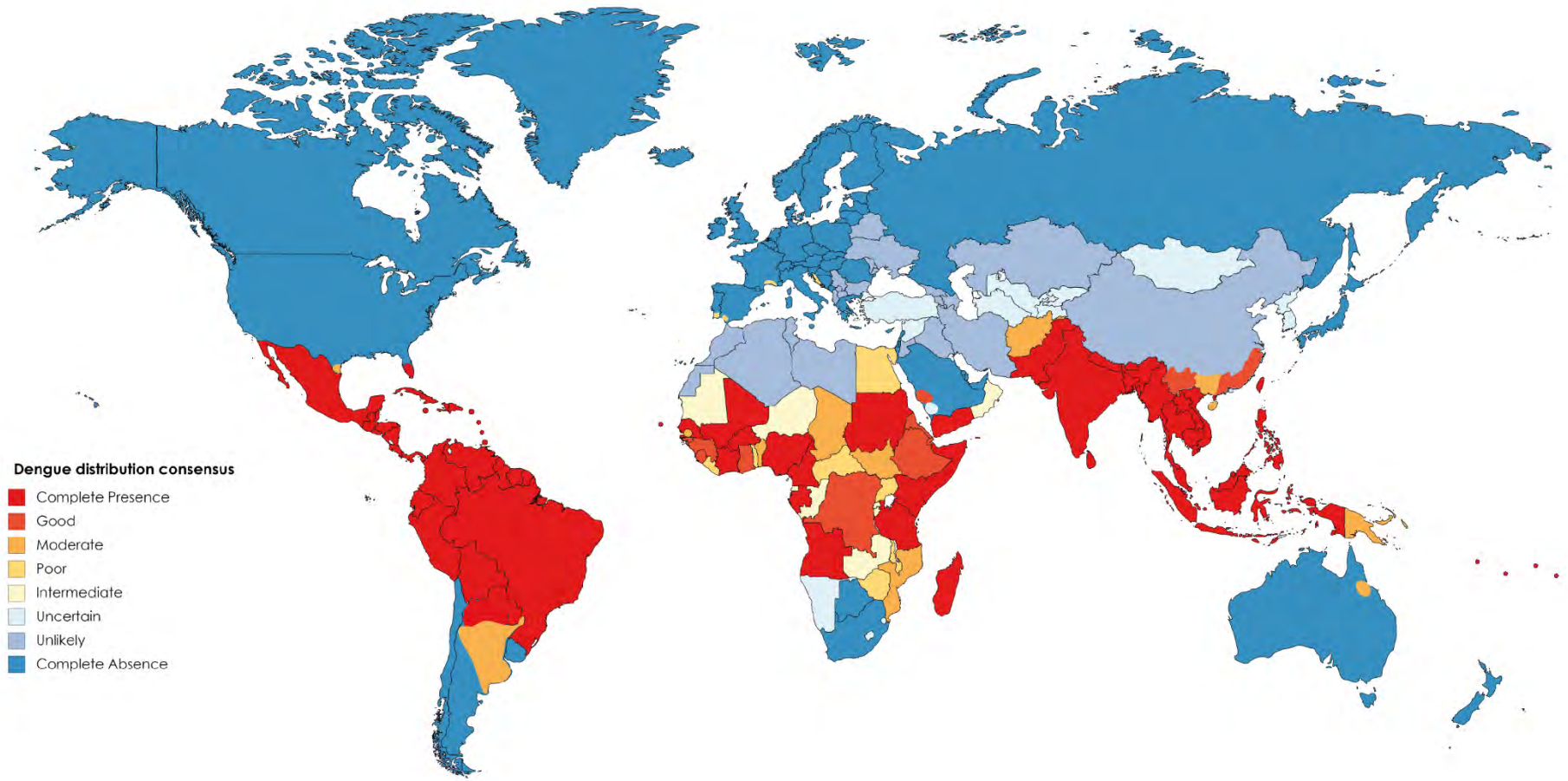

Figure 1. The global distribution of dengue. Adapted from [1,8], CDC Dengue heatmap (/www.healthmap.org/dengue), and data from the European Centre for Disease Prevention and Control (ECDC) (www.ecdc.europa.eu/en/dengue). National and local consensus of complete presence (red) or absence (blue) reported by local transmission. This map does not take into account imported dengue cases by travelers.

1.1.2.2 Symptom Classification

A previous classification established by WHO in 1997 differentiated dengue fever (DF), dengue shock syndrome (DSS) and dengue hemorrhagic fever (DHF). In 2009, WHO revised the classification in dengue without complications and severe dengue. Severe dengue is defined by one of these complications: shock syndrome or respiratory distress caused by plasma leakage or fluid accumulation, severe bleeding, or organ impairment [9].

1.1.2.3 Secondary dengue infection

Following DENV infection with one serotype, the adaptive immune response will provide long-term immunity to this serotype and short-term protection (3 months to 2 years) against heterologous serotype infection [10]. However, with vanning heterologous protection, the risk of severe dengue with secondary infection increases. Cross-reactive antibodies induced by the primary infection bind the heterologous serotype and facilitate virus entry into target cells via Fc receptors. This phenomenon is called antibody-dependent enhancement (ADE). Antibody-FC receptor interaction is an alternative DENV entry mechanism during ADE in the course on secondary heterologous infection [11]. ADE also contributes to decreasing immune response and antiviral response against the infection, through FC receptor signaling which prevent lysosomal degradation of DENV [12].

1.1.2.4 Diagnosis

Diagnosis will depend on the time after disease onset [9]. Before 5 days, viral RNA is detected by nucleic acid amplification, the virus is isolated in cell culture or viral protein NS1 is detected by immunoassay. After 5 days, DENV does not persist in blood,

but NS1 is still detected for a few days, especially during primary infection. From about 4 days onwards, IgM antibodies can be detected, with a peak at 10-14 days, before decreasing and disappearing after 3 months. IgGs appear later, from day 10 onwards, at lower concentration and remains detectable for life. Serological assay may not be sufficient for detection due to cross-reactivity with other flaviviruses, especially in regions where flaviviruses circulate or for patients vaccinated against yellow fever or Japanese encephalitis.

1.2. DENV vectors

1.2.1. *Aedes aegypti* and *Aedes albopictus*

The main vector of DENV is *Aedes aegypti* mosquito. It is highly adapted to urban areas as it preferentially breeds in man-made containers with stagnant water. It mainly bites humans during the day and can take several blood meals from different people, increasing chances of transmission [13]. *Aedes albopictus*, the second major vector of DENV, is found in peri-urban and rural areas and feeds on humans as well as other mammals [14]. Both species are quickly colonizing new regions, spreading risk of infection to new regions [5]. Multiple factors such as urbanization, globalization, trade, population growth, travel and global warming are associated with the enlarged distribution of the two vectors [15]. Population growth in urban tropical areas closely correlates with the increase in dengue epidemics [16]. Higher population density amplifies DENV transmission dynamic, illustrated by the fact that a mosquito can bite several people during a blood meal [17]. Urbanization increases larval development by providing more oviposition sites and enhancing mosquito survival [18]. Globalization and large scale travels spread the virus across different countries and continents

[19,20]. The impact of climate change on DENV distribution has been modeled [21]. Temperature rise and new precipitation patterns facilitates geographical expansion of the vectors. Annual number of people exposed to *Aedes* vectors was projected to increase drastically by 12 to 134% by 2050, depending on different scenario, with new territories affected such as Australia, Europe and North America.

Life cycle of mosquitoes contains four separate stages which takes approximately over 8-10 days: egg, larvae, pupae and adult. An adult female mosquito lays up to 200 eggs inside containers holding water. When submerged in water, eggs hatch into larvae after 1-2 days. Aquatic larvae feed on microorganism and develop into pupae after approximately 5 days. Pupae are mobile in water and do not feed. They emerge into adult flying mosquitoes after 2-3 days. A couple of days later, male and female adults start to mate. The female will need a blood meal to produce eggs. Adult *Aedes* mosquitoes can live for more than 1 month. Mosquitoes can fly about 200 meters after emerging. *A. aegypti* females bite almost exclusively humans during daylight hours, preferentially early in the morning and in the evening, outdoor and indoor.

DENV is maintained at low level in endemic highly dense urban area. Epidemic episodes contribute to the persistence of the virus. Multiple DENV serotypes can circulate in the same area. *Aedes* mosquito will be infected by blood-feeding on a human in the viremic phase of DENV infection (**Fig 2)**. Extrinsic incubation period, the time taken by the virus to multiply and be present in mosquito saliva, is usually 10-14 days. Infected mosquitoes can infect several humans during subsequent bites. About 5-10 days after being bitten by DENV-infected mosquito, a person develops high viremia that persists approximately 7 days. During this period, an infected person can transmit the virus to a new mosquito.

DENV sylvatic cycle exists between Non-Human Primates (NHPs) and *Aedes* forest mosquitoes in rainforests of Southeast Asia (Malaysia) an West Africa (Senegal) [22]. Contrary to the YFV, no evidence exist for a sylvatic cycle in America [23]. DENV found in NHPs in south America are likely spill back from human viruses [24].

1.2.2. DENV cycle in mosquito

Following a blood meal on an infected human, DENV reach the mosquito midgut where it infects and multiplies in epithelium [25] (**Fig 2)**. Blood meal is digested within 48 hours, while replication in the midgut continues and reach a peak at 7 days after ingestion. DENV then disseminates in the whole mosquito body, including salivary glands which are fully infected at 10-14 days post infectious blood meal. Mosquitoes can then transmit DENV to human via saliva during subsequent blood feeding. Throughout its infection cycle in the mosquito, DENV replicates in different tissues and cell types, involving specific physiological changes at each stage.

In mosquitoes, DENV is confronted to complex barriers from the midgut to salivary glands [26]. After the blood meal, the virus needs to infect the midgut epithelium and to overpass an extracellular matrix called basal lamina (BL) to disseminate from midgut to secondary tissues. After crossing the midgut barrier, new virion can infect fat body and nerve tissues, but hemocytes are likely an important target for the next step of arbovirus amplification [27]. DENV then infect lateral and median lobes of salivary glands [25] where viral replication will lead to the release of new viral particles in the excretory canal of the gland. At that point, the virus is associated with apoptosis and mosquito saliva containing proteins and enzymes having immune response modulating properties [28], which suggest that saliva is an important factor in virus transmission to human host.

The ability of a mosquito to acquire and propagate DENV through all these steps is defined as vector competence. The competence is related to host genetic factors such as innate immune response and tissue barriers [29]. For instance, *Ae. aegypti* endogenous RNA interference pathway is involved in arbovirus infection in the midgut and can be virus dose-dependent to overtake host defense [30]. Enhancing RNAi pathway in mosquito can improve the midgut infection barrier (MIB) to DENV after cell entry and decrease the vector competence [31]. Mosquito RNAi effector polymorphism is also a key factor to DENV resistance [32]. The MIB can also be associated to resistance of midgut epithelial cells to viral infection, due to filtration by the extracellular matrix or a lack of host membrane receptor of targeted cells. Precisely, the 67kDa protein described as a DENV receptor in midgut cells, is identified as a marker of vector competence for DENV in *Ae. aegypti* mosquito [33,34]. Infection of salivary glands is likely receptor-mediated and dependent on mosquito strain, similarly to midgut infection. Compatibility between mosquito strain and virus strain to bind and infect tissue especially at the midgut and salivary gland levels are part of endogenous factor that are independent of virus-dose interaction and define vector competence [35].

Among the host endogenous factor, it can be hypothesized that the metabolite composition of certain tissues, especially in lipid constituting cell membranes, such as the midgut or the salivary glands play a major role in such barriers. Furthermore, exogenous nutritional content in lipid and sugar could affect vector competence for arbovirus, as observed for West Nile virus [36]

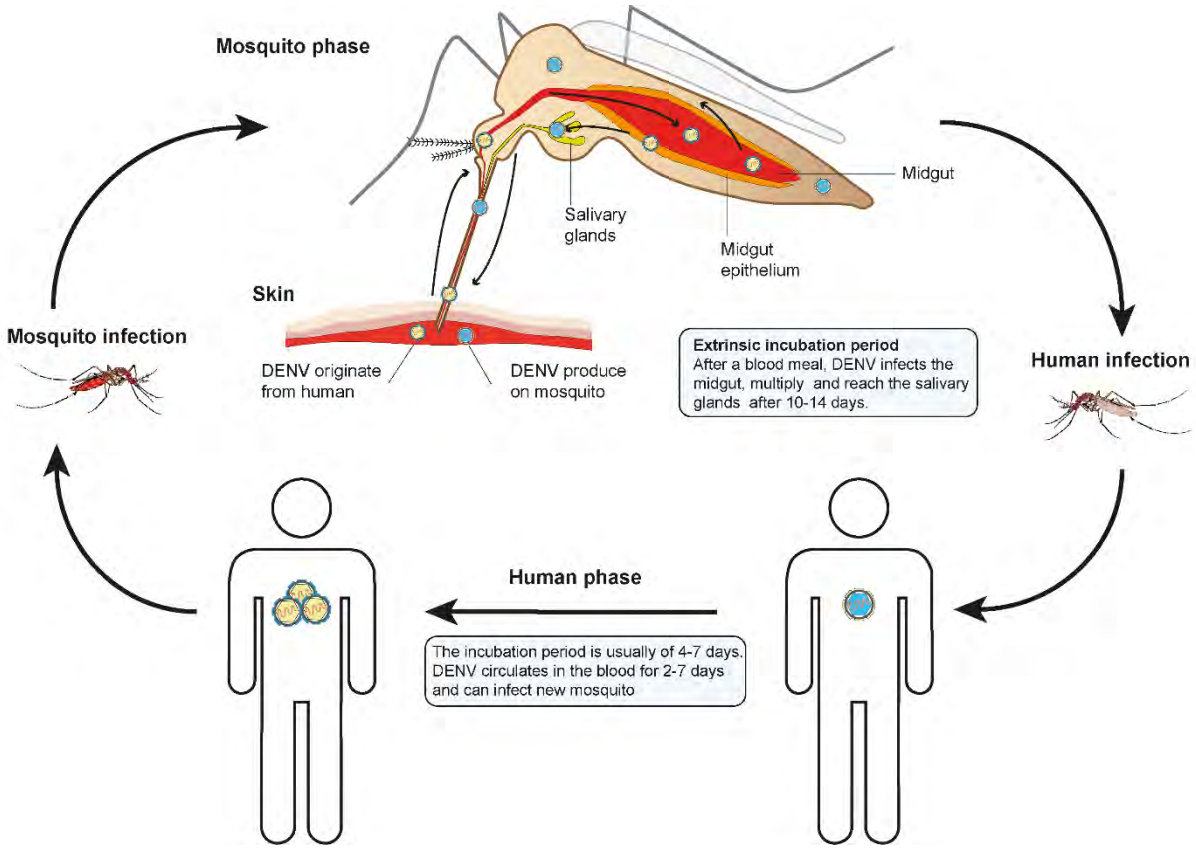

Figure 2. DENV cycle in humans and mosquitoes.

1.3. Dengue virus (DENV)

1.3.1. DENV biology

DENV belongs to the *Flavivirus* genus of the Flaviviridae family. Other pathogenic Flaviviruses include Yellow Fever virus (YFV), West Nile virus (WNV), Japanese encephalitis virus (JEV), tick-borne encephalitis virus (TBEV) and Zika virus (ZIKV) (**Fig 3)**. DENV is composed of four antigenically and genetically different subtypes, called serotype 1 to 4. DENV has the ability to infect and propagate in two different hosts, human and mosquito.

DENV presumably evolved from sylvatic strains in Africa or Asia from non-human primates [37,38]. The four independent DENV serotypes likely involved different host switch events.

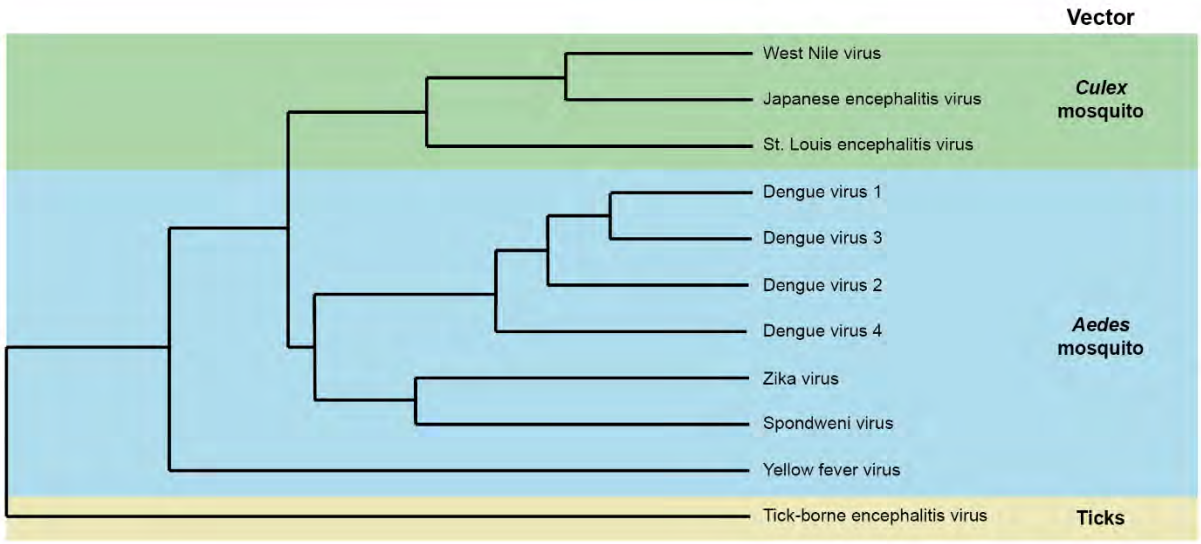

Figure 3. Phylogenetic tree of mosquito borne *flavivirus*. The dendrogram is based on amino acid sequence of the virus polyprotein. Colors differentiate the vectors [39]. *Aedes* mosquitoes vector DENV, ZKV, YFV and the Spondweni virus. *Culex* genus mosquitoes vector WNV, JEV and St. Louis encephalitis virus. Ticks (*Ixodes* genus) are vectors of the tick-borne encephalitis virus.

DENV are enveloped viruses with a spherical shape of 50 nm diameter. The virus is composed by a lipid envelope associated with 2 structural proteins, the envelope (E) and membrane (M) proteins. Within the viral envelope, the RNA viral genome is associated with the capsid (C) protein. Importantly, the lipid bilayer is the only component that does not come from the viral genome, but from the endomembrane compartment of the host cell.

The genome is a single-stranded positive sense RNA ((+)ssRNA) of about 11kb that encodes ten proteins. The + genome is used as template for the – genome synthesis, protein synthesis and for packing into new viral particles. Three structural proteins, E, pr-membrane (prM) and C; and 7 non-structural (NS) proteins, NS1, NS2A,

NS2B, NS3, NS4A, NS4B and NS5 are encoded in a polyprotein. During assembly, a RNA-capsid complex recruits a lipid bilayer membrane, in which the E and prM are embedded. Virions exist in mature and immature form depending on the presence of pr protein, which is shed during maturation.

E protein (53 kDa) is involved in viral entry into targeted cells by binding to cellular receptors and triggering viral and cellular membranes fusion [40]. In mature form, 90 homodimers of E proteins are arranged on the surface, by sets of 3 E homodimers in 30 rafts. E ectodomain is composed of 3 connected domains (DI-III) and a fusion loop at the tip of DII [41]. DI is the central structure, DII contains a fusion loop important for the fusion of viral and cell membranes, and DIII is exposed at the particle surface with cellular-binding motifs. In immature form, E and prM protein are associated in heterodimers forming spike. The prM protein (21 kDa) participate in the formation and the maturation of new virion. During maturation of newly produced particles, pr peptide is cleaved from the M peptide through the secretory pathway involving pH-dependent reaction and host protease. In mature virion, M protein is anchored into the viral membrane by two transmembrane helices under the E protein. It is also important to note that temperature induces structural changes in viral particles. A virus incubated at 28°C, daytime mosquito body temperature, will have a smooth surface, while at human body temperature of 37°C, the virus has a rough and heterogeneous structure due to specific arrangement of the E proteins [42]. This underlines that the virus surface is not a static but a dynamic structure. This conformational amplitude is called viral breathing [43]. Different conformations can exist and this does not have any consequences on the interaction of the virus with target cells [44]. The C proteins (12kDa) are associated in homodimer and act as RNA

chaperone with RNA-binding activity. This complex forms the viral ribonucleoprotein (RNP).

The NS proteins are involved in viral replication and packing, operating in endoplasmic reticulum (ER) and secretory pathway of the cell. NS1 is associated with intracellular membrane and can be secreted (sNS1). NS1 participates in early viral genome replication [45]. The secretory form activates the innate immune system and is associated with vascular leakage in severe dengue [46]. NS2A is a membrane protein involved in RNA replication and viral assembly [47]. NS2B act as a cofactor of NS3 which has several functions, especially during RNA synthesis with helicase and capping activities. NS4A is a membrane protein associated with the formation of the replication complex (RC). NS4B has inhibitory capacity against interferon (IFN) response [48]. NS5 has the biggest size and is highly conserved. Several functions are associated with NS5, such as suppression of IFN system, RNA synthesis and capping. DENV genome contains also two untranslated regions UTR: a short 5' UTR of ~100 nucleotides and a longer 3' UTR of ~450 nucleotides, both highly structured. Those UTR are involved in genome replication [49].

1.3.2. DENV cellular life cycle

1.3.2.1 Virus entry

Susceptible cells contain attachment factors on the surface that allow contact with viral particles through E binding. This promotes virus entry. Multiple cell types can be infected in vitro, including epithelial, endothelial, muscular, dendritic, mast cells and hepatocytes, monocytes and mosquito cells [8]. Different DENV receptors have been candidates in mammalian and mosquito cells, consistent with the ability of the virus to

infect a diversity of cells, as well as 2 different hosts [50,51]. Glycosaminoglycans (GAG) such as heparan sulfate, dendritic cells lectin receptor (DC-SIGN), macrophage mannose receptor (MR), lipopolysaccharide (CD14), heat-shock protein 70 and 90 (HSP70/90), binding-immunoglobulin protein GRP78 and TIM/TAM phospholipid receptors were identified on mammalian cells. On mosquito cells, the chaperone prohibitin protein was identified as receptor by interaction with E [52]. A set of proteins and glycoproteins, some of which related to heat shock protein family, were also candidates as mosquito cell receptor for DENV [51].

After virus adsorption to cell surface, entry occurs mainly by clathrin-dependent endocytosis. DENV has been preferentially found on cell surface of clathrin-coated pit [53]. Alternative entry pathways exist but are minor and found only on mammalian Vero cell line [54]. On mosquitoes cells, only the clathrin-mediated endocytosis pathway was observed four the four DENV serotypes [55,56]. An invagination in the plasma membrane is created and closed by dynamin to form a clathrin-coated vesicle. The endosomal vesicle is transported inside the cell by a mechanism involving actin filaments [57].

At this step the enveloped virus is contained in a vesicle delimited by a lipid bilayer. The endosomal low-pH induces molecular changes on the E proteins leading to viral and endosomal membrane fusion and release of the viral RNP into the cytoplasm. The homodimer of E rearranges in trimers under the acidification, which makes the fusion loop accessible and facilitates interaction with the outer lipid layer of the endosome membrane [40]. The E protein then folds back and induces hemifusion of monolayers followed by pore formation. Cellular vacuolar ATPase are important for endosome acidification and its inhibition blocks DENV infection [58,59].

1.3.2.2 Polyprotein translation

After release from the endosomes, the RNP is in cytoplasm and undergoes capsid uncoating. The single open reading frame (ORF) is translated into a long polyprotein associated with ER membranes, processed by viral and host proteases into the 3 structural proteins (C, prM, E) and the 7 NS proteins (NS1, NS2A, NS2B, NS3, NS4A, NS4B, and NS5) [58]. The genome is likely recruited to the ER to initiate translation with ribosomes. It is also suggested that translation starts into the cytosol and continues in ER when the transmembrane domain of the C protein emerges from ribosomes. Actually, the full-length polyprotein has yet to be observed, suggesting rapid cleavage of viral proteins. The polyprotein intertwines with the ER membrane: NS2A, NS2B, NS4A and NS4B have transmembrane domains and are anchored in the ER bilayer. C, NS3 and NS5 are on the cytoplasmic side, when prM, E and NS1 are on the lumen side. Polyprotein processing is realized by viral and cellular proteases. NS3/NS2B complex cleaves proteins on the cytoplasmic side, while a host peptidase cleaves those in the lumen. A small part of immature C remains in the ER after the cleavage. The cleavage of NS4A and NS4B leave a 2K peptide inserted in the ER membrane. The translation process highly involves ER membrane, and several proteins remain anchored in ER.

1.3.2.3 Replication

Viral replication requires viral proteins, host factors and viral RNA. The positive strand viral genome ((+)ssRNA) is copied into antigenome ((-)ssRNA), which is then used as a template for genome replication. Viral synthesis involves membrane rearrangements via lipid membrane invagination to ensure efficient RNA synthesis in replication complex (RC) [60,61]. RC may also protect viral replication from host defense mechanisms.

DENV replication complex structure has been characterized in human and mosquito cells [62,63]. In mammalian cells, membrane alterations induced by DENV have different shapes, from convoluted membranes (CM), double-membrane vesicles (Ve), tubular structures (T) and vesicle packets (VP), derivating from ER. Open pores were observed in Ve, allowing probably transport of building block from the cytoplasm for RNA synthesis and/or release of newly synthetized RNA for encapsidation. VP are composed of small groups of Ve formed by ER membranes rearrangement containing viral replication sites. Vesicles induced by DENV contain NS proteins and dsRNA intermediates in RC, suggesting active RNA synthesis [63]. Those distinct structures were also observed in mosquito cells, except for CM. Formation of different structures suggest specific modifications of host membranes induced by DENV replication. Vesicle formation may be induced by NS4A protein due to its transmembrane domain acting on the luminal leaflet on the ER [64,65]. Membrane invagination close a cytoplasmic window containing NS1, NS3 and NS5 [64]. Inside a vesicle, replication complex organization is represented as a complex containing dsRNA associated with NS3/NS2B protease/helicase and NS5 methyl-transferase-polymerase [66]. NS3 has helicase activity to unfold dsRNA during RNA synthesis, while NS5 is the RNA-dependent-RNA polymerase (RdRp) and methyltransferase involved in newly synthetized RNA, that also cap RNA by its triphosphatase activity. NS4B ER-anchored protein binds the NS3/NS2B enzymes as factor to support replication. It was observed that the cleavage of the 2K peptide associated with NS4A is important to induce membrane arrangement in RC [64]. Furthermore, NS4A induces rearrangement and phosphorylation of vimentin intermediate filaments to support DENV RC at the perinuclear site [67], suggesting the involvement of the cytoskeleton. NS2A transmembrane protein is essential for RNA synthesis and involved in the RC

organization [47]. NS1 is found in the lumen side of the ER, and connect to the RC via transmembrane interactions, probably by interaction with NS4B as shown during WNV infection [68]. Role of NS1 in viral replication is currently not reported.

1.3.2.4 Assembly

DENV assembly occurs at the ER with C, prM and E proteins assembling with viral genomes to bud towards ER lumen. NS2A as well may be required for viral assembly [47]. NS3 is required for *flavivirus* RNA packing into viral particles, without involving helicase and protease activity [69,70]. The C protein is enough to fold RNA and participates in spontaneous encapsidation [71]. Encapsidated viral RNA is probably released from RC through the pores, but viral RNA transport to assembly sites remain unclear. Once assembled, flaviviruses form immature particles characterized by spikes of trimeric prM and E form [72]. Maturation of flaviviruses occurs through Golgi and trans-Golgi networks and requires an acidic environment [73]. pH induces molecular rearrangement of prM and E protein, enabling access to prM for furin host protease. Cleavage of prM releases pr and maintain M on the envelope. Immature or partially immature virions are also produced and have alter infectious capacity.

1.4. Prevention and treatment

1.4.1. Antiviral developments

No antiviral against DENV is currently available and only symptomatic care is provided to patients [74]. It is recommended to stay hydrated and avoid anticoagulant such as aspirin-containing drugs. For severe dengue patients in shock syndrome,

intravenous fluid supplementation is essential and prophylactic platelet transfusion is performed, although the latter does not prevent bleeding [75].

Multiple drugs with *in vitro* antiviral activity against DENV have been tested in clinical trials (chloroquine, balapiravir, celgosivir, lovastatin), without success in preventing disease or lowering viremia [76]. Ivermectin is currently in clinical trial in phase II/III in children and adult patients (ClinicalTrials.gov number NCT02045069). DENV-2-infected *Aedes albopictus* mosquito treated with ivermectin have shown a 50% decrease in infection rate and almost complete clearance of DENV RNA [77]. Ivermectin also inhibits *in vitro* replication of flaviviruses, mainly YFV and DENV with a lower effect for the later, by targeting NS3 helicase activity [78]. Ivermectin is usually used to treat parasite infections in humans such as malaria [79,80]. Other drugs that target NS proteins such as NS3 and NS5 have been studied, but none reached clinical trials [81]. Recently a DENV inhibitor targeting NS4B was under development [82]. Neutralizing monoclonal antibodies are also candidates for dengue treatment [83]. Several bioactive compounds from natural products display anti-dengue activity, but have not been studied further [84–86].

1.4.2. Vaccines

Dengue vaccine against the four DENV serotypes is needed for the prevention and control strategy. Dengue vaccine development have been on the road since the end of the first half of the 20th century [87].

1.4.2.1. Dengvaxia, a partially efficacious vaccine

Dengvaxia is a DENV vaccine produced by Sanofi-Pasteur. It is a live attenuated tetravalent vaccine composed of the nonstructural genes of yellow fever vaccine strain 17D and envelope (E) and pre-membrane (prM) genes of the four DENV

serotypes. Four chimeric yellow fever dengue (CYD) vaccine are combined into a single formulation. The vaccination scheme remains long with 0, 6 and 12 months boosters. The vaccine is registered in 20 dengue-endemic countries and in the United States of America (USA) in May 2019 [88] and in the European Union [89]. However, its use remains low as it has poor efficacy in protecting against all dengue serotypes and seronegative people [90–92].

During the immunization programs in Brazil and Philippines, an increase risk of severe dengue in vaccinated seronegative group was observed, resulting in a low vaccine uptake. In September 2018, WHO recommended that only people with past DENV infection be vaccinated, after highly specific screening test, in the age range 9-45 years [93]. The U.S. Food and Drug Administration (FDA) approved the vaccine in people ages of 9-16 years who have laboratory-confirmed previous dengue infection and who live in endemic areas of the US [94]. In case when screening is not possible, vaccination could be administrated in areas with 80% seroprevalence or more by 9-year-old. Furthermore, DENV seropositive traveler in a high endemic country could consider the vaccination. This vaccine limitations highlights the urgent needs for rapid diagnostic of dengue serostatus in endemic countries.

1.4.2.2. Other vaccine in clinical trial

Two other vaccines are currently in clinical trial phase III [89]. The vaccine developed by Takeda (TDV) is in clinical trials in several countries in Asia and Latin America (ClinicalTrials.gov, NCT02747927). This vaccine is a live attenuated tetravalent dengue vaccine based on the backbone of DENV-2 and contains the E and prM genes of the other three serotypes. The vaccine developed by National Institute of Allergy and Infectious Diseases (NIAID) and Butantan Institute (TV003/TV005) and

licensed by Merck in the USA, is currently in clinical trials in Brazil (ClinicalTrials.gov, NCT02406729). This vaccine is a live attenuated tetravalent vaccine with mutations in 3' UTR, while DENV-2 is a chimeric virus containing the capsid and NS protein genes from DENV-4 and prM and E genes from DENV-2. The vaccine induces seroconversion to four serotypes up to 90% of naïve adults [95]. Estimated study completion are respectively by 2021 and 2025 for Takeda and NIAID vaccines. These new candidate vaccines will be challenged on seronegative patients with particular scrutiny on safety issues.

1.4.3. Vector control

Control of mosquito vectors and diminution of human-vector contact is a strategic approach to reduce DENV infection [9]. Vector management targets the two main vectors, *A. aegypti* and *A. albopictus*. Vector control includes environmental, biological and chemical methods.

1.4.3.1. Environmental methods

Environmental methods intent to reduce mosquito breeding sites by elimination of larval habitats [9]. Modification of water supply and water storage in household is essential to control vector population. It implies the use of water pipes instead of free access water such as wells and traditional water-storage systems. Otherwise, water-storage containers need improvement to avoid mosquito access for oviposition by using covers or polystyrene beads. Solid waste such as used tires and plastic containers need efficient environmental management to decrease larval habitats in urban areas.

Some urbanization programs, such as in Singapore [96], take into account the urban disease vector problem during housing construction, on construction sites and through specialized infrastructure. For example, roof gutters are prohibited and home owners must ensure maintenance of water storages.

Vector control can also be managed by using mosquito traps. Mosquito traps use carbon dioxide or ultraviolet-A as attractants and aspirate mosquitoes with a vacuum fan [74]. Other traps use water or organic lure.

1.4.3.2. Biological method

Wolbachia-infected mosquitoes

Wolbachia is a gram-negative bacteria naturally present in 70% of insect species [97], including certain mosquito disease vectors [98]. The bacteria modify host reproduction to ensure its dispersion. Males infected with *Wolbachia* produce a sterile progeny, meaning no hatching, after mating with non-infected females. The phenomenon is called Cytoplasmic Incompatibility (CI). *Wolbachia*-induced sterility is a population suppression strategy used to eradicate *A. aegypti* populations [99]. Release of *Wolbachia*-infected *A. aegypti* males, exploiting the CI phenotype, is used in programs in Singapore [100], US and China. Furthermore, *Wolbachia* infection in female mosquitoes reduces virus multiplication [101] and is transmitted maternally. Because of these two traits, replacement of the wild population with *Wolbachia*-infected mosquitoes has been used to decrease transmission. *Wolbachia*-infected mosquitoes have been released in large scales in Australia, Brazil, Colombia [102], Vietnam and Indonesia [103].

Genetically modified mosquitoes

Insect genetic engineering is another strategy used to control mosquito populations [104]. The most common genetically modified mosquitoes make use of a lethal gene insertion to sterilize progeny with wild populations, hence reduce population sizes. Male *A. aegypti* are introgressed with dominant lethal gene (i.e., RIDL) [105]. When engineered males mate with wild-type females, offspring are not viable and die at larval stages. This strategy has been tested in the field and showed encouraging result to suppress local mosquito population [106]. These strategies require very large quantities of modified mosquitoes, as well as increased knowledge of the vector ecology to foresee impacts of the modifications.

Larvicide organisms

Mosquito larvae control is conducted using bacteria and animals. *Bacillus thuringiensis israelensis* (Bti) produced endotoxins are able to kill mosquito larvae, by permeabilizing cell membranes and inducing cell death [107]. However, mosquitoes that survived Bti treatment will have fitness benefit compared to congeners not under larvicide pressure [108]. Larvivorous fish and small crustaceans (Copedod) have been used to reduce larvae in container [74]. Some fish species (*Gambusa affinis*) are insecticide tolerant, allowing combination with chemical control. Nevertheless, those species do not target specifically *Aedes* larvae and can affect other insect species, and their introduction into a new environment can affect biodiversity.

1.4.3.3. Chemical methods

Insecticides

Insecticide use is the most common method to control mosquito population. Chemical control targets either the larval or adult stage, mainly by neurotoxic insecticides. However, insecticides have adverse environmental and health effects and are less effective due to evolution of insecticide resistance.

Larvicides are used to control larval stage and are amenable for water containers [9]. Those compounds are complementary to environmental interventions and restricted to area where water containers are difficult to reach. The challenge is to target only mosquito vector and not to alter water quality. Three classes of larvicides are generally used. Insect growth regulators affect hormones and disrupt the development of young insect. Organophosphates act as nerve agents by disrupting acetylcholine action, resulting in mosquito death. Biopesticides from bacteria toxin such as Bti toxin or the neurotoxin Spinosad can be used. Some larvicides are used for treatment of drinking-water, such as pyriproxyfen, temephos and methoprene at specific dosages.

Adulticides target adult vector to impact mosquito densities in large scale by spraying or fogging [9]. Space spraying is used to prevent epidemic or in emergency situation. Spraying is usually focused where dengue cases have been reported or in high-density population area (school, hospitals, housing). In emergencies, treatments can be applied every 2-3 days for 2 weeks. Significant suppression of adult mosquito populations in high risk area may require application once or twice a week. Organophosphates (Fenitrothion, Malathion) and pyrethroids (cyphenothrin, metofluthrin) are generally used for spraying application against vector. Pyrethroids alter signaling in nervous system by alteration of sodium channels. Insecticide derived

from bioactive compounds (terpenoids, alkaloids, pyrethrins, anthraquinones, saponins, monoterpenes) have also shown larvicidal, ovicidal and insecticidal activities [74]. Carbamates, organochlorines (i.e., DDT) are other classes of insecticides but are now rarely used.

Individual protection against vector uses mosquito repellent or Insecticide-treated materials (ITMs). The most widely used repellents are DEET (N, N-diethyl- 3-methylbenzamide), IR3533 (3-[N-acetyl-N-butyl]-aminopropionic acid ethyl ester) or Picardin (1-piperidinecarboxylic acid, 2-(2-hydroxyethyl)-1-methylpropylester). Oil extract from lemongrass (*Cymbopogon nardus*, *Cymbopogon citratus*) have repellant activity against *A. aegypti* and are used in sprays, lotion and bracelet for temporary individual protection [109]. Insecticide-treated bed nets (ITN) and long-lasting insecticides-nets (LLIN) incorporate insecticide in the fabric and reduces vector borne disease transmission.

Insecticide resistance

Chemical control with insecticides has been efficient in controlling *Aedes* mosquito population before resistance to all four classes of insecticides occurred [110–114]. Rising of mosquito resistance to insecticides have been observed in more than 60 countries, with resistance to 2 or more classes [115]. It is proposed that low density of mosquito carry resistance genes that allow them to survive after insecticide exposure. The offspring of resistant mosquitoes will have a fitness advantage and be the dominant group of mosquito population [116].

Multiple resistance mechanisms have been identified in *A. aegypti* mosquito [117], including metabolic detoxification and modification of the insecticide-target site. More precisely, mutations in the sodium channel, on acetylcholinesterase or on GABA

receptors will induce insecticide resistance against pyrethroids, organophasphate and cyclodiene, respectively. Metabolic detoxification is due to overexpression/modification of cytochrome P450 genes, esterases and glutathione transferases (GST), which are able to metabolize different types of insecticides [110].

The variety of insecticides for public health is limited and their use led to evolution of resistant populations. Insecticide resistance management is essential to slow down the evolution of resistance and maintain efficiency of vector control. Reduction of insecticide pressure in vector control, agriculture and domestic use is essential. Alternation of insecticides with different modes of action, spread over different areas, use of mixture of insecticides, and nonchemical alternatives are strategies to manage resistances [118]. Development of novel chemicals focusing not on annihilating the vector but on blocking viral transmission is another unexploited strategy to fight the dengue global burden.

Vector competence and tolerance to infection

It is commonly reported that viral infection barely impacts physiology and fitness of mosquitoes [119,120]. However, rather than resisting infection, it seems that the mosquito tolerates infection by limiting damages [121]. This tolerance allows mosquito survival and high viral load, essential for virus transmission to humans. Different tolerance mechanisms have been suggested in midgut, such as immune pathways, tissue repair via stem cell division, metabolic adaptation, stress responses and microbiota-induced tolerance [122].

2. The metabolome

2.1. Overview

Metabolites are small molecules that determine the physiological state of cells and include carbohydrates, amino acids, lipids, nucleotides, hormones and vitamins. The metabolome is the set of all metabolites. Metabolites are usually presented as the end product of processes related to genes, transcripts and proteins. Consequently, any upstream bio cellular alterations result in metabolic changes and metabolome profiling brings information about the phenotype.

The metabolism is separated in several pathways, which are interconnected and converge on the tricarboxylic (TCA) cycle **(Fig 4)**. TCA produces metabolic intermediates and contributes to energy production in the form of adenosine triphosphate (ATP). TCA cycle starts with acetyl-CoA, which is produced by catabolism of carbohydrates, mainly glucose, via glycolysis. In the TCA cycle, the acetyl group is oxidized to produce energy. Acetyl-CoA is also used for fatty acid and lipid biosynthesis, including phospholipids, sphingolipids and glycerolipids. Acetyl-CoA can be reversely produced by fatty acid catabolism via the β-oxidation. TCA cycle is connected with amino acid metabolism through shared intermediates and, thus, indirectly influences protein translation. Eventually, nucleic acids originate from the pentose phosphate pathway, which derives from glycolysis.

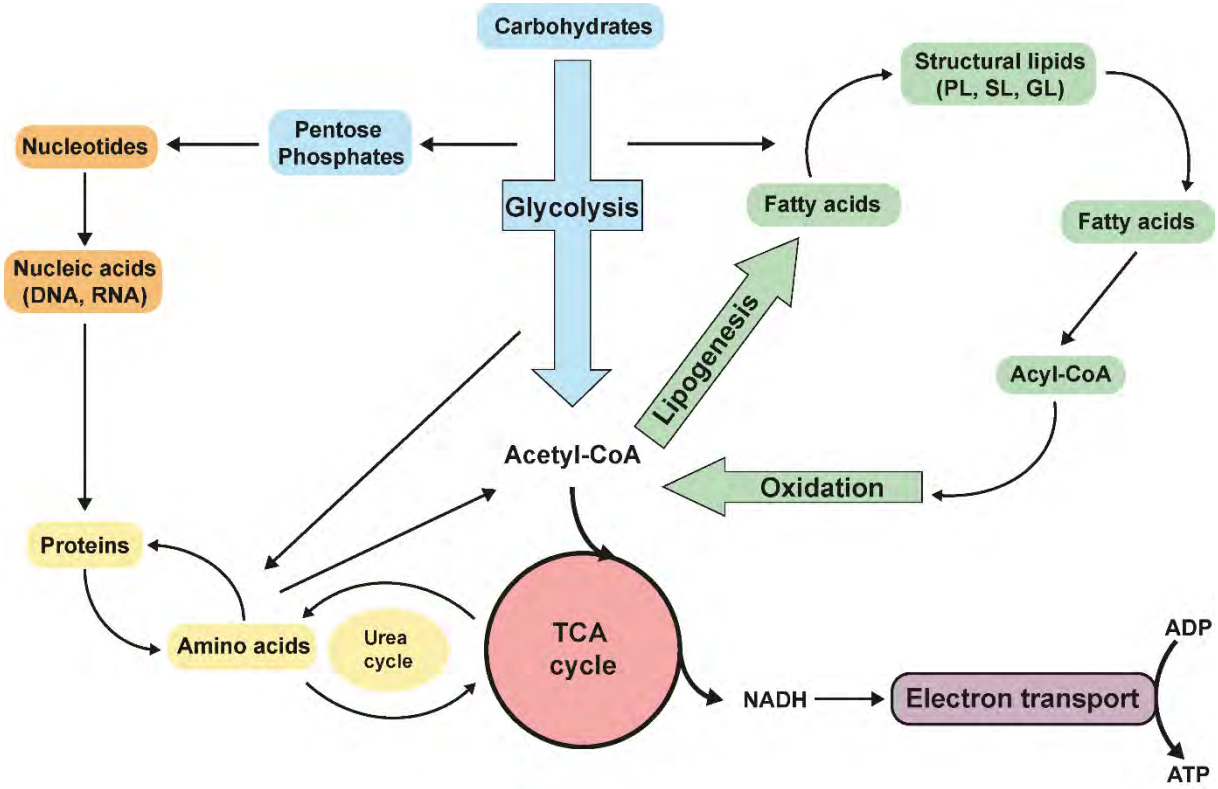

Figure 4. Overview of the metabolism. The general metabolism is composed of metabolic pathways that converge onto the tricarboxylic cycle (TCA) via acetyl-CoA intermediate production. Breakdown of carbohydrates by the glycolysis, oxidation of fatty acids and amino acids pathways lead to acetyl-CoA production. Acetyl-CoA is used as precursor for fatty acids generation and structural lipid pathways. Glycolysis results in the production of pentose phosphates involved in nucleotide production. The TCA cycle produces precursors of amino acids and the reducing agent NADH, which feeds into the electron transport chain to produce chemical energy in the form of ATP. TCA, tricarboxylic cycle; PL, phospholipid; SL, sphingolipid; GL, glycerolipid; NADH, nicotinamide adenine dinucleotide; ADP, adenosine diphosphate: ATP, adenosine triphosphate.

2.2. Energy pathways

The central energy pathways are the glycolysis, beta-oxidation and citric acid cycle [123]. The first two aim to break down glucose and lipids to provide acetyl-CoA, a 2-carbon molecule donor, which drives electron donor production and generates energy in the form of ATP.

The TCA pathway is central for many metabolite turnovers [124]. The reactions occur in the matrix of the mitochondria over eight different steps. The first step is the fusion of acetyl-CoA with oxaloacetate by a citrate synthase to form citrate. Citrate is converted in 2 steps in isocitrate by an aconitase enzyme. Isocitrate dehydrogenase next catalyzes dehydrogenation and decarboxylation of isocitrate into alpha-ketoglutarate. This reaction generates NADH, the electron donor used for oxidative phosphorylation. Alpha-ketoglutarate is converted into succinyl-CoA by an alpha-ketoglutarate dehydrogenase, producing an another NADH molecule. Succinyl-CoA produces succinate via a succinate thiokinase, which generates one GTP molecule used for ATP production. Succinate is transformed into fumarate by a succinate dehydrogenase, generating one FADH2 molecule, another electron donor. A fumarase converts fumarate into malate, which is finally transformed in oxaloacetate by malate dehydrogenase, producing a third NADH molecule. TCA cycle intermediates are used by other pathways such as gluconeogenesis, lipid and amino acid pathways. Electron donors, NADH and FADH2 produced in the TCA cycle then feeds into the electron transport chain, also called oxidative phosphorylation, to produce ATP by ATP synthase.

2.3. Lipid metabolism

2.3.1. Overview

The lipidome is the set of all lipids in an organism. In eukaryotic cells, thousands of different lipids are produced and 5% of the genes are involved in their synthesis [125]. Lipid metabolism fulfills different important functions for cell homeostasis. Lipids play roles in energy storage, essentially via triacylglycerol stored in lipid droplets, and energy conversion pathway. Membrane biogenesis is another important process, involving sterols and fatty acids. It allows intracellular elements to be compartmentalized by boundaries. Membrane lipids are associated with critical cellular events such as cell division, fusion, membrane trafficking, endocytosis and exocytosis. Various chemical properties of lipids enable protein anchorage, dispersion, aggregation and multiple enzymatic reactions. Lipids can also act as secondary messengers when degraded, in cellular recognition processes and signal transduction. Furthermore, lipidic membranes are closely associated with virus life cellular cycle, especially for enveloped virus.

Lipid classification is dictated by hydrophobic and hydrophilic characteristics [126]. Their chemical structure is divided in eight large categories: fatty acyls, glycerolipids, glycerophospholipids, sphingolipids, sterol lipids, prenol lipids, saccharolipids and polyketides.

2.3.2. Lipid biogenesis

Lipid biogenesis or lipogenesis is the process by which acetyl-CoA is synthesized into fatty acids. The synthesis starts with the formation of malonyl-CoA from acetyl-CoA, via two acetyl-CoA carboxylases (ACC) [127]. In the cytoplasm, fatty acid synthase (FAS) then catalyzes repeated additions of acetyl-CoA to produce

mainly palmitic acid (palmitate), a 16-carbon saturated fatty acid (C16:0), and in minor amount a 18-carbon stearic acid (C18:0). Palmitic or stearic acids undergo elongation or unsaturation to generate other types of fatty acids [128]. Chain elongation is happening mainly in the endoplasmic reticulum (ER) and produces acyl chains greater than 16 carbons for membrane lipids, by successive 2-carbon condensation. Mitochondrial elongation is less important and is required for mitochondrial membrane biogenesis. These fatty acids are used as components of membrane lipids or can be esterified in triacylglycerol for energy storage.

Mono-unsaturated fatty acids (MUFA) are produced through oxidative desaturation by desaturase; hydrogen removal results in double bond formation. The first double bond introduced is in carbon position 9 (Δ9). In animals, poly-unsaturated fatty acids (PUFA) result from the insertion of other double bonds between the existing bond and the end carbon. Insects, however, can desaturate on either side of the existing bond. Consequently, different PUFA species are found in insect and mammals. Unsaturated fatty acids have naturally cis double bonds.

Oxidation of fatty acids occurs in mitochondria and peroxisomes via the mechanism of β-oxidation [129]. Fatty acids need first to be activated by conversion into fatty acyl-CoA thioesters via an acyl-CoA synthetase. In mitochondria, this reaction occurs at the outer membrane. The inner mitochondrial membrane is impermeable to CoA, so the acyl residues have to be carried by carnitine via carnitine palmitoyltransferase I to cross this barrier and reach the mitochondrial matrix where β-oxidation is located. At this place, acylcarnitine are transformed in acyl-CoA thioesters by carnitine palmitoyltransferase II to enter the β-oxidation spiral. Oxidative degradation is composed of four steps: dehydrogenation, hydration, second dehydrogenation and a final thiolytic cleavage. The final product of one cycle of β-

oxidation are 2 carbon shortened acyl-CoA. Complete degradation continues until the carbon chain is completely cut into acetyl-CoA. Mitochondrial oxidation generates acetyl-CoA for energy metabolism and ketogenesis, and provides energy for oxidative phosphorylation. The peroxisome is specialized in oxidation of long and very long fatty acid.

2.3.3. Phospholipid metabolism

Phospholipids are major constituent of cellular membranes [130]. They are composed of one hydrophilic head group, a glycerol backbone and two hydrophobic fatty acyl chains, which combine through the hydrophobic parts in a bilayer. Phospholipids provide a barrier between cellular content and external environment, enabling intracellular organelle formation and compartmentalization of different cellular activities. Phospholipids are mainly produced in the endoplasmic reticulum. The most abundant phospholipids in eukaryotic membranes are phosphatidylcholine (PC), representing up to 50% of phospholipid content, phosphatidylethanolamine (PE), phosphatidylserine (PS), phosphatidylinositol (PI), phosphatidylglycerol (PG), cardiolipin (CL) and phosphatidic acid (PA). Each categories are distinguished by their different head group [131] (**Fig 5)**. While PCs are the main phospholipids in mammalian, PEs are the preponderant ones in mosquito cells PE [132–134].

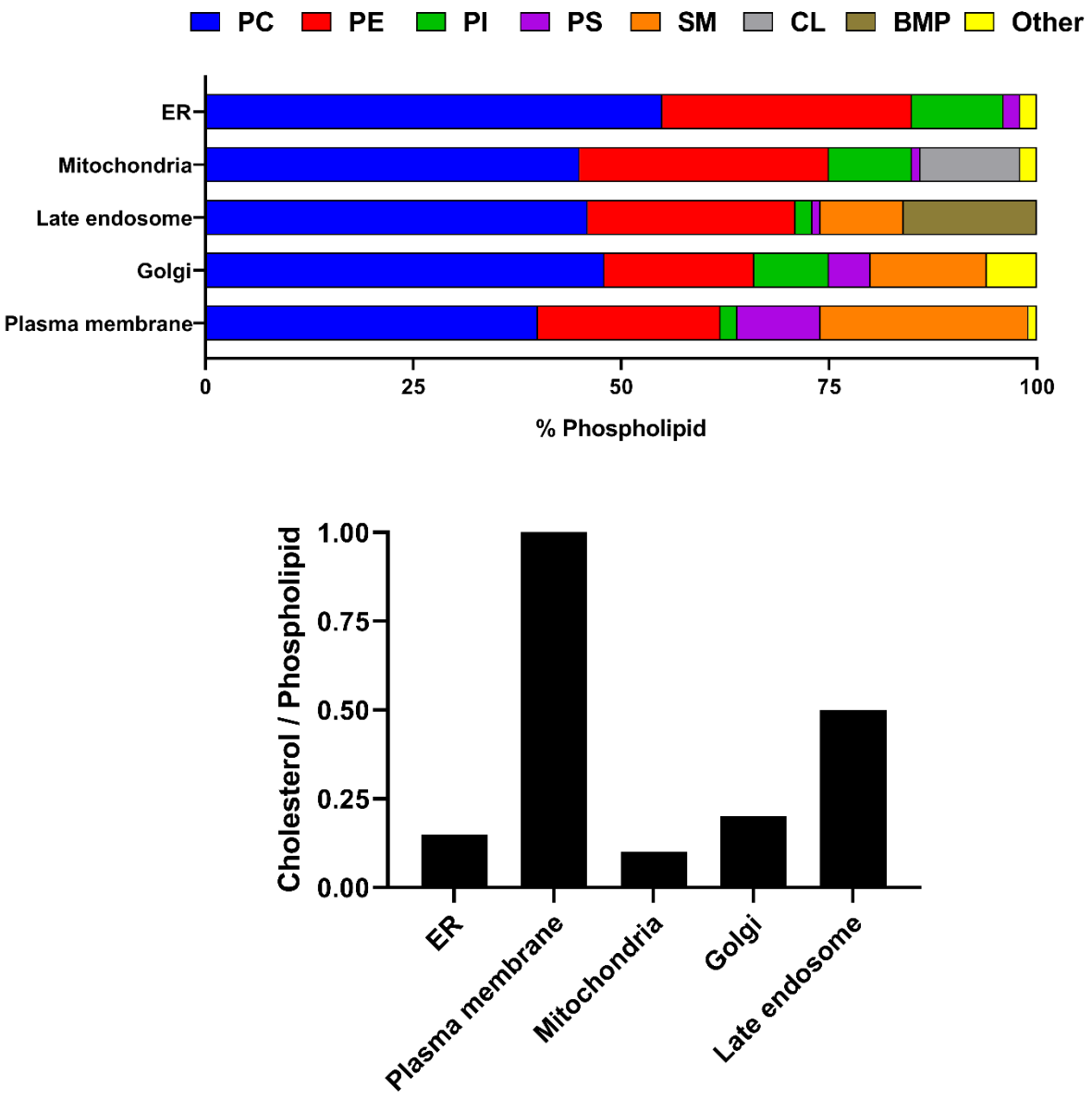

Figure 5. Phospholipid composition of cell membranes. Composition of phospholipid species expressed as percentage of the total phospholipids in mammals. The distributions in plasma membrane, endoplasmic reticulum, mitochondria, Golgi and late endosome are shown. Molar ratio of cholesterol to phospholipid is presented in the same membranes.

The fatty acyl chains of phospholipids can have different carbon number and degree of saturation. Those variable structures give them different biochemical proprieties. Sphingolipid (SL) belong to a different lipid membrane species, although their structure function in cell membranes are similar to PC [135]. Most abundant SL are ceramides and sphingomyelins (SM).

Endoplasmic reticulum is where the bulk of structural lipids (i.e., phospholipids, ceramides and cholesterols) are produced [136]. A subfraction of the ER attached to the mitochondria, the mitochondria-associated membranes (MAM), contains also specific enzyme for lipid biosynthesis [137]. The ER, as the first secretory organelle, contains all intermediates and endproducts of complex lipid pathways, except for sterol and sphingolipids which are rapidly transported into other membranes. Mitochondria is also a major site of lipid biosynthesis, especially for LysoPA, PA and PG used for CL synthesis, a product that is unique to this organelle. Mitochondrial PEs are produced by PS decarboxylation. Mitochondrial inner membrane is composed of high density PG and CL and a high PE/PC ratio [138]. The golgi is more specialized in sphingolipid production and the final steps of PC synthesis [139]. Plasma membranes and early endosome contain more sterol and sphingolipid than PL, due to the required property of resistance to mechanical stress. Plasma membrane is not a major place for structural lipids synthesis, even if lipid regulation can occur by sphingolipid turnover, lipid degradation and signaling [140]. Plasma membrane contain PS on the inner side. Flipping of PS and their exposure on the cell surface is a marker for apoptosis that leads to recognition and uptake by macrophages [141]. Late endosome contains less PS and sterol but a high concentration of bis(monoacylglycerol)phosphate (BMP), a lipid associated with fusion and sphingolipid degradation [142,143].

2.3.3.1. Phospholipid (PL) biogenesis

PL biogenesis is a highly conserved pathway. It involves multiple enzymes in different organelles and results in the production of hundreds of different PL species. PL *de novo* biogenesis is initiated by two types of acyl-transferases that sequentially add two acyls to one glycerol-3-phosphate (G3P) (**Fig. 6**) [130,144,145]. The first addition is realized in the ER or mitochondria membrane by glycerol-3-phosphate acyltransferase (GPAT) to produce lysophosphatidic acid (LysoPA). LysoPAs formed in mitochondria are transferred to the ER prior to the second acylation [149]. The second addition is catalyzed by 1-acyl-sn-glycerol-3-phosphate O-acyltransferases (AGPAT) that transform LysoPA in phosphatidic acid (PA), in the ER principally [146].

The PA produced is composed of fatty acid (FA) at first and the second carbons of the glycerol molecule, called sn1 and sn2 positions respectively . FA in sn1 is generally saturated or monounsaturated, while FA in sn2 is polyunsaturated (PUFA) with long chains. The most abundant FAs in PA are palmitic acid (16:0), stearic acid (18:0), and oleic acid (18:1) at sn1; and linoleic acid (LA; 18:2), arachidonic acid (ARA; 20:4), eicosapentaenoic acid (EPA; 20:5), or docosahexaenoic acid (DHA; 22:6) at sn2 (**Fig 7)**. The diversity of FA in PA produces a multiplicity of unique PL species. PAs are then used to produce all PLs, positioning AGPATs as rate-limiting enzymes of PL biogenesis. PA forms either DAG or CDP-DAG, each generating a different set of PL.

Synthesis of CDP-DAG involves condensation of cytidine triphosphate (CTP) with PA, via CDP-diacylglycerol synthase. This reaction occurs in ER and mitochondria membrane. CDP-DAG produces PI and PG, the latter being transformed in CL by combination with a second PG. Inositol and CDP-DAG are condensed in PI by PI synthase. Inositol is originated from diet, recycling or biosynthesis from glucose. PI is the precursor of several phosphorylated derivates (PIPs) called also phosphoinositides

that are involved in cell signaling. PG is synthesized from a phosphatidylglycerol phosphate intermediate (PGP) by PGP synthase and PGP phosphatase in both ER and mitochondria. CL or diphosphatiylglycerol is produced by combination of PG and CDP-DG via cardiolipin synthase. PG induces another PL synthesis called bis(monoacylglycerol)phosphate (BMP), via a complex biosynthetic pathway of acylations.

DAG is synthesized by phosphatidic acid phosphatase (PAP) from PA. DAG is required for triacylglycerol (TAG) and biosynthesis of the aminophospholipids (AminoPL), namely PC, PE and PS [130]. *De novo* PC and PE synthesis is conducted mainly through the Kennedy pathway [147] within the ER, using the CDP-choline and CDP-ethanolamine intermediates. Choline and ethanolamine are first rapidly phosphorylated by choline/ethanolamine kinases (CK/EK). Phosphocholine and Phosphoethanolamine then form CDP-choline and CDP-ethanolamine with CTP by the rate-limiting enzyme CTP:phosphocholine/ethanolamine cytidyltransferase (CT/ET). Diacylglycerol (DAG) incorporates the phosphocholine/ethanolamine group from cytidine-diphosphocholine/ethanolamine by DAG:CDP-choline cholinephosphotranferase (CPT) or DAG:CDP-ethanolamine ethanolaminephosphotranferase (EPT) to produce PC and PE. PS is produced by head exchange reaction from PC or PE and is catalyzed by PS synthase (PSS1 or PSS2). PS biosynthesis directly via CDP-DAG pathway was found only in plants and yeast [148]. PCs are also involved in SM synthesis with ceramide by sphingomyelin synthase (SMS).

Alternative pathways exist for PC and PE syntheses. The alternative pathway for PE biosynthesis is the Psd pathway in mitochondria inner membrane. It involves PS decarboxylation to PE by a PS decarboxylase (PSD) [149,150]. PC can also be

synthetized in a minor pathway via ethanolamine methylation of PE by PE methyltransferase (PEMT), principally in hepatocytes. AminoPLs such as PC and PE are also produced by reacylation of LysoPLs [151].

Choline is an essential nutrient and must be imported from the diet to meet metabolic needs. Methylation of PE into PC and hydrolysis of the choline part is a minor mechanism for choline recycling . Inside cells, choline is rapidly phosphorylated by CK. Choline can also be converted in acetylcholine in neurons or in betaine in the liver and kidney for methionine biosynthesis [151]. The CT reaction limits the rate of PC biosynthesis, making phosphocholine present in higher concentration than CDP-Choline. CT enzyme, and DAG and PC components modulate PC biosynthesis by feed-back and feed-forward mechanism.

Ethanolamine used for PE biosynthesis derives from the diet in the form of lipids [152]. Smaller amount of ethanolamine is produced by PE degradation. Gut-associated bacteria can convert ethanolamine in acetaldehyde, a precursor for acetyl-CoA generation [153].

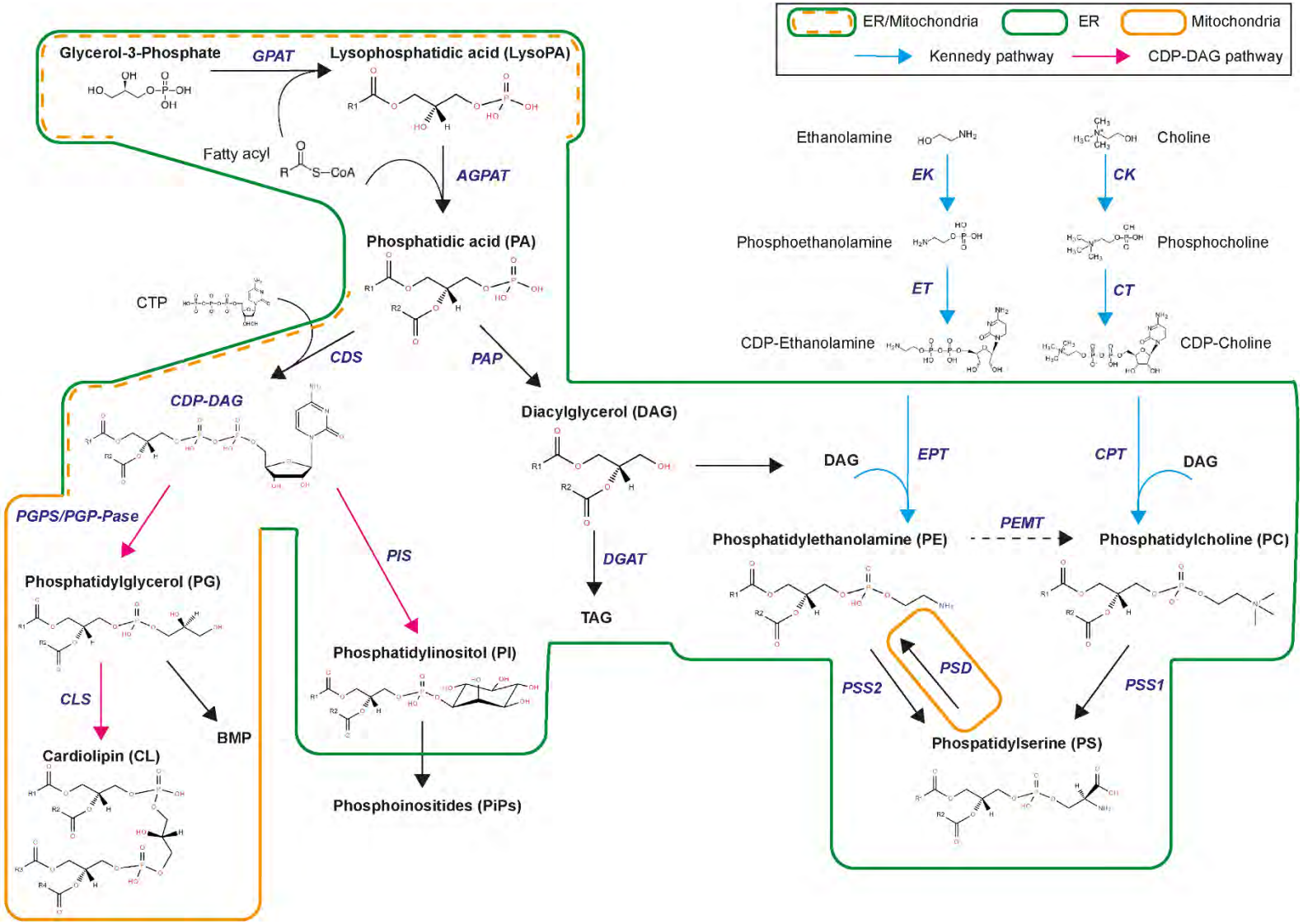

Figure 6: Biosynthetic pathway of phospholipids

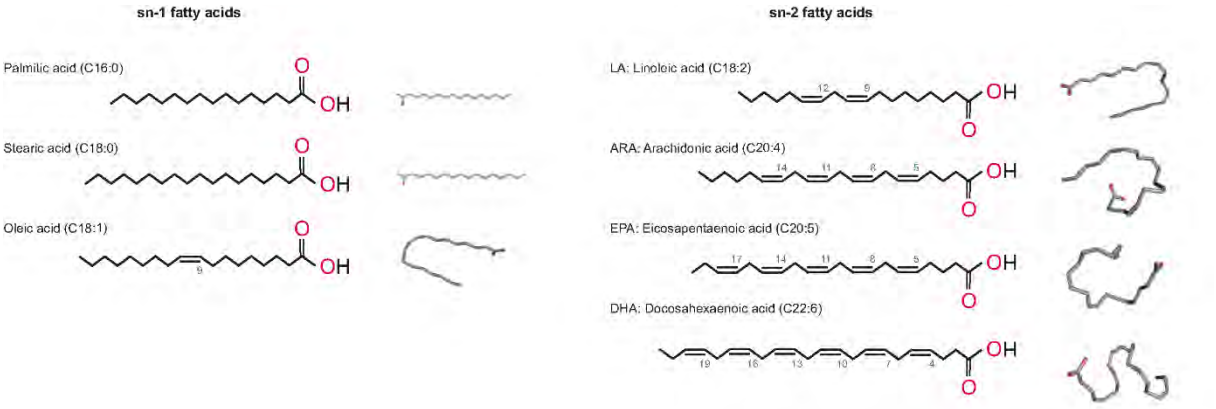

Figure 7. Structures of common fatty acids in phospholipids. The commonly FA present in sn-1 and sn-2 acyl chain of PL are represented in linear form and 2D conformation structure.

2.3.3.2. Phospholipid remodeling

Diversity of fatty acyls in PL does not only result from *de novo* synthesis pathway, but also from remodeling through the Land's cycle [154]. Newly synthetized PL can be hydrolyzed at the sn-2 position by phospholipase A2 (PLA2) to produce 1-acyl lysophospholipid (**Fig 8)**. This LysoPL is reacylated by lysophospholipid acyltransferase (LPLAT) via incorporation of another fatty acid in sn-2 position and form a new PL species [154]. Remodeling ensures maintenance of PL membrane composition and cell signaling. LysoPL and FA released by PLA2 activity can serve as intermediates for lipid signaling synthesis, such as platelet-activating factor (PAF), eicosanoids and prostaglandins [155].

Among LPLAT, lysophosphatidylcholine acyltransferases (LPCATs) were discovered for their PC remodeling activity. LPCATs actually have also LysoPE, LysoPS and LysoPG acyltransferase activities used in PL remodeling. Four members of LPCAT were identified. LPCAT1 and LPCAT2 are member of the AGPAT family and are found in ER membrane and lipid droplets. Remodeling by LPCAT1-2 are important in lipid droplet size regulation and their lipid surface organization [156]. LPCAT3 and

LPCAT4 membrane-bound O-acyltransferase (MBOAT) family, are also in ER membrane. Each LPCAT have specific acyl substrate preference, enzymatic activity and tissue localization in mammals. LPCAT3 is the most expressed LPCAT in different cell types and is responsible for the majority of LysoPC acyltransferase activity.

PLA2 enzymes have a multitude of isoforms and functions, other than in the Land's cycle [157]. Four main categories of PLA2 exist: secreted PLA2 is most studied in bees and snake venoms and in pancreatic juices in mammals; cytosolic PLA2 is recruited in membrane by Ca^{2+}-dependent translocation; calcium-independent PLA2 [158,159]; and platelet activating factor (PAF) lipoprotein associated PLA2. Another impact of PLA2 during PL hydrolysis is the release of PUFA for eicosanoids biosynthesis such as prostaglandin, thromboxane and prostacyclin, all active lipid mediators.

Others phospholipase enzymes can hydrolyze PL (**Fig 8A)**, [160]. Phospholipase A1 (PLA1) hydrolyze the sn-1 to produce 2-acyl lysophospholipid. PLA1 function is largely unknow but they likely have role in production of LysoPS, LysoPI and LysoPA. Phospholipase B (PLB) is able to hydrolyze both the sn-1 and sn-2 fatty acids of PC, PE and PI [161]. Phospholipase C (PLC) and Phospholipase D (PLD) are phosphodiesterase. PLC cleaves the glycerophosphate bond, while PLD removes the headgroup. PLC produce DAG and phosphorylated headgroup, in a specific way on PC or PI depending of the enzyme. PLD releases headgroup and produces PA, but can also catalyze exchange of the headgroup by transphophatidylation to produce a new PL. In mammals, PLD is important for cell signaling due to PA remodeling, the central lipid of PL biosynthesis and a lipid mediator

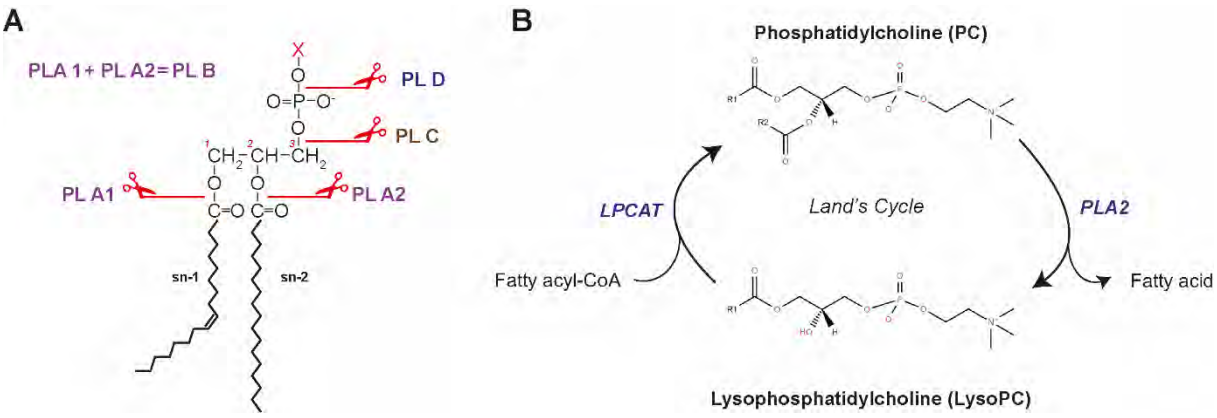

Figure 8. Phospholipid remodeling. A. sites of cleavage by the different phospholipases, B. Land's cycle showing remodeling of PC and LysoPC.

2.3.3.3. Phospholipid structure and biochemical property

Structure and membrane curvature

Nature of PL molecular composition confers specific structural proprieties, impacting membrane comportment and organization inside the cell (**Fig. 9**). Structure of PL depends on the headgroup size and acyl chain composition [162].

PC and PS have a polar headgroup and parallel fatty acyl chains that confer a cylindrical geometry and enable linear bilayer formation. Usually, they have one cis unsaturated acyl chain, making the membrane fluidic at room temperature. Sphingolipids are composed of only one acyl chain, resulting in a cylindrical geometry as well. When inserted in lipid bilayers however, sphingolipids produce a tighter membrane because of their smaller steric hinderance than PC and PS.

PE, PA, DAG and CL have a small headgroup and two fatty acyls that result in inverted conical geometry. When inserted in the inner layer of a lipid bilayer, those lipid species impose a negative curvature. Conversely, LysoPC, LysoPE and PI confers positive curvature in the same condition due to large headgroups and small acyl chains.

Sterols and non-polar lipids are highly abundant in cell membranes. Cholesterol, the main sterol species in mammals and insects, consists of a small polar headgroup and a large apolar body, enables to integrate among the non-polar fatty acid chains of PL in membrane. Cholesterols are preferentially associated with SM and PC in membranes and increase fluidity [163,164]. Lipid rafts are enriched in SM and cholesterol, and are involved in the assembly of signaling proteins.

Insertion of PE in mostly PC bilayers induces membrane curvature, allowing phenomena of fusion, fission and budding [165]. The curvature is also induced by lipid asymmetric distribution among both lipid leaflets. Abundance of PE and PS on the inner monolayer of plasma membrane induces neutral to negative curvature [166].

Membrane asymmetry

Lipid asymmetry refers to a non-random distribution of lipid species in lipid bilayers. It induces biophysical properties that promotes certain cellular functions [166,167]. A well-known example is the organization of negative PS in plasma membrane. In normal cells, PS are found in the cytoplasmic side where they associate with numerous enzymes such as kinase proteins. During specific event, PS move to the outer leaflet, exposing their negative polar head to the extracellular side and inducing signaling such as apoptosis.

In plasma membrane, PC and SM are generally found in the outer leaflet, while PE, PS and PI are found in the inner leaflet [131]. Lipids in the ER are symmetrically distributed between the two leaflets, while Golgi, endosome and plasma membranes have asymmetric distribution.

Phospholipid asymmetry is maintained by lipid transporters [168]. Flippases are ATP-dependent aminoPL translocases that transport lipids inward. Floppases are

ATP-binding cassette (ABC) transporters that transport lipids outward. PL scramblases induce lipid asymmetry by migrating lipids between the two-membrane layers. PL scramblases induce PS externalization in apoptotic cells or to start coagulation process [167].

Electrostatics

Electrostatic charges depend on negatively charged lipids, i.e. PS and phosphoinositides PIPs. They are highly present in plasma membrane, especially on the cytosol side, and are low abundance in ER membranes [168,169]. Distribution of the membrane electric changes is associated with lipid asymmetry. Furthermore, the charge of different PL is pH-dependent. PC and PE are zwitterionic, while PS, PA, PG, CL an PI are anionic at pH 7 [170]. Consequently, pH gradient modifies electric charges and consequently lipid distribution on inner and outer leaflet [171]. Electric charges are critical to orientate transmembrane proteins. Positively-charged peptides will interact with negatively-charged lipids in the inner leaflet to integrate the protein in the lipid bilayer and position it adequately [166].

Packing defects

Lipid packing defects refer to heterogenous lipid arrangements that loosen lipid bilayer and increase fluidity, facilitating protein insertion [172] (**Fig 8)**. Ratio between small and large headgroups and ratio between saturated and unsaturated acyl chains influence lipid packing. Low packing in the ER is induced by high concentration of unsaturated PL and lack of cholesterol [173], while plasma membrane has high packing due to saturated structural lipids and sterols. Packing defects also influence fluidity [132].

Lipid phase

Membrane lipid organization is induced by the different characteristic described previously, provoke different membrane phase behavior [131]. External factors such as temperature, pressure, composition of the aqueous phase influence the assembly of the different lipid phases.

The lamellar phase, known as the lipid bilayer, is found in biological membranes with polar headgroups of lipids face the aqueous environment on both sides and acyl chains associated inside [174]. Most biomembranes are organized in lamellar liquid phase with a liquid disordered (Ld) phase which contains floating “rafts” of liquid ordered (Lo) phase. Liquid phases are characterized by the lateral mobility of lipids within the bilayer. Gel phase, also called solid phase, can exist in *in vitro* system, where lipid lose lateral mobility and become more packed.

Membrane lipids are also able to form non-lamellar transitory phase, like hexagonal or cubic phases, making specific local structures within membranes [175]. Hexagonal phase can be type I (HI) consisting of cylinder or spheric micelles with the polar head outside of the tubules, and type II (HII) with inverted micelles where the fatty acyl chains are directed outward from the tubules. Combination of HII phase and lamellar phase can form cubic phase. HII and cubic phase establish aqueous channel.

Lamellar phase is formed by non-curvature lipids PC, PG, PI. The Ld phase is enriched in saturated lipids, especially SM, and cholesterol, while the Lo phase in enriched in unsaturated PL. Gel or solid-like phase is induced by lipids with long and saturated chains, high amount of cholesterol and low temperature. Non-lamellar phase, hexagonal and cubic phases exist temporarily during fusion, fission and pore formation and may be important for enzymatic activity [175]. Negative curvature lipids, PE, PS,

PA form hexagonal II and cubic phase, while positive curvature lipids LysoPL form hexagonal I phase.

Protein insertion

Membrane proteins modify the behavior of lipid membranes and should not be overlooked when discussing lipid properties. Insertion of these proteins is influenced by the physicochemical parameters of membrane, such as curvature, electrostatics and lipid packing [176]. Once inserted, the proteins perturb the hydrophobicity and provoke a mismatch between protein and lipid, then affecting the thickness and membrane organization [172]. Consequently, protein function is tightly regulated by lipid interactions.

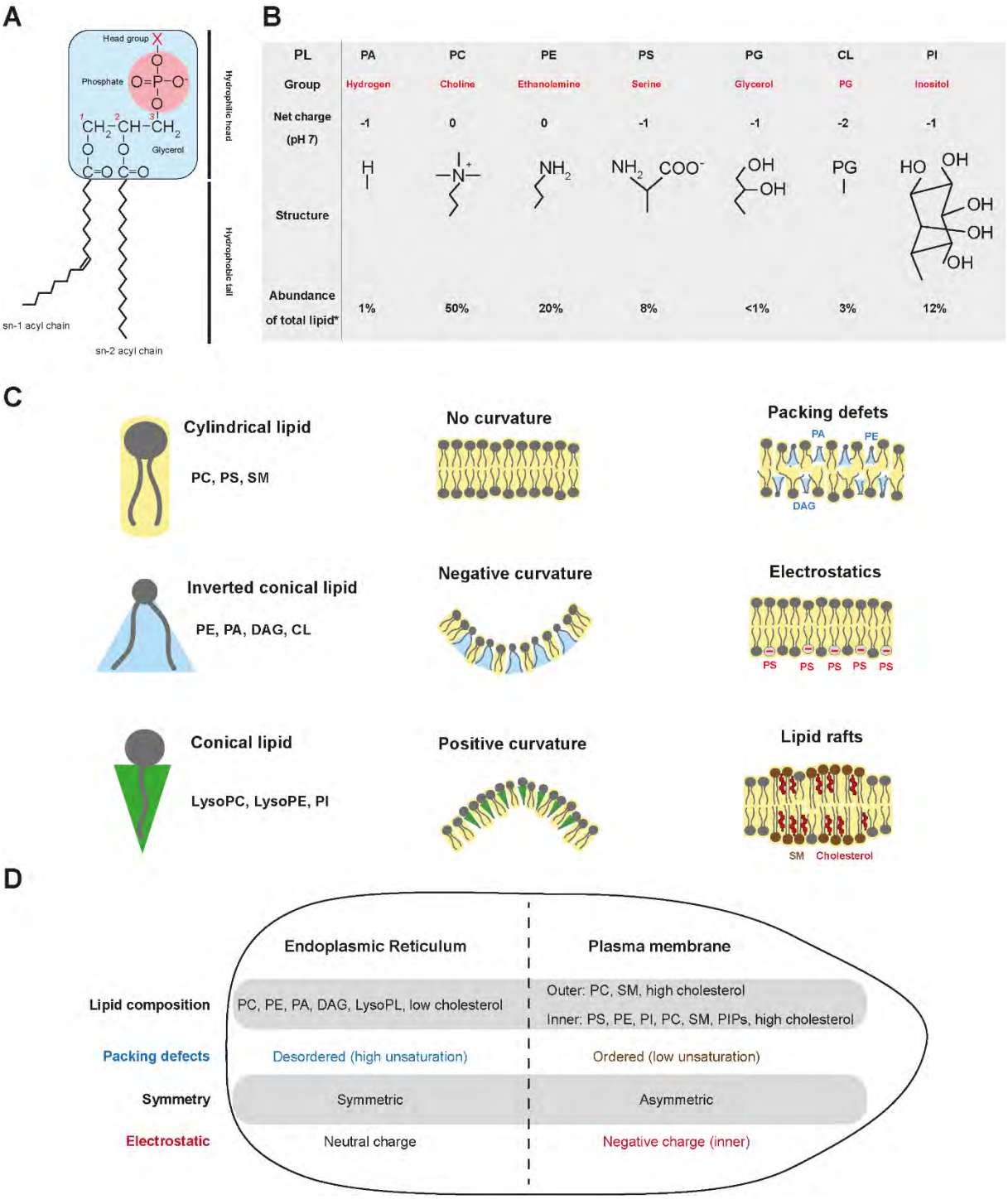

Figure 9. Phospholipid structure and biochemical properties.

2.3.4. Lipid droplet: a lipid storage constrained by phospholipids

Lipid droplets (LD) are essential for the cell storage of carbons via neutral lipids, TAG and sterol esters. These storage bodies are constrained by a layer of PL (mainly PC an PE) and proteins [177]. The LD monolayer composition is closed to the one in ER, showing a common origin [178]. LD are mobilized by lipases, perilipin, to provide lipid substrate for PL synthesis, fatty acid pathway and lipid mediator production [179]. LD also contain enzymes of the PC biosynthesis pathway that allows the production of CDP-Choline [180]. However, LD lack of CPT to finalize PC production, suggesting a role as an intermediary donor to the ER where PC biosynthesis is completed. LD can also perform PL remodeling through phospholipase PLA2 and LPCAT.

2.3.5. Specificity of mosquito lipid metabolism

There exist important differences in the way insects metabolize lipids [181]. Insects obtain cholesterol and essential fatty acids from their diet. For blood feeders, ingested blood provides numerous lipid species, mainly TAG, PL, cholesterylesters and FA. In the midgut, lipolysis takes place with lipases that hydrolyze TAG and several phospholipases. Fatty acids are absorbed in midgut cells and used to produce phospholipids, TAG and DAG via the PA pathway. DAG is transported through hemolymph in association with a lipophorin carrier to reach the fat body for conversion in TAG and lipid storage. Lipids stored in the fat body are then mobilized and delivered to targeted tissues that require energy or FA metabolic process, such as oocyte development and flight muscle [182]. Lipophorin is also involved in *A. aegypti* mosquito immune response and is regulated by parasite infection [183].

Fatty acids are also synthesized from glucose and amino acids, which is important given the mosquito's diet that feeds on sugar and high-protein blood. FA,

phospholipid and Glycerolipid synthesis have the same pattern as in mammals, with difference on the number of enzyme isoforms [182]. One particularity of insect is the capacity to produce Poly-unsaturated fatty acids (PUFA) with specific desaturase, contrary to mammals, given a wide range of PL species insect-specific [184]. The phospholipids composition of A.aegypti cells have confirmed a major abundance of PC and PE, and detection of all other PL species [134,185]. Subcellular fractions isolated from mosquito cells show a common system to the mammalian phospholipid pathway. Furthermore, membrane composition is analogous to mammals [186], suggesting an highly conserved metabolism.

2.3.6. PL mediated signaling and innate immunity

Insect and mosquito developed several immune systems in antiviral defense [187–189]. Several major immune signaling pathways are involved in antiviral protection, including the Janus kinase/signal transducers and transcription activator pathway (JAK-STAT), immune deficiency pathway (IMD), the Toll pathway, the Jun-N-terminal Kinase (JNK) pathway and the RNA interference pathway (RNAi).

The JAK-STAT pathway is triggered by Dome transmembrane receptor via Upd or Vago binding and induces phosphorylation of STAT transcription factor by Janus kinases (JAKs) and activates JAK-STAT-regulated genes [187]. IMD pathway is activated by PGRP membrane receptor through binding with ligand and trigger signaling via IMD and several kinases and caspases which induce phosphorylation of Rel2 transcription factor and activate transcription of anti-microbial effectors. Toll pathway signal transduction is triggered by the recognition of pathogen derived ligands by pattern recognition receptors (PRR) and leads to the cleavage of the cytokine

Spaetzle which binds the Toll membrane receptor and induces association with MyD88, Tube and Pelle adaptors proteins. This leads to activation of Rel1 transcription factor and activates subsequent transcription of antimicrobial peptides genes (AMPs). The RNAi pathway is stimulated by dsRNA inside infected cells and uses enzymes expressed in the cytoplasm. Dicer-2 recognized dsRNA and associates with RISC complex in order to degrade RNA [190].

RNAi is continually activated and modulates DENV infection in Ae. aegypti and is an important factor of vector transmission [191]. Those pathways are part of the mosquito anti-DENV defense and restricts DENV replication in mosquito midgut tissues, where effectors are up-regulated by infection [189,192–196]. However, DENV also induces suppression of mosquito immune responses such as down-regulation of AMPs in early infection in mosquito [195]. For instance, DENV NS proteins can suppress RNAi and STAT signaling in mammalian and insect cells [197,198].

Interactions have been described between Ae. aegypti immune responses to pathogens and lipid metabolism. Bacterial Gram +, fungi and parasite infection induce fat body genes expression related to lipid metabolism through regulation by the Toll signaling pathway [183]. In DENV-infected *A. aegypti* mosquitoes [199], gene associated with LD biosynthesis are regulated. Furthermore, activation of both the Toll and IMD pathways increase LD number in mosquito cells.

The increase of lipid species during DENV infection in mosquito [200], especially fatty acids related to lipid mediators, such as prostaglandin, can be involved in the mosquito immune defense against viral infection. Prostaglandin (PG) are produced by phospholipid hydrolysis containing C20 polyunsaturated fatty acids, via phospholipase A2. PG play a role in the regulation of immunity and inflammation [201] and have be found regulated by bacterial and parasites infection

in mosquito [202].

Inflammatory response, autophagy, apoptosis, coagulation and T-cell recognition are all mediated by PLs and their degradation products [155]. Activated immune cells are known to produce several PL-derivated species, such as phosphoinositides (PIPs), oxidized phospholipids or plasmalogen-PC known as the platelet activating factor (PAF). PLA2 hydrolysis activity is involved in platelet activation, inflammation with prostaglandin produced by the release of the ARA fatty acid, and cyclooxygenase-mediated pathways of ARA in immune cells [155,203].

LD accumulation is often reported in response to bacterial or viral infection. In mammalians cells, activation of the Toll-like receptor (TLR) induces the production of LD that participate in the interferon (IFN) response [204,205]. Anionic PLs, such as PG and PI, negatively modulate TLR signaling, likely to prevent inflammatory processes [206]. Stimulation of acyltransferase activity by *AGPAT* overexpression to convert LysoPA to PA induces enhancement of tumor necrosis factor-α (TNF-α) and interleukin-6 (IL-6) cytokines, in mammalian cells [207]. TNF- α and IL-6 are both cell signaling pro-inflammatory cytokines, emphasizing the link between PL and inflammatory response.

2.4. Metabolomics

Metabolomics is an emerging “omics” that identifies and quantifies metabolites from cells, biofluids, tissues and organisms [208]. Metabolomics is a powerful method to detect altered metabolic pathways upon infection [209,210]. Metabolomics can reveal major changes in the four main metabolite groups: nucleotides, carbohydrates, lipids and amino acids [211].

There are two metabolomics strategies: untargeted and targeted metabolomics [208,212]. Untargeted metabolomics is the comprehensive analysis of all known and unknown measurable compounds in a sample. Annotation with *in silico* libraries or experimental database is then primordial. The untargeted approach allows the discovery of new compounds and exploration of non-model organism metabolome. Targeted metabolomics focuses on annotated molecular species. This requires *a priori* knowledge of the targeted metabolites. It is generally associated with internal standards for quantitative or semi-quantitative assay. Sample preparation and metabolite extractions will depend on the metabolites classes targeted and the strategy [212–215].

Different analytical methods are used separately or in combination to qualify changes in metabolite concentrations. The three main methods are nuclear magnetic resonance (NMR) spectroscopy, liquid chromatography-mass spectrometry (LC-MS) and gas chromatography-mass spectrometry (GC-MS). NMR spectroscopy, commonly proton (^{1}H-NMR) or carbon -13 NMR, is based on the spin states of nuclei and their transition upon exposure to a magnetic field [216]. NMR has high reproducibility, does not require complex sample preparation, is nondestructive and noninvasive and high number of metabolites can be detected rapidly in a single measurement [217]. Mass spectrometry (MS) is generally coupled with chromatographic separation method such as liquid chromatography (LC) or gas chromatography (GC) to simplify separation and identification of compounds. MS-based metabolomics provide higher sensitivity (even more so when different ionization techniques are used) and selectivity than NMR. MS analysis required more sample preparation than NMR [218]. GC and LC separates compound based on their specific mass-to-charge ratio (m/z). GC-MS aims to detect volatile metabolites, while LC-MS provide detection of a wide range of compounds

based on ion property and metabolite polarity [219]. Reversed-phase LC-MS (RPLC-MS) is used to separate apolar or semi-polar compounds, while hydrophilic interaction liquid chromatography (HILIC) separates polar metabolites [220]. Tandem MS (MS/MS) is used for optimal metabolite annotation. In MS/MS, the first MS allows the selection of an ion that is then decomposed in the second MS, providing more in-depth ion characteristics of the compound [220,221].

Spectral data acquired are pre-processed and normalized before annotation [222]. Common processing steps include baseline correction, spectral alignment, normalization and scaling. Baseline correction is essential to correct signal intensity deviation. Alignment is performed in order to correct peak shifts between samples. Normalization is used to correct variations between samples to make them more comparable to each other. Normalization in the total ion current (TIC) is commonly applied. Scaling allow to make the features more comparable. Commonly used scaling methods include range scaling, autoscaling, and Pareto scaling [223]. Metabolite differences between sample groups are calculated by statistical analysis. Multivariate methods such as principal component analysis (PCA) and partial least squares discriminant analyses (PLS-DA) are widely used for metabolic fingerprinting [224]. PCA is used to visualize trends and detect outliers, while PLS-DA helps to predict metabolite classification and identify biomarkers [222]. Accurate metabolite annotation is crucial for functional interpretations of perturbed metabolic pathways. The Metabolomics Standards Initiative (MSI) proposes four levels of identification [225]: identified compounds, putatively annotated compounds, putatively characterized compound classes and unknown compounds. Compounds are identified based on similar mass with databases and support from retention time and spectral fragmentation [226]. Comparison with databases from Human Metabolome Database

HMDB [227], METLIN [228], ChEBI [229], PubChem [230], MassBank [231], LIPID MAPS [232] and LipidBlast [233] are used. However, there is a lack of non-model organism metabolite database (i.e., for mosquitoes) that complicates metabolomic studies in *Aedes*. Determination of unknown metabolite classes based on their spectral similarity with annotated metabolites is a useful strategy for non-model organisms, such as mosquitoes. For spectral similarity, MS/MS spectra are aligned to one other in order to construct molecular similarity networks. Metabolites are then connected according to their fragmentation similarity, generating clouds of same-class compounds [234].

3. Metabolic alterations upon DENV infection

Viruses depend on host metabolism to provide energy and molecules for their multiplication. Infection may dramatically disrupt host metabolic pathways through virus metabolic diversion for its own benefits or through host response against the pathogen. The use of metabolomics to study DENV interaction with the metabolome is relatively recent. Identification and quantification of modulated metabolites will shed light on DENV-host interactions and reveal potential targets to block mosquito transmission.

3.1. Alteration of energy pathways

Energy conversion pathways are highly perturbed during DENV infection in human hepatic cell line [235]. Specifically, DENV down regulates TCA-associated proteins such as aconitase, ATP citrate synthase, pyruvate dehydrogenase, and upregulates citrate synthase. The mitochondrial energy function is also altered through

downregulation of important proteins (such as dihydrolipoamide dehydrogenase) [235], resulting in structural alteration and decrease of ATP content and energy charge [236].

DENV induces and requires carbon metabolism, particularly glycolysis, for efficient replication [237]. The glycolytic pathway is altered at the beginning of DENV infection in human fibroblasts, while its inhibition decreased DENV replication and virion production. Mechanistically, DENV NS1 enhances the activity of the glycolytic enzyme glyceraldehyde-3-phosphate dehydrogenase (GAPDH), a major enzyme in glucose catabolism [238]. GAPDH was also up regulated in hepatocellular infected cells, whereas several glycolysis enzyme were down regulated (phosphoglycerate kinase, pyruvate kinase, aldose reductase) [235].

TCA is affected by DENV infection in *Aedes albopictus* mosquitoes [239]. Protein expression of several enzymes associated to TCA cycle (aconitase, isocitrate dehydrogenase and malic enzyme) and oxidative phosphorylation (ATP synthase, ATPase and NADH dehydrogenase) were significantly down or up regulated after DENV infection in C6/36 cells and in salivary glands, midgut and, especially, in the fat body. Other proteins, enolase and α-glucosidase, involved in carbohydrate metabolism, are also up-regulated after DENV infection in *Aedes albopictus* [239] and *Aedes aegypti* [240]. Those studies suggest changes in global metabolism and energy pathways in *Aedes* mosquitoes. DENV1-4 increased secretion of essential amino acids isoleucine, tryptophan, and phenylalanine [241], suggesting interference with the phenylalanine and alanine pathways, which contribute to TCA cycle.

3.2. Lipids as biomarker of dengue infection

Metabolomics is widely used for to profile human sera and to explore disease impact on physiology. Human serum from patients infected by DENV1-3 revealed strong alterations of lipids during early stages and a reversion to normal at the recovery phase [242]. The two main classes of structural membrane lipids, PL and SL, are highly perturbed. The PL phosphatidylcholine (PC), lysophosphatidylcholine (LysoPC) and lysophosphatidylethanolamine (LysoPE) decreased simultaneously with platelet count. Increase of sphingomyelin (SM) correlated with decrease of lymphocytes. PC, lysoPC and SM thus show potential as prognostic markers. LysoPC and LysoPE are usually decreased during severe dengue and DHF [243–245]. Even if other PL classes, such as phosphatidylinositol (PI) and as phosphatidyserine (PS), were also detected and modulated on dengue serum patients, PC species are the most altered in the sera of DENV-infected patients [246].

Phospholipase A2 (PLA2), the enzyme catalyzing the degradation of PL in lysophospholipids (LysoPL), was highly increased in sera of DENV-3 patients [247]. Modulation of PL and LysoPL observed in different studies may be attributed to PLA2 activation by DENV. The other products resulting from PL hydrolysis are free fatty acids, such as arachidonic acid (ARA), and are also elevated in serum of infected patients [242,243].

Triacylglycerol (TAG) is elevated in serum of DENV-infected patients [244,246,248]. TAG are important molecules species for lipid storage and can provide fatty acid for energy metabolism or lipogenesis. Compounds involved in lipid degradation for energy metabolism, such as acylcarnitine, are highly modulated in dengue severe patients [242,249,250]. The levels of such metabolites associated with

severe dengue correlate with liver damage and alteration of liver enzymes transaminases.

Fatty acid (FA) synthesis is perturbed in humans upon DENV infection. NS3 protein interacts with fatty acid synthase (FAS) to relocalize the enzyme to DENV replication complexes and enhances its activity, possibly to increase FA availability for replication [251]. Autophagy in Huh-7 cells is elevated by DENV infection, also contributing to increase fatty acid production [252]. Conversely, fatty acid catabolism is also activated through increase in β-oxidation with DENV-induced autophagy [252] and increase in ω-oxidation [241], the latter being a rescue pathway for fatty acid synthesis [253]. These mechanisms corroborates fatty acid results in serum of dengue patients.

Studies with humanized mice confirmed that DENV decreased PC, PE and LysoPE, while it increased SM and acylcarnitine [254]. These studies established the potential of lipids, particularly PL, as biomarkers to predict dengue clinical outcome [255]. Beyond the use of lipid biomarkers to predict dengue infection, the mechanisms associated to such alteration of membrane lipids remain to be elucidated.

3.3. Lipid regulations in DENV-infected mosquito

Few studies have reported lipid alterations by DENV in mosquitoes. Lipidomics in mosquito cells showed that DENV reconfigures the lipid profile, altering the membrane lipids such as phospholipids (PL) and sphingolipids (SL) [256]. Among PL, PC was the most regulated class, followed by LysoPC, the product of its hydrolysis. A similar alteration is observed in DENV-infected midguts, with a particular alteration in SL [257]. Functional characterization of lipids was obtained by chemical inhibition of lipid synthesis. As observed in human cells, inhibition of FAS by C75 in mosquito cells,

decreased DENV replication at early stage of infection [256]. As observed on human sera and human cell line, membrane lipid remains one of the most altered class upon DENV-infection on *Aedes* mosquito

3.4. DENV cellular cycle is intricately linked to membrane lipids

3.4.1. Lipid virus structure

Composition of f*lavivirus* lipid envelope is only characterized for WNV [258]. The envelope is rich in sphingolipid (SM and ceramide) and PL. Among PL, PC is the most abundant, followed by PS and plasmalogen-PC. PE, plasmalogen-PE, LysoPE and LysoPC are present in lower proportions. Moreover, the charge distribution of C protein suggests its capacity to interact with lipid membranes [259] and LD, the latter plays an important role in virus particle formation [260].

3.4.2. Attachment and entry

Phospholipids mediate DENV attachment to host cells. TIM/TAM phospholipid receptors are entry factors in mammalian cells and bind directly or indirectly to PS on the lipid viral envelope, acting as coreceptors [261]. PE at the surface of the virus bilayer is a ligand for human TIM, and promotes entry of DENV and WNV [262]. Human CD300a is another phospholipid receptor that binds directly DENV particle through viral PE and PS association and mediates virus entry [263].

Cholesterol is highly present in plasma membrane, where it associates with phospholipids and sphingolipids in lipid-ordered raft domains. Cholesterol depletion inhibits *flavivirus* entry and replication, as shown for DENV and JEV [96]. DENV entry is also reduced by cell supplementation with cholesterol or by pretreating the virus with cholesterol [264]. It suggests that cholesterol incorporate into the viral lipid bilayer envelope, subsequently altering entry. Cholesterol inhibition or cell supplementation

suggest that cholesterol homeostasis in cell membrane is a critical factor for DENV entry [265].

Early endosome membranes have a lipid composition close to plasma membrane, containing sphingolipids, PS and sterols [131]. Late endosome contains less sterol and higher abundance of anionic lipid PS and BMP. The DENV fusion process was reported to be PL-dependent, especially for anionic PS and BMP in late endosome [266].

3.4.3. Translation

DENV polyprotein translation takes place in ER lipid membranes. Cholesterol-rich lipid rafts present in ER are important in DENV polyprotein processing [267]. The membrane protein complex (EMC) in the ER in association with transmembrane NS4A and NS4B are required for DENV polyprotein folding and post-translational stability [268,269]. In absence of EMC, viral membrane protein adopts an incorrect topology in the ER membrane that leads to NS4A-B viral protein degradation. However, little is known about the phospholipid alteration of the ER caused by the translation process.

3.4.4. Replication and assembly

The DENV replication complexes (RC) drastically modify the lipid membrane of the ER [60,61]. Membrane lipids and host cellular proteins are essential for formation of the RC. A cellular chaperone protein DNAJC14 acts as a protein scaffold to modulate and maintain the vesicle packet formation [270]. RTN3.1A is also localized in the *flavivirus* RC and is associated directly or indirectly with NS4A protein to promote membrane remodeling [271]. LysoPC species is required for the formation of WNV replication complex and is involved in membrane curvature [272]. In WNV-infected

cells, phospholipase A2 (PLA2) activity is increased to produce LysoPC and contribute to the flaviviral replication complex formation [256].

The virus demand for lipids required for membrane remodeling is mechanistically illustrated by the redistribution of the fatty acid synthase (FAS) at replication site by NS3 interaction [273]. FAS is activated by NS3 and stimulates malonyl-CoA incorporation into fatty acids. This activity should produce palmitate that is then used for complex lipid biogenesis. This redistribution of FAS is mediated by Rab18, a host Rab GTPase located in ER and lipid droplets (LD) [274]. LD, the lipid storage organelle, might act as a source of lipid for energy and membrane reorganization. Autophagy is another process required for efficient DENV replication via viral NS protein induction [275], which generates free fatty acids, likely for energy supply or to provide structural lipids [276]. LD lipophagy is activated by NS4A interaction with AUP1, a LD-associated acyltransferase [277]. AUP1 acyltransferase activity is enhanced by NSA4 and may provide PL for DENV infectious process.

Lipid droplets originating from ER are modified and involved in DENV assembly via C protein [260]. The number of LD increases during DENV infection, requiring production of lipids constituent such as DAG and PL.

In summary, we have seen that all stages of the DENV cellular cycle require the host membrane environment (**Fig 10**). From attachment to the release of new virions, the virus is constantly interacting with multiple species of structural lipids. Mature viral particles attach to the targeted cells through multiple host receptors that involve PL as co-factors. Viral entry is achieved mainly by endocytosis in a fine-balanced cholesterol membrane context. In late endosome, the viral E protein undergoes pH-dependent

rearrangement and promotes viral and endosomal membranes fusion to release the nucleocapsid, which is uncoated and release the positive strand-RNA ((+)ssRNA). The genomic RNA is translated in a single polyprotein by the host machinery in the bilayer ER membrane at cholesterol-enriched lipid rafts. Post-translational process stabilizes and ensures proper folding of new viral proteins by interacting with the host membrane protein complex (EMC). Individuals transmembrane NS proteins provoke formation of Vesicle Packets (VP), which derive from ER membrane. Fatty acids and PL productions are induced by Lipid droplet (LD) autophagy via NS4A-AUP1 interaction. Fatty acid synthesis is relocalized at replication site via NS3 and Lipid Droplet (LD) trafficking mediated by Rab18. LysoPC that allow membrane curvature and invagination are produced by enhancement of PLA2 activity and redirected to RC. Combination of NS4A interaction with Host Factors (HF: RTN3.1A and DNAJC14) maintain vesicle formation for efficient Replication Complex (RC) establishment. NS proteins are associated into the RC with RNA to initiate transcription. New ((+)ssRNA) produced is released from vesicles and assemble with capsid, membrane (prM) and envelope (E) proteins embedded into the host ER bilayer. Immature particles bud off from the ER lumen through the trans-Golgi network, in which low pH induces prM and E rearrangement that exposes prM to furin host protease and induces pr cleavage. Mature virions are released into the extracellular space with pr peptide through interaction with the plasma membrane.

3.5. Lipids as targets for DENV antivirals

Given the importance of the membrane environment and the host lipid metabolism, lipids appear as a promising target to block DENV infection. Inhibitor of fatty acid synthase (C75) can alter DENV infection, while direct inhibition of certain lipid species or lipid supplementation disrupt DENV multiplication. Inhibition of the first enzyme

involved in lipid biogenesis, acetyl-Coenzyme A carboxylase (ACC) reduces DENV infection in human cell lines and infected mice [278]. Activators of adenosine monophosphate-activated protein kinase (AMPK), an important pathway regulating lipid metabolism and glycolysis, has anti-DENV activity [279]. Sphingolipid and cholesterol metabolism are also targeted to block *flavivirus* infection [280]. Inhibition by nordihydroguaiaretic acid (NDGA) compounds of the sterol regulatory element-binding proteins (SREBP) pathway that regulates expression of enzymes involved in cholesterol and FA biosynthesis disrupts *flavivirus* infection [281,282]. It is interesting to observe that the phospholipid pathways and PL are a less preferential target to develop DENV antivirals.

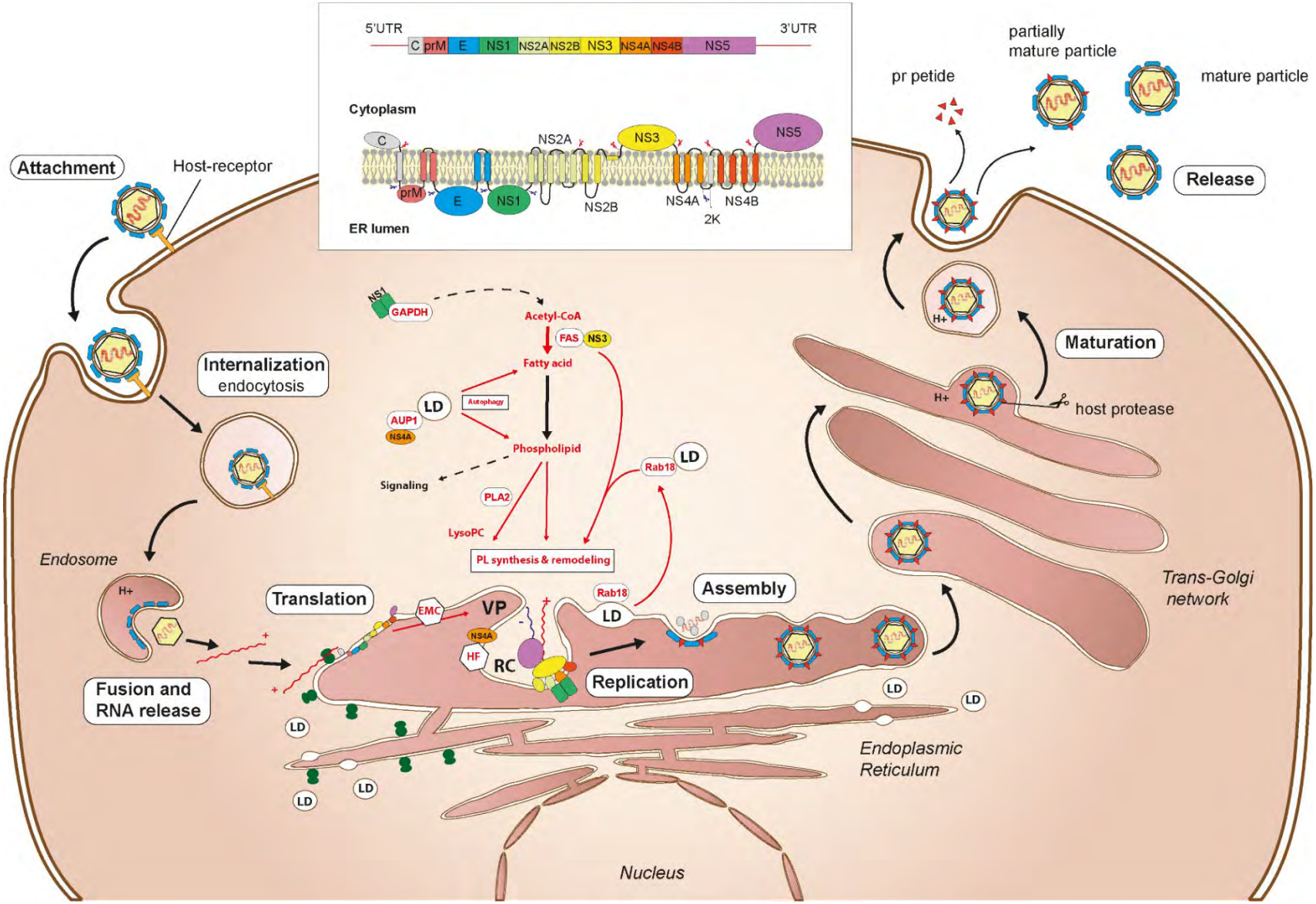

Fig 10. DENV life cycle.

4. Aim of the thesis

Multiple evidences demonstrate the paramount roles of host lipids in DENV infection both in the mammalian and insect hosts. Recent studies characterized the lipidome modulations in mosquito cell lines and midguts at early stages of the DENV cycle. However, there is a dearth of information about the molecular mechanisms that orchestrate these lipidome modulations.

The objective of this work is to characterize the metabolomic changes in *Aedes aegypti*, to decipher how the virus reconfigures the lipidome and characterize the molecular function of the altered lipids. To this end, we designed a high-resolution metabolomics pipeline to profile metabolome alterations and used molecular and cell biology to characterize the function.

In chapter 2, we revealed a major phospholipid reconfiguration throughout the DENV mosquito cycle, in cells, midguts, and whole mosquitoes. We further identified the mosquito gene AGPAT1, involved in PL *de novo* biosynthesis, as a host factor altered by DENV to promote the infection, associated with major regulation of AminoPL, especially PC and PE. In chapter 3, we demonstrated the importance of the Kennedy pathway and PC/PE biogenesis for DENV multiplication. By isotope labeling throughout ethanolamine and choline supplementation, we showed that a PL remodeling is induced by DENV infection. We further focus on different step of the DENV cellular life cycle and showed that the viral replication step is associated with the aminoPL biosynthetic pathway.

This work extends our understanding of mosquito-virus interaction and metabolic requirement for DENV infection. It reveals the importance of phospholipids needs and host biosynthetic factor regulation during the DENV mosquito cycle. In

addition, it describes a novel model of virus-induced lipid membrane reorganization by a balance between PE/PC biogenesis and PL remodeling. Finally, it underlines the key role of aminoPL in the DENV replication mechanism. Decipher interactions between DENV and lipids in mosquitoes can help to identify compounds to block transmission.

CHAPTER 2 – Dengue virus reduces AGPAT1 expression to alter phospholipids and enhance infection in *Aedes aegypti*

1. Presentation of the publication

The chapter 2 aims to expand our understanding of mosquito-virus interaction by studying the metabolic changes induced during DENV infection in *Aedes aegypti* mosquito. We combined a metabolomic approach by Liquid chromatography–high resolution mass spectrometry and gene silencing to underline the role of lipid membrane for DENV transmission. We highlighted the importance of aminophospholipids metabolites and their reconfiguration during DENV infection. We further identified a mechanism associated with the phospholipid metabolism, where DENV regulates a mosquito host factor to enhance its infection. The results of this work are presented in the following research article, which was published on December 9, 2019 in the Plos Pathogens journal.

PLOS PATHOGENS

RESEARCH ARTICLE

Dengue virus reduces *AGPAT1* expression to alter phospholipids and enhance infection in *Aedes aegypti*

Thomas Vial[1,2], Wei-Lian Tan[2], Benjamin Wong Wei Xiang[2], Dorothée Missé[3], Eric Deharo[1], Guillaume Marti[1☯*], Julien Pompon[2,3☯*]

1 UMR 152 PHARMADEV-IRD, Université Paul Sabatier-Toulouse 3, Toulouse, France, **2** Programme in Emerging Infectious Diseases, Duke-NUS Medical School, Singapore, **3** MIVEGEC, IRD, CNRS, Univ. Montpellier, Montpellier, France

☯ These authors contributed equally to this work.
* guillaume.marti@univ-tlse3.fr (GM); julien.pompon@ird.fr (JP)

OPEN ACCESS

Citation: Vial T, Tan W-L, Wong Wei Xiang B, Missé D, Deharo E, Marti G, et al. (2019) Dengue virus reduces *AGPAT1* expression to alter phospholipids and enhance infection in *Aedes aegypti*. PLoS Pathog 15(12): e1008199. https://doi.org/10.1371/journal.ppat.1008199

Editor: Glenn Randall, The University of Chicago, UNITED STATES

Received: May 30, 2019

Accepted: November 7, 2019

Published: December 9, 2019

Peer Review History: PLOS recognizes the benefits of transparency in the peer review process; therefore, we enable the publication of all of the content of peer review and author responses alongside final, published articles. The editorial history of this article is available here: https://doi.org/10.1371/journal.ppat.1008199

Data Availability Statement: Raw data were deposited in the MassIVE data repository under number MSV000083868; ftp://massive.ucsd.edu/MSV000083868/.

Abstract

More than half of the world population is at risk of dengue virus (DENV) infection because of the global distribution of its mosquito vectors. DENV is an envelope virus that relies on host lipid membranes for its life-cycle. Here, we characterized how DENV hijacks the mosquito lipidome to identify targets for novel transmission-blocking interventions. To describe metabolic changes throughout the mosquito DENV cycle, we deployed a Liquid chromatography–high resolution mass spectrometry (LC-HRMS) workflow including spectral similarity annotation in cells, midguts and whole mosquitoes at different times post infection. We revealed a major aminophospholipid reconfiguration with an overall early increase, followed by a reduction later in the cycle. We phylogenetically characterized acylglycerolphosphate acyltransferase (AGPAT) enzyme isoforms to identify those that catalyze a rate-limiting step in phospholipid biogenesis, the acylation of lysophosphatidate to phosphatidate. We showed that DENV infection decreased *AGPAT1*, but did not alter *AGPAT2* expression in cells, midguts and mosquitoes. Depletion of either AGPAT1 or AGPAT2 increased aminophospholipids and partially recapitulated DENV-induced reconfiguration before infection *in vitro*. However, only AGPAT1 depletion promoted infection by maintaining high aminophospholipid concentrations. In mosquitoes, AGPAT1 depletion also partially recapitulated DENV-induced aminophospholipid increase before infection and enhanced infection by maintaining high aminophospholipid concentrations. These results indicate that DENV inhibition of *AGPAT1* expression promotes infection by increasing aminophospholipids, as observed in the mosquito's early DENV cycle. Furthermore, in AGPAT1-depleted mosquitoes, we showed that enhanced infection was associated with increased consumption/redirection of aminophospholipids. Our study suggests that DENV regulates aminophospholipids, especially phosphatidylcholine and phosphatidylethanolamine, by inhibiting *AGPAT1* expression to increase aminophospholipid availability for virus multiplication.

Funding: This work was supported by a grant from National Medical Research Council, Singapore, (NMRC/ZRRF/0007/2017) awarded to JP, a grant from the Ministry of Education, Singapore, (MOE2015-T3-1-003) partially awarded to JP, and by the Duke-NUS Signature Research Programme funded by the Agency for Science, Technology and Research (A*STAR), Singapore, and the Ministry of Health, Singapore. The funders had no role in study design, data collection and analysis, decision to publish, or preparation of the manuscript.

Competing interests: The authors have declared that no competing interests exist.

Author summary

Dengue is endemic in tropical and subtropical regions, and has now encroached onto temperate regions because of the geographic expansion of its vector, *Aedes aegypti*. In the absence of effective vaccine and curative drug, the sole intervention relies on containment strategies using insecticide. However, occurrence of insecticide resistance diminishes vector control efficacy. Here, we explore the nascent field of mosquito metabolomics as part of our discovery effort for new transmission-blocking targets. Dengue virus (DENV) relies on host metabolome, specifically the lipid membrane to complete its life-cycle. However, little is known about how DENV subverts the mosquito physiology. Using high-resolution mass spectrometry, we described metabolic changes incurred by DENV throughout the mosquito cycle, from cellular replication onset to systemic infection. Membrane phospholipids were highly reconfigured and were associated with reduced expression of *AGPAT1*, an enzyme involved in their biogenesis. AGPAT1 depletion partially recapitulated DENV-induced metabolic reconfiguration and enhanced infection by maintaining high phospholipid concentrations. These phospholipids were then consumed/redirected later in the mosquito DENV cycle. Our work comprehensively describes metabolic changes associated with DENV infection. In addition, we reveal how DENV subdues the lipidome for its benefit by demonstrating the role of phospholipids in mosquito infection.

Introduction

Increased global distribution of dengue virus (DENV) is driven by the expansion of its mosquito vectors, mainly *Aedes aegypti* [1]. An estimated 400 million infections occur yearly in over 100 countries [2] and cause a range of symptoms from flu-like illness to potentially lethal complication called severe dengue. Without approved antiviral drug, treatment is limited to supportive care. Although dengue vaccine is now licensed in several countries, it has variable efficacy against all dengue serotypes [3], and is only suitable for dengue-seropositive patients [4]. To curb dengue epidemics, containment strategy mainly relies on vector control that includes the use of insecticides [5]. However, insecticide resistance is rapidly developing, compromising the efficacy of the only available intervention [6]. Characterization of viral metabolic requirements in mosquitoes will identify targets for novel chemical-based control strategies [7].

As obligate and intracellular parasites, viruses rely on the host to fulfill their metabolite requirements. Glycolysis, amino acid and lipid pathways provide the energy and structural compounds necessary for multiplication. In human cells, DENV alters energy [8,9], glycolysis [10], nucleic acid [11], mitochondrial [12] and lipid metabolisms [13–15]. As an envelope virus, DENV is particularly dependent on host-derived lipid membranes, with which it interacts for entry, replication, translation, assembly and egress [7,16]. In mosquito cells and midgut, DENV reconfigures the lipid profile as indicated by lipidomics [17,18] and transcriptomics [19], particularly altering the membrane lipids such as phospholipids (PL) and sphingolipids. Chemical inhibition of lipid synthesis confirmed the DENV requirements for lipids in human and mosquito cells [20]. Several mechanisms related to elevated autophagy [13] and recruitment of lipogenesis enzymes to the replication complex [21] have been elucidated in the mammalian host. However, how DENV reconfigures lipids in mosquitoes remains unknown.

PL *de novo* biogenesis is initiated by two types of acyl-transferases that sequentially add two acyls to one glycerol-3-phosphate (G3P) [22,23]. The second addition is catalyzed by 1-acyl-sn-glycerol-3-phosphate O-acyltransferases (AGPAT) that transform lysophospatidate

(lysoPA) in phosphatidate (PA) [24]. PAs are then used to produce all PLs, positioning AGPATs as rate-limiting enzymes of PL biogenesis. PLs are produced within the endoplasmic reticulum and subject to swift reconfiguration to meet the cell needs [25,26]. DENV translation, replication and assembly harness the endoplasmic reticulum membranes, suggesting potential alteration of PL biogenesis.

Following an infectious blood meal, DENV infects the mosquito midgut, multiplies, and propagates to the whole mosquito body, including salivary glands, from where it is expectorated during subsequent blood feeding [27]. Throughout various infected tissues, the virus modifies its metabolic environment. In this study, we aim to understand how DENV modifies mosquitoes' metabolome. Using high-resolution mass spectrometry, we explored the metabolic changes throughout the DENV cycle, in *Ae*. *aegypti* Aag2 cell line, midguts and whole mosquitoes at different times post infection. Infection-induced metabolic alteration mostly affected PLs and was associated with *AGPAT* expression regulations. Combining metabolomic profiling with RNAi-mediated AGPAT depletions, we partially recapitulated the infection-induced PL reconfiguration and demonstrated its pro-viral impact. Eventually, PL profiling upon infection both *in vitro* and *in vivo* in PL-altered environments indicated that increased PL redirection/consumption favored virus multiplication. Our study reveals how DENV reconfigures the metabolome and identifies PLs as important components in the virus life-cycle.

Results

Mosquito phospholipidome is reconfigured throughout DENV infection

To describe the metabolic changes in *Ae*. *aegypti*, we designed an untargeted multidimensional approach that covered the different stages of DENV cycle (Fig 1A). Extracts from Aag2 cells at 6, 12, 24 and 48 h post infection (hpi) represented changes caused by entry, initiation of replication, replication and virion production (S1A and S1B Fig) [28]. Extracts from midguts at 1 and 7 days post oral infection (dpi) represented infection onset and replication peak, respectively (S1C and S1CD Fig) [27]. Extracts from whole mosquitoes at 1, 7 and 14 dpi represented the different dissemination stages in the mosquito body (S1C and S1CD Fig) [27]. The extracts were analyzed using a Liquid Chromatography-High Resolution Mass Spectrometry (LC-HRMS) metabolomic workflow that detects polar and nonpolar metabolites (S2 Fig). We detected 667, 486 and 1121 compounds in the cells, midgut and whole mosquitoes, respectively (Table 1). Comparison of MS spectra with available non-mosquito databases enabled the annotation of 77% of the peaks. To annotate the remaining mosquito-specific metabolites, we deployed MS spectral similarity network (S3 Fig; S1 Table) [29]. Based on the spectral similarity with database-identified features, we identified the class of 20 MS features without homologues in the databases, increasing the identification coverage to 77, 70 and 82% in the cells, midguts and whole mosquitoes, respectively (Table 1). Among all annotated metabolites, we detected 29% of PLs, 21% of non-PL lipids, 8% of amino acids and peptides, 5% of organic acids, 4% of carbohydrates and 33% of other minor classes (fewer than 3 occurrences). The distribution of metabolite classes indicates that the metabolomic workflow had a broad coverage, although slightly biased towards lipids.

Infection regulated 67, 24 and 181 unique metabolites in cells, midguts and whole mosquitoes, respectively (Fig 1B; S2 Table). The PL class had the highest number of regulated metabolites in the midgut and mosquito, and the third most regulated in cells. Fatty acyls were also differentially regulated in the three tissue levels, while amino acids and carbohydrates were regulated in cells and mosquitoes.

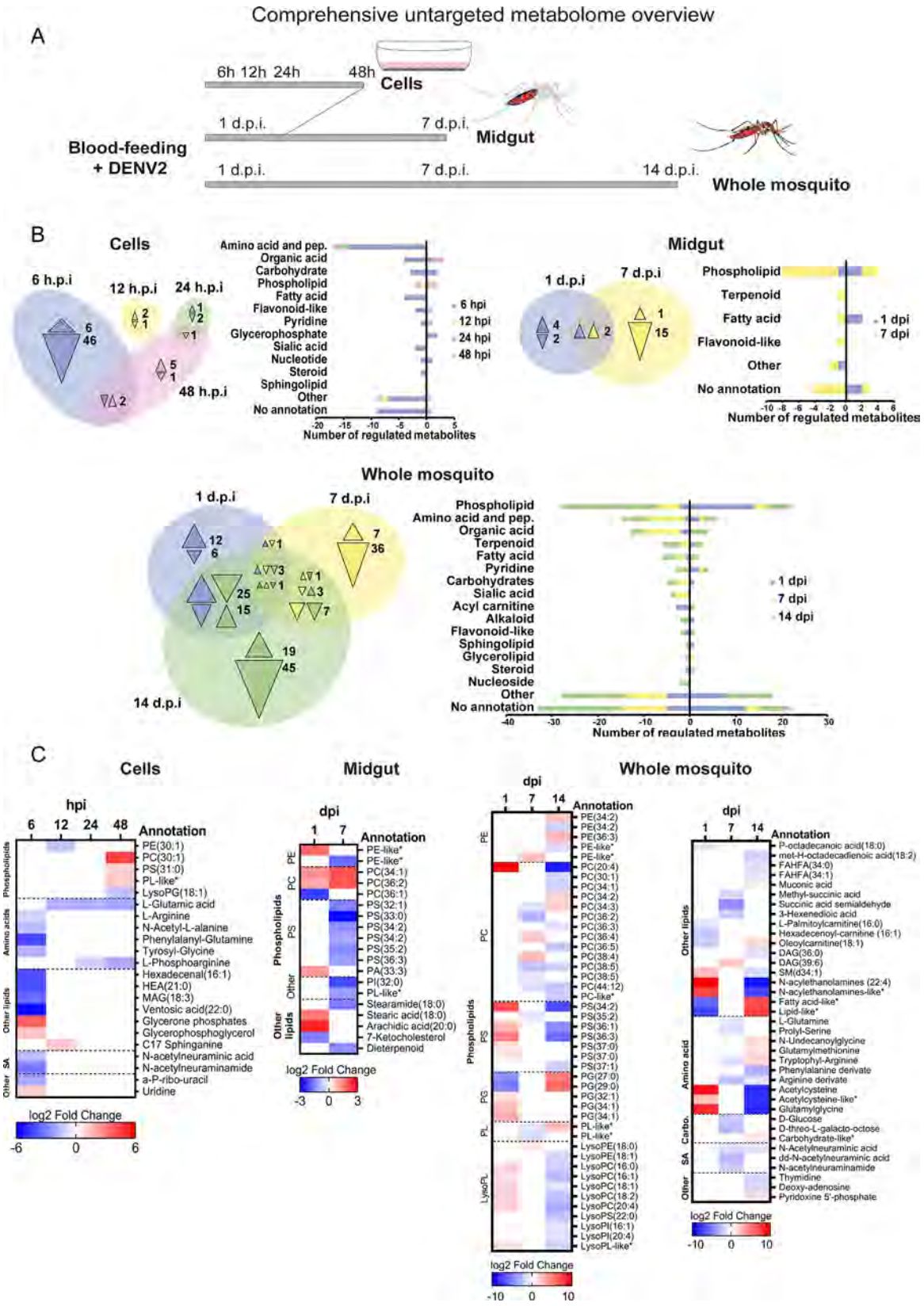
Comprehensive untargeted metabolome overview
A
6h 12h 24h
48h
Cells
1 d.p.i.
7 d.p.i.
Midgut
Blood-feeding
+ DENV2
1 d.p.i.
7 d.p.i.
14 d.p.i.
Whole mosquito
B
Cells
6 h.p.i
12 h.p.i
24 h.p.i
48 h.p.i
Amino acid and pep.
Organic acid
Carbohydrate
Phospholipid
Fatty acid
Flavonoid-like
Pyridine
Glycerophosphate
Sialic acid
Nucleotide
Steroid
Sphingolipid
Other
No annotation
6 hpi
12 hpi
24 hpi
48 hpi
Number of regulated metabolites
Midgut
1 d.p.i
7 d.p.i
Phospholipid
Terpenoid
Fatty acid
Flavonoid-like
Other
No annotation
1 dpi
7 dpi
Number of regulated metabolites
Whole mosquito
1 d.p.i
7 d.p.i
14 d.p.i
Phospholipid
Amino acid and pep.
Organic acid
Terpenoid
Fatty acid
Pyridine
Carbohydrates
Sialic acid
Acyl carnitine
Alkaloid
Flavonoid-like
Sphingolipid
Glycerolipid
Steroid
Nucleoside
Other
No annotation
1 dpi
7 dpi
14 dpi
Number of regulated metabolites
C
Cells
hpi
Annotation
PE(30:1)
PC(30:1)
PS(31:0)
PL-like*
LysoPG(18:1)
L-Glutamic acid
L-Arginine
N-Acetyl-L-alanine
Phenylalanyl-Glutamine
Tyrosyl-Glycine
L-Phosphoarginine
Hexadecenal(16:1)
HEA(21:0)
MAG(18:3)
Ventosic acid(22:0)
Glycerone phosphates
Glycerophosphoglycerol
C17 Sphinganine
N-acetylneuraminic acid
N-acetylneuraminamide
a-P-ribo-uracil
Uridine
log2 Fold Change
Midgut
dpi
Annotation
PE-like*
PE-like*
PC(34:1)
PC(36:2)
PC(36:1)
PS(32:1)
PS(33:0)
PS(34:2)
PS(34:2)
PS(35:2)
PS(36:3)
PA(33:3)
PI(32:0)
PL-like*
Stearamide(18:0)
Stearic acid(18:0)
Arachidic acid(20:0)
7-Ketocholesterol
Dieterpenoid
log2 Fold Change
Whole mosquito
dpi
Annotation
PE(34:2)
PE(34:2)
PE(36:3)
PE-like*
PE-like*
PC(20:4)
PC(30:1)
PC(34:1)
PC(34:2)
PC(34:3)
PC(36:2)
PC(36:3)
PC(36:4)
PC(36:5)
PC(38:4)
PC(38:5)
PC(38:5)
PC(44:12)
PC-like*
PS(34:2)
PS(35:2)
PS(36:1)
PS(36:3)
PS(37:0)
PS(37:0)
PS(37:1)
PG(27:0)
PG(29:0)
PG(32:1)
PG(34:1)
PG(34:1)
PL-like*
PL-like*
LysoPE(18:0)
LysoPE(18:1)
LysoPC(16:0)
LysoPC(16:1)
LysoPC(18:1)
LysoPC(18:2)
LysoPC(20:4)
LysoPS(22:0)
LysoPI(16:1)
LysoPI(20:4)
LysoPL-like*
log2 Fold Change
dpi
Annotation
P-octadecanoic acid(18:0)
met-H-octadecadienoic acid(18:2)
FAHFA(34:0)
FAHFA(34:1)
Muconic acid
Methyl-succinic acid
Succinic acid semialdehyde
3-Hexenedioic acid
L-Palmitoylcarnitine(16:0)
Hexadecenoyl-carnitine (16:1)
Oleoylcarnitine(18:1)
DAG(36:0)
DAG(39:6)
SM(d34:1)
N-acylethanolamines (22:4)
N-acylethanolamines-like*
Fatty acid-like*
Lipid-like*
L-Glutamine
Prolyl-Serine
N-Undecanoylglycine
Glutamylmethionine
Tryptophyl-Arginine
Phenylalanine derivate
Arginine derivate
Acetylcysteine
Acetylcysteine-like*
Glutamylglycine
D-Glucose
D-threo-L-galacto-octose
Carbohydrate-like*
N-Acetylneuraminic acid
dd-N-acetylneuraminic acid
N-acetylneuraminamide
Thymidine
Deoxy-adenosine
Pyridoxine 5'-phosphate
log2 Fold Change

Fig 1. Aminophospholipid composition is altered throughout DENV infection in mosquitoes. (A) Schematic of the multidimensional strategy deployed to profile the mosquito metabolome after DENV infection. Aag2 mosquito cells were infected with DENV at an MOI of 5 and collected at 6, 12, 24 and 48 h post infection (hpi). Mosquitoes were orally infected with 10^7 pfu/ml of DENV. Midguts and whole mosquitoes were collected at 1, 7 and 14 days post infection (dpi). Metabolic extracts were analyzed by LC-HRMS as in S2 Fig. (B) Venn diagrams show regulated metabolites at the different time points and bars indicate class distribution within tissue levels. Triangles indicate direction of regulation and are color-coded with regards to the time point. Uninfected condition was used as control. (C) Fold changes of annotated and significantly regulated metabolites ($|\log_2$ fold change$| > 1$ and p-value < 0.05) by DENV in cells, midguts and mosquitoes as compared to mock infection. Only metabolites from the general metabolism (i.e., lipid, carbohydrate, amino acid and peptide, nucleotide and nucleoside, sialic acid) are shown. *, indicates metabolite annotations determined by spectral similarity. Carbo., carbohydrate; SA, sialic acid; PL, phospholipid; PE, phosphatidylethanolamine; PC, phosphatidylcholine; PS, phosphatidylserine; PA, phosphatidic acid; PI, phosphatidylinositol; PG, phosphatidylglycerol; LysoPS, lysophosphatidylserine; LysoPC, lysophosphatidylcholine; LysoPE, lysophosphatidylethanolamine; LysoPG, lysophosphatidylglycerol; LysoPI, lysophosphatidylinositol; SM, Sphingomyelin; DAG, Diacylglycerol; MAG, Monoacylglycerol; FAHFA, Fatty Acid ester of Hydroxyl Fatty Acid; NAE, N-acylethanolamine; HEA, Heneicosanoic acid; pep., peptides.

https://doi.org/10.1371/journal.ppat.1008199.g001

Several classes of PLs were regulated in all three tissues (Fig 1C, S4 Fig). Aminophospholipids (aminoPL) are the major constituents of membranes and are synthesized in the endoplasmic reticulum [30]. AminoPLs include phosphatidylethanolamine (PE), phosphatidylcholine (PC) and phosphatidylserine (PS) [31]. Although infection altered different species of aminoPLs in the different tissue-time combinations, we observed a general increase at the beginning of DENV cycle, followed by a reduction at the end. In cells, the majority of regulated aminoPLs (3 out of 5) were upregulated at 48 hpi. In midguts and mosquitoes a total of 9 aminoPLs were increased at 1 dpi, whereas 15 and 14 were reduced at 7 and 14 dpi, respectively.

Phosphatidylglycerols (PG) are another group of PL. Although PGs have a lower abundance than aminoPLs, they are also constituents of membranes and synthesized in the mitochondria [32]. Although only detected in mosquito extracts, PGs responded differently to infection when compared with aminoPLs (Fig 1C). Two shorter PGs decreased at 1 dpi and increased at 14 dpi, and three longer PGs were upregulated at 1 dpi.

Lysophopholipids (lysoPL) are produced from fatty acid remodeling of the different PL classes [33]. In cells, one lysoPG was downregulated at 48 hpi (Fig 1C). In mosquitoes, the lysoPCs followed the same trend as aminoPLs, with 6 increasing at 1 dpi and decreasing at 14 dpi.

Different types of PL precursors were regulated. PA, the direct precursor of all PLs [24,31], was upregulated at 1 dpi in midgut, similar to aminoPLs. Two diacylglycerols (DAG), intermediates for PE and PC productions, were up and downregulated in mosquitoes at 7 and 14 dpi, respectively. Fatty acyls can be incorporated into a glycerol head to produce PL and were regulated. Fatty acyls with an ethanolamine group can be related to PE either via degradation or as a precursor. Similar to aminoPLs, two acyl-ethanolamine increased at 1 dpi and decreased at 14 dpi in mosquitoes. In accordance with previous studies [34], one sphingomyelin was regulated in mosquitoes and one cholesterol compound was depleted in midgut.

Our comprehensive metabolomic profiling revealed that DENV infection profoundly reconfigures the phospholidome. The aminoPLs including PE, PC and PS increased at the

Table 1. Summary of metabolites detected across mosquito tissues. ¶MS Finder (HMDB, ChEBI, LipidMAPS, LipidBlast) score annotation ≥ 5; * p-value < 0.05 as indicated by unpaired t-test and $|\log_2$ Fold Change$| \geq 1$.

Tissue	Aag2 cells				*A. aegypti* Midgut		*A. aegypti* Mosquito		
Unique peak detected with MS/MS	667				486		1121		
Annotated peaks (%)¶	77%				70%		82%		
Metabolites significantly regulated*	**6 hpi**	**12 hpi**	**24 hpi**	**48 hpi**	**1 dpi**	**7 dpi**	**1 dpi**	**7 dpi**	**14 dpi**
Total	54	3	4	9	8	18	63	59	119
Annotated (%)	83%	100%	100%	89%	75%	72%	73%	78%	79%

https://doi.org/10.1371/journal.ppat.1008199.t001

beginning of DENV cycle and decreased later on. A large phospholipidome reconfiguration was previously observed in DENV-infected midguts at 3, 7 and 11 dpi [18]. However, in this previous kinetic study, PLs were mostly up-regulated throughout the infection cycle. They reported a decrease in lysoPL abundance, which we observed at 14 dpi in mosquitoes. The authors also noted an increase in sphingolipids, which we saw in mosquitoes but only for one species. Those variations between the studies can stem from methodological differences in extraction and analyses, or from biological differences in mosquito colony and virus strain. Taken together, our results and those of others indicate that DENV infection reconfigures lipid membrane composition.

DENV infection modulates expression of *AGPAT1* that is involved in PL biogenesis

To determine how PLs are reorganized upon DENV infection, we first characterized the rate-limiting AGPAT enzymes in *Ae. aegypti* (Fig 2A). In humans, there are five AGPAT isoforms with different activities depending on four motif sequences [35]. Motifs I and IV bind to acyl-CoA and catalyze lysoPA to PA acylation, while motifs II and III bind to lysoPA. Human AGPAT (hAGPAT) 1 and 2 are localized in the endoplasmic reticulum and have the highest acyltransferase activity and lysoPA affinity [36]. hAGPAT3-5 have lower transferase activity and target different substrates that lysoPA such as lysoPL, participating in PL remodeling [37]. *Aedes aegypti* also has five AGPAT isoforms: AGPAT1 (AAEL011898), AGPAT2 (AAEL001000), AGPAT3 (AAEL011902), AGPAT4 (AAEL014026) and AGPAT5 (AAEL011901). Based on amino acid similarity, AGPAT1, 2, 3 and 5 cluster with hAGPAT1 and 2, whereas AGPAT4 clusters with hAGPAT3-5 (Fig 2B; S5 Table). Further classification based on functional motifs that are define the biochemical activity [38] establishes AGPAT1, 2, 3 as homologues of hAGPAT1 and 2 (Table 2), suggesting that they all share the acyltransferase activity and lysoPA affinity.

To test whether infection-induced phospholipidome reconfiguration is associated with AGAPT regulation, we quantified *AGPAT1* and *2* expressions. Interestingly, we observed that *AGPAT1* was downregulated at 24 and 48 hpi in cells, at 1 and 7 dpi in midguts and at 1, 7 and 14 dpi in mosquitoes (Fig 2C–2E). In contrast, *AGPAT2* was not significantly regulated in cells, midguts and mosquitoes (Fig 2C–2E). This partially corroborates a transcriptomic study [39] that shows *AGPAT1* downregulation and *AGPAT2* upregulation at 1, 2 and 7 days post DENV-inoculation in mosquitoes (S5 Fig). To test whether virus replication was required for *AGPAT1* down-regulation, we incubated cells with UV-inactivated virus (S6A Fig). *AGAPT1* expression did not vary between mock and UV-inactivated DENV at 24 and 48 hpi (S6B Fig), indicating that active infection is required.

Altogether, our results and those of others suggest that *AGPAT1* down-regulation correlates with DENV phospholipidome reconfiguration.

Depletion of AGPAT1 but not AGPAT2 promotes DENV infection by increasing aminoPL concentrations in cells

Based on the association between the infection-induced phospholipidome reconfiguration and *AGPAT1* down-regulation, we hypothesized that AGPAT1 mediates the phospholipidome reconfiguration that promotes DENV infection. First, we described how both AGPAT1 and 2, the latter used as control, regulate PL biogenesis in non-infected mosquito cells. LC-HRMS polar mode detection was used to target phospholipid metabolites (S2 Fig). Depletion of either AGPAT1 or 2 increased the concentrations of aminoPLs (Fig 3A–3C; S6 Table), as previously observed in human cells [40]. Strikingly, PC (34:1), PC (38:5) and G3P were upregulated by both AGPAT1 and 2 depletion. AGPAT2 depletion also increased two other PCs and

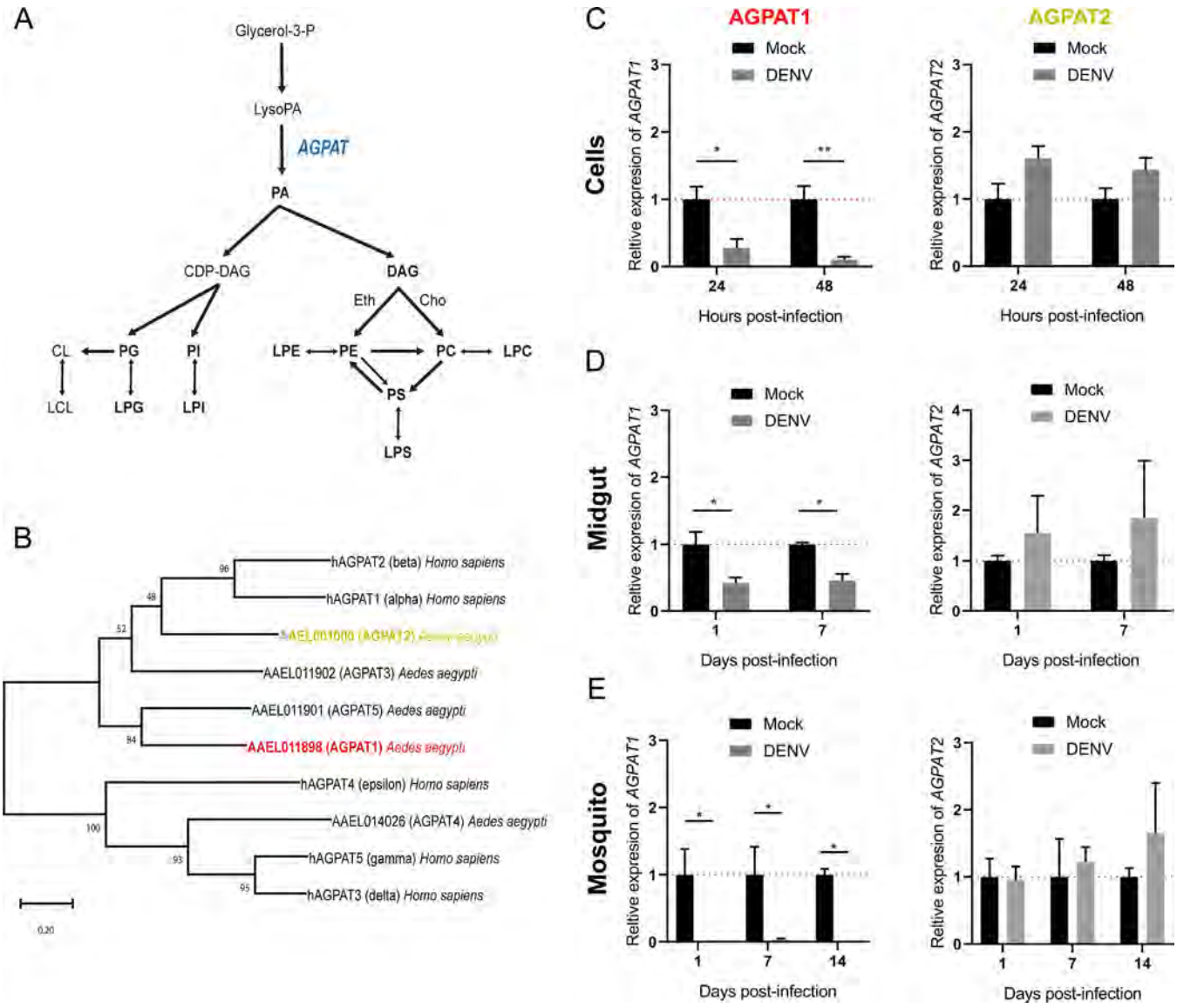

Fig 2. DENV infection decreases *AGPAT1* but not *AGPAT2* expression. (A) An overview of phospholipid biogenesis. Sequential additions of two acyl-coA to one G3P produce a LysoPA and a PA. Several AGPATs mediate the second addition. PA forms either DAG or CDP-DAG, each generating a different set of phospholipids. DAG produces aminophospholipids by addition of a Cho or Eth group. Aminophospholipids are also produced by acylation of lysoPL and base group modifications. CDP-DAG produces PI and PG, the latter being transformed in CL by combination with a second PG. Phospholipases cleave off an acyl chain from PL to produce lysoPL. G3P, glycerol-3-phosphate; LysoPA, lysophosphatidate; PA, phosphatidate; AGPAT, acyl-sn-glycerol-3-phosphate acyltransferases; DAG, diacylglycerol; CDP-DAG, cytidine diphosphate diacylglycerol; PC, phosphatidylcholine; LPC, lysophosphatidylcholine; Cho, choline; PE, phosphatidylethanolamine; LPE, lysophosphatidylethanolamine; Eth, ethanolamine; PS, phosphatidylserine; LPS, lysophosphatidylserine; PI, phosphatidylinositol; LPI, lysophosphatidylinositol; PG, phosphatidylglycerol; LPG, lysophosphatidylglycerol; CL, cardiolipin; LCL, lysocardiolipin. (B) Maximum likelihood tree between AGPATs from *Ae. aegypti* and humans. (C) *AGPAT1* and *AGPAT2* expressions in DENV-infected cells at 24 and 48 hpi with an MOI of 5. Expressions of *AGPAT1* and *AGPAT2* (D) in midguts at 1, 7 dpi and (E) in whole mosquitoes at 1, 7 and 14 dpi with DENV at 10^7 pfu/ml. (C-E) *Actin* expression was used for normalization. Bars show means ± s.e.m from 4 independent wells or 3 pools of 5 midguts or 5 mosquitoes. *, p-value < 0.05; **, p-value<0.01; as indicated by unpaired t-test.

https://doi.org/10.1371/journal.ppat.1008199.g002

decreased two forms of sphinganine, a precursor of sphingolipid biosynthesis [41] (Fig 3D; S7A Fig), and six amino acids or nucleoside (arginine, cysteine, methionine, glutamic acid, oxidized glutathione and adenosine) (S6 Table). Of note, depletion of one of the AGPATs did not alter expression of the other (S8 Fig), indicating the enzyme-specificity of the aminoPL

Table 2. Acyltransferase motif comparison between human and *Ae. aegypti* AGPAT homologues. Purple indicates amino acid residues highly conserved across all hAGPATs and yellow in hAGPAT1 and 2 only.

Specie	Protein	RefSeq	Amino acids	Motif I acyl-CoA binding and catalysis	Motif II LPA binding	Motif III LPA binding	Motif IV acyl-CoA binding and catalysis
Homo sapiens	hAGPAT1 (alpha)	NP_006402	283	VSN H QS S L D LL G M	A GV I F I D R K R	V FPEGT RN H	VPIV P I V M SS
Homo sapiens	hAGPAT2 (beta)	NP_006403	278	VSN H QS I L D MM G L	G GV F F I N R Q R	IY PEGT RN D	VPIV PV V Y SS
Homo sapiens	hAGPAT3 (gamma)	NP_064517	376	IL N H NFEI D FLCG	LEIV F CK R KW	LYC EGT R FT	YHLL P RTKGF
Homo sapiens	hAGPAT4 (delta)	NP_064518	378	V L N H KFEI D FLCG	TEMV F CS R KW	IHC EGT R FT	HHLL P RTKGF
Homo sapiens	hAGPAT5 (epsilon)	NP_060831	364	LA N H QS TV D WIVA	QHGGIYVKRS	I FPEGT R YN	HVLT P RIKAT
Ae. aegypti	AGPAT1 (AAEL011898)	EAT35978	273	LM N H QS A L D LVVL	WGTL F I N R KN	F FPEGT R GD	GY I Q PV V I S K
Ae. aegypti	AGPAT2 (AAEL001000)	EAT47921	398	V A N H QS S L D IL G M	S G LI F I D R KN	V FPEGT R RN	L PI M PV V Y SS
Ae. aegypti	AGPAT3 (AAEL011902)	EAT35981	308	MA N H QS SM D IL G L	A G IT F I N R KN	IY PEGT R FP	VPI I PV V F S H
Ae. aegypti	AGPAT4 (AAEL014026)	EAT33698	387	LM N H TYEV D WLVG	AEFV F LE R SF	LNA EGT R FT	HHLI P RTKGF
Ae. aegypti	AGPAT5 (AAEL011901)	EAT35980	280	LI N H QS AI D IVML	V GV V F I D R KN	I FPEGT R HD	SI I QSIIV S K

https://doi.org/10.1371/journal.ppat.1008199.t002

alterations. These results confirm the roles of AGPAT1 and 2 in PL biogenesis, and reveal differences between the two enzymes.

To test whether AGPAT-mediated reconfiguration of aminoPLs promotes DENV infection, we quantified infection in cells depleted of either AGPAT1 or 2. While DENV titer was not altered by AGPAT2 depletion, it increased 2.09 ± 0.36 fold (p-value = 0.0012) following AGPAT1 depletion (Fig 3E). Next, we described how DENV infection altered the lipidome in cells depleted of either AGPAT1 or 2. Infection in AGPAT1-depleted cells, but not in AGPAT2-depleted cells, mostly increased aminoPLs as compared to infected wild-type cells (Fig 3C, S7 Table). Specifically, two PEs, two PCs, two PSs, and one lysoPE were upregulated (Fig 3F; S7B Fig). These results indicate that: (i) depletion of AGPAT1 prior infection amplifies the aminoPL increase observed in early mosquito DENV infection (Fig 1C), and (ii) AGPAT1-mediated aminoPL reconfiguration is associated with increased DENV production. Therefore, *AGPAT1* downregulation by infection generates a pro-viral environment.

To test whether AGPAT1 effect on DENV was related to aminoPLs, we modified the AGPAT1-induced reconfiguration of aminoPLs by media supplementation. In PL biogenesis, PA produces DAG, which is transformed into PE by addition of ethanolamine (Fig 2A). Extracellular source of ethanolamine influences phospholipid metabolism [42], especially PEs that were altered by AGPAT1 depletion (Fig 3F). Therefore, we measured the impact on DENV gRNA of ethanolamine supplementation upon AGPAT1 depletion. Controls were non-depleted cells without supplementation (standard media that does not contain ethanolamine), non-depleted cells with ethanolamine supplementation and AGPAT1-depleted cells without supplementation. While ethanolamine supplementation did not alter gRNA in non-depleted cells, the increase observed upon AGPAT1-depletion was reverted to non-depleted non-supplemented control when ethanolamine was supplemented (S9 Fig). These results confirm the role of AminoPLs in AGPAT1 increase of DENV multiplication and incriminate metabolites downstream of DAG as important for DENV.

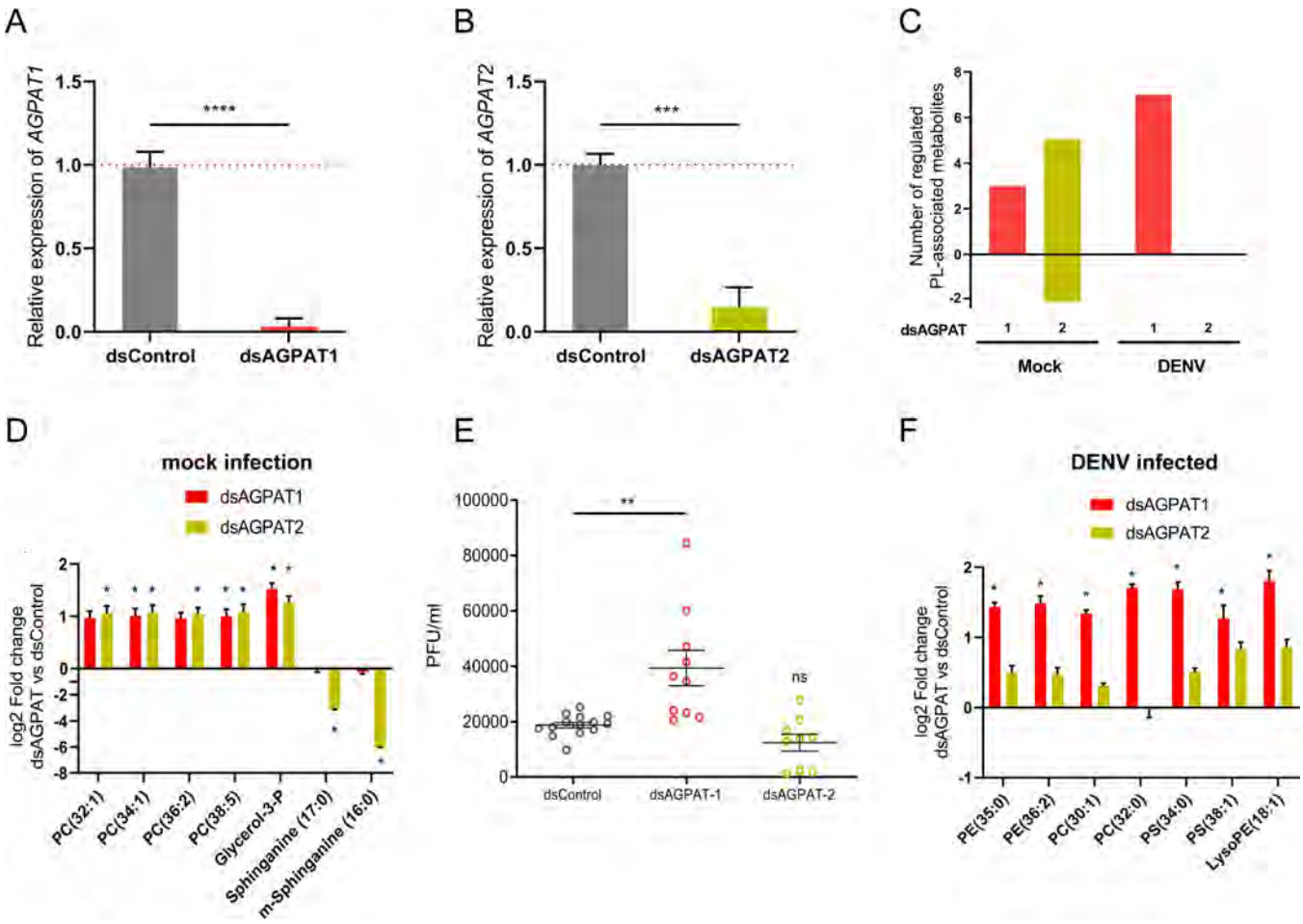

Fig 3. AGPAT1 but not AGPAT2 depletion increases DENV multiplication and aminoPL in cells. Aag2 cells were transfected with either dsRNA against *AGPAT1* or *2* (dsAGPAT1 or 2) or with dsRNA control (dsControl). At 24 h post transfection, cells were infected with DENV at MOI of 1 or mock infected. Supernatant was collected at 48 hpi. Expressions of (A) *AGPAT1* and (B) *AGPAT2* in mock-infected cells at 72 h post transfection. *Actin* expression was used for normalization. Bars show mean ± s.e.m. (C) Number of phospholipid-related metabolites significantly regulated. (D) Impact of AGPAT1 or 2 depletion on the lipidome of mock-infected cells at 72 h post transfection. *, p-value <0.05 and $|\log_2$ fold change$| > 1$. (E) Impact of AGPAT1 or 2 depletion on DENV production at 48 hpi as determined by plaque forming unit (pfu) assay. Bars show mean ± s.e.m. and each point represents independent wells. (F) Impact of AGPAT1 or 2 depletion on the lipidome of infected cells at 48 hpi. *, p-value < 0.05 and $|\log_2$ fold change$| > 1$. (A, B, D and F) result from three biological replicates. (A, B) ***; p-value < 0.001; ****, p-value < 0.0001, as indicated by unpaired t-test. (E) **, p-value < 0.01, as indicated by Dunnett's test. PE, phosphatidylethanolamine; PC, phosphatidylcholine; PS, phosphatidylserine; LPE, lysophosphatidylethanolamine.

https://doi.org/10.1371/journal.ppat.1008199.g003

AGPAT1 depletion promotes DENV infection by amplifying aminoPL reconfiguration in mosquitoes

To further characterize how AGPAT1-mediated PL alteration increases DENV infection, we depleted AGPAT1 in mosquitoes (Fig 4A). We first described how AGAPT1 regulates PLs in mosquitoes that fed on a non-infectious blood meal (Fig 4B; S10 Fig; S8 Table). As in cells, AGPAT1 mostly regulated aminoPLs and their derivatives (S8 Table). At 2 days post oral feeding, one DAG and one PA, two key precursors of PLs, and one PS were increased. At 7 days post oral feeding, eight lysoPLs (one lysoPI, two lysoPGs, one lysoPS, two lysoPEs and two lysoPCs) were downregulated, similarly to those in DENV-infected wild-type mosquitoes at 14 dpi (Fig 1C). Strikingly, some metabolites were similarly regulated by either AGPAT1-depletion or DENV infection. PS (34:2) was upregulated by either AGPAT1-depletion at 2 days post oral feeding or DENV infection at 1 dpi. LysoPI (20:4), lysoPE (18:1), lysoPC (16:1) and lysoPC

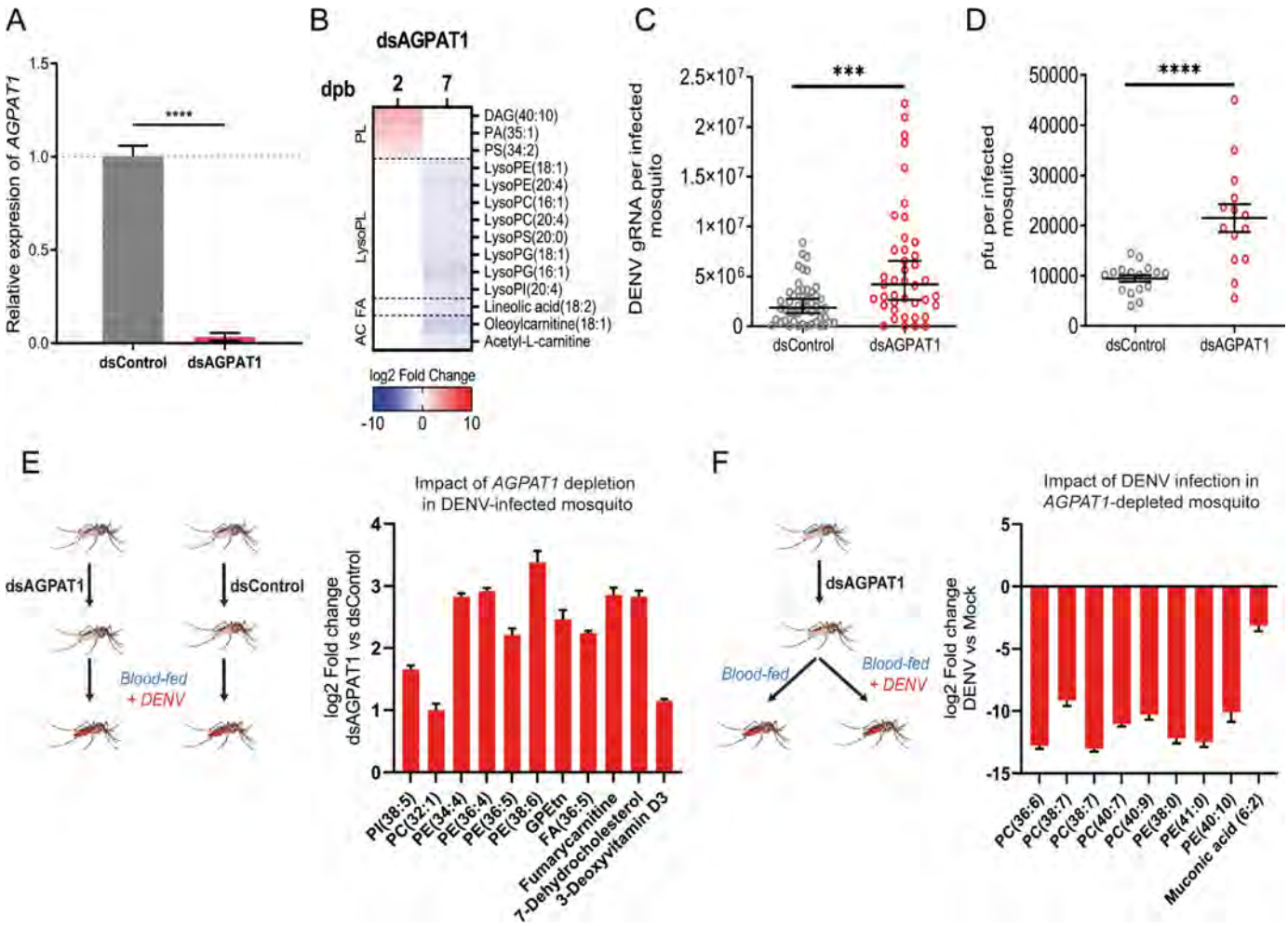

Fig 4. AGPAT1 depletion increases DENV multiplication and consumption of aminoPLs in mosquitoes. Mosquitoes were injected with either dsRNA against *AGPAT1* (dsAGPAT1) or dsRNA control (dsControl). Two days later, mosquitoes were orally fed with non-infectious blood or infectious blood containing DENV at 10^7 pfu/ml. (A) Validation of *AGPAT1* silencing in non-infected mosquitoes at two days post dsRNA injection. *Actin* expression was used for normalization. Bars show mean ± s.e.m. from 3 pools of 5 mosquitoes each. ****, p-value < 0.0001 as indicated by unpaired t-test. (B) Impact of AGPAT1 depletion on the lipidome of mosquitoes at 2 and 7 days post non-infectious blood feeding (dpb). Impact of AGPAT1 depletion on (C) DENV gRNA copies and (D) viral load measured as pfu/ml at 7 days post oral infection (dpi). Bars indicate mean (C) or geometric means ± 95% CI (D) with each dot representing one mosquito. ***, p-value < 0.001 ****, p-value < 0.0001 as indicated by unpaired t-test (C) or Mann-Whitney test (D). (E) Impact of AGPAT1 depletion on the lipidome of infected mosquitoes at 7 dpi. (F) Impact of infection on the lipidome of AGPAT1-depleted mosquitoes at 7 dpi. (B, E, F) Only regulated metabolites are shown (p-value < 0.05 and $|\log_2$ fold change$| > 1$). PL, phospholipid; FA; fatty acyl; AC, acylcarnitine; DAG, diacylglycerol; PA, phosphatidic acid; PS, phosphatidylserine; LPE, lysophosphatidylethanolamine; LPC, lysophosphatidylcholine; LPS, lysophosphatidylserine; LPG, lysophosphatidylglycerol; LPI, lysophosphatidylinositol; PE, phosphatidylethanolamine; PC, phosphatidylcholine; PI, phosphatidylinositol; GPEtn, glycerophosphoethanolamine.

https://doi.org/10.1371/journal.ppat.1008199.g004

(20:4) were reduced by either AGPAT1-depletion at 7 days post oral feeding or DENV infection at 14 dpi. At 7 days post oral feeding in AGPAT1-depleted mosquitoes, one fatty acyl, two acylcarnitines, oleoylcarnitine (18:1) and acetyl-L-carnitine, were decreased. Of note, one of the regulated acylcarnitines (i.e., oleoylcarnitine) was inversely regulated by DENV infection at 14 dpi (Fig 1C). These results show that AGPAT1 depletion partially reproduces the aminoPL reconfiguration caused by DENV infection.

Next, we found that AGPAT1-depletion increased DENV gRNA (p-value = 0.0004) and titer (p-value < 0.0001) at 7 dpi in whole mosquito (Fig 4C and 4D), confirming that AGPAT1 depletion induces a pro-viral environment *in vivo*. However, the pro-viral impact of AGPAT1 depletion was not observed on infection rate (S11A Fig) and at 2 dpi on gRNA (S11B Fig). We

repeated the experiment using a lower inoculum for oral infection and similarly observed no effect at 2 dpi but a moderate increase of gRNA ($p = 0.0421$) at 7 dpi (S11C–S11E Fig). It is intriguing that AGPAT1 depletion only increased infection at 7 dpi. This may indicate that DENV infection is necessary to amplify AGPAT1-mediated alteration in establishing a proviral environment. To characterize the AGPAT1-induced proviral environment, we compared the lipidome of infected mosquitoes that were AGPAT1 depleted or not. AGPAT1-depletion increased aminoPL concentrations at 7 dpi (Fig 4E; S9 Table). Specifically, one PC, four PEs and one glycerophosphoethanolamine were upregulated. By artificially modulating the metabolome, we revealed that AGPAT1 depletion favors DENV by increasing aminoPL concentrations.

When profiling metabolic changes throughout mosquito DENV cycle, we observed that aminoPLs were reduced at the end of DENV cycle (Fig 1C). To test whether this reduction occurred when aminoPL concentrations were increased by AGPAT1 depletion (Fig 4E), we examined how DENV modifies the lipidome in AGPAT1-depleted mosquitoes. Control mosquitoes were depleted of AGPAT1 and fed a non-infectious blood meal. At 7 dpi, aminoPLs were drastically decreased by DENV despite AGPAT1-depletion enhancement (Fig 4F; S10 Table). Specifically, three PEs and five PCs were reduced more than 100 folds. These results suggest that, by reproducing infection-induced aminoPL reconfiguration, AGPAT1 depletion amplifies the DENV reconfiguration, thereby promoting infection. Altogether, our results indicate that DENV inhibits *AGPAT1* expression to increase the amplitude of aminoPLs consumption/redirection for virus multiplication.

Discussion

By combining observational and manipulative approaches *in vitro* and *in vivo*, we deciphered how DENV hijacks the mosquitoes' metabolome. We deployed metabolomic profiling throughout the mosquito DENV cycle, and revealed an overall increase in aminoPLs, followed by a reduction at the end of the cycle. We next showed that aminoPL reconfiguration is partially mediated by infection-induced *AGPAT1* down-regulation, which increases aminoPL concentrations. Because AGPAT1 depletion promotes virus multiplication, our study discovers a mechanism whereby DENV reconfigures the metabolome to its benefit. Furthermore, we show that in an environment richer in aminoPLs (AGPAT1 depletion), infection reduces aminoPL concentrations at a higher and earlier rate than in a wild-type organism, while increasing virus production. This suggests that DENV consumes/redirects aminoPLs, although this is based on correlations between indirect lipidome alteration and virus multiplication. Altogether, we propose a model whereby DENV regulates aminoPL enzymes to increase aminoPL concentrations early during the cycle and consumes/redirects them for its multiplication.

We revealed that DENV-induced phospholipidome reconfiguration is partially mediated by lowering *AGPAT1* expression. Indeed, *AGPAT1* was downregulated upon infection and its depletion partially recapitulated DENV-induced aminoPL reconfiguration both *in vitro* and *in vivo*. That we only partially recapitulated the DENV-induced phospholipidome reconfiguration suggests that other enzymes, such as those directly producing and those hydrolyzing aminophospholipids [43], play a role. AGPAT enzymes can influence PL composition at several levels. By catalyzing the second acylation that produces PA (Fig 2A), AGPAT enzymes are responsible for a rate-limiting step in PL biogenesis [35]. However, we did not observe PA reduction upon AGPAT1 depletion and instead reported an alteration of aminoPLs. This pattern was previously observed in hAGPAT-depleted human cells [40] and was attributed to compensation by other AGPAT isoforms. Lack of AGPAT1 may unbalance substrate competition with other isoforms with different lysoPA and acyl affinity [44]. Consequently, this can

influence PA structure and subsequent PL composition. In addition, certain AGPAT isoforms can transfer acyls to lysoPL, thus, participating in PL remodeling independently of *de novo* synthesis [45]. In mosquito cells, AGPAT2 depletion also altered PL profile. However, *AGPAT2* expression is not reduced by DENV infection and its depletion does not impact virus multiplication. The correlation between expression of *AGPAT* isoforms and their impacts on infection indicates a fine regulation of metabolism by DENV, and identifies a new mechanism by which the virus hijacks the host phospholipidome.

The expression of *AGPATs* is regulated either directly through their transcription factors or indirectly by altering the endoplasmic reticulum topology. Sterol regulatory element binding proteins (SREBP) coordinate fatty acid, sterol and phospholipid metabolisms by transcriptionally regulating enzymes, such as acyl transferases [46]. DENV protein interaction with SREBP, as described with other transcription factors [47], could alter *AGPAT* expressions. In support of this, chemical inhibition of SREBP blocks DENV replication [48]. Alternatively, AGPAT activity is influenced by substrate accessibility, which depends on membrane topology [36]. Several DENV proteins are embedded in the endoplasmic reticulum membrane and modify its topology [49,50]. This can alter endoplasmic reticulum-located AGPAT activity, PL profile and activate acyl-transferase expressions to restore homeostasis [51].

DENV intricately interacts with aminoPL-containing membranes and a change as we report can alter several stages of its life-cycle, such as entry, replication, translation, assembly and egress [7,16]. DENV interacts with the plasma membrane for entry and fusion, and with the endoplasmic reticulum membrane for translation, replication and assembly [28]. These membranes are mostly composed of PE and PC, and PS in lower proportions [52]. Their fluidity and topology are determined by the aminoPL structure and concentration. The cylindrical shape of PCs stabilizes lipid bilayers, whereas the conical shape of PEs induces curvature. Several flavivirus-aminoPL interactions have been described in human cells. PLs present in the DENV envelope are recognized by cellular ligands and mediate entry [53,54]. Replication of flaviviruses induce the invagination of the endoplasmic reticulum by altering PE [55,56] and lysoPC compositions [43]. Alternatively, *AGPAT* expressions could alter anti-viral immune response [57]. In mammalian cells, *AGPAT* overexpressions amplify cellular signaling of cytokine [58] that can reduce DENV infection in mosquito cells [59]. Although the precise function of AGPAT1-regulated aminoPLs is unknown and may be multifactorial, previous studies and ours indicate that membrane aminoPL reconfiguration influences DENV multiplication.

In conclusion, our study determines the importance of aminoPL reconfiguration for DENV infection. We also reveal the underlying mechanism for viral phospholipidome reconfiguration. The intricate metabolic interactions between DENV and mosquitoes represents a target to control transmission.

Materials and methods

Aedes aegypti mosquitoes and cell line

The *Aedes aegypti* colony was established in 2010 from Singapore and was reared at 28˚C and 60% relative humidity with 12h:12h light:dark cycle. Eggs hatched in milliQ water were fed with a mix of fish food (TetraMin fish flakes), yeast and liver powder (MP Biomedicals). Adults were held in rearing cages (Bioquip) supplemented with water and 10% sucrose solution. *Aedes aegypti* Aag2 cells [60] were grown in RPMI-1640 medium (Gibco) with 10% filtered fetal bovine serum (FBS) (Hyclone) and 1% Penicillin-Streptomycin (Gibco). For media supplementation, 2 mM of ethanolamine (Sigma) was added to Aag2 growth medium. Cells were maintained in vented culture flasks in a humidified incubator with 5% CO_2 at 28˚C. BHK-21

(baby hamster kidney) (ATCC CCL-10) cells were grown in the same media and maintained at 37˚C with 5% CO_2.

Dengue virus

Dengue virus serotype-2 strain ST (DENV) was collected from the Singapore General Hospital in 1997 [61]. DENV was propagated alternatively in Vero (ATCC CCL-81) and C6/36 (ATCC CRL-1660) cells. Virus titer was determined by plaque assay using BHK-21 cells. DENV supernatant was exposed to UV light from biosafety cabinet (Sterilgard III advance, the Baker Company) for 1h at room temperature for inactivation.

Oral infection of mosquitoes

Two- to four-day-old adult female mosquitoes were starved for 24h before oral feeding on a blood meal containing 40% volume of washed erythrocytes from SPF pig's blood (PWG Genetics, Singapore), 5% of 100 mM ATP (Thermo Fisher Scientific), 5% of human serum (Sigma-Aldrich) and 50% of DENV-2 in RPMI media (Gibco). The virus titer in the blood meal was 2 x 10^7 pfu/ml and validated by plaque assay. Blood was maintained at 37˚C using hemotek membrane feeder system (Discovery Workshops) with sausage casing for 1.5 h. A control group was allowed to feed on the same mix of SPF pig blood meal without virus. Engorged mosquitoes were visually selected and maintained at 28˚C with water and 10% sucrose solution.

Cell inoculation

5 x 10^6 cells were inoculated with DENV at an MOI of 5 in serum-free RPMI media for 1h. The inoculum was then replaced with 2% FBS RPMI media. Mock infection was used as negative control.

Metabolite extraction from mosquitoes, midguts and cells

At 1, 7 and 14 days post-oral feeding, 10 mosquitoes in 500 μl of ice-cold methanol and water ratio of 80:20 (LCMS grade, Thermo Fisher) were homogenized with bead Mill homogenizer (FastPrep-24, MP Biomedicals) and sonicated for 15 min in an ultrasonic bath (J.R. Selecta) at 4˚C. Homogenates were centrifuged at 10,000 rpm for 1 min at 4˚C to collect 400 μl supernatant. Pellets were further extracted twice by addition of 500 μl of methanol:water (80:20), followed by centrifugation. Supernatants were combined and vacuum-dried (Speed-Vac, Thermo-Scientific) before storage at -20˚C. At 1 and 7 days post-oral feeding, 10 midguts were homogenized in 200 μl of the methanol:water (80:20) solution and 120 μl of supernatant was collected three times with the same protocol. At 6, 12, 24 and 48 h post-inoculation, cells were washed with room temperature 0.9% NaCl and collected in 2 ml of ice-cold methanol:water (80:20) by scraping. Cells were homogenized by ultrasound and extracted thrice as detailed above by adding 500 μl of ice-cold methanol:water (80:20). Three biological replicates were conducted per condition.

LC-HRMS metabolism profiling

Dry extracts were normalized at 2 mg/mL in methanol:water 80:20 solution and metabolites were detected using two methods. Compounds from medium range polarity to lipophilic substances were detected using a UPLC-UV-QTOF-MS^E instrument (Xevo G2 QTof, Waters) mounted on an electrospray ionization (ESI) source, with a UPLC BEH C18 Acquity column (100 × 2.1 mm i.d., 1.7 μm, Waters) equipped with a guard column. Mobile phase A was of

0.1% formic acid in water, B was 0.1% formic acid in acetonitrile. The flow rate was 400 μl/min and the gradient ran with 98% A for 0.5 min to 20% B over 3.5 min, 98% B for 8 min, held at 98% B for 3 min, and returned in 0.5 min to initial conditions (98% A), finally held for 3.5 min to assure equilibration before the subsequent analysis. Detection was performed at 254 nm by TOF-MS in both electrospray (ESI) negative mode with voltage at 2.5 kV and positive mode with voltage at 3.0 kV. The m/z range was 100–1200 Da with a scan time of 0.1 s. All detected ions were fragmented using MS^E scan with an energy collision ramp from 20 to 50 eV. All analyses were acquired using leucine enkephalin as the lock mass at a concentration of 400 pg/μl and flow rate 7 μl/min. The injection volume was 2 μl and samples were kept at 10˚C during the whole analysis.

Polar metabolites were profiled using a UPLC-LTQ Orbitrap XL instrument (Ultimate 3000, Thermo Fisher Scientific, Hemel Hempstead, UK) set at 15,000 resolution, with a ZicpHilic column (150 × 2.1 mm i.d., 5 μm, SeQuant, Merck). Mobile phase A was 20 mM ammonium acetate buffered at pH 9 and B was acetonitrile. The flow rate was 250 μl/min and the gradient ran from 90% B for 0.5 min to 40% B over 18 min, held at 40% B for a further 3 min, and then returned in 0.5 min to initial conditions (90% B) finally held for 5 min before subsequent analysis. The *m/z* range was 100–1500 and ISpray voltage at 4.2 kV (positive mode) and 3.0 kV (negative mode). Each full MS scan was followed by data dependent MS/MS on the two most intense ions using stepped CID fragmentation mode at 35% normalized collision energy, isolation width of 2 u and activation Q set at 0.250.

Data analysis and visualization

Peak detection and alignment were performed using MS-DIAL (ver. 3.12) [62]. Peak annotation was done using MS-finder (ver. 3.04) [63] with HMDB, ChEBI, LipidMAPS and LipidBlast databases, allowing a level 2.2 of metabolite identification [64,65]. Data were normalized by total ion chromatogram (TIC) and features lower than 2-fold average blank were removed. Each LC-HRMS condition was analyzed separately before concatenation. Data were normalized by auto-scaling before selecting regulated metabolites with more than 2-fold intensity change and a p-value < 0.05 with FDR adjustment as indicate by unpaired t-test using MetaboAnalyst (ver. 4.0) [66]. To account for physiological variations between the different time-tissue combinations, the t-tests were done by comparing the same tissue in infected and uninfected conditions within each time. Uninfected condition was used as control. PCA for quality control was performed with MetaboAnalyst (ver. 4.0). MS/MS similarity metabolic networks with cut-off $> 60\%$ were generated with MS-Finder for each LC-HRMS mode-tissue combination.

dsRNA-mediated RNAi

Templates for dsRNA against AAEL011898 and AAEL001000 were PCR amplified with primers flanked with a T7 promoter (S3 Table) from mosquito cDNA. dsRNA was synthetized with megaScript T7 transcription kit (Thermo Fisher Scientific), extracted in DEPC-treated water and annealed by slowly cooling down from 95˚C. Control dsRNA targeting LacZ was produced [67]. Two- to five-day-old cold-anesthetized female mosquitoes were intrathoracically injected with 69 nl of 3 mg/ml of dsRNA by using Nanoject II injector (Drummond Scientific). Mosquitoes were then maintained at 28˚C with water and 10% sucrose solution before oral infection as detailed above. Cells were seeded at 2 x 10^5 per 24-well plate and transfected after 24h with 1 μg of dsRNA by using TransIT-mRNA Transfection kit (Mirusbio). Infection with DENV was done one day post transfection.

Quantification of DENV genomic RNA

Single mosquitoes or tissues were homogenized in 350μl of TRK lysis buffer (Omega Bio-tek) using a bead Mill homogenizer (FastPrep-24, MP Biomedicals). Total RNA was extracted using E.Z.N.A. Total RNA kit I (Omega Bio-tek) and eluted in 30μl of DEPC-treated water. Genomic RNA (gRNA) was quantified with one-step RT-qPCR using iTaq Universal probe kit (Bio-Rad) and primers and probes targeting the DENV Envelope [68]. The 12.5 μl reaction mix contained 1 μM of forward and reverse primers, 0.125 μM of probe and 4 μl of RNA extract. Quantification was conducted on a CFX96 Touch Real-Time PCR Detection System (Bio-Rad). Thermal profile was 50˚C for 10 min, 95˚C for 1 min and 40 cycles of 95˚C for 10 sec and 60˚C for 15 sec.

An absolute standard curve was generated by amplifying fragments containing the qPCR target using a forward primer tagged with T7 promoter; forward: 5'-CAGGATAAGAGGTT CGTCTG-3' and reverse: 5'-TTGACTCTTGTTTATCCGCT-3', resulting in a 453bp fragment. The fragment was reverse transcribed using MegaScript T7 transcription kit (Ambion) and purified using E.Z.N. A. Total RNA kit I. The total amount of RNA was quantified using a Nanodrop (Thermo Fisher Scientific) to estimate copy number. Ten times serial dilutions were made and used to generate absolute standard equation for gRNA. In each subsequent RT-qPCR plate, five standards were added to adjust for threshold variation between plates. The infection rate was calculated by dividing the number of samples with detectable gRNA over total number of samples.

Titration

Titration was conducted by plaque assay with BHK-21 cells as described previously [69]. Briefly, 80–90% confluent cells were inoculated with serial 10-fold dilutions of samples for 1h. Cells were then incubated with 1% carboxyl-methyl cellulose (CMC) (Merck) for 5 days, fixed with 4% formaldehyde (Merck) -PBS and stained with 1% crystal violet (Sigma-Aldrich) solution to count plaque forming units (pfu).

Quantification of gene expression

Total RNA from five mosquitoes was extracted using E.Z.N.A. Total RNA kit I, treated with RapidOut DNA Removal kit (Thermo Fisher Scientific) and reverse transcribed with iScript cDNA Synthesis Kit (Bio-Rad). Gene expression was quantified using iTaq Universal SYBR Green Supermix (Bio-Rad) and primers detailed in S4 Table. *Actin* expression was used for normalization. Quantification was conducted in a CFX96 Touch Real-Time PCR Detection System (Bio-Rad). Thermal profile was 95˚C for 1 min and 40 cycles of 95˚C for 10 sec and 60˚C for 15 sec. Three biological replicates were conducted.

Statistical analysis

Differences in gRNA copies per infected mosquito were tested on values using unpaired t-test or Mann-Whitney test depending on the normal distribution estimated with D'agostino and Pearson normality test. Differences in percentages were tested using χ^2 test. Tests were performed with GraphPad PRISM software (ver. 6.01).

AGPAT sequence alignment

Amino acid sequence homology was determined by MEGA X software (ver. 10.0.5), using Maximum Likelihood and bootstrapping. FASTA sequences (S5 Table) were retrieved from ncbi.nlm.nih.gov.

Supporting information

S1 Fig. Quantification of DENV infection in Aag2 cells, *A. aegypti* mosquito and midgut. (A) DENV gRNA copies in Aag2 cells at 6, 12, 24 and 48h post-infection with DENV at MOI = 5. Points from 4 repeat and standard errors show geometric mean ± 95% CI. (B) Plaque titer (plaque forming unit—pfu) in supernatant from Aag2 cells at 6, 12, 24 and 48h post-infection. Aag2 cells were infected with DENV at MOI = 5 and virus titer was calculated using plaque assay. Each point represents one well. (C) DENV gRNA copies per infected mosquitoes and dissected midguts at 1, 7 and 14 days post-oral infection with 10^7 pfu/ml. Each point represents one mosquito or midgut. Bars show geometric mean ± 95% CI. (D) Infection rate in whole mosquito and midgut at 1, 7 and 14 days post-oral infection. Bars represent percentages ± s.e.
(TIF)

S2 Fig. LC-HMRS analytical pipeline. Liquid Chromatography-High Resolution Mass Spectrometry (LC-HRMS) pipeline used to detect polar and nonpolar metabolites.
(TIF)

S3 Fig. Spectral similarity network from mosquito MS features. Example of a molecular spectral network for Ae. aegypti mosquito at 14 days post-infection using MS features detected with the non-polar LC condition and MS negative mode. Line length represents the MS/MS score similarity. Ontology for unknown features was determined based on the proximity with database-identified features.
(TIF)

S4 Fig. Ion intensity of regulated metabolites in cells, midguts and mosquitoes infected with DENV and mock. Normalized ion intensity was calculated after total ion chromatography normalization and auto scaling from three biological replicates. Conditions with significantly regulated metabolites (p-value <0.05 and $|\log2 \text{ fold change}| > 1$) were indicated with an asterisk. Only metabolites from the general metabolism (i.e., lipid, carbohydrate, amino acid and peptide, nucleotide and nucleoside, sialic acid) are shown. †, indicates metabolite annotated by spectral similarity. Carbo., carbohydrate; SA, sialic acid; PL, phospholipid; PE, phosphatidylethanolamine; PC, phosphatidylcholine; PS, phosphatidylserine; PA, phosphatidic acid; PI, phosphatidylinositol; PG, phosphatidylglycerol; LysoPS, lysophosphatidylserine; LysoPC, lysophosphatidylcholine; LysoPE, lysophosphatidylethanolamine; LysoPG, lysophosphatidylglycerol; LysoPI, lysophosphatidylinositol; SM, Sphingomyelin; DAG, Diacylglycerol; MAG, Monoacylglycerol; FAHFA, Fatty Acid ester of Hydroxyl Fatty Acid; NAE, N-acylethanolamine; HEA, Heneicosanoic acid; pep., peptides.
(TIF)

S5 Fig. AGPAT genes are regulated by DENV infection, from Colpitts transcriptomic data. *Ae. aegypti* female mosquitoes were inoculated with DENV serotype 2 and collected at 1, 2 and 7 days post inoculation for transcriptomic analysis using microarray. Data from 3 separate infections. AGAPAT 1–5 were found significantly regulated by DENV infection. Data retrieved from (Colpitts et al., 2011, PMID: 21909258).
(TIF)

S6 Fig. UV-inactivated DENV does not regulate *AGPAT1* expression. Aag2 cells were infected with an MOI of 5 of DENV (DENV-WT), UV-inactivated DENV (DENV-UV) or mock. Cells were analyzed at 24 and 48 hours post-infection (hpi). (A) DENV gRNA copies. Bars show geometric means ± 95% C.I. (B) *AGPAT1* expression relative to *Actin* level. Bars show arithmetic means ± s.e.m. (A-B) Each point represents an independent well. ***, p-

value < 0.001 as determined by unpaired t-test.
(TIF)

S7 Fig. Metabolomic impact of AGPAT1 and AGPAT2 depletion and infection in cells as measured by ion intensity. Aag2 cells were transfected with dsRNA against *AGPAT1* (dsAGPAT1) or *AGPAT2* (dsAGPAT2) or a dsRNA control (dsControl). 24h later, cells were infected with DENV at MOI of 1. (A) Ion intensity of regulated metabolites in mock cells at 72h post transfection. (B) Ion intensity of regulated metabolites in infected cells at 24 hpi. Normalized ion intensity was calculated after total ion chromatography normalization and auto scaling from three replicates. Conditions with significantly regulated metabolites (p-value <0.05 and $|\log2 \text{ fold change}| > 1$) were indicated with an asterisk. PE, phosphatidylethanolamine; PC, phosphatidylcholine; PS, phosphatidylserine; LPE, lysophosphatidylethanolamine.
(TIF)

S8 Fig. *AGPAT1* and *2* expression in cells after the other AGPAT depletion. Aag2 cells were transfected with dsRNA against *AGPAT1* or *2* (dsAGPAT1 or 2). Control cells were transfected with dsRNA control (dsControl). Cells were collected 72h post dsRNA. (A) *AGPAT1* expression in AGPAT2-depleted cells. (B) *AGPAT2* expression in AGPAT1-depleted cells. Bars show mean ± s.e.m from 3 biological replicates. ns, non-significant, as indicated by unpaired t-test.
(TIF)

S9 Fig. Ethanolamine supplementation partially rescued infection increase upon AGPAT1 depletion. 24h before infection, Aag2 cells were transfected with dsRNA against AGPAT1 (dsAGPAT1) or with dsRNA control (dsControl) and reared in standard growth media or the same media supplemented with 2mM ethanolamine. Cells were infected with DENV at MOI of 1 and gRNA copy was quantified 48h later. Bars show geometric means ± 95% C.I. Each point represents an independent well. *, p-value < 0.05; **, p-value < 0.01 as determined by unpaired t-test.
(TIF)

S10 Fig. Metabolomic impact of AGPAT1 and AGPAT2 depletion in uninfected mosquitoes as measured by ion intensity. Two days post dsRNA injection against *AGPAT1* (dsAGPAT1) or control (dsControl), mosquitoes were orally infected with DENV at 10^7 pfu/ml. Metabolomic analyses were performed at 2 and 7 dpi. Normalized ion intensity was calculated after total ion chromatography normalization and auto scaling from three replicates. Conditions with significantly regulated metabolites (p-value <0.05 and $|\log2 \text{ fold change}| > 1$) were indicated with an asterisk.
(TIF)

S11 Fig. Impact of AGPAT1-depletion in mosquitoes on DENV infection rate and gRNA copies. Mosquitoes were injected with either dsRNA against *AGPAT1* (dsAGPAT1) or dsRNA control (dsControl). Two days post injection, mosquitoes were orally fed with either non-infectious blood or DENV infectious blood. Impact of AGPAT1 depletion on (A) infection rate and (B) DENV gRNA copies at 2 days post oral infection (dpi) with 10^7 pfu/ml. (C-E) Impact of AGPAT1 depletion on infection rate (C) and DENV gRNA copies at 2 (D) and 7 (E) dpi with 10^6 pfu/ml. Bars indicate percentage ± s.e. (A, C) or geometric means ± 95% C.I. (B, D, E) with each dot representing one mosquito. *, p-value < 0.05 as indicated by Mann-Whitney test.
(TIF)

S1 Table. Identification of mosquito specific metabolites by spectral similarity.
(DOCX)

S2 Table. Metabolites detected from cell, midgut and whole mosquito with differential regulation upon DENV infection. The three tabs contain compound detected on cell, midgut and mosquito with the following information: ionization mode (positive and negative), phase detection (polar and non-polar), the mass average m/z between replicate, the retention time average Rt in minutes between replicates, the MS/MS spectrum fragmentation and intensity, adducts [M+H]+ and [M-H]-, metabolites of importance in Fig 1C, regulated compound with abundance between DENV-infected and uninfected samples (p-value < 0.05 and $|\log2 \text{ fold change}| \geq 1$) and annotation classes with the first 3 ranks of identification by MS-Finder.
(XLSX)

S3 Table. Primers for dsRNA.
(DOCX)

S4 Table. Primers for Real-Time qPCR.
(DOCX)

S5 Table. AGPAT FASTA protein sequences.
(DOCX)

S6 Table. Metabolites detected from uninfected cell, after AGPAT1 or AGPAT2 depletion. The table contains compound detected on cell with the following information: ionization mode (positive and negative), the mass average m/z between replicate, the retention time average Rt in minutes between replicates, the MS/MS spectrum fragmentation and intensity, adducts [M+H]+ and [M-H]-, metabolites of importance in Fig 3C, regulated compound with abundance between dsAGPAT1 or 2 and dsControl samples (p-value < 0.05, $|\log2 \text{ fold change}| \geq 1$) and annotation classes with the first 3 ranks of identification by MS-Finder.
(XLSX)

S7 Table. Metabolites detected from DENV-infected cell at 48 hpi, after AGPAT1 or AGPAT2 depletion. The table contains compound detected on cell with the following information: ionization mode (positive and negative), the mass average m/z between replicate, the retention time average Rt in minutes between replicates, the MS/MS spectrum fragmentation and intensity, adducts [M+H]+ and [M-H]-, metabolites of importance in Fig 3E, regulated compound with abundance between dsAGPAT1 or 2 and dsControl samples (p-value < 0.05, $|\log2 \text{ fold change}| \geq 1$) and annotation classes with the first 3 ranks of identification by MS-Finder.
(XLSX)

S8 Table. Metabolites detected from uninfected mosquito after AGPAT1 depletion. The two tabs contain compound detected on cell after 2 or 7 days post blood feeding with the following information: ionization mode (positive and negative), the mass average m/z between replicate, the retention time average Rt in minutes between replicates, the MS/MS spectrum fragmentation and intensity, adducts [M+H]+ and [M-H]-, metabolites of importance in Fig 4B, regulated compound with abundance between dsAGPAT1 and dsControl samples (p-value < 0.05, $|\log2 \text{ fold change}| \geq 1$) and annotation classes with the first 3 ranks of identification by MS-Finder.
(XLSX)

S9 Table. Metabolites detected from DENV-infected mosquito after dsAGPAT1 depletion or dsControl. The table contains compound detected on cell with the following information:

ionization mode (positive and negative), the mass average m/z between replicate, the retention time average Rt in minutes between replicates, the MS/MS spectrum fragmentation and intensity, adducts [M+H]+ and [M-H]-, metabolites of importance in Fig 4E, regulated compound with abundance between dsAGPAT1 and dsControl samples (p-value < 0.05, $|\log2$ fold change$| \geq 1$) and annotation classes with the first 3 ranks of identification by MS-Finder.
(XLSX)

S10 Table. Metabolites detected from DENV-infected or uninfected mosquito after AGPAT1 depletion. The table contains compound detected on cell with the following information: ionization mode (positive and negative), the mass average m/z between replicate, the retention time average Rt in minutes between replicates, the MS/MS spectrum fragmentation and intensity, adducts [M+H]+ and [M-H]-, metabolites of importance in Fig 4F, regulated compound in dsAGPAT1 condition only, regulated compound with abundance between DENV-infected and Mock samples in dsControl or dsAGPAT1 condition (p-value < 0.05, $|$ log2 fold change$| \geq 1$) and annotation classes with the first 3 ranks of identification by MS-Finder.
(XLSX)

Acknowledgments

We are grateful to Dr. Mariano Garcia-Blanco for constant support and the Pompon/Garcia-Blanco's team for comments on a previous version. We thank Dr. Eng Eong Ooi for providing the ST virus. We also thank the Mass spectrometry platform, Université de Toulouse, ICT, UPS, Toulouse, France.

Author Contributions

Conceptualization: Dorothée Missé, Guillaume Marti, Julien Pompon.

Data curation: Thomas Vial.

Formal analysis: Thomas Vial, Guillaume Marti, Julien Pompon.

Funding acquisition: Eric Deharo, Julien Pompon.

Investigation: Thomas Vial, Wei-Lian Tan, Benjamin Wong Wei Xiang, Guillaume Marti.

Methodology: Thomas Vial, Guillaume Marti, Julien Pompon.

Supervision: Eric Deharo, Guillaume Marti, Julien Pompon.

Visualization: Thomas Vial.

Writing – original draft: Thomas Vial, Guillaume Marti, Julien Pompon.

Writing – review & editing: Thomas Vial, Dorothée Missé, Eric Deharo, Guillaume Marti, Julien Pompon.

References

1. Gubler DJ. The Global Emergence/Resurgence of Arboviral Diseases As Public Health Problems. Arch Med Res. 2002; 33: 330–342. https://doi.org/10.1016/s0188-4409(02)00378-8 PMID: 12234522
2. Bhatt S, Gething PW, Brady OJ, Messina JP, Farlow AW, Moyes CL, et al. The global distribution and burden of dengue. Nature. 2013; 496: 504–507. https://doi.org/10.1038/nature12060 PMID: 23563266
3. Capeding MR, Tran NH, Hadinegoro SRS, Ismail HIHM, Chotpitayasunondh T, Chua MN, et al. Clinical efficacy and safety of a novel tetravalent dengue vaccine in healthy children in Asia: a phase 3,

randomised, observer-masked, placebo-controlled trial. The Lancet. 2014; 384: 1358–1365. https://doi.org/10.1016/S0140-6736(14)61060-6

4. WHO. Dengue vaccine: WHO position paper–September 2018. 2018. Available: http://apps.who.int/iris/bitstream/handle/10665/274315/WER9336.pdf?ua=1
5. WHO SEARO, Regional Office for South-East Asia. Comprehensive guidelines for prevention and control of dengue and dengue haemorrhagic fever. New Delhi, India: World Health Organization Regional Office for South-East Asia; 2011. Available: http://www.searo.who.int/entity/vector_borne_tropical_diseases/documents/SEAROTPS60/en/
6. Liu N. Insecticide Resistance in Mosquitoes: Impact, Mechanisms, and Research Directions. Annu Rev Entomol. 2015; 60: 537–559. https://doi.org/10.1146/annurev-ento-010814-020828 PMID: 25564745
7. Villareal VA, Rodgers MA, Costello DA, Yang PL. Targeting host lipid synthesis and metabolism to inhibit dengue and hepatitis C viruses. Antiviral Res. 2015; 124: 110–121. https://doi.org/10.1016/j.antiviral.2015.10.013 PMID: 26526588
8. Pando-Robles V, Oses-Prieto JA, Rodríguez-Gandarilla M, Meneses-Romero E, Burlingame AL, Batista CVF. Quantitative proteomic analysis of Huh-7 cells infected with Dengue virus by label-free LC–MS. J Proteomics. 2014; 111: 16–29. https://doi.org/10.1016/j.jprot.2014.06.029 PMID: 25009145
9. Allonso D, Andrade IS, Conde JN, Coelho DR, Rocha DCP, da Silva ML, et al. Dengue Virus NS1 Protein Modulates Cellular Energy Metabolism by Increasing Glyceraldehyde-3-Phosphate Dehydrogenase Activity. J Virol. 2015; 89: 11871–11883. https://doi.org/10.1128/JVI.01342-15 PMID: 26378175
10. Fontaine KA, Sanchez EL, Camarda R, Lagunoff M. Dengue Virus Induces and Requires Glycolysis for Optimal Replication. Sandri-Goldin RM, editor. J Virol. 2015; 89: 2358–2366. https://doi.org/10.1128/JVI.02309-14 PMID: 25505078
11. Birungi G, Chen SM, Loy BP, Ng ML, Li SFY. Metabolomics Approach for Investigation of Effects of Dengue Virus Infection Using the EA.hy926 Cell Line. J Proteome Res. 2010; 9: 6523–6534. https://doi.org/10.1021/pr100727m PMID: 20954703
12. El-Bacha T, Midlej V, Pereira da Silva AP, Silva da Costa L, Benchimol M, Galina A, et al. Mitochondrial and bioenergetic dysfunction in human hepatic cells infected with dengue 2 virus. Biochim Biophys Acta BBA—Mol Basis Dis. 2007; 1772: 1158–1166. https://doi.org/10.1016/j.bbadis.2007.08.003 PMID: 17964123
13. Heaton NS, Randall G. Dengue Virus-Induced Autophagy Regulates Lipid Metabolism. Cell Host Microbe. 2010; 8: 422–432. https://doi.org/10.1016/j.chom.2010.10.006 PMID: 21075353
14. Diop F, Vial T, Ferraris P, Wichit S, Bengue M, Hamel R, et al. Zika virus infection modulates the metabolomic profile of microglial cells. PLOS ONE. 2018; 13: e0206093. https://doi.org/10.1371/journal.pone.0206093 PMID: 30359409
15. Cui L, Lee YH, Kumar Y, Xu F, Lu K, Ooi EE, et al. Serum Metabolome and Lipidome Changes in Adult Patients with Primary Dengue Infection. Michael SF, editor. PLoS Negl Trop Dis. 2013; 7: e2373. https://doi.org/10.1371/journal.pntd.0002373 PMID: 23967362
16. Martín-Acebes MA, Vázquez-Calvo Á, Saiz J-C. Lipids and flaviviruses, present and future perspectives for the control of dengue, Zika, and West Nile viruses. Prog Lipid Res. 2016; 64: 123–137. https://doi.org/10.1016/j.plipres.2016.09.005 PMID: 27702593
17. Perera R, Riley C, Isaac G, Hopf-Jannasch AS, Moore RJ, Weitz KW, et al. Dengue Virus Infection Perturbs Lipid Homeostasis in Infected Mosquito Cells. PLoS Pathog. 2012; 8. https://doi.org/10.1371/journal.ppat.1002584 PMID: 22457619
18. Chotiwan N, Andre BG, Sanchez-Vargas I, Islam MN, Grabowski JM, Hopf-Jannasch A, et al. Dynamic remodeling of lipids coincides with dengue virus replication in the midgut of Aedes aegypti mosquitoes. PLOS Pathog. 2018; 14: e1006853. https://doi.org/10.1371/journal.ppat.1006853 PMID: 29447265
19. Xi Z, Ramirez JL, Dimopoulos G. The Aedes aegypti Toll Pathway Controls Dengue Virus Infection. PLoS Pathog. 2008; 4. https://doi.org/10.1371/journal.ppat.1000098 PMID: 18604274
20. Martín-Acebes MA, Blázquez A-B, Jiménez de Oya N, Escribano-Romero E, Saiz J-C. West Nile Virus Replication Requires Fatty Acid Synthesis but Is Independent on Phosphatidylinositol-4-Phosphate Lipids. Wang T, editor. PLoS ONE. 2011; 6: e24970. https://doi.org/10.1371/journal.pone.0024970 PMID: 21949814
21. Heaton NS, Perera R, Berger KL, Khadka S, LaCount DJ, Kuhn RJ, et al. Dengue virus nonstructural protein 3 redistributes fatty acid synthase to sites of viral replication and increases cellular fatty acid synthesis. Proc Natl Acad Sci U S A. 2010; 107: 17345–17350. https://doi.org/10.1073/pnas.1010811107 PMID: 20855599
22. Fagone P, Jackowski S. Membrane phospholipid synthesis and endoplasmic reticulum function. J Lipid Res. 2009; 50: S311–S316. https://doi.org/10.1194/jlr.R800049-JLR200 PMID: 18952570
23. Takeuchi K, Reue K. Biochemistry, physiology, and genetics of GPAT, AGPAT, and lipin enzymes in triglyceride synthesis., Biochemistry, physiology, and genetics of GPAT, AGPAT, and lipin enzymes in

triglyceride synthesis. Am J Physiol Endocrinol Metab Am J Physiol—Endocrinol Metab. 2009;296, 296: E1195, E1195–209. https://doi.org/10.1152/ajpendo.90958.2008 PMID: 19336658

24. Athenstaedt K, Daum G. Phosphatidic acid, a key intermediate in lipid metabolism. Eur J Biochem. 1999; 266: 1–16. https://doi.org/10.1046/j.1432-1327.1999.00822.x PMID: 10542045

25. Gillespie LK, Hoenen A, Morgan G, Mackenzie JM. The Endoplasmic Reticulum Provides the Membrane Platform for Biogenesis of the Flavivirus Replication Complex. J Virol. 2010; 84: 10438–10447. https://doi.org/10.1128/JVI.00986-10 PMID: 20686019

26. Aktepe TE, Mackenzie JM. Shaping the flavivirus replication complex: It is curvaceous! Cell Microbiol. 2018; 20: e12884. https://doi.org/10.1111/cmi.12884 PMID: 29933527

27. Salazar MI, Richardson JH, Sánchez-Vargas I, Olson KE, Beaty BJ. Dengue virus type 2: replication and tropisms in orally infected Aedes aegypti mosquitoes. BMC Microbiol. 2007; 7: 9. https://doi.org/10.1186/1471-2180-7-9 PMID: 17263893

28. Barrows Nicholas J., Mariano A. Garcia-Blanco. Biochemistry and Molecular Biology of Flaviviruses. Chem Rev. 2018; 118: 4448–4482. https://doi.org/10.1021/acs.chemrev.7b00719 PMID: 29652486

29. Tsugawa H. Advances in computational metabolomics and databases deepen the understanding of metabolisms. Curr Opin Biotechnol. 2018; 54: 10–17. https://doi.org/10.1016/j.copbio.2018.01.008 PMID: 29413746

30. van Meer G, Voelker DR, Feigenson GW. Membrane lipids: where they are and how they behave. Nat Rev Mol Cell Biol. 2008; 9: 112–124. https://doi.org/10.1038/nrm2330 PMID: 18216768

31. Vance JE. Phospholipid Synthesis and Transport in Mammalian Cells. Traffic. 2015; 16: 1–18. https://doi.org/10.1111/tra.12230 PMID: 25243850

32. Lagace TA, Ridgway ND. The role of phospholipids in the biological activity and structure of the endoplasmic reticulum. Biochim Biophys Acta BBA—Mol Cell Res. 2013; 1833: 2499–2510. https://doi.org/10.1016/j.bbamcr.2013.05.018 PMID: 23711956

33. Yamashita A, Hayashi Y, Nemoto-Sasaki Y, Ito M, Oka S, Tanikawa T, et al. Acyltransferases and transacylases that determine the fatty acid composition of glycerolipids and the metabolism of bioactive lipid mediators in mammalian cells and model organisms. Prog Lipid Res. 2014; 53: 18–81. https://doi.org/10.1016/j.plipres.2013.10.001 PMID: 24125941

34. Mackenzie JM, Khromykh AA, Parton RG. Cholesterol Manipulation by West Nile Virus Perturbs the Cellular Immune Response. Cell Host Microbe. 2007; 2: 229–239. https://doi.org/10.1016/j.chom.2007.09.003 PMID: 18005741

35. Yamashita A, Hayashi Y, Matsumoto N, Nemoto-Sasaki Y, Oka S, Tanikawa T, et al. Glycerophosphate/Acylglycerophosphate Acyltransferases. Biology. 2014; 3: 801–830. https://doi.org/10.3390/biology3040801 PMID: 25415055

36. Dircks LK, Ke J, Sul HS. A Conserved Seven Amino Acid Stretch Important for Murine Mitochondrial Glycerol-3-phosphate Acyltransferase Activity. J Biol Chem. 1999; 274: 34728–34734. https://doi.org/10.1074/jbc.274.49.34728 PMID: 10574940

37. Lu B, Jiang YJ, Zhou Y, Xu FY, Hatch GM, Choy PC. Cloning and characterization of murine 1-acyl-sn-glycerol 3-phosphate acyltransferases and their regulation by PPARalpha in murine heart. Biochem J. 2005; 385: 469–477. https://doi.org/10.1042/BJ20041348 PMID: 15367102

38. Yamashita A, Nakanishi H, Suzuki H, Kamata R, Tanaka K, Waku K, et al. Topology of acyltransferase motifs and substrate specificity and accessibility in 1-acyl-sn-glycero-3-phosphate acyltransferase 1. Biochim Biophys Acta BBA—Mol Cell Biol Lipids. 2007; 1771: 1202–1215. https://doi.org/10.1016/j.bbalip.2007.07.002 PMID: 17707131

39. Colpitts TM, Cox J, Vanlandingham DL, Feitosa FM, Cheng G, Kurscheid S, et al. Alterations in the Aedes aegypti Transcriptome during Infection with West Nile, Dengue and Yellow Fever Viruses. Rice CM, editor. PLoS Pathog. 2011; 7: e1002189. https://doi.org/10.1371/journal.ppat.1002189 PMID: 21909258

40. Gale SE, Frolov A, Han X, Bickel PE, Cao L, Bowcock A, et al. A Regulatory Role for 1-Acylglycerol-3-phosphate-O-acyltransferase 2 in Adipocyte Differentiation. J Biol Chem. 2006; 281: 11082–11089. https://doi.org/10.1074/jbc.M509612200 PMID: 16495223

41. Merrill AH. Sphingolipid and Glycosphingolipid Metabolic Pathways in the Era of Sphingolipidomics. Chem Rev. 2011; 111: 6387–6422. https://doi.org/10.1021/cr2002917 PMID: 21942574

42. Lipton BA, Davidson EP, Ginsberg BH, Yorek MA. Ethanolamine metabolism in cultured bovine aortic endothelial cells. J Biol Chem. 1990; 265: 7195–7201. PMID: 2110161

43. Liebscher S, Ambrose RL, Aktepe TE, Mikulasova A, Prier JE, Gillespie LK, et al. Phospholipase A2 activity during the replication cycle of the flavivirus West Nile virus. PLoS Pathog. 2018;14. https://doi.org/10.1371/journal.ppat.1007029 PMID: 29709018

44. Hollenback D, Bonham L, Law L, Rossnagle E, Romero L, Carew H, et al. Substrate specificity of lysophosphatidic acid acyltransferase β—evidence from membrane and whole cell assays. J Lipid Res. 2006; 47: 593–604. https://doi.org/10.1194/jlr.M500435-JLR200 PMID: 16369050

45. Prasad SS, Garg A, Agarwal AK. Enzymatic activities of the human AGPAT isoform 3 and isoform 5: localization of AGPAT5 to mitochondria. J Lipid Res. 2011; 52: 451–462. https://doi.org/10.1194/jlr.M007575 PMID: 21173190

46. Coleman RA, Lee DP. Enzymes of triacylglycerol synthesis and their regulation. Prog Lipid Res. 2004; 43: 134–176. https://doi.org/10.1016/s0163-7827(03)00051-1 PMID: 14654091

47. Ashour J, Laurent-Rolle M, Shi P-Y, García-Sastre A. NS5 of Dengue Virus Mediates STAT2 Binding and Degradation. J Virol. 2009; 83: 5408–5418. https://doi.org/10.1128/JVI.02188-08 PMID: 19279106

48. Merino-Ramos T, Jiménez de Oya N, Saiz J-C, Martín-Acebes MA. Antiviral Activity of Nordihydroguaiaretic Acid and Its Derivative Tetra-O-Methyl Nordihydroguaiaretic Acid against West Nile Virus and Zika Virus. Antimicrob Agents Chemother. 2017; 61. https://doi.org/10.1128/AAC.00376-17 PMID: 28507114

49. Miller S, Kastner S, Krijnse-Locker J, Bühler S, Bartenschlager R. The Non-structural Protein 4A of Dengue Virus Is an Integral Membrane Protein Inducing Membrane Alterations in a 2K-regulated Manner. J Biol Chem. 2007; 282: 8873–8882. https://doi.org/10.1074/jbc.M609919200 PMID: 17276984

50. Fajardo-Sánchez E, Galiano V, Villalaín J. Spontaneous membrane insertion of a dengue virus NS2A peptide. Arch Biochem Biophys. 2017; 627: 56–66. https://doi.org/10.1016/j.abb.2017.06.016 PMID: 28666739

51. Caviglia JM, Dumm INT de G, Coleman RA, Igal RA. Phosphatidylcholine deficiency upregulates enzymes of triacylglycerol metabolism in CHO cells. J Lipid Res. 2004; 45: 1500–1509. https://doi.org/10.1194/jlr.M400079-JLR200 PMID: 15175356

52. Meer G van, Kroon AIPM de. Lipid map of the mammalian cell. J Cell Sci. 2011; 124: 5–8. https://doi.org/10.1242/jcs.071233 PMID: 21172818

53. Richard AS, Zhang A, Park S-J, Farzan M, Zong M, Choe H. Virion-associated phosphatidylethanolamine promotes TIM1-mediated infection by Ebola, dengue, and West Nile viruses. Proc Natl Acad Sci U S A. 2015; 112: 14682–14687. https://doi.org/10.1073/pnas.1508095112 PMID: 26575624

54. Carnec X, Meertens L, Dejarnac O, Perera-Lecoin M, Hafirassou ML, Kitaura J, et al. The Phosphatidylserine and Phosphatidylethanolamine Receptor CD300a Binds Dengue Virus and Enhances Infection. J Virol. 2016; 90: 92–102. https://doi.org/10.1128/JVI.01849-15 PMID: 26468529

55. Xu K, Nagy PD. RNA virus replication depends on enrichment of phosphatidylethanolamine at replication sites in subcellular membranes. Proc Natl Acad Sci U S A. 2015; 112: E1782–E1791. https://doi.org/10.1073/pnas.1418971112 PMID: 25810252

56. Belov G. Less Grease, Please. Phosphatidylethanolamine Is the Only Lipid Required for Replication of a (+)RNA Virus. Viruses. 2015; 7: 3500–3505. https://doi.org/10.3390/v7072784 PMID: 26131959

57. Sim S, Jupatanakul N, Dimopoulos G. Mosquito Immunity against Arboviruses. Viruses. 2014; 6: 4479–4504. https://doi.org/10.3390/v6114479 PMID: 25415198

58. West J, Tompkins CK, Balantac N, Nudelman E, Meengs B, White T, et al. Cloning and expression of two human lysophosphatidic acid acyltransferase cDNAs that enhance cytokine-induced signaling responses in cells. DNA Cell Biol. 1997; 16: 691–701. https://doi.org/10.1089/dna.1997.16.691 PMID: 9212163

59. Kanthong N, Laosutthipong C, Flegel TW. Response to Dengue virus infections altered by cytokine-like substances from mosquito cell cultures. BMC Microbiol. 2010; 10: 290. https://doi.org/10.1186/1471-2180-10-290 PMID: 21078201

60. Barletta ABF, Silva MCLN, Sorgine MHF. Validation of Aedes aegypti Aag-2 cells as a model for insect immune studies. Parasit Vectors. 2012; 5: 148. https://doi.org/10.1186/1756-3305-5-148 PMID: 22827926

61. Schreiber MJ, Holmes EC, Ong SH, Soh HSH, Liu W, Tanner L, et al. Genomic Epidemiology of a Dengue Virus Epidemic in Urban Singapore. J Virol. 2009; 83: 4163–4173. https://doi.org/10.1128/JVI.02445-08 PMID: 19211734

62. Tsugawa H, Cajka T, Kind T, Ma Y, Higgins B, Ikeda K, et al. MS-DIAL: data-independent MS/MS deconvolution for comprehensive metabolome analysis. Nat Methods. 2015; 12: 523–526. https://doi.org/10.1038/nmeth.3393 PMID: 25938372

63. Tsugawa H, Kind T, Nakabayashi R, Yukihira D, Tanaka W, Cajka T, et al. Hydrogen Rearrangement Rules: Computational MS/MS Fragmentation and Structure Elucidation Using MS-FINDER Software. Anal Chem. 2016; 88: 7946–7958. https://doi.org/10.1021/acs.analchem.6b00770 PMID: 27419259

64. Sumner LW, Amberg A, Barrett D, Beale MH, Beger R, Daykin CA, et al. Proposed minimum reporting standards for chemical analysis Chemical Analysis Working Group (CAWG) Metabolomics Standards

Initiative (MSI). Metabolomics Off J Metabolomic Soc. 2007; 3: 211–221. https://doi.org/10.1007/s11306-007-0082-2 PMID: 24039616

65. Tsugawa H, Nakabayashi R, Mori T, Yamada Y, Takahashi M, Rai A, et al. A cheminformatics approach to characterize metabolomes in stable-isotope-labeled organisms. Nat Methods. 2019; 16: 295. https://doi.org/10.1038/s41592-019-0358-2 PMID: 30923379

66. Chong J, Soufan O, Li C, Caraus I, Li S, Bourque G, et al. MetaboAnalyst 4.0: towards more transparent and integrative metabolomics analysis. Nucleic Acids Res. 2018; 46: W486–W494. https://doi.org/10.1093/nar/gky310 PMID: 29762782

67. Fraiture M, Baxter RHG, Steinert S, Chelliah Y, Frolet C, Quispe-Tintaya W, et al. Two Mosquito LRR Proteins Function as Complement Control Factors in the TEP1-Mediated Killing of Plasmodium. Cell Host Microbe. 2009; 5: 273–284. https://doi.org/10.1016/j.chom.2009.01.005 PMID: 19286136

68. Johnson BW, Russell BJ, Lanciotti RS. Serotype-Specific Detection of Dengue Viruses in a Fourplex Real-Time Reverse Transcriptase PCR Assay. J Clin Microbiol. 2005; 43: 4977–4983. https://doi.org/10.1128/JCM.43.10.4977-4983.2005 PMID: 16207951

69. Manokaran G, Finol E, Wang C, Gunaratne J, Bahl J, Ong EZ, et al. Dengue subgenomic RNA binds TRIM25 to inhibit interferon expression for epidemiological fitness. Science. 2015; 350: 217. https://doi.org/10.1126/science.aab3369 PMID: 26138103

3. Supplement information

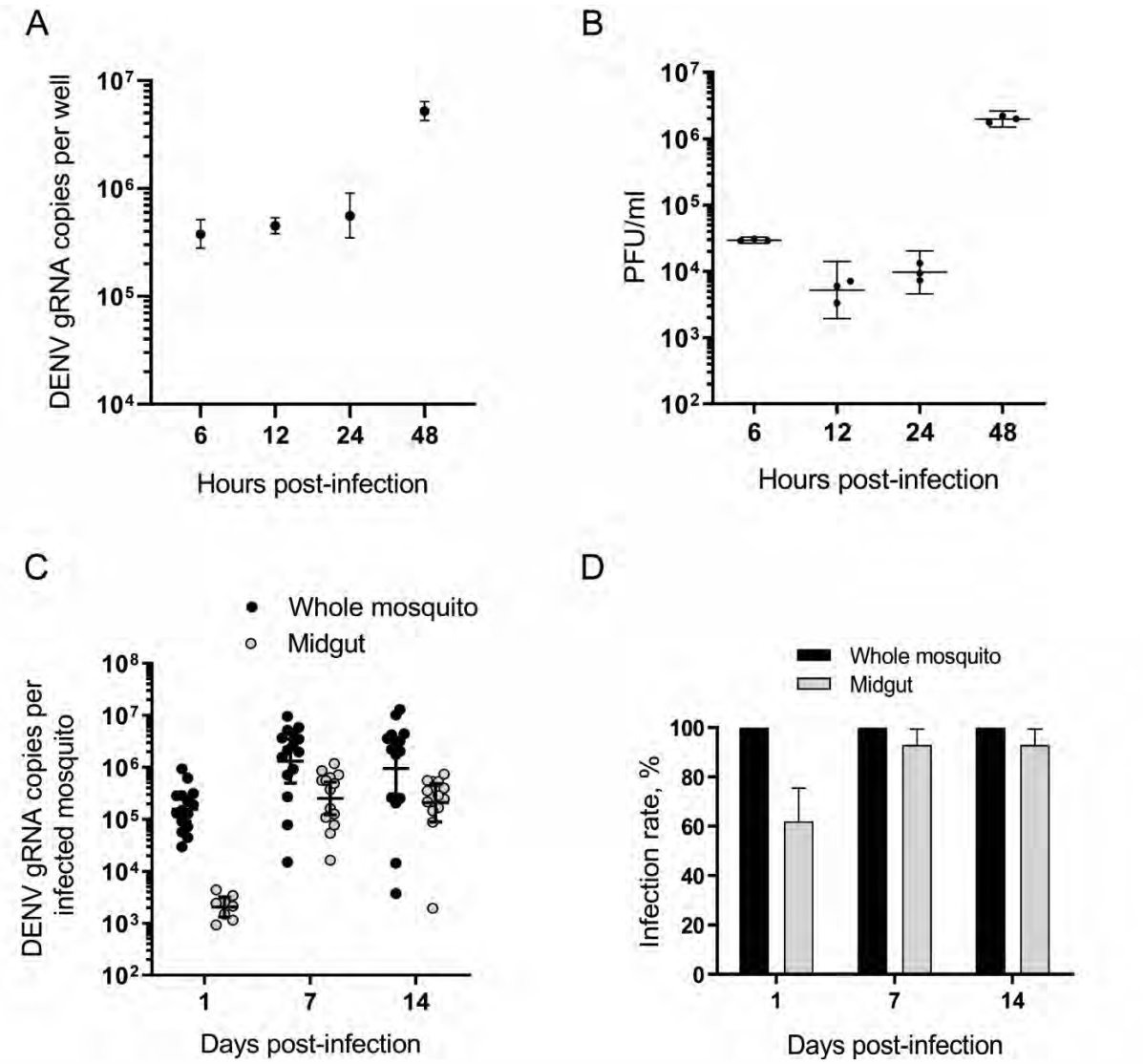

Figure S1. Quantification of DENV infection in Aag2 cells, *A. aegypti* mosquito and midgut. (A) DENV gRNA copies in Aag2 cells at 6, 12, 24 and 48h post-infection with DENV at MOI = 5. Points from 4 repeat and standard errors show geometric mean ± 95 % CI. (B) Plaque titer (plaque forming unit - pfu) in supernatant from Aag2 cells at 6, 12, 24 and 48h post-infection. Aag2 cells were infected with DENV at MOI = 5 and virus titer was calculated using plaque assay. Each point represents one well. (C) DENV gRNA copies per infected mosquitoes and dissected midguts at 1, 7 and 14 days post-oral infection with 10^7 pfu/ml. Each point represents one mosquito or midgut. Bars show geometric mean ± 95 % CI. (D) Infection rate in whole mosquito and midgut at 1, 7 and 14 days post-oral infection. Bars represent percentages ± s.e.

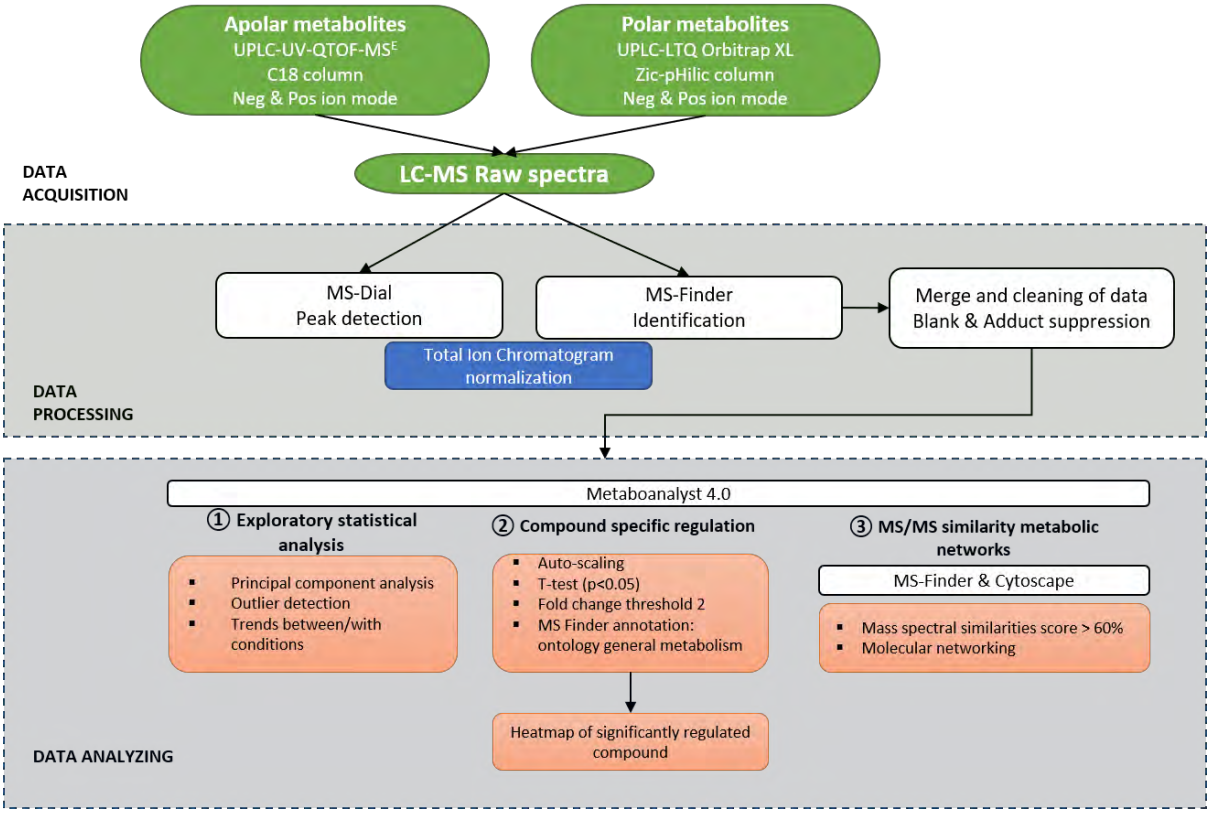

Figure S2. LC-HMRS analytical pipeline. Liquid Chromatography-High Resolution Mass Spectrometry (LC-HRMS) pipeline used to detect polar and nonpolar metabolites.

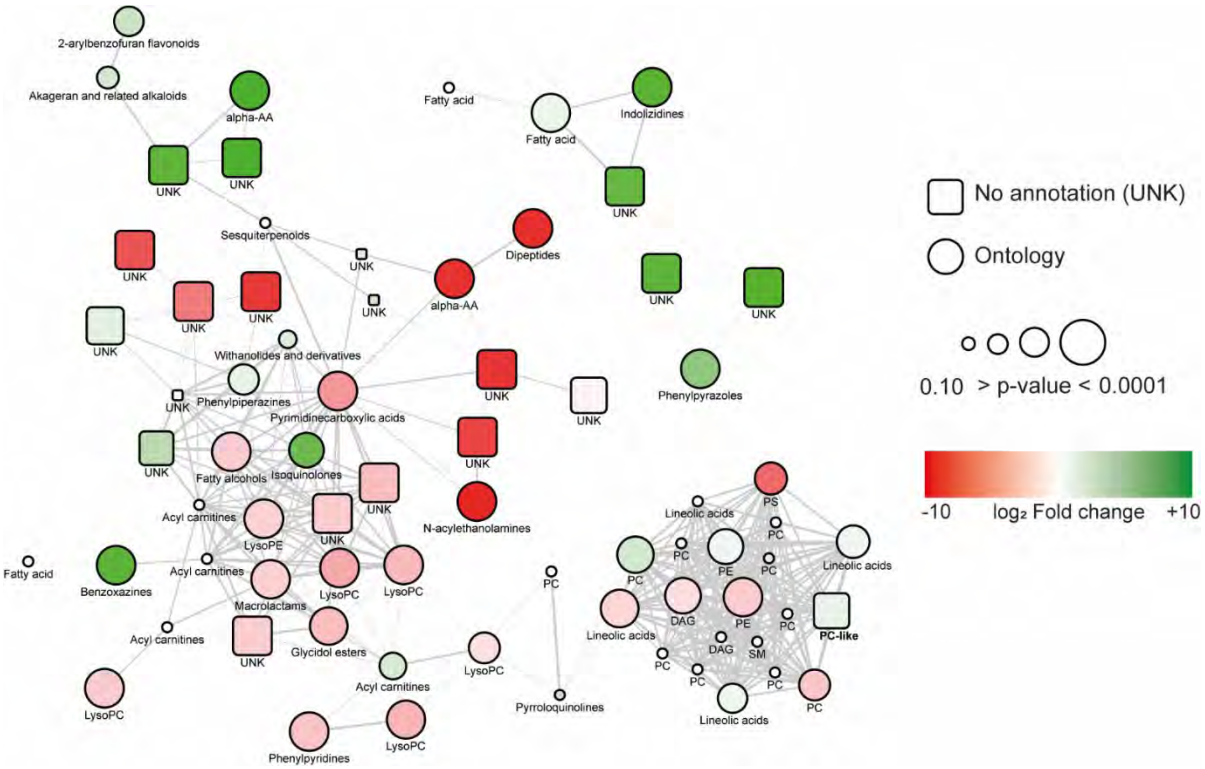

Figure S3. Spectral similarity network from mosquito MS features. Example of a molecular spectral network for Ae. aegypti mosquito at 14 days post-infection using MS features detected with the non-polar LC condition and MS negative mode. Line length represents the MS/MS score similarity. Ontology for unknown features was determined based on the proximity with database-identified features.

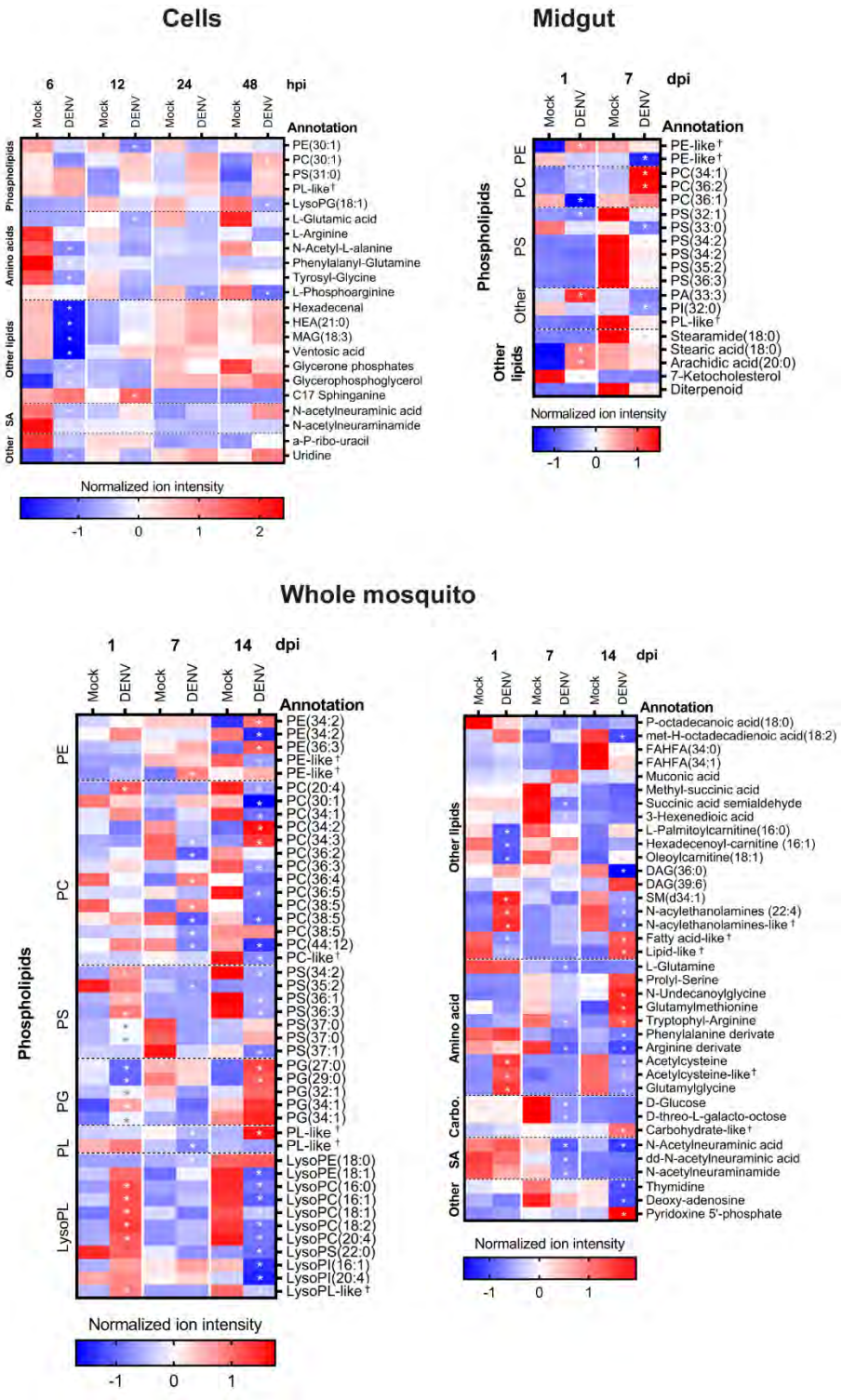

Figure S4. Ion intensity of regulated metabolites in cells, midguts and mosquitoes infected with DENV and mock. Normalized ion intensity was calculated after total ion chromatography normalization and auto scaling from three biological replicates. Conditions with significantly regulated metabolites (p-value <0.05 and |log2 fold change| >1) were indicated with an asterisk. Only metabolites from the general metabolism (i.e., lipid, carbohydrate, amino acid and peptide, nucleotide and nucleoside, sialic acid) are shown. †, indicates metabolite annotated by spectral similarity. Carbo., carbohydrate; SA, sialic acid; PL, phospholipid; PE,

phosphatidylethanolamine; PC, phosphatidylcholine; PS, phosphatidylserine; PA, phosphatidic acid; PI, phosphatidylinositol; PG, phosphatidylglycerol; LysoPS, lysophosphatidylserine; LysoPC, lysophosphatidylcholine; LysoPE, lysophosphatidylethanolamine; LysoPG, lysophosphatidylglycerol; LysoPI, lysophosphatidylinositol; SM, Sphingomyelin; DAG, Diacylglycerol; MAG, Monoacylglycerol; FAHFA, Fatty Acid ester of Hydroxyl Fatty Acid; NAE, N-acylethanolamine; HEA, Heneicosanoic acid; pep., peptides.

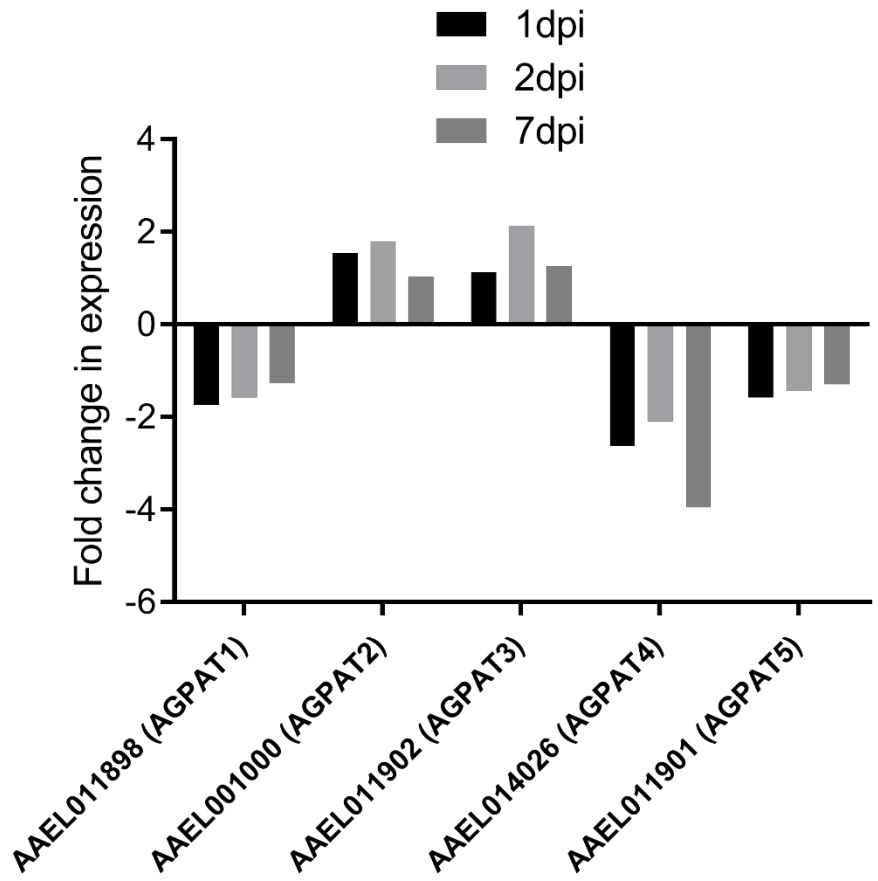

Figure S5. AGPAT genes are regulated by DENV infection, from Colpitts transcriptomic data. *Ae. aegypti* female mosquitoes were inoculated with DENV serotype 2 and collected at 1, 2 and 7 days post inoculation for transcriptomic analysis using microarray. Data from 3 separate infections. AGAPAT 1-5 were found significantly regulated by DENV infection. Data retrieved from (Colpitts et al., 2011, PMID: 21909258).

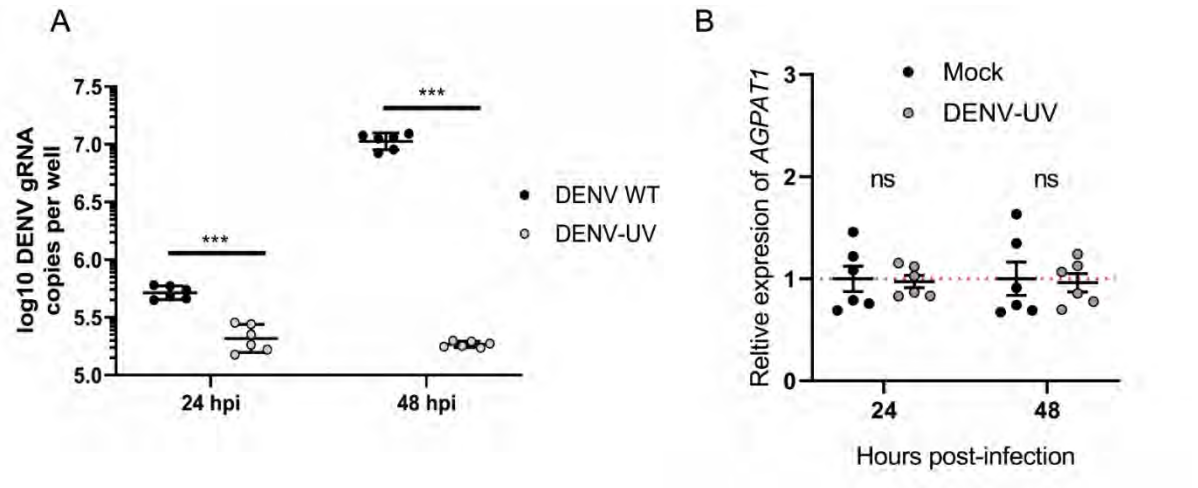

Figure S6. UV-inactivated DENV does not regulate *AGPAT1* expression.

Aag2 cells were infected with an MOI of 5 of DENV (DENV-WT), UV-inactivated DENV (DENV-UV) or mock. Cells were analyzed at 24 and 48 hours post-infection (hpi). (A) DENV gRNA copies. Bars show geometric means ± 95 % C.I. (B) *AGPAT1* expression relative to *Actin* level. Bars show arithmetic means ± s.e.m. (A-B) Each point represents an independent well. ***, p-value < 0.001 as determined by unpaired t-test.

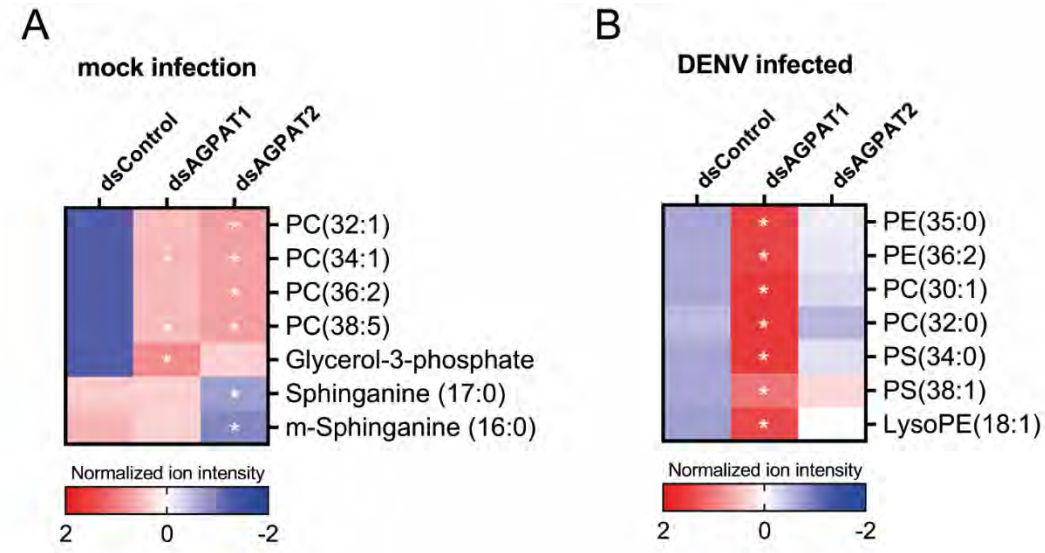

Figure S7. Metabolomic impact of AGPAT1 and AGPAT2 depletion and infection in cells as measured by ion intensity. Aag2 cells were transfected with dsRNA against *AGPAT1* (dsAGPAT1) or *AGPAT2* (dsAGPAT2) or a dsRNA control (dsControl). 24h later, cells were infected with DENV at MOI of 1. (A) Ion intensity of regulated metabolites in mock cells at 72h post transfection. (B) Ion intensity of regulated metabolites in infected cells at 24 hpi. Normalized ion intensity was calculated after total ion chromatography normalization and auto scaling from three replicates. Conditions with significantly regulated metabolites (p-value <0.05 and |log2 fold change| >1) were indicated with an asterisk. PE, phosphatidylethanolamine; PC, phosphatidylcholine; PS, phosphatidylserine; LPE, lysophosphatidylethanolamine.

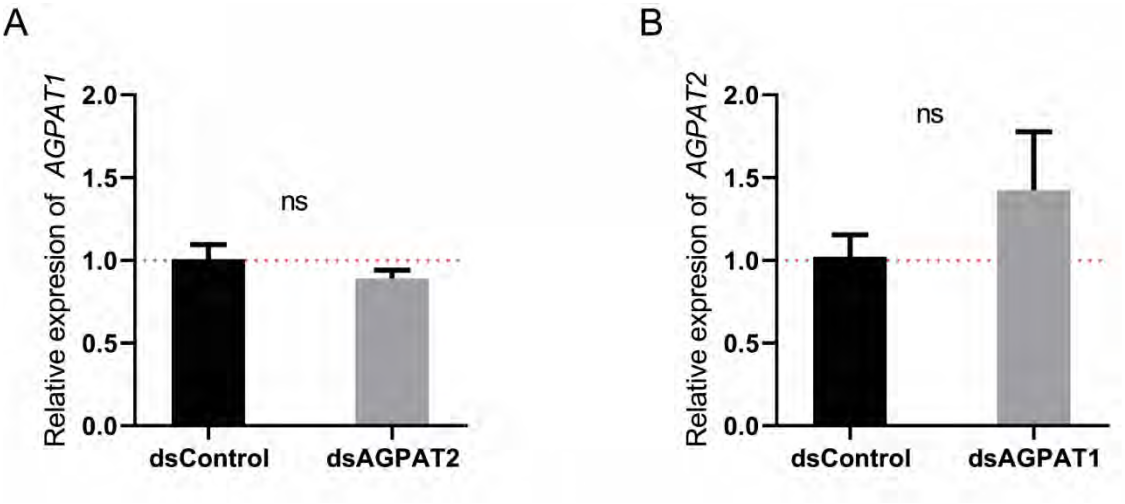

Figure S8. *AGPAT1* and *2* expression in cells after the other AGPAT depletion. Aag2 cells were transfected with dsRNA against *AGPAT1* or *2* (dsAGPAT1 or 2). Control cells were transfected with dsRNA control (dsControl). Cells were collected 72h post dsRNA. (A) *AGPAT1* expression in AGPAT2-depleted cells. (B) *AGPAT2* expression in AGPAT1-depleted cells. Bars show mean ± s.e.m from 3 biological replicates. ns, non-significant, as indicated by unpaired t-test.

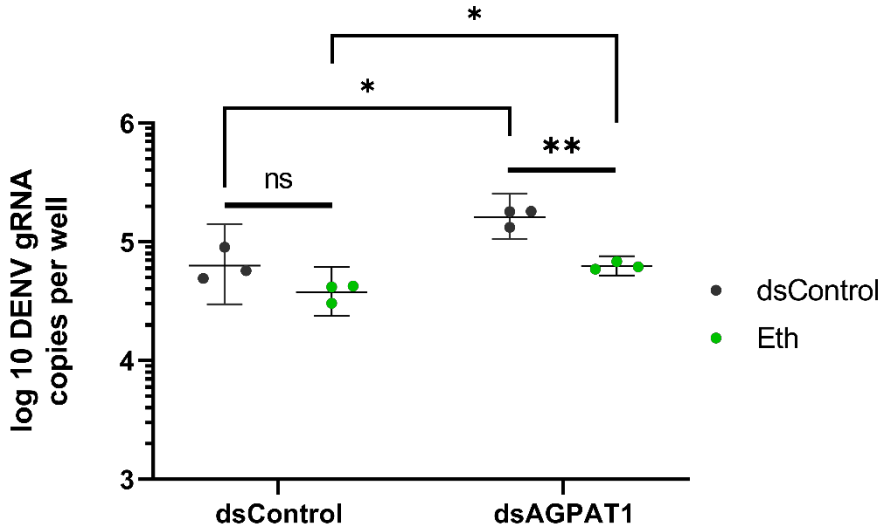

Figure S9. Ethanolamine supplementation partially rescue wild-type infection after AGPAT1 depletion. Aag2 cells were transfected with dsRNA against AGPAT1 (dsAGPAT1) or with dsRNA control (dsControl), with standard growth media or media supplemented with 2mM ethanolamine (Eth). At 24 h post transfection, cells were infected with DENV at MOI of 1. DENV gRNA copies were analyzed at 48 hours post-infection (hpi). Bars show geometric means ± 95 % C.I. Each point represents an independent well. *, p-value < 0.05, **, p-value < 0.01 as determined by unpaired t-test.

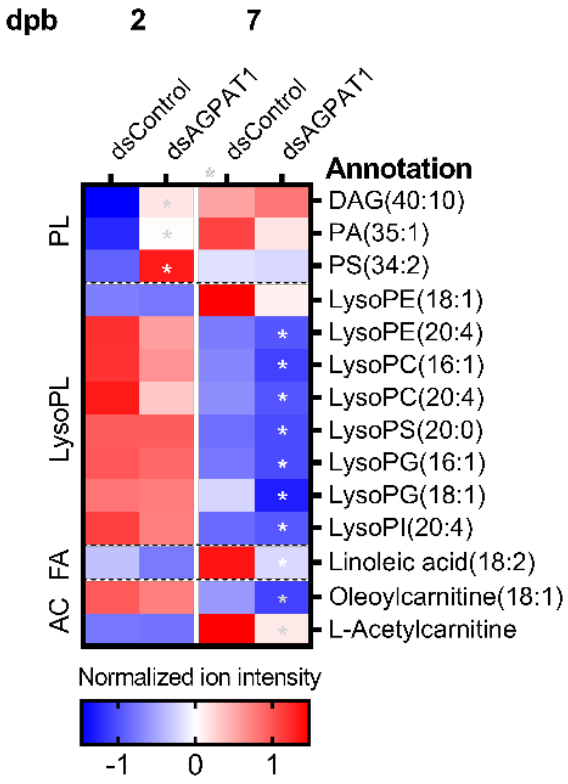

Figure S10. Metabolomic impact of AGPAT1 and AGPAT2 depletion in uninfected mosquitoes as measured by ion intensity. Two days post dsRNA injection against *AGPAT1* (dsAGPAT1) or control (dsControl), mosquitoes were orally infected with DENV at 10^7 pfu/ml. Metabolomic analyses were performed at 2 and 7 dpi. Normalized ion intensity was calculated after total ion chromatography normalization and auto scaling from three replicates. Conditions with significantly regulated metabolites (p-value <0.05 and |log2 fold change| >1) were indicated with an asterisk.

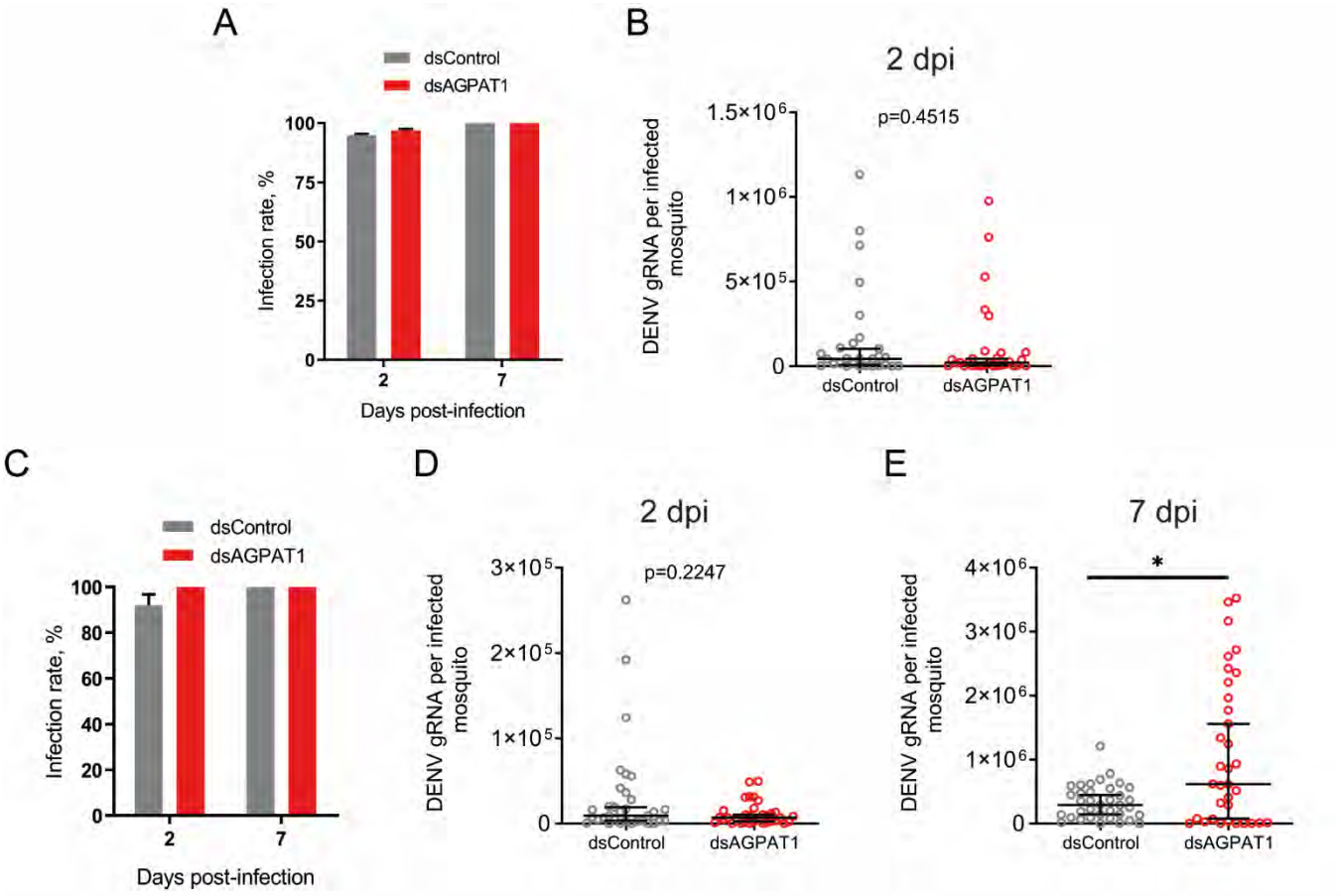

Figure S11. Impact of AGPAT1-depletion in mosquitoes on DENV infection rate and gRNA copies. Mosquitoes were injected with either dsRNA against *AGPAT1* (dsAGPAT1) or dsRNA control (dsControl). Two days post injection, mosquitoes were orally fed with either non-infectious blood or DENV infectious blood. Impact of AGPAT1 depletion on (A) infection rate and (B) DENV gRNA copies at 2 days post oral infection (dpi) with 10^7 pfu/ml. (C-E) Impact of AGPAT1 depletion on infection rate (C) and DENV gRNA copies at 2 (D) and 7 (E) dpi with 10^6 pfu/ml. Bars indicate percentage ± s.e. (A, C) or geometric means ± 95% C.I. (B, D, E) with each dot representing one mosquito. *, p-value < 0.05 as indicated by Mann-Whitney test.

Table S1. Identification of mosquito specific metabolites by spectral similarity.

	Suggested annotation	Mass m/z	Time course	Similarity score	Similarity features mass	Similarity features Ontology
Cells	Phospholipid	1004.0799	48 hpi	0.67	227.2018	Long-chain fatty acids
				0.64	171.0119	Glycerophosphates
Midgut	Phospholipid	695.311	1 dpi	0.97	716.4861	Phosphatidylserines
				0.96	742.5027	Phosphatidylserines
				0.95	714.5056	Phosphatidylethanolamines
				0.90	740.5221	Phosphatidylethanolamines
				0.89	711.2864	Saccharolipids
				0.88	729.4831	Xanthophylls
				0.81	715.5099	Acyclic diterpenoids
				0.80	716.5167	Phosphatidylethanolamines
				0.76	719.4855	Phosphatidylglycerols
				0.71	740.5191	Phosphatidylethanolamines
				0.67	717.4706	Phosphatidylglycerols
	Phospholipid	701.4858	7 dpi	0.83	711.2864	Saccharolipids
				0.81	716.5167	Phosphatidylethanolamines
				0.78	715.5099	Acyclic diterpenoids
				0.78	729.4831	Xanthophylls
				0.74	253.2168	Long-chain fatty acids
				0.68	740.5221	Phosphatidylethanolamines
				0.68	716.4861	Phosphatidylserines
				0.62	717.4706	Phosphatidylglycerols
	Phospholipid	707.1689	7 dpi	0.97	219.175	Sesquiterpenoids
				0.95	469.3869	Stilbenes
				0.94	284.2951	Carboximidic acids
				0.93	481.3505	Brassinolides and derivatives
				0.87	553.2563	Benzodioxoles
				0.85	775.5345	Glycosyldiacylglycerols
				0.85	850.5543	Phosphatidylserines
				0.76	437.1938	3'-prenylated isoflavanones

				0.66	522.3557	Lysophosphatidylcholines
				0.66	427.3893	Cycloartanols and derivatives
				0.93	794.5101	Glycosphingolipids
	Phospholipid	846.5413	7 dpi	0.94	818.5106	Phosphatidylethanolamines
				0.98	820.5248	Oligopeptides
	Phospholipid	628.3821	14 dpi	0.84	466.3301	Lysophosphatidylethanolamines
				1.00	312.3264	Morpholines
				0.99	516.307	Lysophosphatidylcholines
				0.99	758.5696	Phosphatidylcholines
				0.91	778.5354	Phosphatidylcholines
				0.91	802.5355	Phosphatidylcholines
	Phospholipid	754.5367	14 dpi	0.73	808.5806	Phosphatidylcholines
				0.69	566.323	Benzoic acids
				0.67	522.356	Lysophosphatidylcholines
				0.67	284.2961	Carboximidic acids
				0.66	808.5842	Phosphatidylcholines
				0.66	780.5518	Phosphatidylcholines
Mosquito				0.67	281.2477	Long-chain fatty acids
				0.67	659.5121	Phosphoethanolamines
				0.65	564.3434	Resorcinols
	Phospholipid	611.3975	7 dpi	0.64	687.4951	Phosphatidic acid
				0.64	714.4923	Phosphatidylethanolamines
				0.63	775.5479	Phosphatidylglycerols
				0.60	734.533	Phosphatidylserines
				0.97	469.2935	Withanolides and derivatives
				0.95	428.3731	Acyl carnitines
				0.90	359.1749	Phenylpiperazines
				0.89	311.2584	Fatty alcohols
	Phospholipid	768.4946	7 / 14 dpi	0.88	518.2646	Harmala alkaloids
				0.87	453.1676	Sulfated steroids
				0.76	480.3088	Lysophosphatidylethanolamines
				0.61	463.2568	Fatty acyl glycosides
		534.2963		0.95	630.4976	Aralkylamines

Lysophospholipid / Acylcarnitine		1 / 14 dpi	0.99	339.2893	Glycidol esters
			0.98	398.3265	Acyl carnitines
			0.66	426.3578	Acyl carnitines
			0.97	428.3731	Acyl carnitines
			0.61	452.277	Acyl carnitines
			0.62	480.3088	Lysophosphatidylethanolamines
			0.98	518.2646	Harmala alkaloids
			0.64	520.3402	Lysophosphatidylcholines
Lysophospholipid	534.2963	1 / 14 dpi	0.64	544.3403	Lysophosphatidylcholines
			0.64	558.2961	Diphenylethers
			0.94	560.312	Macrolactams
N-acylethanolamines	376.2597	1 / 14 dpi	0.83	376.3156	N-acylethanolamines
Lipid	107.086	1 / 14 dpi	0.87	219.1751	Sesquiterpenoids
			0.72	337.1053	Coumestans
			0.95	135.0809	Alkylthiols
			0.90	425.1364	Ginkgolides and bilobalides
Fatty acid	192.16	1 / 14 dpi	0.96	216.1964	Medium-chain fatty acids
			0.94	156.1386	Indolizidines
Carbohydrate	198.1861	14 dpi	0.69	839.3719	Sugar acids and derivatives
			0.80	359.1749	Phenylpiperazines
Acyl-Amino acid	616.1778	7 / 14 dpi	0.64	164.0408	N-acyl-L-alpha-amino acids
Pyrazinecarboxamides	789.4676	1 / 14 dpi	0.66	414.2152	Pyrazinecarboxamides
Hydroxypyrimidines	234.9183	14 dpi	0.75	184.0742	Hydroxypyrimidines
Hydroxypyrimidines	376.2597	1 / 14 dpi	0.78	184.0739	Hydroxypyrimidines
			0.80	184.0742	Hydroxypyrimidines
Hydroxypyrimidines	768.4946	7 / 14 dpi	0.94	184.0739	Hydroxypyrimidines
			0.97	184.0742	Hydroxypyrimidines

Table S3. Primers for dsRNA.

Gene name	Gene code	Fragment size	Forward primer	Reverse primer
AGPAT 1	AAEL011898	364	TAATACGACTCACTATAGGGTTAA GCGCATGCCGTAAAAA	TAATACGACTCACTATAGGGTTG GTACAGAGATAGGCGGG
AGPAT 2	AAEL001000	346	TAATACGACTCACTATAGGGGGCC TACTTTTGCAGTTTGAA	TAATACGACTCACTATAGGGCGA GTTGATCATCAGCACAAA
LacZ	/	370	TAATACGACTCACTATAGGGTACC CGTAGGTAGTCACGCA	TAATACGACTCACTATAGGGTAC GATGCGCCCATCTACAC

Table S4. Primers for Real-Time qPCR

Gene name	Gene code	Forward primer	Reverse primer
AGPAT1	AAEL011898	TAAGCGCATGCCGTAAAAAT	GTGGCCGTAAAAGCATGAG
AGPAT2	AAEL001000	GGCCTACTTTTGCAGTTTGAA	CGAGTTGATCATCAGCACAAA
Actin	AAEL011197	GAACACCCAGTCCTGCTGACA	TGCGTCATCTTCTCACGGTTAG

Table S5. AGPAT FASTA protein sequence.

>NP_006402.1 1-acyl-sn-glycerol-3-phosphate acyltransferase alpha [Homo sapiens]

MDLWPGAWMLLLLFLLLLFLLPTLWFCSPSAKYFFKMAFYNGWILFLAVLAIPVCAVRGRV
ENMKILRLMLLHIKYLYGIRVEVRGAHHFPPSQPYVVVSNHQSSLDLLGMMEVLPGRCVPIA
KRELLWAGSAGLACWLAGVIFIDRKRTGDAISVMSEVAQTLLTQDVRVWVFPEGTRNHNGS
MLPFKRGAFHLAVQAQVPIVPIVMSSYQDFYCKKERRFTSGQCQVRVLPPVPTEGLTPDDV
PALADRVRHSMLTVFREISTDGRGGGDYLKKPGGGG

>NP_006403.2 1-acyl-sn-glycerol-3-phosphate acyltransferase beta isoform a precursor [Homo sapiens]

MELWPCLAAALLLLLLLVQLSRAAEFYAKVALYCALCFTVSAVASLVCLLRHGGRTVENMSII
GWFVRSFKYFYGLRFEVRDPRRLQEARPCVIVSNHQSILDMMGLMEVLPERCVQIAKRELL
FLGPVGLIMYLGGVFFINRQRSSTAMTVMADLGERMVRENLKVWIYPEGTRNDNGDLLPFK
KGAFYLAVQAQVPIVPVVYSSFSSFYNTKKKFFTSGTVTVQVLEAIPTSGLTAADVPALVDTC
HRAMRTTFLHISKTPQENGATAGSGVQPAQ

>NP_064517.1 1-acyl-sn-glycerol-3-phosphate acyltransferase gamma [Homo sapiens]

MGLLAFLKTQFVLHLLVGFVFVVSGLVINFVQLCTLALWPVSKQLYRRLNCRLAYSLWSQLV
MLLEWWSCTECTLFTDQATVERFGKEHAVIILNHNFEIDFLCGWTMCERFGVLGSSKVLAKK
ELLYVPLIGWTWYFLEIVFCKRKWEEDRDTVVEGLRRLSDYPEYMWFLLYCEGTRFTETKH
RVSMEVAAAKGLPVLKYHLLPRTKGFTTAVKCLRGTVAAVYDVTLNFRGNKNPSLLGILYGK
KYEADMCVRRFPLEDIPLDEKEAAQWLHKLYQEKDALQEIYNQKGMFPGEQFKPARRPWT
LLNFLSWATILLSPLFSFVLGVFASGSPLLILTFLGFVGAASFGVRRLIGVTEIEKGSSYGNQE
FKKKE

>NP_064518.1 1-acyl-sn-glycerol-3-phosphate acyltransferase delta [Homo sapiens]

MDLAGLLKSQFLCHLVFCYVFIASGLIINTIQLFTLLLWPINKQLFRKINCRLSYCISSQLVMLLE
WWSGTECTIFTDPRAYLKYGKENAIVVLNHKFEIDFLCGWSLSERFGLLGGSKVLAKKELAY

VPIIGWMWYFTEMVFCSRKWEQDRKTVATSLQHLRDYPEKYFFLIHCEGTRFTEKKHEISM
QVARAKGLPRLKHHLLPRTKGFAITVRSLRNVVSAVYDCTLNFRNNENPTLLGVLNGKKYHA
DLYVRRIPLEDIPEDDDECSAWLHKLYQEKDAFQEEYYRTGTFPETPMVPPRRPWTLVNWL
FWASLVLYPFFQFLVSMIRSGSSLTLASFILVFFVASVGVRWMIGVTEIDKGSAYGNSDSKQK
LND

>NP_060831.2 1-acyl-sn-glycerol-3-phosphate acyltransferase epsilon [Homo sapiens]

MLLSLVLHTYSMRYLLPSVVLLGTAPTYVLAWGVWRLLSAFLPARFYQALDDRLYCVYQSM
VLFFFENYTGVQILLYGDLPKNKENIIYLANHQSTVDWIVADILAIRQNALGHVRYVLKEGLKW
LPLYGCYFAQHGGIYVKRSAKFNEKEMRNKLQSYVDAGTPMYLVIFPEGTRYNPEQTKVLS
ASQAFAAQRGLAVLKHVLTPRIKATHVAFDCMKNYLDAIYDVTVVYEGKDDGGQRRESPTM
TEFLCKECPKIHIHIDRIDKKDVPEEQEHMRRWLHERFEIKDKMLIEFYESPDPERRKRFPGK
SVNSKLSIKKTLPSMLILSGLTAGMLMTDAGRKLYVNTWIYGTLLGCLWVTIKA

>EAT35978.1 AAEL011898-PA [*Aedes aegypti*]

MTTTNSELLGLAFMAFFIITLSSTARYYFKFFCFIILSVVCAVGPVPLMLLRPRDYRNALLPAYL
CTKFGKMLGASFEVRGRENVNRQHGGVVLMNHQSALDLVVLAYLWPIVGRATVVAKREVL
YMFPFGLACWLWGTLFINRKNQRSAKSAINNESKAINEKQAKILFFPEGTRGDGDSLLPFKK
GSFHVAIEAQGYIQPVVISKYHFLNSKAKLFNRGQNIIKILPEVSCVGLTKDDMPQLMDRVQR
MMQSEYEALSDESLAINNLSKSL

>EAT47921.1 AAEL001000-PA [*Aedes aegypti*]

MKAYFCSLKLFSLFPTLRHATWPHFLFLQRDDISAAITSEPTSSCDDRVLLFYFQNVGGMNT
TLAKYLLACKGTMASYYEIFLICGIILMPIFYETSHKFRYFFKFFIYYFVLMINSIILIPAMMFRAK
DVRNLIWAGTFCRPISTVLGIKWELRGADILSRDEAYVIVANHQSSLDILGMFDFWHVMNKC
TVIAKKELLYTGPFGVAAWLSGLIFIDRKNAEKAHVAMNECTDMLKEKRIKLWVFPEGTRRN
TNEIHPFKKGAFHTAVRSQLPIMPVVYSSYGSFLDDKAKILNNGHVIVTTLEPIETKGLTSDDI
PELMERVRNVMMDTFKATTKEVENKYSVNSTKNGGVGLSGSKLRLRCIDDLIKPKLASSRRL
NASANGSPTKESAVYRRKE

>EAT35981.1 AAEL011902-PA [*Aedes aegypti*]

MTDCTLCHYVGLLVKYYLYAWIIGVGVWFLLIIASKVGSDGNKFRYYAKYGMIYYATQAFTTL
FAPFSLLRPRNPANAGIICAVASKASSLLPITWELRNARILREAEGAVVMANHQSSMDILGLEI
LWSTMRNVISIAKKEMLFIVPFGPAAWLAGITFINRKNRPSAMKTLDGCKRKMVEQGFKMYI
YPEGTRFPERGMLPFKKGGFHTAIEAGVPIIPVVFSHIYFIDAKKYSFKPGHVIMNVLEPIPTK
GLTKDNLDALITRTRDAMMAEYERLSAEMDANLANPKWVKASRPRFVTYDGKKTN

>EAT33698.1 AAEL014026-PA [*Aedes aegypti*]

MHLCFAISYFTSGLIINTAQCILYFGLKPFNKRLYRKIGYYLCYSFYSQLVFLADWWSGSTLYI
YISDEDLKHCGKEHVLLLMNHTYEVDWLVGWMFCEKVKVLGNCKAYAKKVIQYIPTVGWA
WKFAEFVFLERSFDKDKEIIGRQIKEIMDYPDPVWLLLNAEGTRFTEKKHEASIKFARDRGMV
ELKHHLIPRTKGFTASLPELRNKSTILDIQLAISKDSPVKPTIFNILNGKPIEAHMHIRRIPFDQV
PEDEGQAAEWLQELFRQKDVMQESFHKHGDFFTGSNVTRKVPVKLHPRLHTLINMVAWNV
LTVVPMFYYLIQLLISGEIMYFSIGTSILIAFYGLMVKAIGMSKISKASSYGSEKKNGQSVHNGP
SSNETTKNK

>EAT35980.1 AAEL011901-PA *[Aedes aegypti*]

MAMEAIISTIKDVFLGSTCVQIMVVSILLSLVWPTFKYYAKLTAILMMSFMVMVVPIPLYFFKPR
WPLNALIPGIVACEIIRWFGVEYEIRGKENINVKNGGVALINHQSAIDIVMLSRLLREFRNIVPV
VKKELFYALPFGIASYLVGVVFIDRKNITSAKDVMKREAVAIQRDNLKLAIFPEGTRHDKDTLL

PFKKGSFHVAIDSQSIIQSIIVSKYGFLDHKKKRFGRGRVIIKILPEISTKGMTKDDINSLVEKCQ
TTMQAEFDALSAEAKQYCHL

CHAPTER 3 – DENV activates phospholipid remodeling for replication

1. Presentation

The chapter 3 is intended to deepen the PL reconfiguration mechanism induced by DENV and to provide insight into the function of PL in DENV cellular life cycle in mosquito. We deployed our metabolomic workflow associated with isotope labelling to study the impact of either activation or inhibition of the aminophospholipid biosynthetic and remodeling pathway on DENV infection. By studying different stages of the cellular viral cycle, we revealed a PL modification by remodeling to ensure DENV replication process. Advanced results of this work are presented in the following section and are intended to be submitted for later publication.

2. Advanced results

2.1. Abstract

Dengue virus (DENV) is a re-emerging arbovirus present in all continent. The virus life cycle involves two different hosts, humans and mosquito species as vector responsible for DENV transmission and epidemics. DENV infection induces host metabolic disorder, by affecting particularly the lipid membrane metabolism. Here, we explored how DENV exploits phospholipids to complete its viral cellular cycle in mosquito. We demonstrated that inhibition of the Kennedy pathway, involved in phosphatidylcholine (PC) and phosphatidylethanolamine (PE) biosynthesis, favors DENV multiplication, while ethanolamine supplementation has the reverse effect by decreasing the infection.

Combining isotope labelling and ethanolamine or choline supplementation, we showed that DENV increases PC and PE biosynthesis by phospholipid remodeling. We further demonstrated that ethanolamine reduced viral replication, without affecting attachment, internalization or translation. These findings support the importance of PC and PE in DENV infection on mosquito and reveal a major role of aminophospholipid remodeling during the replication process.

2.2. Introduction

Dengue virus (DENV) is transmitted by *Aedes aegypti* mosquito[1] and is a global public health concern due to the wide and expanding distribution of its vector[283]. DENV is an enveloped single-stranded positive-sense RNA ((+)RNA) virus[8] that relies on host membrane for its cellular cycle. Lipids in DENV envelope attach to plasma membrane receptors to enter cells through endocytosis[8][53]. Upon internalization, DENV envelope fuses with plasma membrane, releasing the viral RNA genome into the cytosol[40]. The single open reading frame is translated into a transmembrane polyprotein by ribosomes associated with endoplasmic reticulum (ER) membrane[58]. After cleavage by host and viral proteases, non-structural viral proteins reconfigure the ER through membrane invagination to form a replication complex (RC) that encompasses vesicle packets (VP) where replication occurs[60,61]. Inside VP, first is produced the negative-sense RNA genome (-ssRNA), which is used as a template for +ssRNA replication. RC and VP structures enable efficient replication and protect from the host defense system. In ER membrane, newly synthetized +ssRNA is assembled into virion with viral structural proteins anchored in a lipid bilayer envelope. Viral particles bud in the ER lumen and undergo maturation through the Golgi and

trans-Golgi membrane networks[72], before being released into extracellular space by fusion between endosome and plasma membranes.

Plasma and endosomal membranes are mainly composed of phospholipids (PL)[284]. PLs contain one hydrophilic head group, a glycerol backbone and two hydrophobic fatty acyl chains. Because of their amphiphilic nature, bilayer associations of PL form cellular barriers. Phosphatidylcholine (PC) and phosphatidylethanolamine (PE) represent more than 50% of cellular PL content. PC and PE *de novo* biosynthesis is conducted in the ER through the highly conserved Kennedy pathway, which is composed of the parallel cytidine 5'-diphosphate (CDP) intermediates, CDP-choline and CDP-ethanolamine branches[147,156,284]. In these, choline (Cho) and ethanolamine (Etn) are integrated into a diacylglycerol (DAG) to form PC and PE, respectively[130]. Both PE and PC then form phosphatidylserine (PS) by head group exchange reaction[149,150]. PC, PE and PS are called aminophospholipids (AminoPL) based on their amine head group. Remodeling of PLs occurs through the Land's cycle[154,156] by deacylation of one acyl chain, forming lysophospholipid (LysoPL)[154], and reacylation to incorporate another fatty acid in the free position of the glycerol backbone, forming different PL species[154]. Together, *de novo* synthesis and remodeling of PLs ensures maintenance and rearrangement of membrane composition, which determine membrane properties and structures[162]. The polar headgroup and parallel acyl chains of PC results in a cylindrical geometry that form planar bilayer membrane. The small headgroup of PE confers an inverted conical geometry, which induces negative curvature[285]. Conversely, LysoPC and LysoPE with one acyl chain promote positive curvature and membrane permeability[285]. PL acyl chain composition is also important for membrane behavior, where high concentration of unsaturated PL leads to low lipid packing which increase membrane

fluidity[173]. Cellular membrane undergoes drastic modifications during DENV infection[62,63], as illustrated by the large PL reconfiguration in both humans and mosquitoes[200,286,287]. Understanding how DENV alters PL composition and the function of these membrane alterations will provide insight into the virus biology and transmission.

Recently, we described a major aminoPL reconfiguration throughout the DENV cycle in *Ae. aegypti* mosquitoes[286]. This reconfiguration is partially caused by DENV-mediated downregulation of *AGPAT1*, the enzyme responsible for synthesis of phosphatidic acid (PA), which feeds into the Kennedy pathway through DAG. We further showed that such inhibition of *de novo* AminoPLs generated a pro-viral environment in mosquitoes. Here, we aim to decipher how DENV reconfigures AminoPL – especially the role of *de novo* synthesis and remodeling - and the function of aminoPL in the viral cellular cycle. Using enzyme depletion to inhibit and precursor supplementation to activate the Kennedy pathway, we showed that *de novo* AminoPL synthesis is detrimental to DENV. Pioneering lipid isotope labelling in mosquitoes, we revealed that DENV aminoPL reconfiguration is initiated through remodeling. Eventually, we showed that activation of the Kennedy pathway does not alter virus attachment, internalization, translation and particle production but hampers replication, resulting in a lower number of infectious particles.

2.3. Results

2.3.1. Inhibition of the Kennedy pathway favors DENV multiplication

To determine how *de novo* AminoPL synthesis influences DENV infection, we depleted the enzymes from different steps of the two branches (CDP-Cho and CDP-Etn) of the

Kennedy pathway in Aag2 mosquito cells (Fig 1A; Fig S1). Both branches have parallel synthesis and, in insects, certain enzymes have overlapping activities, recognizing substrates from either branches[147]. We depleted the kinase responsible for Cho and Etn transformation into phosphocholine (CK) and phosphoethanolamine (EK), respectively; the two transferases that synthesize CDP-Cho (CT) and CDP-Etn (ET); the two transferases identified in Diptera that synthesize both PC and PE by introgression of DAG (E/CPT1 and E/CPT2), which have dual specificity for both CDP-choline and CDP-ethanolamine[288,289]. We also depleted the synthetase (PSS1) and decarboxylase (PSD) responsible for PC transformation into PS and PS transformation into PE, respectively. Upon gene depletion, we measured DENV infection by quantifying gRNA in cells and infectious particle production (plaque-forming unit, pfu) in supernatant at 48 h post infection (hpi). Both parameters showed identical pattern. Whereas the first step (EK/CK) of the Kennedy pathway and the second step (ET) of the CDP-Etn branch did not alter virus multiplication, synthesis inhibition of CDP-choline and *de novo* PC and PE by E/CPT1 and 2 increased gRNA and pfu/ml (Fig. 1B and C). Of note, E/CPT enzymes catalyze the rate-limiting step in the Kennedy pathway[147]. Alteration of PS synthesis and decarboxylation did not significantly influence particle production, however, PSD depletion, resulting in a decrease of alternative PE synthesis, moderately increased DENV gRNA.

To characterize the pro-viral metabolic environment induced by inhibition of *de novo* AminoPL synthesis, we quantified changes in PLs in enzyme-depleted mosquito cells as compared to wild-type upon DENV infection. Overall, pro-viral conditions (CT, E/CPT1 and E/CPT2 and to a lower extent PSD) induced a major AminoPL increase, including several compounds from PC, PE, PS, sphingomyelin (SM), LysoPC, LysoPE and lysophosphatidylinositol (LysoPI) classes (Fig 1D; Fig S2). However, neutral

conditions (EK/CK and ET) also induced a large AminoPL reconfiguration with several metabolites overlapping with pro-viral conditions. To correlate unique metabolite profiles with DENV titer in the different conditions, we performed a partial least squares regression (PLS)[290,291]. Higher concentration in PC(30:1) and PS(34:0) were the best predictors (highest VIP scores) of higher DENV titer (Fig 1E). Then, three LysoPCs, one LysoPE, one LysoPI, SM(34:1) and PS(40:4) correlated with DENV production. Altogether, those results demonstrate that inhibition of *de novo* AminoPL synthesis favors DENV production. This is in accordance with our previous observation that synthesis inhibition of precursors for the Kennedy pathway favors virus production in cells and mosquitoes[286]. More specifically, the new results show that reduction of PC and PE *de novo* synthesis but not PS synthesis promote DENV. In spite of Kennedy pathway inhibition, DENV infection increases concentrations of PC and PS, which associate with higher viral production. Importantly, LysoPLs are also largely increased, suggesting initiation of PL remodeling, which can produce these pro-viral PC and PS.

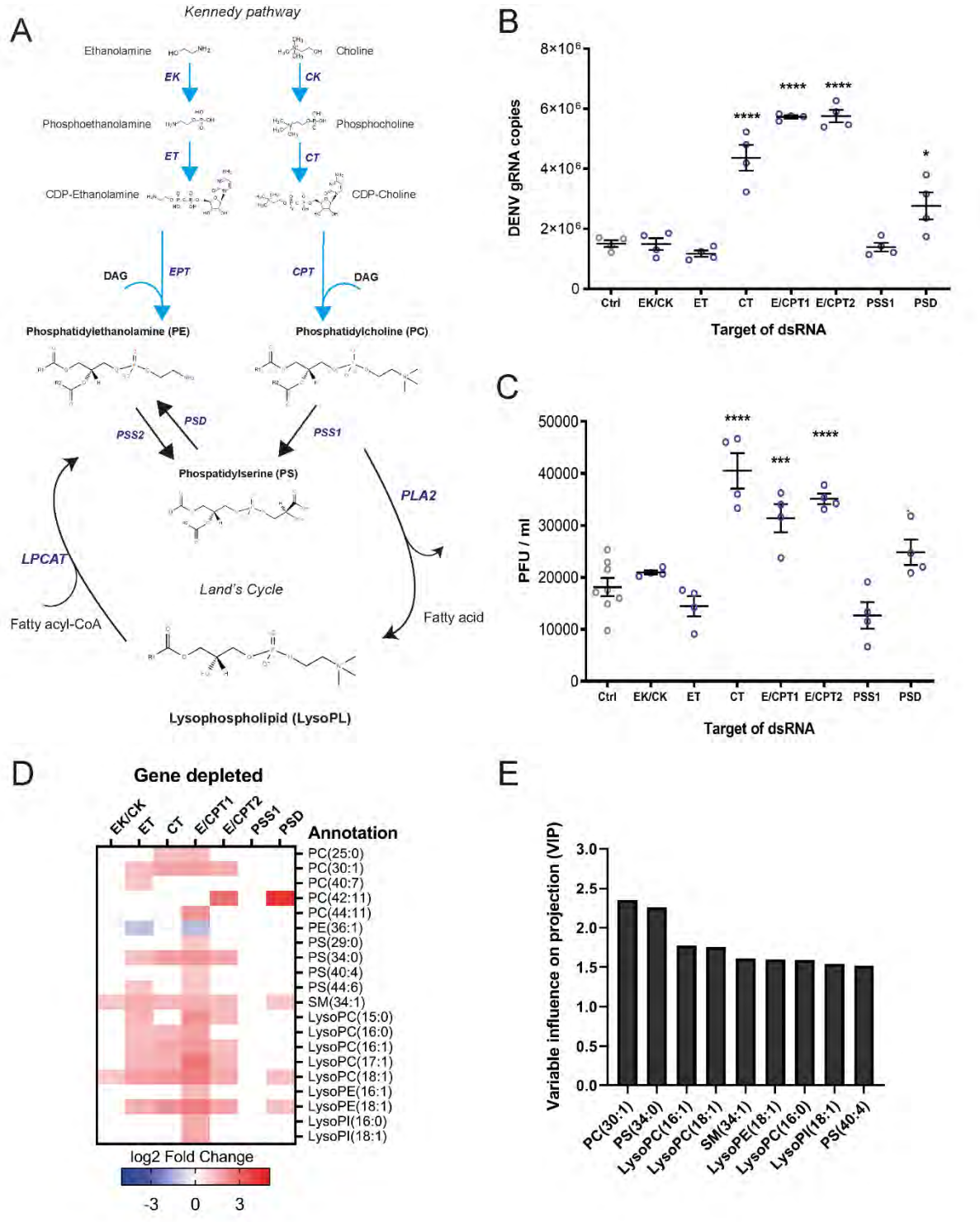

Fig 1. Impact of Kennedy pathway inhibition on DENV and phospholipid reconfiguration. Aag2 cells were transfected with dsRNA targeting different enzymes of the Kennedy pathway or control dsRNA (Ctrl). 24 h later, cells were infected with DENV at a MOI of 1 or mock. Samples were collected at 48hpi. (A) Scheme of the

Kennedy pathway and Land's cycle. Ethanolamine (Etn) and choline (Cho) are phosphorylated by ethanolamine/choline kinase (EK/CK) and then integrate a cytidine diphosphate group by CTP:phosphocholine/ethanolamine cytidyltransferase (CT/ET). The CDP-ethanolamine and CDP-choline formed incorporate a diacylglycerol (DAG) by DAG:CDP-choline cholinephosphotranferase (CPT) or DAG:CDP-ethanolamine ethanolaminephosphotranferase (EPT) to produce PC and PE, respectively. In mosquitoes, these enzymes catalyze both PE and PC. PS is produced by head exchange reaction from PC or PE by PS synthase (PSS). PE is reversely produced by PS decarboxylase (PSD). PL remodeling starts with deacylation by phospholipase A2 (PLA2) to produce lysophospholipids (LysoPL). LysoPL are then reacylated by lysophospholipid acyltransferase (LPLAT) via incorporation of another fatty acid to form a new PL species. (B) Impact of gene depletion on DENV gRNA copies. Bars show mean ± s.e.m. and each point represents one well-repeat. (C) Impact of gene depletion on DENV plaque-forming unit (pfu) assay. Bars show mean ± s.e.m. and each point represents one well-repeat. (D) DENV phospholipidome reconfiguration upon gene depletion. Fold changes of annotated and significantly regulated metabolites (|log2 fold change| > 1 and p-value < 0.05) upon DENV as compared to dsRNA control. (E) Variable influence on projection (VIP) for each metabolite. Bars show VIP score > 1.5 as determined by PLS analysis with DENV production (pfu/ml). (B, C) *, p-value < 0.05; ***, p-value < 0.001; **** p-value < 0.0001 as determined by Dunnett's multiple comparison test. PC, phosphatidylcholine; LysoPC, lysophosphatidylcholine; PE, phosphatidylethanolamine; LysoPE, lysophosphatidylethanolamine; PS, phosphatidylserine; LPI, lysophosphatidylinositol; SM, sphingomyelin.

2.3.2. Activation of the CDP:Ethanolamine branch of the Kennedy pathway reduces DENV multiplication

To test whether *de novo* AminoPL synthesis alters DENV multiplication, we activated the Kennedy pathway by supplementing mosquito cells with either Etn or Cho (Fig. 1A)[292]. While Etn was too small and apolar to be detected in our metabolomics workflow, uptake of Cho was confirmed in Cho supplemented cells (Fig. 2A). Interestingly, Cho was also increased upon Etn supplementation. This could be explained by induction of PC recycling and choline homeostasis[293], and is indicative of Etn uptake. Overall, AminoPLs were similarly regulated by either Cho or Etn supplementations, suggesting interconnections and compensation mechanisms between the two branches of the Kennedy pathway[293]. We observed an increase of two PC and one PS species. Interestingly, LysoPLs were largely decreased (7 downregulated out of 11 regulated). These results show that supplementation with Kennedy pathway precursors activates *de novo* AminoPL synthesis and inhibits partially PL remodeling.

We then quantified the effect of Etn and Cho supplementations on DENV gRNA at 6, 24 and 48 hpi (Fig 2B), and on DENV production (pfu/ml in supernatant) at 48 hpi (Fig 2C). At 48 hpi, Cho supplementation significantly increased gRNA replication and slightly enhanced pfu/ml, whereas Etn supplementation drastically inhibited both gRNA and pfu/ml (Fig 2B and C). However, while supplementation did not influence replication at 6 hpi, both Etn and Cho supplementation inhibited gRNA at 24 hpi (Fig 2B). The difference in the impact of Cho supplementation at 24 and 48 hpi may reflect the balance between precursor-mediated and DENV-mediated PL reconfiguration. If this is the case, higher pressure from DENV infection should revert the negative impact

of Cho. Accordingly, at a higher MOI, Cho supplementation did not alter gRNA quantity at 24 hpi (Fig S3).

To characterize DENV-mediated PL reconfiguration when Kennedy pathway is activated, we profiled the phospholipidome of Etn- and Cho-supplemented cells upon DENV infection at 6, 24 and 48 hpi. At 6 hpi, Kennedy pathway precursors (Cho and phosphocholine) increased in cells supplemented with either Etn or Cho (Fig 2D; Fig S4). Together with the observed decrease in PC, PE and PS, it is suggestive of inhibition of the Kennedy pathway. At 24 hpi, two LysoPCs and several sphingomyelin (SM), the latter being produced from LysoPCs, increased in both supplementations, indicating activation of PC remodeling. At the same time point upon Etn supplementation, only PC(34:1) and two PEs increased, while all other regulated PCs and PEs were downregulated upon Cho supplementation. At 48 hpi, all regulated PCs, PSs, SMs and LysoPCs were similarly upregulated in both supplementations. However, while nine PEs were similarly upregulated in both supplementations, three other PEs only increased upon Etn supplementation. Altogether, these observations indicate that DENV induces PL remodeling through deacylation of PC. Consequently, activation of *de novo* PC and PE synthesis restricts the proportion of remodeled PLs that favor DENV and reduces early virus infection. There exists a balance between *de novo* synthesis and remodeling of PL[294]. In our conditions, DENV-mediated PC remodeling counterbalances the negative effect of *de novo* PCs at 48 hpi. Inversely, *de novo* PEs forced by Etn supplementation are less efficiently remodeled by DENV and hamper infection. In accordance, LysoPEs that indicate PE remodeling were downregulated upon both supplementations at 48 hpi.

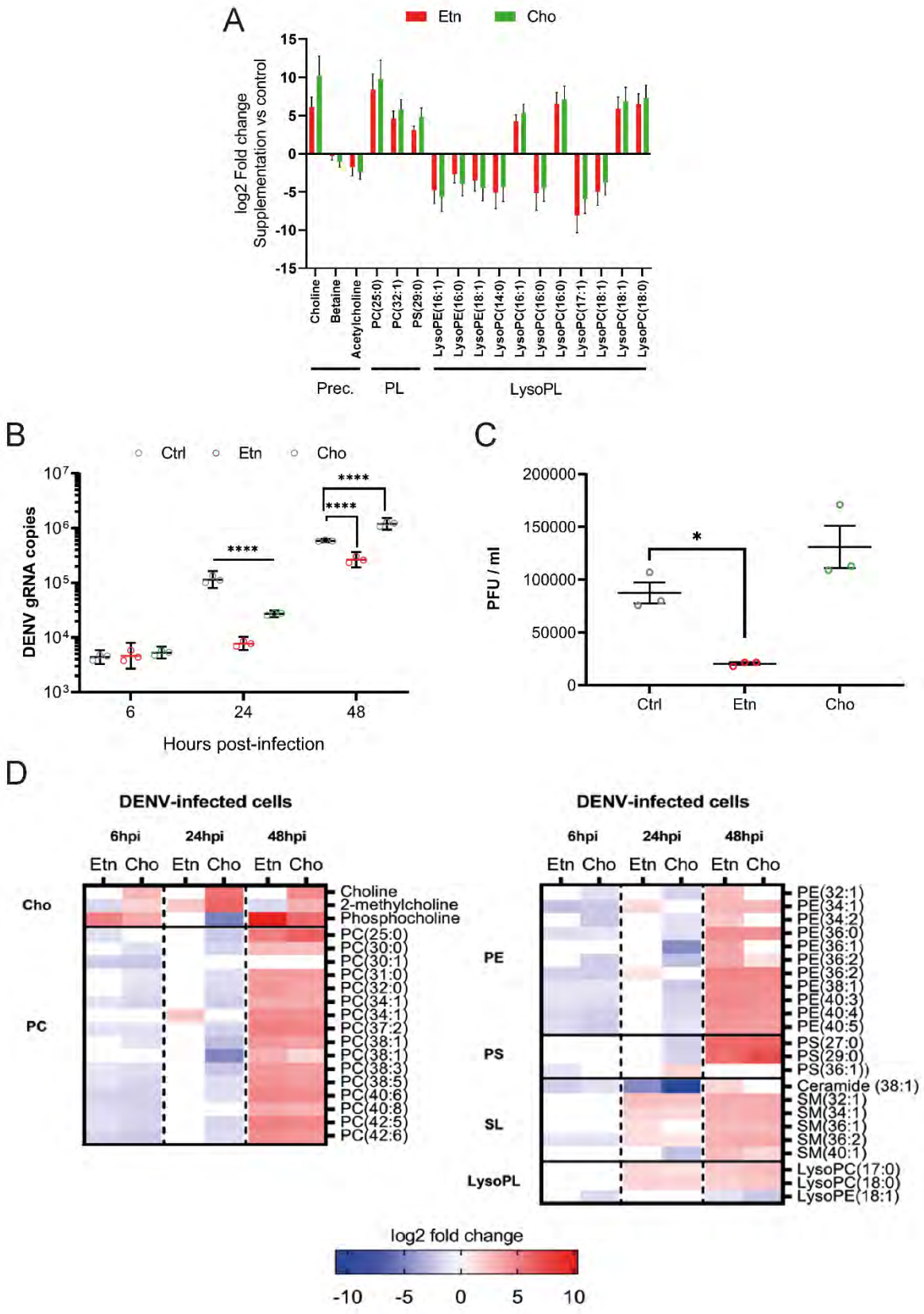

Fig 2. Impact of Kennedy pathway activation on DENV and phospholipid reconfiguration. Aag2 cells were supplemented with either ethanolamine (Etn) or

choline (Cho) for 24h before infection with DENV at a MOI of 1 or mock. (A) Impact of the supplementations on the phospholipidome before infection. Fold changes of significantly regulated metabolites (|log2 fold change| > 1 and p-value <0.05) as compared to control media are shown. (B) Impact of the supplementations on DENV gRNA at 6, 24 and 48 hpi. Bars show geometric means ± 95% C.I. Each point represents an independent well-repeat. ***, p-value < 0.001; ****, p-value < 0.0001 as determined by Dunnett's multiple comparison test. (C) Impact of the supplementations on DENV production as determined by plaque forming unit (pfu). Bars show mean ± s.e.m. *, p-value < 0.05, as determined by unpaired t-test. (D) Impact of the supplementations on the phospholipidome at 6, 24 and 48 hpi. Fold changes of significantly regulated metabolites (|log2 fold change| > 1 and p-value <0.05) as compared to media control within same time-point are shown. Cho; choline intermediates; PE, phosphatidylethanolamine; PC, phosphatidylcholine; PS, phosphatidylserine; LysoPC, lysophosphatidylcholine; LysoPE, lysophosphatidylethanolamine; SM, Sphingomyelin.

2.3.3. DENV reconfigures PLs through remodeling first and then de novo synthesis

To determine the effect of DENV on the biosynthesis of PE and PC, separately, we isotopically labeled each branch of the Kennedy pathway (i.e., CDP:Etn and CDP:Cho branches) and monitored changes in isotopically labeled metabolites. Aag2 cells were supplemented with ^{13}C-Etn, ^{13}C-Cho or non-isotopic precursors. Isotopically labeled metabolites were detected and annotated by comparing retention time (RT) and mass m/z between labeled and non-labeled metabolites (Fig 3A; Fig S5; Table S1). Isotopically labeled metabolites have similar RT as the same non-labeled metabolites and a m/z + 2. Before infection, in ^{13}C-Etn supplemented cells, we detected five

labeled-PE and, in ^{13}C-Cho supplemented cells, we detected labeled-Cho and three labeled-PCs (Table S1). This confirmed that our labeling strategy differentiated the two branches of the Kennedy pathway and that isotopes were incorporated in PE and PC before infection.

Upon infection, we monitored changes in labeled PLs at 1, 6, 24 and 48 hpi as compared to mock. Many new PLs were labeled in both ^{13}C-Etn and ^{13}C-Cho supplemented cells, indicating activation of PL reconfiguration in both branches (Fig 3B and C; Table S1 and S2). In ^{13}C-Etn samples, two LysoPEs were first induced at 1 hpi, and then at 24 and 48 hpi (Fig 3D; Table S2), suggesting that pre-labelled PE were deacylated to form LysoPE early and throughout infection. At 24 and 48 hpi, four monounsaturated PEs and three polyunsaturated PEs were increased by DENV. This increase in PE can stem from *de novo* synthesis (incorporation of ^{13}C-Etn through the Kennedy pathway) or remodeling (reacylation of LysoPE through the Lands cycle). However, because *de novo* synthesis does not produce polyunsaturated PL[295], it is highly probable that remodeling is activated by DENV to reconfigure PE. In support of DENV-activated deacylation, one PE-Ceramide that is generated by PE deacylation and incorporation of ceramide[135] was increased at 24 hpi. We also observed an increase in two polyunsaturated PCs in ^{13}C-Etn cells at 24 hpi. PE conversion into PC has not been reported in insects but exists in other organisms[296]. In ^{13}C-Cho supplemented cells (Fig 3E; Table S2), we did not detect LysoPC despite the previous observation of DENV activation of PC remodeling (Fig 2). This may reflect a technical limitation. Indeed, the lower number of labeled PC than labelled PE prior infection (Table S1) indicates that fewer PCs were labeled. Deacylation may have occurred for non-labeled PC. At 24 hpi, labeled-Cho increased, indicating activation of the Kennedy pathway, which is supported by increase of four monounsaturated PCs (Fig 3E; Table

S2). Altogether, the isotopic labeling strategy confirms PL reconfiguration and indicates that DENV induces first remodeling and then *de novo* synthesis.

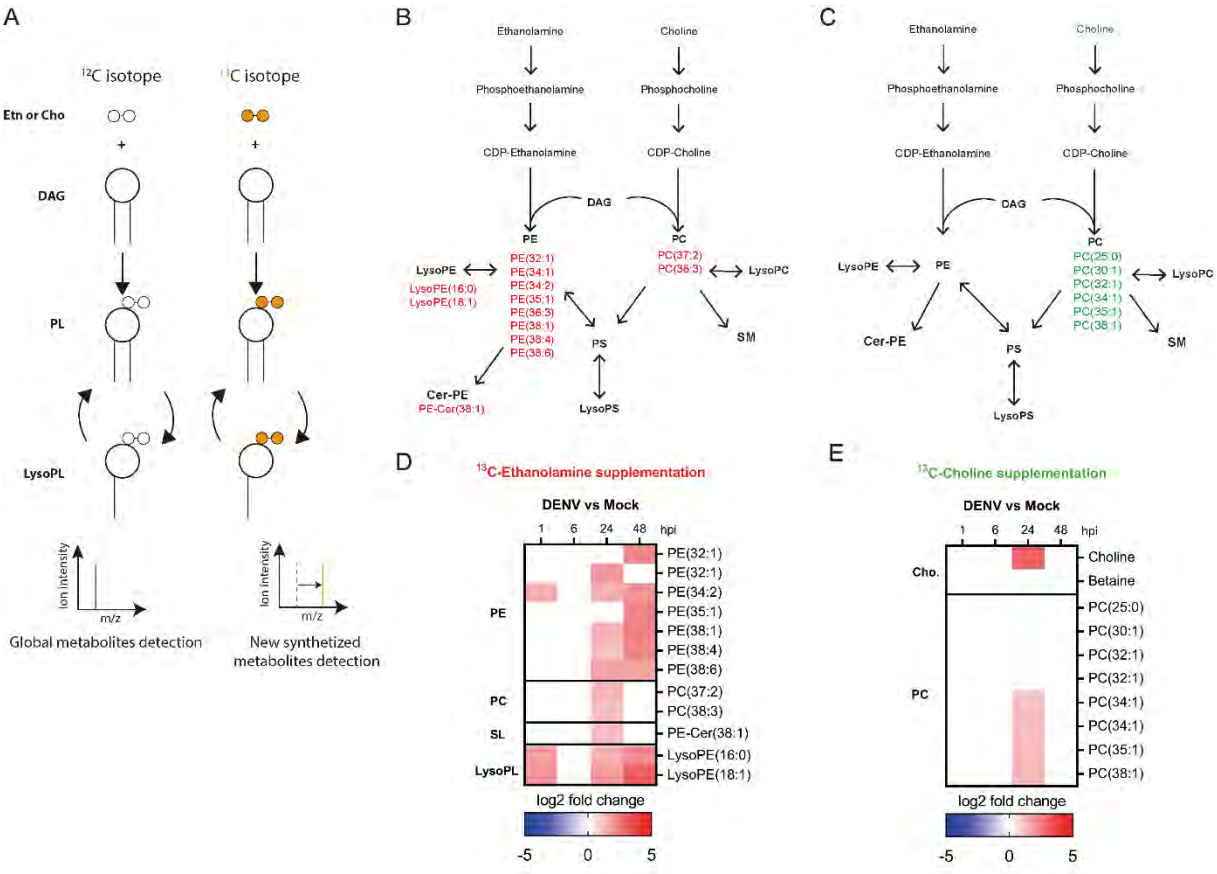

Fig 3. Impact of DENV on each of the branches of Kennedy pathway. Aag2 cells were supplemented with either isotope labeled ^{13}C ethanolamine (Etn) or choline (Cho). 24 h later, cells were infected with DENV at MOI 1 or mock. ^{13}C enrichment was quantified at 1, 6, 24 and 48h post infection. (A) Experimental design of isotope labeling tracking. Position in the Kennedy pathway of labeled PL upon (B) ^{13}C-Etn and (C) ^{13}C-Cho supplementation. Impact of DENV on labeled metabolites at 1, 6, 24 and 48 hpi upon (B) ^{13}C-Etn and (C) ^{13}C-Cho supplementation. Fold changes of annotated and significantly regulated metabolites (|log2 fold change| > 1 and p-value < 0.05) as compared to mock. PE, phosphatidylethanolamine; PC, phosphatidylcholine; PS,

phosphatidylserine; LysoPE, lysophosphatidylethanolamine; LysoPC, lysophosphatidylcholine; LysoPS, lysophosphatidylserine; SM, Sphingomyelin; Cer, Ceramide, DAG; diacylglycerol, CDP; cytidine -5'- diphosphate.

2.3.4. Kennedy pathway activation hampers replication

To determine what step(s) of DENV cellular cycle requires PL reconfiguration, we evaluated the impact of Etn and Cho supplementations on virus attachment, internalization, translation, replication and infectivity. PLs are present in plasma membrane and could influence attachment and internalization. To estimate attachment and internalization, we quantified attached and internalized gRNA from DENV grown in control media in cells supplemented with Cho or Etn. Attached and internalized gRNA were not altered by cell supplementations (Fig 4A). To investigate translation, we quantified production of NS3 as early as we detected it (3 hpi) and every hour until 6 hpi. NS3 expression did not change between supplemented and control cells (Fig 4B). DENV replication is initiated by antigenome (-ssRNA) production in PL-rich ER. We performed a kinetic of -ssRNA production from 1 to 24 hpi every 3 h and first detected it at 9 hpi (Fig 4C). Strikingly, from 9 hpi for Cho supplementation and from 12 hpi for Etn supplementation, -ssRNA was reduced and remained lower than control until the end of the kinetic. We then quantified +ssRNA, used for translation and virus packaging at the same time points, which roughly encompass the first replication cycle[58]. +ssRNA decreased from 1 to 9 hpi in all conditions and increased from 12 hpi (Fig 4D). In accordance with –ssRNA template appearance, it indicates that production of +ssRNA does not start before 12 hpi in Aag2 cells. From 12 and until 21 hpi, both supplementations reduced +ssRNA quantity. At 24 hpi, while Etn supplementation still reduced replication, Cho supplementation did not significantly alter replication anymore. We previously observed a similar difference between Etn

and Cho supplementations for gRNA (i.e., +ssRNA) and infectious particles (pfu/ml) at 48 hpi (Fig. 2B and C). We then quantified the attachment and internalization efficiency of DENV produced from Etn and Cho supplemented cells. DENV envelope contains PLs that are involved in these processes and could have been modified in supplemented cells. While attached and internalized gRNA from Etn-produced viruses was identical to control, Cho-produced DENV attached better but did not internalize better (Fig 4E). DENV envelope can exchange lipids with the media[265]. To control that attachment and internalization reflected changes due to assembly, we quantified attachment and internalization for control-grown DENV that were pre-incubated with Etn or Cho before attachment and internalization assays. Quantity of attached and internalized gRNA was no longer changed between treatments (Fig S6). Eventually, we quantified virus infectivity by calculating the ratio of gRNA to pfu in supernatant at 24 and 32 hpi. Importantly, while infectious particles (pfu/ml) was reduced upon Etn supplementation, gRNA copies were not significantly altered by supplementation (Fig 4F and G). This discrepancy resulted in an increase of gRNA/pfu ratio upon Etn supplementation (Fig 4H). Altogether, our analysis indicates that alteration of DENV-mediated PL reconfiguration by Etn and Cho supplementation chiefly hampers replication by reducing –ssRNA and +ssRNA productions and decreasing infectivity, the latter likely caused by genome defects. While replication deficiency occurs for both Etn and Cho supplementation, Cho-mediated alteration is temporary and Etn-mediated alteration lasts at least until 48 hpi in mosquito cells.

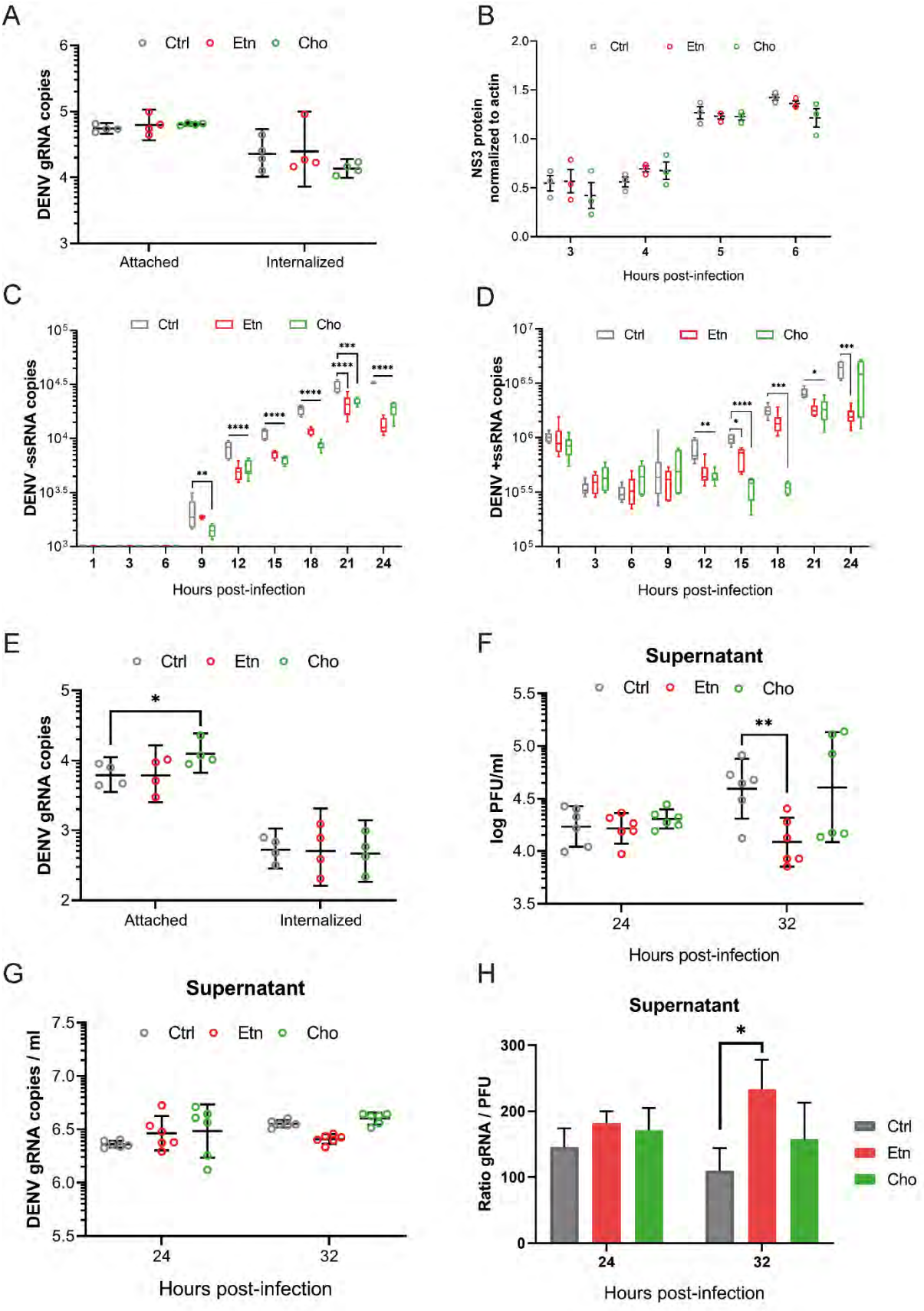
A
Ctrl
Etn
Cho
DENV gRNA copies
Attached
Internalized
B
NS3 protein normalized to actin
Hours post-infection
C
DENV -ssRNA copies
Hours post-infection
D
DENV +ssRNA copies
Hours post-infection
E
DENV gRNA copies
Attached
Internalized
F
Supernatant
log PFU/ml
Hours post-infection
G
Supernatant
DENV gRNA copies / ml
Hours post-infection
H
Supernatant
Ratio gRNA / PFU
Hours post-infection

Fig 4. Impact of Kennedy pathway activation on DENV cellular cycle. Aag2 cells were supplemented with either Etn or Cho or control media (Ctrl) for 24 h before infection with DENV at a MOI of 1. Impact of supplementations (A) on attachment and internalization; (B) on translation as measured by NS3 level normalized to b-actin at 3, 4, 5 and 6 hpi; on replication as measured by (C) -ssRNA and (D) +ssRNA per well at 1, 3, 6, 9, 12, 15, 18, 21 and 24 hpi; (E) on attachment and internalization for virus grown in supplemented media; on virus infectivity as measured by (F) pfu/ml, (G) gRNA/ml and (H) ratio of gRNA/pfu in supernatant at 24 and 32 hpi. (A, E, F, G) Bars show geometric means ± 95% C.I. Each point represents an independent well. (B, H) Bars show mean ± s.e.m. (C-D) Tukey box plots. (C-D, F-H) Six biological replicates were collected from 2 independent experiments. *, p-value < 0.05; **, p-value < 0.01; ***, p-value < 0.001; ****, p-value < 0.0001 as determined by Dunnett's multiple comparisons test.

2.4. Discussion

Several studies, including ours[286], support that DENV infection in mosquitoes[200,256] and mammals[243–245] is associated with PL reconfiguration. Here, we address two important questions to understand the metabolic interactions between DENV and its vector: how DENV reconfigures PLs and what is the function of the PL alterations? There are two ways PL are generated: *de novo* synthesis through the Kennedy pathway and remodeling through the Land's cycle. Using enzyme depletion to inhibit and precursor supplementation to activate the Kennedy pathway, we robustly demonstrate the negative effect of *de novo* synthesis on DENV multiplication. By monitoring the phospholipidome upon Kennedy pathway alterations and by using PL isotope labeling in mosquito cells, we showed that DENV induced PL

deacylation, the first step of the Land's cycle. PL synthesized from the Kennedy and Land's pathway have different saturation levels. The Kennedy pathway incorporates saturated or monounsaturated acyl chains, whereas Land's cycle removes saturated chains and replaces them with polyunsaturated chains[295]. Our findings suggest a model whereby *de novo* synthetized PLs do not favor DENV multiplication and DENV induces remodeling to reconfigure PLs for its multiplication. Of note, the pro-viral reconfiguration induced by infection depends on infection intensity and is, thus, expected to amplify with infection. There is probably not one specific PL species that is required for DENV multiplication. For instance, the PC(30:0) and PS(34:1) that were associated with higher DENV multiplication upon Kennedy pathway inhibition were also associated with unfavorable conditions upon Kennedy pathway activation. Further, while PE and PC *de novo* synthesis reduces DENV, PE *de novo* synthesis is more resistant to DENV-mediated reconfiguration, despite DENV-induced deacylation as for PC. PEs have an inverse conic shape that induces negative curvature, whereas LysoPLs have a conic shape that induces a positive curvature of different angle depending on the head group[295]. Adequate metabolic environment relies on a combination of the different PLs. Our results reveal the role of aminoPL remodeling in DENV multiplication.

By testing the impact of Kennedy pathway activation on each step of the DENV cellular cycle, we determine that PL reconfiguration is required for replication. Another *flavivirus* member, West Nile Virus (WNV), induces LysoPC generation in human cells by activation of phospholipase A2 (PLA2)[297]. Because LysoPC localizes to RC and inhibition of PLA2 blocks DENV replication by altering RC shape, the authors proposed that a certain LysoPC species is required for replication. Although for another *flavivirus*, we propose a more complex picture for PL requirements for replication. A new role for

PLA is emerging in reacylation of LysoPLs and, thus, in remodeling new PLs[295]. Additionally, DENV recruits the fatty acid synthase (FAS), the main enzyme for lipogenesis, at replication site by interaction with NS3 viral protein[273]. The need for FA at replication site may be required to feed new FA into PL remodeling. The conservation in remodeling enzymes may also represent an evolution towards replication in two different hosts, human and mosquito. VP where replication occurs contain NS proteins and viral RNA[63]. It is proposed that the joint actions of transmembrane NS4A and NS4B, and NS2 and NS1 assist in the formation of invaginated ER membrane that results in RC and VP[298]. Perturbation of ER membrane homeostasis by introgression of viral proteins induces the ER stress response, which promotes membrane expansion by PL synthesis[299] and is required for replication[300]. PL remodeling not only modifies ER membrane curvature and fluidity required for RC and VP formations, but also increases permeability, which facilitates protein introgression.

We identified that Kennedy pathway activation through Etn supplementation reduced DENV multiplication. Etn cannot be synthesized by insects and has to be provided by the food source, most probably blood, which contains it at 2 µM[153]. Etn may represent another blood source that influence DENV infection in mosquitoes and could be a targeted for transmission-blocking strategy.

2.5. Materials and methods

Cell line

Aedes aegypti Aag2 cells[301] were cultured in RPMI-1640 medium (Gibco) with 10% filtered fetal bovine serum (FBS) (Hyclone) and 1% Penicillin-Streptomycin (Gibco).

For media supplementation, 2mM of either choline chloride (Sigma), ethanolamine (Sigma), choline-$^{13}C_2$ chloride (Sigma) or ethanolamine-$^{13}C_2$ (Sigma) was added to Aag2 growth medium 24 h before infection. Cells were maintained in vented culture flasks in a humidified incubator with 5% CO_2 at 28°C. BHK-21 (baby hamster kidney) (ATCC CCL-10) cells were cultured in the same media and maintained at 37°C with 5% CO_2.

Dengue virus

Dengue virus serotype-2 strain ST (DENV) was collected from the Singapore General Hospital in 1997[302]. DENV was propagated alternatively in Vero (ATCC CCL-81) and C6/36 (ATCC CRL-1660) cells. Virus titer was determined by plaque assay using BHK-21 cells[286].

dsRNA-mediated RNAi

Templates for dsRNA against AAEL009765 (EK/CK, ethanolamine/choline kinase), AAEL011564 (CT, CTP:phosphocholine cytidyltransferase), AAEL014395 (E/CPT1, DAG:CDP-choline ethanolamine/cholinephosphotranferase 1), AAEL011841 (E/CPT2, DAG:CDP-choline ethanolamine/cholinephosphotranferase 2), AAEL005651 (ET, CTP:phosphoethanolamine cytidyltransferase), AAEL010223 (PSD, PS decarboxylase) and AAEL008393 (PSS, PS synthase) were PCR amplified from *Ae. aegypti* cDNA with primers (Table S3) flanked with T7 promoter. dsRNA was synthetized with megaScript T7 transcription kit (Thermo Fisher Scientific), purified with E.Z.N.A. Total RNA kit I (Omega Bio-tek) in DEPC-treated water and annealed by slowly cooling down. Control dsRNA targeting LacZ was produced similarly from a plasmid[303]. 2 x 10^5 Aag2 cells were transfected with 1 µg of dsRNA by using TransIT-mRNA Transfection kit (Mirusbio).

Quantification of gene expression

Total RNA from Aag2 cells was extracted using E.Z.N.A. Total RNA kit I, treated with RapidOut DNA Removal kit (Thermo Fisher Scientific) and reverse transcribed with iScript cDNA Synthesis Kit (Bio-Rad). Gene expression was quantified using iTaq Universal SYBR Green Supermix (Bio-Rad) and primers detailed in Table S4*. Actin* expression was used for normalization. Quantification was conducted in a CFX96 Touch Real-Time PCR Detection System (Bio-Rad). Thermal profile was 95°C for 1 min and 40 cycles of 95°C for 10 sec and 60°C for 15 sec. Three biological replicates were conducted.

Quantification of DENV genomic RNA (gRNA)

Total RNA from cells was extracted using E.Z.N.A. Total RNA kit I (Omega Bio-tek) and eluted in 30µl of DEPC-treated water. Total RNA from supernatant was extracted using QIAamp Viral RNA Mini Kit (Quiagen) and eluted in 40µl of AVE buffer. gRNA was quantified with one-step RT-qPCR using iTaq Universal probe kit (Bio-Rad) and primers and probes targeting the DENV Envelope[304]. The 12.5 µl reaction mix contained 1 µM of forward and reverse primers, 0.125 µM of probe and 4 µl of RNA extract. Quantification was conducted on a CFX96 Touch Real-Time PCR Detection System (Bio-Rad). Thermal profile was 50˚C for 10 min, 95˚C for 1 min and 40 cycles of 95˚C for 10 sec and 60˚C for 15 sec. An absolute standard curve was generated by amplifying the qPCR target using a forward primer tagged with a T7 promoter; forward: 5'-CAGGATAAGAGGTTCGTCTG-3' and reverse: 5'-TTGACTCTTGTTTATCCGCT-3', resulting in a 453bp fragment. The fragment was reverse transcribed using MegaScript T7 transcription kit (Ambion) and purified using E.Z.N. A. Total RNA kit I. The total amount of RNA was quantified using a Nanodrop (Thermo Fisher Scientific) and used

to estimate copy number. Ten times serial dilutions were made and used to generate absolute standard equation. In each subsequent RT-qPCR plate, five standards were added to adjust for threshold variation between plates.

Titration

Titration was conducted by plaque assay with BHK-21 cells as described previously[305]. Briefly, 80-90% confluent cells were inoculated with serial 10-fold dilutions of samples for 1h. Cells were then incubated with 1% carboxyl-methyl cellulose (CMC) (Merck) media for 5 days, fixed with 4% formaldehyde (Merck)-PBS and stained with 1% crystal violet (Sigma-Aldrich) solution to count plaque forming units (pfu).

Metabolite extraction

Cells were washed with room temperature 0.9 % NaCl, collected in 500 µl of ice-cold 80:20 methanol(LCMS grade, Thermo Fisher):water by scraping and sonicated for 15 min in an ultrasonic bath at 4°C. Homogenates were centrifuged at 10,000 rpm for 1 min at 4°C and 400 µl of supernatant was collected. Pellets were extracted a second time by addition of 500 µl of 80:20 methanol:water, then sonicated and centrifugated before collecting 400 µl of supernatant. Combined supernatants were vacuum-dried (Speed-Vac, Thermo-Scientific) and stored at -20°C. Three biological replicates were conducted per condition.

LC-HRMS metabolic profiling

Dry extracts were normalized at 2 mg/mL in 80:20 methanol:water solution. Metabolites were profiled using a UPLC- Q Exactive Plus hybrid quadrupole-Orbitrap

instrument (Ultimate 3000, Thermo Fisher Scientific, Hemel Hempstead, UK) set at 15,000 resolution, with a Zic-pHilic column (150 × 2.1 mm i.d., 5 µm, SeQuant®, Merck). Mobile phase A was 20 mM ammonium acetate buffered at pH 9 and B was acetonitrile. The flow rate was 200 µl/min and the gradient ran from 90 % B for 0.5 min to 40 % B over 18 min, was held at 40 % B for an additional 3 min, returned in 0.5 min to initial condition (90 % B) finally and was held for 5 min before subsequent analysis. The *m/z* range was 100–1500, ISpray voltage at 4.2 kV in positive mode and 3.0 kV in negative mode. Each full MS scan was followed by data dependent MS/MS on the two most intense ions using stepped CID fragmentation mode at 35 % normalized collision energy, isolation width of 2 u and activation Q set at 0.250.

Data analysis and visualization

Raw data were converted to abf files (Reifycs, Japan). Peak detection and alignment were performed using MS-DIAL (ver. 4.12) [306]. Peak annotation was done using MS-finder (ver. 3.26) [307] with HMDB, ChEBI, LipidMAPS and LipidBlast databases, allowing a level 2.2 of metabolite identification [225,308]. Data were normalized by total ion chromatogram (TIC) and features lower than 2-fold average blank were removed. Data were normalized by auto-scaling before selecting regulated metabolites with more than 2-fold intensity change and a p-value < 0.05 as indicated by unpaired t-test with FDR adjustment using MetaboAnalyst (ver. 4.0) [309]. PCA was performed for quality control with MetaboAnalyst (ver. 4.0). Isotope tracking analysis was performed using MS-DIAL. Peak detection and alignment were achieved first on the non-labelled sample data to build a library of compounds with known mass (M), retention time (RT) and annotation. Peak detection and alignment were then performed on ^{13}C labelled sample data and compared with non-labelled sample data. Peaks exclusively detected

in ^{13}C labelled sample data with a similar RT and a M+2 compared to a compound from non-labelled samples were considered isotopically labelled.

Attachment and internalization assays

2 x 10^5 Aag2 cells were chilled at 4°C for 15 min and inoculated with DENV at a MOI of 1 in serum-free media for 30 min at 4°C. Cells were washed with pre-chilled 2% FBS media. To quantify attached viruses, cells were lysed in 350 µL of TRK lysis buffer (E.Z.N.A. RNA kit I) and total RNA was extracted to quantify gRNA. To quantify internalization, cells were incubated with 350µl of 2% FBS medium at 28°C, 5% CO_2 for 1h. The medium was then replaced with 200µl of 2mg/ml pronase (Sigma) in serum free medium for 5 min on ice to remove virus particles on cell surface. Cells were washed twice with 10% FBS media and lysed in 350 µL of TRK lysis buffer to extract RNA and quantify gRNA from internalized viruses.

Translation assay

10^6 Aag2 cells were inoculated with DENV at a MOI of 1 in serum-free media for 1h. After infection, cells were washed with PBS before adding new fresh pre-warmed complete media with respective supplementation. At 3, 4, 5 and 6 hours post-infection, cells were washed twice with PBS, scrapped in 70 µL of RIPA lysis buffer (ThermoFisher) and sonicated for 10 min in an ultrasonic bath (J.R. Selecta) at 4°C. Protein concentration was measured by BCA assay (ThermoFisher) and 20µg was fractioned under denaturing conditions in 10% polyacrylamide gel (Bio-Rad). Antibodies used were anti-DENV-2 NS3 (CTX124252, Genetex) and anti-beta-actin (SC-47778, Santa-Cruz).

Replication assay

2.5 x 10^5 Aag2 cells were inoculated with DENV at a MOI of 1 or 5 in serum-free RPMI for 1h at 28°C. After infection, cells were washed with PBS before adding new fresh pre-warmed complete media with respective supplementation. At 1, 3, 6, 9, 12, 15, 18, 21 and 24 hours post-infection, cells were washed twice with PBS and lysed in 350 µL of TRK lysis buffer to extract RNA and quantify +strand and –strand gRNA.

Statistical analysis

Differences in gRNA copies were tested on log-transformed values using unpaired t-test or Dunnett's multiple comparisons test. Tests were performed with GraphPad PRISM software (ver. 8.02). For multivariate analysis, data were imported into SIMCA-P (ver. 15.0, Sartorius Stedim Biotech, Umetrics, Umeå, Sweden). To check for data consistency and outliers, data were analyzed with principal component analysis (PCA). The data were then pareto scaled for the partial least squares (PLS) regression analysis with DENV activity in PFU as the Y input. Variable importance for the projection (VIP) scores were used to rank variables according to their correlation with DENV activity.

3. Supplement information

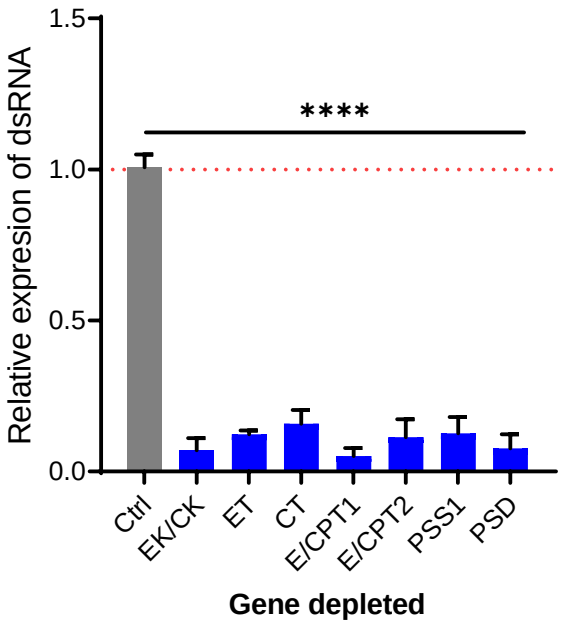

Fig S1. Kennedy pathway gene expression after silencing. Aag2 cells were transfected with either dsRNA against 7 genes of the Kennedy pathway or with dsRNA control (Control). Validation of Kennedy pathway gene silencing in in mock-infected cells at 72 h post transfection. Actin expression was used for normalization. Bars show mean ± s.e.m. ****, p-value < 0.0001 as indicated by Dunnett's multiple comparisons test or unpaired t-test. EK/CK, ethanolamine/choline kinase; ET, CTP:phosphoethanolamine cytidyltransferase; CT, CTP:phosphocholine cytidyltransferase; E/CPT, DAG:CDP-ethanolamine/choline ethanolamine/cholinephosphotranferase; PSS1, PS synthase; PSD, PS decarboxylase.

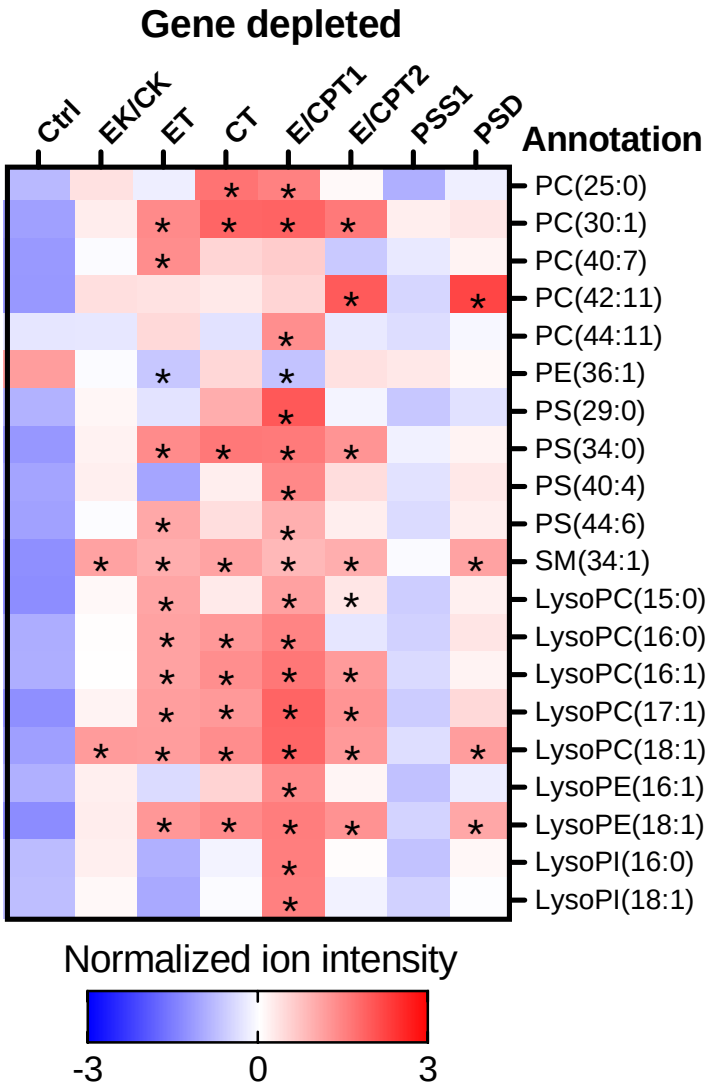

Fig S2. Ion intensity of regulated metabolites in DENV-infected cells after Kennedy pathway gene depletion. Normalized ion intensity was calculated after total ion chromatography normalization and auto scaling from three biological replicates. Conditions with significantly regulated metabolites (p-value <0.05 and |log2 fold change| >1) were indicated with an asterisk. PE, phosphatidylethanolamine; PC, phosphatidylcholine; PS, phosphatidylserine; LysoPC, lysophosphatidylcholine; LysoPE, lysophosphatidylethanolamine; LysoPI, lysophosphatidylinositol; SM, Sphingomyelin.

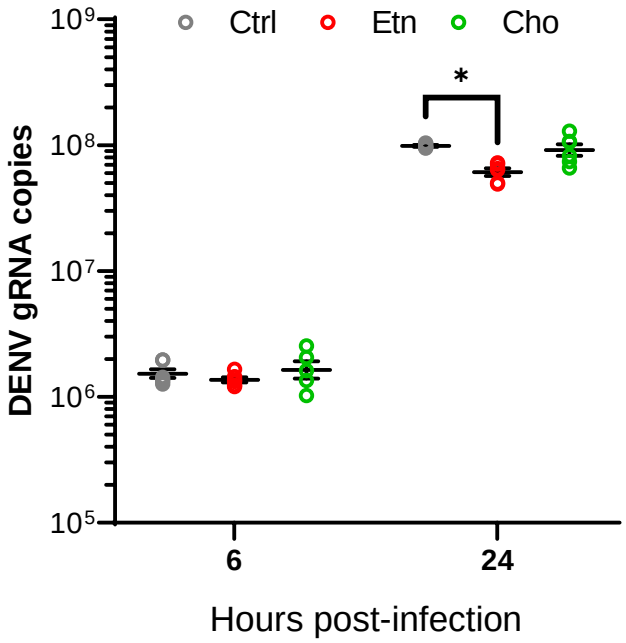

Fig S3. Impact of ethanolamine and choline supplementation on DENV replication at MOI 5. Aag2 cells were supplemented with either ethanolamine (Etn) or choline (Cho) and compared to standard growth media (control). At 1-day post supplementation, cells were infected with DENV at MOI 5. Quantification of DENV gRNA at 6 and 24 hpi. * p-value < 0.05, as determined by Dunnett's multiple comparisons test.

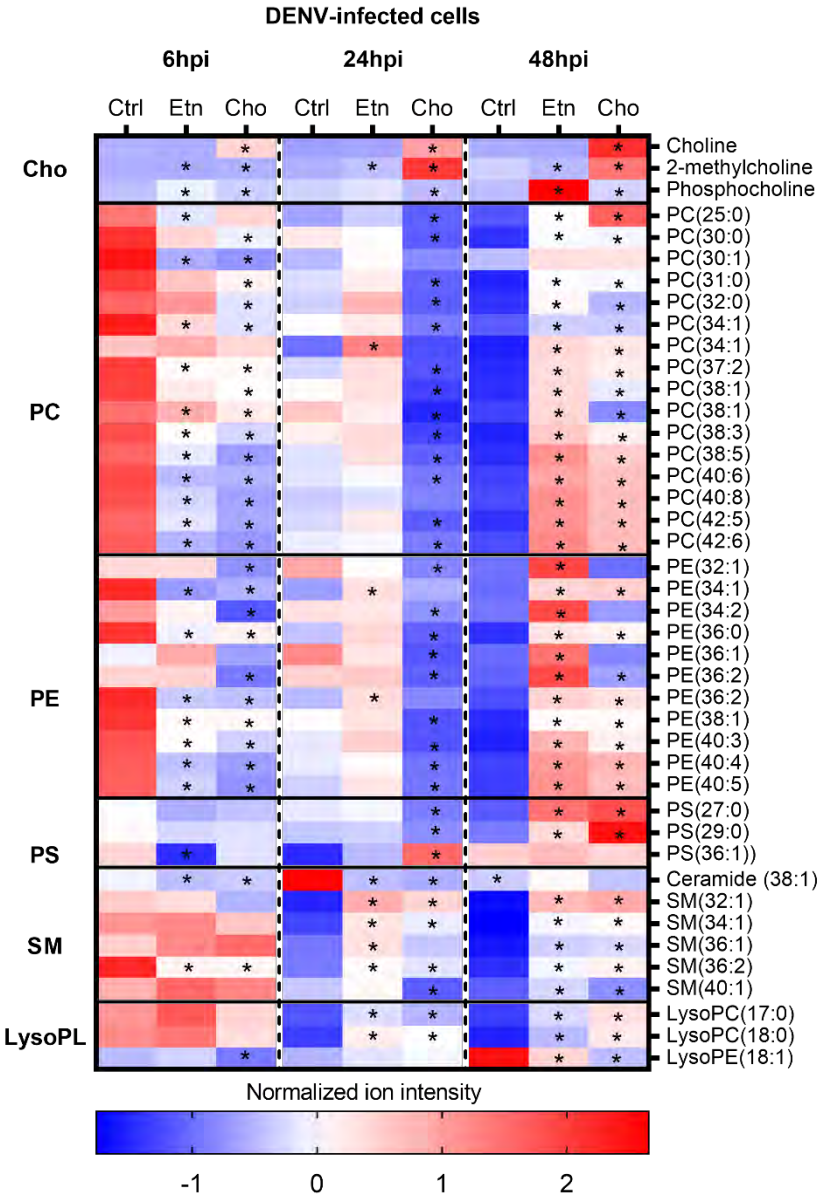

Fig S4. Ion intensity of regulated metabolites in choline or ethanolamine supplemented cells infected with DENV. Normalized ion intensity was calculated after total ion chromatography normalization and auto scaling from three biological replicates. Conditions with significantly regulated metabolites (p-value <0.05 and |log2 fold change| >1) were indicated with an asterisk. Cho, choline; PE, phosphatidylethanolamine; PC, phosphatidylcholine; PS, phosphatidylserine; LysoPL, lysophospholipid LysoPC, lysophosphatidylcholine; LysoPE, lysophosphatidylethanolamine; SM, Sphingomyelin;

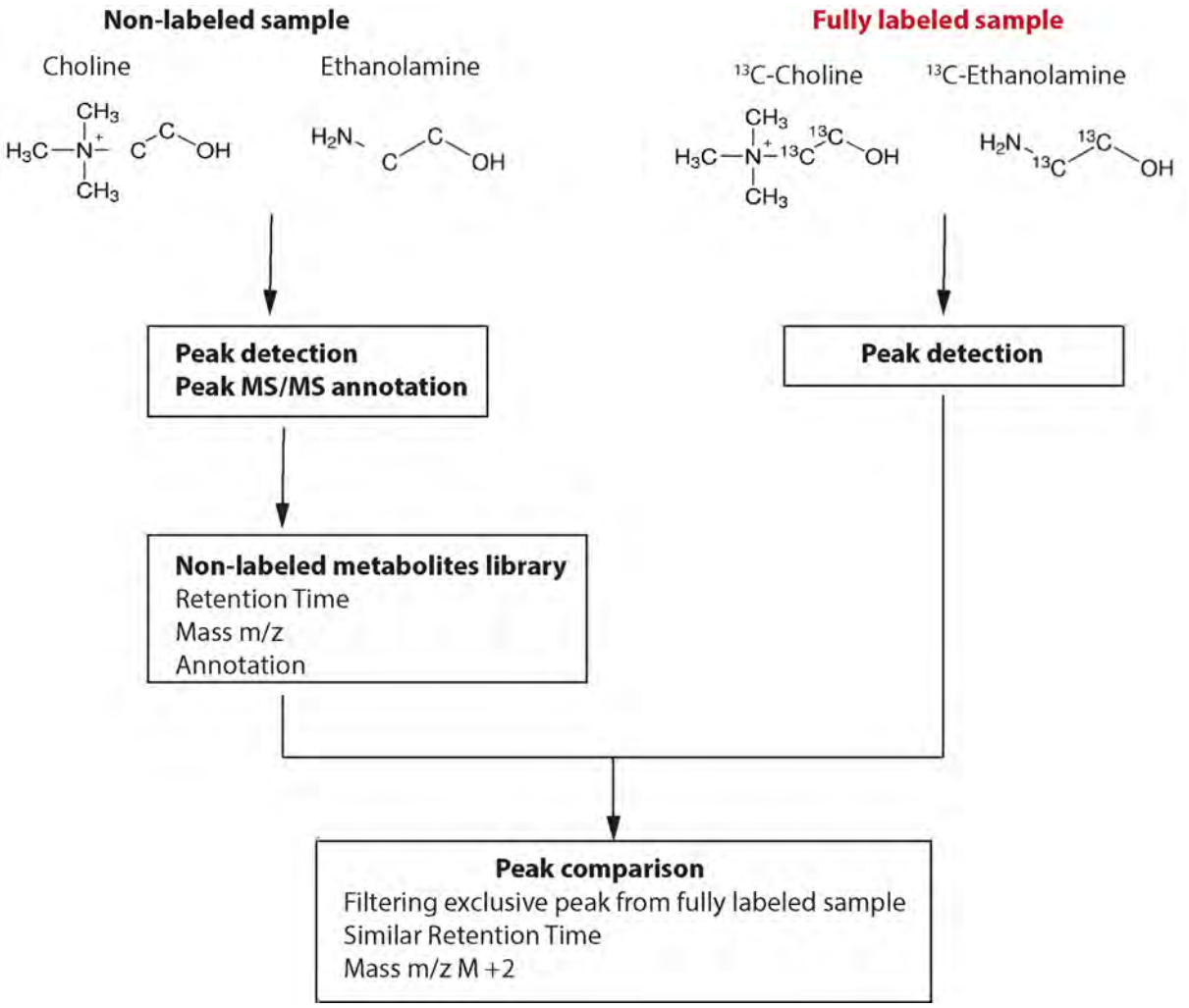

Fig S5. Isotope labeled ^{13}C ethanolamine (Etn) or choline (Cho) incorporation on phospholipid metabolites on mock-infected cells.

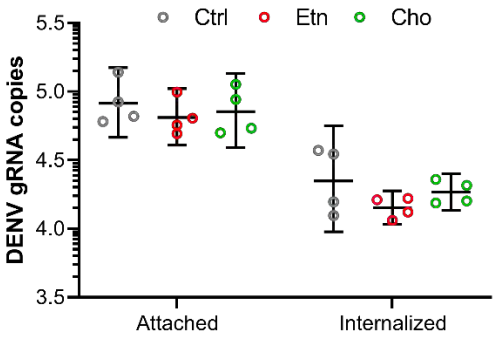

Fig S6. Impact of ethanolamine and choline pre-treated virus on attachment and internalization. (A) Attachment and internalization evaluation by gRNA quantification on DENV infected cells by pre-incubated for 30 min DENV with ethanolamine (Etn), choline (Cho) or with standard growth media (control).

Table S1. Isotope labeled ^{13}C ethanolamine (Etn) or choline (Cho) incorporation on phospholipid metabolites in mock-infected cells 24 hours after supplementation.

	^{13}C fully labeled		**Non-labeled**		
Supplementation	**RT**	**Mass m/z**	**Annotation**	**RT**	**Mass m/z**
Ethanolamine	2.976	692.5139	PE(18:1(9Z)/14:0)	2.939	690.5084
Ethanolamine	2.842	718.5323	PE(16:0/18:2(9Z,12Z))	2.895	716.5224
Ethanolamine	3.155	720.5444	PE(18:1(9Z)/16:0)	3.229	718.5375
Ethanolamine	2.897	720.5446	PE(18:1(9Z)/16:0)	2.944	718.5377
Ethanolamine	6.446	744.5445	PE(16:0/20:3(8Z,11Z,14Z))	6.499	742.5374
Choline	11.184	106.1078	Choline	11.167	104.1067
Choline	7.634	668.4445	PC(16:0/9:0(COOH))	7.635	666.4341
Choline	6.527	706.5334	PC(14:0/16:1(9Z))	6.514	704.5219
Choline	6.503	734.5647	PC(14:0/18:1(11Z))	6.501	732.5535

Table S2. Isotope labeled ^{13}C ethanolamine (Etn) or choline (Cho) incorporation on phospholipid metabolites in DENV and mock-infected cells between 25 and 72 hours after supplementation.

	^{13}C fully labeled				Non-labeled		
Supplementation	**RT**	**Mass m/z**	**DENV regulated**	**Time**	**Annotation**	**RT**	**Mass m/z**
Ethanolamine	2.485	766.5332	yes (Up)	24h	PE(16:0/22:6(4Z,7Z,10Z,13Z,16Z,19Z))	2.544	764.5216
Ethanolamine	2.614	770.5588	yes (Up)	24-48h	PE 38:4|PE 18:1_20:3	2.536	768.5520
Ethanolamine	2.757	776.6061	yes (Up)	24-48h	PE 38:1	2.652	774.5992
Ethanolamine	2.942	734.5592	yes (Up)	48h	PE(20:1(11Z)/15:0)	2.736	732.5531
Ethanolamine	2.925	718.5321	yes (Up)	6-24-48h	PE(16:0/18:2(9Z,12Z))	2.892	716.5224
Ethanolamine	3.168	692.5135	yes (Up)	48h	PE(18:1(9Z)/14:0)	3.323	690.5065
Ethanolamine	3.006	692.5134	yes (Up)	24h	PE(14:0/18:1(9Z))	3.039	690.5067
Ethanolamine	6.358	810.5977	yes (Up)	24h	PC 38:3	6.356	812.6126
Ethanolamine	6.435	802.6281	yes (Up)	24h	PC 37:2	6.392	800.6150
Ethanolamine	5.231	719.5968	yes (Up)	24h	PE-Cer(d16:1(4E)/22:0)	5.22	717.5901
Ethanolamine	5.852	482.3155	yes (Up)	6-24-48h	LysoPE(18:1(9Z)/0:0)	5.869	480.3085
Ethanolamine	5.929	456.2997	yes (Up)	6-24-48h	LysoPE(16:0/0:0)	5.928	454.2927
Choline	11.2	106.1135	yes (Up)	24h	Choline	11.189	104.1068
Choline	5.786	120.0807	no	/	Betaine	7.531	118.0861
Choline	7.635	668.4404	no	/	PC(16:0/9:0(COOH))	7.634	666.4340
Choline	6.525	706.5344	no	/	PC 30:1	6.511	704.5210
Choline	6.505	720.5438	no	/	PC O-32:1	6.526	718.5772
Choline	6.498	734.5615	no	/	PC(18:0/14:1(9Z))	6.494	732.5531
Choline	6.465	748.5726	yes (Up)	24h	PC O-34:1	6.511	746.6069
Choline	6.445	762.5900	yes (Up)	24h	PC 34:1	6.465	760.5835
Choline	6.446	776.6052	yes (Up)	24h	PC 35:1	6.444	774.5966
Choline	6.434	818.6527	yes (Up)	24h	PC 38:1	6.456	816.6458

Table S3. Primers for dsRNA synthesis

Gene name	Gene code	Fragment size	Forward primer	Reverse primer
EK/CK	AAEL009765	301	GGCTTAGGGGATCGAGAGAC	GTCATCGTTGGCGTTATTGTT
CT	AAEL011564	305	CCGGTACGGTTGTACGGA	CGCCTCAAGGTTTCGATTTA
CPT1	AAEL014395	395	ATCATCGCGAATGCAATTTT	CAGCTGTAGGGCATGGACTT
CPT2	AAEL011841	312	GACCCTGTTCTACTGTGCCC	AACAGGAACGGTATGATGGG
ET	AAEL005651	313	ACGGAGCTCGGAGGCTTACT	TCGTCAACCCATTTAATGCC

PSD	AAEL010223	314	GGTCTGTACTCGACCGCTTT	GCATTGTCGGGTGATTTCTT
PSS	AAEL008393	337	GTGGACGATATTTCGCTGGA	TAAAATTCCGTAACGTGGGG
LacZ	/	370	TACCCGTAGGTAGTCACGCA	TACGATGCGCCCATCTACAC

Table S4. Primers for RT-qPCR

Gene name	Gene code	Forward primer	Reverse primer
EK/CK	AAEL009765	GGCTTAGGGGATCGAGAGAC	GTCATCGTTGGCGTTATTGTT
CT	AAEL011564	CCGGTACGGTTGTACGGA	CGCCTCAAGGTTTCGATTTA
CPT1	AAEL014395	ATCATCGCGAATGCAATTTT	CAGCTGTAGGGCATGGACTT
CPT2	AAEL011841	GACCCTGTTCTACTGTGCCC	AACAGGAACGGTATGATGGG
ET	AAEL005651	ACGGAGCTCGGAGGCTTACT	TCGTCAACCCATTTAATGCC
PSD	AAEL010223	GGTCTGTACTCGACCGCTTT	GCATTGTCGGGTGATTTCTT
PSS	AAEL008393	GTGGACGATATTTCGCTGGA	TAAAATTCCGTAACGTGGGG
Actin	AAEL011197	GAACACCCAGTCCTGCTGACA	TGCGTCATCTTCTCACGGTTAG

CHAPTER 4 – Discussion

The work presented here enabled the exploration of the role of lipid mosquito metabolism in the DENV infectious. As a first step, we deployed a metabolomics approach using liquid-chromatography-mass spectrometry workflow, to study the reconfiguration of phospholipid by DENV across the mosquito cycle. The phospholipid regulation was partially due to DENV-mediated reduction of a host metabolic factor, an acylglycerophosphate acyltransferase (AGPAT1) involved in phospholipid biogenesis. Such *AGPAT1* downregulation provides a beneficial environment for the viral infection. Reconfiguration of phosphatidylethanolamine (PE) and phosphatidylcholine (PC) were highly associated with DENV multiplication. We then refine the role of DENV in the PC and PE biogenesis pathway and support the importance of aminophospholipids for the replication of DENV infection in mosquito. We revealed that PL remodeling is more beneficial for DENV infection than *de novo* PL synthesis. Altogether, our study highlights the potential for disruption of phospholipid reconfiguration through aminoPL pathway interference as a strategy to block DENV mosquito transmission.

1. DENV alters the phospholipid metabolism for its benefits in mosquito

1.1. Mosquito phospholipid species reconfiguration during DENV infection

Lipid profiling of DENV infection is widely reported in human patients by analyzing alteration of serum and blood samples. Phospholipids, glycerolipids and sphingolipids families have been reported as lipid biomarkers of DENV infection [242–245]. Two studies have shown lipid perturbation in the *Aedes* vector, in mosquito cell line and midgut [200,256]. Membrane lipids were globally increased in DENV-infected *Aedes albopictus* cell line and on blood-fed *Ae. aegypti* midguts. In the present report, we described the lipid alteration in *Ae. aegypti* mosquito cell line, in midgut and in whole *Ae. aegypti* mosquito at strategic time points of the infection cycle to profile DENV metabolic alteration throughout the main mosquito vector life cycle. It is interesting to compare the DENV infectious profiles described in *Aedes* mosquito.

Perera and al., showed the impact of high DENV infection (multiplicity of infection of 20) at 36 and 60 hours post-infection in *Ae. albopictus* cell line, to quantify peak and late stage of replication as well as cellular stress increase [256]. In our study, we choose to represent the early stages of DENV-infection in *Ae. aegypti* mosquito cell between 6 and 48 hours (multiplicity of infection of 5), encompassing the changes induced during the first cycle of infection. We showed a very early decrease of lipid intermediates such as fatty acid and glycerolipid, while unsaturated phospholipid PC and PS species were increased at 48 hours. In *Ae. albopictus* cell, an increase of phospholipids and sphingolipids species, PC, LysoPC, LysoPE, SM and ceramides, was observed mainly at 36 hpi in infected cell and endomembrane fractions containing the DENV replication complex. Majority of PC species upregulated had unsaturated fatty acyl chains, likely synthetized from PL remodeling[154], which contributes to PL

recycling with incorporation of polyunsaturated fatty acid. LysoPL, resulting from PL hydrolysis by phospholipase activity, were highly increased in infected cells at 36 hpi, which is consistent with the remodeling and unsaturated PL regulation. It is interesting to note that PE, a major PL in insect that is involved in membrane curvature, was not regulated in global cell extract, but increased in isolated endomembrane fractions. PL intermediates, were increased in endomembrane fraction. Sphingolipid species, such as SM and ceramides were increases in *Ae. Albopictus* cells. While SM and ceramides were detected, we did not observe regulation on *Ae. Aegypti* cells. Those lipid species are evidence of both lipogenesis and lipolysis and indicate a renewal within the lipid membrane metabolism. The difference observed between Perera group and our results can be explained by the different mosquito species, the intensity of DENV infection and the collection time. However, it is clear that infection perturbs lipid homeostasis in both mosquito cell type and induces PL increase as the infection progress.

DENV-infection on *Aedes aegypti* midgut showed also membrane lipid modulation. Perera group described global upregulation of phospholipids PC, PE, PS, PG, lysophospholipid LysoPI, glycerolipids and sphingolipids, on midgut between 2 and 11 days after infectious blood-feeding [200]. In our study, we studied infected midgut between 1 and 7 days and showed an early increase of PA, the central intermediate in PL biogenesis. Lipid intermediates, PE and PC were also elevated, while anionic PS were decreased. PC and PE, the main cellular PLs were increased in both studies, emphasizing their modulation in infected midgut. However, PS has a different behavior. PS is generally associated with cell signaling and apoptosis. Difference in mosquito and DENV strain and physiological state of mosquito may result in different cellular phenomena which results in metabolic differences. We described

on whole mosquito the global increase of PL and especially LysoPL early in the infection and then a decrease of PL and LysoPL as the infection progress. By going further in the mosquito infectious cycle, we underline the consumption/ redirection of the PL content as the infection progresses. Finally, a lipid enrichment/consumption with functions in membrane architecture and membrane expansion is generally observed on DENV-infected mosquito.

1.2. DENV reduces the phospholipid biogenesis AGPAT1 gene

Acyltransferase enzymes are considered as major enzymes in lipid metabolism [310]. Phosphatidic acid is known to be the common intermediate for the synthesis of phospholipid and glycerolipid [146]. GPAT and AGPAT localized into membranes are involved in PA synthesis by two successive step of free fatty acyl incorporation into a glycerol molecule. Most fatty acids are “transferred” by these two enzymes. Several enzymes have been identified in the GPAT/AGPAT family [311]. Four well-conserved domains are involved in acyltransferases activities of these enzymes. The acyl-CoA specificity of GPAT/AGPAT determines the acyl composition of all *de novo* synthesized phospholipids and glycerolipids. Human AGPAT1 and AGPAT2 possess the highest affinity for LysoPA and acyltransferase activity involve in the conversion of LysoPA to PA [312]. Those enzymes are localized in the endoplasmic reticulum. Nevertheless, other role have been assigned to human AGPATs. It has been shown that AGPAT may be associated with cellular signaling by cytokine induction [207]. In the work presented previously, we phylogenetically characterized several mosquito AGPATs based on functional motifs defining substrates affinity and acyltransferase activity [313] as compared to human AGPAT. We identified 2 mosquito AGPATs with sequence similarity to human AGPAT1 and human AGPAT2, suggesting PA biosynthesis activity

of the mosquito AGPATs a potential immune signaling properties. We demonstrated that DENV reduced AGPAT1 expression *in vitro* and *in vivo* on mosquito and midgut, throughout the mosquito life cycle. Interestingly, mosquito AGPAT2 was not reduced upon DENV infection. *Aedes aegypti* transcriptome study showed a downregulation of AGPAT1 and an upregulation of AGPAT2 during DENV infection [314]. This difference in virus impact between the two AGPAT isoforms involved in the same mechanism of PA generation suggests a viral specific regulation depending on the sequence of the targeted proteins.

It is known that the endomembrane, and more specifically the endoplasmic reticulum membrane is used as a platform for translation, replication and assembly processes during DENV infection [315]. Furthermore, the endoplasmic reticulum is the site of structural lipids production [136], as it contains enzymes, intermediates and endproducts of the lipid pathways. Mitochondrial membranes also contain lipid biosynthesis enzyme involved in LysoPA and PA generation. The mitochondria-associated membranes (MAM) attached to the ER contains the lipid synthesis machinery [137]. This membrane network undergoes drastic modification upon viral infection. Viral polyprotein is anchored in the ER membrane after its translation and is then processed by host and viral proteases to produce single viral proteins, many of which remain anchored to the membrane such as prM, E, NS2A, NS2B, NS4A and NS4B and can modify membrane topology [64,316]. Viral replication then recruits host protein and induce membrane arrangement for the biogenesis of the replication complex. Those viral modifications made to the ER membrane might affect the pre-existing host protein-lipid environment. Membrane topology alteration may impair transmembrane protein function. Lipid bilayer stress can disrupt ER-resident proteins [317]. ER stress is characterized by accumulation of unfolded or misfolded proteins in

the ER, known as the unfolded protein response (UTR) [318]. ER induced-stress can disrupt lipid metabolism, such as glycerolipid and cholesterol biosynthesis [319]. Conversely, aberrant lipid metabolism and saturated fatty acids can induce ER stress leading to dramatic effect on cell survival [320–322]. All these suggest that ER membrane stress imposed by DENV infectious process might affect AGPAT1 activity, by membrane anchorage alteration, acyl substrate specificity modification or transferase activity impairment. In our work we showed the reduction of AGPAT1 gene expression during DENV infection, which implies a regulation at the gene or mRNA level. Moreover, an active infection was necessary to reduce AGPAT1 gene expression, as showed with inactivated virus which did not modify AGPAT1 regulation. AGPAT2, another mosquito isoform of acyltransferase was not subject to regulation of its expression, suggesting a specific DENV regulation on AGPAT1.

In this context, we can question how acylglycerophosphate acyltransferase are transcriptionally regulated. The expression of AGPAT is regulated either directly by transcription factor or indirectly by alteration of PL content, ER stress response or endoplasmic reticulum topology modification. It is know that several lipid metabolism pathways are regulated transcriptionally by the sterol regulatory element binding proteins (SREBP) [310,323]. Evidence of SREBP role in DENV infection was shown by inhibiting viral replication using chemical inhibition of SREBP [282]. However, the role of SREBP pathway in the ER membrane rearrangement induced during DENV infection was not demonstrated [324]. ER modification was independent of SRBEP activation, but dependent of viral protein expression and lipid reabsorption into the ER. This suggest that phospholipid metabolism alteration upon DENV infection, through the modulation of central lipid biosynthetic enzyme, may be impacted directly by host PL species and viral proteins. AUP1, a membrane protein localized in ER and lipid

droplets, contains acyltransferase domain and enable generation of phospholipids which is dependent on ubiquitylation. DENV exploits the acyltransferase activity of AUP1 through NS4A and NS4B interaction, which trigger lipophagy and induce DENV production [277]. This underlines the viral requirement of lipid modulation as observed with AGPAT1 reduction and phospholipid reconfiguration. Taken together, AGPAT1 enzyme regulation and PL reconfiguration upon DENV infection show a specific viral-host interaction within the PL metabolism.

1.3. Phospholipid remodeling contributes to DENV infection

De novo synthetized phospholipid and pre-existing phospholipids are known to have different acyl species diversity. The fatty acid remodeling system regulates the acyl compositions of *de novo* synthetized phospholipids [295,325]. While saturated or monounsaturated C16 and C18 fatty acid are commonly incorporated in *de novo* produced lipids, polyunsaturated fatty acids such as arachidonic acid, are usually introduced during the fatty acid remodeling. Remodeling enable to meet the cell needs for new PL species which are not produced upstream. As PA biosynthesis, the remodeling process requires acyltransferase reactions. Isoforms of GPAT/AGPAT can possess acyltransferase activity for lysophospholipids, contributing to PL remodeling. Human AGPAT3-5 target different substrates that LysoPA, such as other LysoPL, which contributes to phospholipid remodeling. Phospholipid can be hydrolyzed and lose one acyl chain under phospholipase activity. This reaction generates lysophospholipid and free fatty acid. Lysophospholipid transferase (LPLAT) can incorporate a new fatty acid species, to form different phospholipids. This remodeling process known as the Land's cycle [154], is crucial for cell membrane maintenance and diversity [154].

In the presented work, we found that AGPAT1 gene depletion enhanced DENV infection in vivo and in vitro on mosquito. This pro-viral phenotype was associated with an increase in aminoPL concentration. We hypothesized that the depletion of AGPAT1 expression, and consequently a decrease of the acyltransferase process for *de novo* PL synthesis, contributes to the DENV infectious cycle. Inhibition of the Kennedy pathway showed also an increase of DENV replication, more specifically on the choline branch of the Kennedy pathway. We could hypothesize that a diminished metabolic activity of de novo phospholipids biosynthesis induces a balance towards the remodeling of existing PL. DENV infection may not contributes only to the *de novo* phospholipid generation, but rather modify existing PLs and change their fatty acid composition in order to modulate a membrane architecture conducive to infection. As detailed above, this dynamic PL remodeling was shown in our work and in recent studies in mosquitoes with the modulation of lipid species such as LysoPL and unsaturated PL [200].

1.4. DENV NS proteins recruit metabolic host protein

Beyond metabolomic alteration and gene expression modulation, it is known that DENV regulates directly host metabolic proteins via NS proteins interaction. Cellular energy metabolism is affected upon DENV infection via NS1 protein [326]. The glyceraldehyde-3-phosphate dehydrogenase (GAPDH), a multifunctional enzyme involved in the glycolysis [327], interacts with intracellular NS1. GAPDH glycolytic activity can be enhanced by NS1 addition in vitro and by DENV infection. Moreover, DENV relocalized GAPDH is the perinuclear region near NS1 expression site. Recruitment and modulation of major glycolytic enzyme by NS protein is consistent with energy alteration and glycolysis requirement in DENV-infected cells [328,329].

Others viruses such as Hepatitis C virus (HCV) and herpes simplex virus-1 enhance glucose consumption and glycolytic flux [330,331]. HCV NS5 protein induces energy modulation through interaction with the glycolytic hexokinase enzyme [331]. Glycolytic metabolites were also found increased during DENV infection [329], demonstrating the link between direct host protein regulation and metabolites modulation. DENV NS3 regulates another major metabolic pathway, by interacting with the fatty acid synthase (FAS) enzyme involved in lipogenesis. FAS is relocalized to DENV replication sites and its activity is enhanced [251]. NS1 and NS3 may be directly responsible for host metabolism modulation by increasing glycolytic and lipogenesis activity. Interestingly, both NS proteins relocalized the targeted metabolic host proteins to perinuclear regions, where viral replication occurs. This recruitment by DENV viral proteins may contribute to energetic needs during viral translation, replication assembly but also for membrane rearrangement induction. Another aspect for host metabolic factor enrolment is the capacity to produce building block necessary for DENV infection. FAS recruitment by NS3 on replication sites can be useful to provide free fatty acid bulk for incorporation into hydrolyzed phospholipid and enhancing PL remodeling. New fatty acids produced, usually saturated, can be further transformed into polyunsaturated fatty acid by fatty acid desaturases, which can be used to diversify the PL composition by remodeling. Simultaneous metabolic pathway could be affected by either direct viral proteins interaction or indirect lipid species alteration, which enable PL remodeling and construction of biochemical platforms for DENV infectious cycle.

2. The DENV viral life cycle is intimately associated with the phospholipids

2.1. Alteration of membrane PL composition for the replication step

Incorporation of ethanolamine in phospholipid showed and increased in LysoPE early during DENV infection, suggesting early remodeling. We also demonstrated the PC/PE reconfiguration during DENV infection on mosquito. DENV-mediated remodeling and aminoPL balance modification could contributes to the optimal concentration of PC, PE, LysoPL in endomembrane hosting the important stages of the viral cycle. PC as a cylindrical lipid, induces a planar membrane and restrict membrane curvature. PC has to be associated with other PL species to induce membrane rearrangement. PE with a small headgroup results in inverted conical geometry, imposing a negative curvature when inserted in a lipid bilayer. LysoPL with large headgroup compared to the small acyl chain, is the reverse of PE by inducing positive membrane curvature. Different association of those PL-induced curvature into a PC membranes can lead to the membrane alteration observed into DENV-infected mammalian and mosquito cells [62,63]. DENV replication occurs in association with virus-induced endomembrane structure that fold around the replication mechanism containing host and viral proteins and viral RNA. LysoPL increases the membrane permeability [285], which can be favorable for molecule incorporation during DENV replication complexes formation.

As we seen with the remodeling, DENV-mediated synthesis of curvature PL may ensure the membrane architecture enable the efficient infectious environment. Construction of different morphology of membranes alterations, such as convoluted membranes, tubular structures and vesicle packets derivate from the ER membrane system, provide the support for viral proteins, genome transport between ribosomes,

replication vesicle and virus assembly sites. Conversely, by supplementing cells with either ethanolamine or choline we showed a modification of the PL cell profile and an activation of PC and PE biogenesis. We can then hypothesize that PL precursor supplementation modify the PL membrane content. By these modifications, we impacted negatively the step of DENV replication, but not the entry neither the translation step. Even if the steps of translation, replication and assembly are intimately associated with intracellular membrane [63], we established a distinct impact on viral replication, which persists with exogenous ethanolamine and impacts the production of viral particles. Otherwise, the replication of West Nile Virus, another member of *flavivirus*, was affected by the inhibition of LysoPL generation [297]. This inhibition was rescued by LysoPL exogenous addition. Moreover, LysoPL generation was linked to subcellular sites of viral replication. Our work extends the previous understanding of how *flavivirus* manipulate the PL balance to favor specifically the step of viral replication.

2.2. Model of phospholipid needs in DENV life cycle

In order to complete its infectious cycle, the virus must adjust the cell lipid homeostasis to provide the platform for its translation, replication and assembly steps. To do this, the virus uses several strategies. It regulates the expression of genes involved in phospholipid metabolism such as AGPAT1. It interacts directly with host factors, such as the interaction of NS3 with FAS, which contributes to fatty acid synthesis and provide substrate for efficient PL synthesis/remodeling. DENV induces enrollment of cellular proteins to maintain membrane structures (RTN3.1A and DNAJC14), and recruits lipid reserve structures such as lipid droplet by NS4-AUP1 and NS3-Rab18 for lipid bulk reserve. These virus-host associations are localized at the site of genome

replication. It results in inducing the biosynthesis and degradation of phospholipids, as well as their remodeling in order to reveal the optimal membrane composition that will lead to membrane rearrangement for the proper conduct of infectious cycle. Viral replication is particularly demanding on this redesigned lipidic environment to build the membrane structures necessary for the establishment of the replication complex, which ensures both the good performance of genome synthesis and protection against cellular factors. PC, PE and LysoPL balance induce the curvature and membrane permeability necessary to maintain this environment.

3. Host lipid metabolism alteration confirms potential antiviral target strategy

As showed in our work with ethanolamine, lipid-related metabolites may be candidates to disrupt DENV replication. We demonstrated relative alteration on DENV particle production on mosquito cells with exogenous ethanolamine. A phospholipid compound, belonging to the phosphatidylinositol (PI) family, showed anti-DENV activity [332]. The PI molecule did not impair DENV entry but blocked the viral replication. The PI suppressed cytokines induced during DENV infection, showing inflammatory responses alteration in DENV-infected cells. Interestingly, the PI did not bind directly to DENV particle which indicates an indirect effect of inhibition mechanism. It would be interesting to follow the impact of lipid-modified blood meal on DENV development in mosquito.

Previous studies have reported other viral infection alteration by lipid molecules. Influenza virus infection is blocked by a lipid derived from the polyunsaturated fatty acid docosahexaenoic acid (DHA), by acting on viral transcript transport [333]. Other PL compound, such as phosphatidylglycerol (PG) and phosphatidylinositol (PI) can

suppress influenza A virus infection and syncytial virus infection [334–336]. The PG compound was also associated with inflammatory signaling. Targeting PL by antibody was applied to treat arenavirus and cytomegalovirus infection in animal models, against phosphatidylserine (PS) [337]. Neutralization of HIV-1 on peripheral blood mononuclear cells was established by anti-phospholipid monoclonal antibodies, which do not neutralize directly the virus but induce effective immune response [338]. Conversely, structural lipid can be important for *flavivirus* infection. Sphingolipid such as sphingomyelin and glycosphingolipid GM3 are essential in West Nile virus and DENV infection [339,340].

Several studies showed chemical inhibition of host metabolic factors altering DENV infection. Fatty acid synthase inhibition by C75 chemical compound is able to impair DENV infection [260]. C75 inhibitor was able to reduce fatty acid incorporation into lipid [251]. Chemical inhibition of phospholipase A2, involved in PL deacylation, can also impair flaviviral infection [297]. Cholesterol, major component of cell membrane is also a target in antiviral strategy. U18666A drug is an intracellular cholesterol inhibitor which blocks DENV and HCV infection [341,342]. Furthermore, the direct involvement of NS protein in host metabolic factor modulation, such as NS3 with FAS and AUP1, provides new insights for further drug conception as antiviral therapies against DENV infection. The need of antiviral therapy due to the absence of treatment and effective vaccines, and the major role of lipid metabolism in DENV infection on mosquito could enhance lipid-targeted strategy to block the transmission.

4. Exogenous factor linked to PL in vector transmission

Human host blood taken during the female mosquito's meal is a large source of lipid and its composition could contribute to the transmission from host to vector as seen with other blood amino acid metabolites enhancing arbovirus replication in mosquito [343]. Blood is composed of fluid plasma and floating cells. Plasma contains water, ions, metabolites such as glucose, amino acids, lipids, proteins (albumin, globulin, fibrinogen, immunoglobulin, heparin, lysozyme, properdin), excretory substances (ammonia, uric acid, creatine) and hormones. Blood cells composition contains erythrocytes carrying hemoglobin, leucocytes and thrombocytes.

Blood contains a wide variety of lipid, with free fatty acids, TAG mainly carried in very low density lipoprotein particles (VDDL), PL in high density lipoprotein (HDL) and in blood cells, and lipoprotein-cholesterol [344]. The most abundant fatty acids in whole blood are C16:0, C18:1 and C18:2 [345,346]. In blood lipid fractions, PC and SM are the main PL classes in the plasma followed by a small concentration of phosphatidylethanolamine [344]. Erythrocytes and thrombocytes contained mainly PC, PE and SM and smaller abundance of PS and PI. For instance, the proportion of PC in blood lipid fractions, which is the main PL in human, is 70-72% in the plasma, 30-36% in erythrocytes, 35-40% in thrombocytes. PC and PE are the main source of choline and ethanolamine to produce de novo and remodeled PL. However, several determinants can influence blood lipids composition, such as diet, age, gender, genetic background, smoking and exercise and therefore may induce variability in the mosquito blood meal associated with lipids depending on the host donor [344]. Blood cells are also a major source of PL, and their concentration, composition and viability are other factors that may influence lipids uptaken by the mosquito.

It would be interesting to assess the impact of different diets on populations with high lipid intake containing ethanolamine carried by PE on DENV transmission from humans to mosquitoes and its ability to transmit to an uninfected host. It could give insight to lipid and especially aminoPL as a factor for vector competence to transmit DENV. It should also be considered that infection in humans induces strong lipid remodeling with an increase in many species of fatty acids and phospholipids in the blood [255,287]. This change in the lipid content of the blood may also be a human factor influencing transmission.

It should important to note that the mosquito's blood meal is usually carried out in several times due to interruption by the host[347]. These multiple blood intakes can therefore successively modify the host's metabolism through the nutrients and properties of the blood and through intrinsic stimulation of mosquito metabolic pathways. A study of the mosquito lipidome in its natural condition is likely to give significantly different information in terms of phospholipid reorganization kinetics.

Mosquito microbiome is another external factor involved on the modulation of pathogen acquisition and transmission [348]. Midgut microbiota is known to enhance protection against pathogen and stimulate mosquito immune system [349,350], however mosquito bacteria were also linked to mosquito metabolism. In Ae. aegypti mosquito, midgut bacteria could play a role in the carbohydrates metabolism [351] and in the digestion process of the blood meal by the lysis of red blood cells and digestion of blood proteins [352]. Given that red blood cells and lipoprotein carrying lipid are a major source of PL, their digestion are highly important for the intake of lipid-derived species such as ethanolamine, choline et fatty acids. It would be interesting to determine this microbial activity upon DENV infection and the bacterial role in the

organization of the lipidome. Midgut bacterial communities was not identified as a factor which explains the susceptibility of the Ae. aegypti mosquito to DENV infection [353,354], however midgut bacteria composition could contributes in PL modulation during DENV infection.

From a general viewpoint, the role of lipid metabolism and PL in mosquito infection and transmission of DENV must take into account the mosquito's bloodmeal behavior, the characteristics of the blood donor and the mosquito microbiota, which plays an essential role in the absorption of external lipid metabolites.

5. A metabolomics approach to vector-pathogen interaction

The work presented in this thesis has expanded the understanding of the lipid metabolism in mosquitoes. We have highlighted the presence of genes involved in phospholipid biosynthesis, which until now had not been studied in mosquitoes. In addition, we were able to describe the mosquito lipidome under different conditions, such as DENV infection and gene depletion of the phospholipid pathway. We confirmed with previous study, the implementation of the metabolomic approach to study a non-model organism without mosquito specific metabolites databases [200]. This method may be applicable to other entomology studies to further investigate the interaction of pathogens with their vectors, and to complement transcriptomic and proteomic studies. The metabolome study strategy was already deployed in *Anopheles* mosquito [355,356]. Targeted phospholipid approach appears as an interesting strategy to adjust the view on the mosquito metabolic alteration upon viral infection.

REFERENCES

1. Bhatt S, Gething PW, Brady OJ, Messina JP, Farlow AW, Moyes CL, et al. The global distribution and burden of dengue. Nature. 2013;496: 504–507. doi:10.1038/nature12060

2. Gubler DJ. The Global Emergence/Resurgence of Arboviral Diseases As Public Health Problems. Arch Med Res. 2002;33: 330–342. doi:10.1016/S0188-4409(02)00378-8

3. Shepard DS, Undurraga EA, Halasa YA, Stanaway JD. The global economic burden of dengue: a systematic analysis. Lancet Infect Dis. 2016;16: 935–941. doi:10.1016/S1473-3099(16)00146-8

4. Selck FW, Adalja AA, Boddie CR. An Estimate of the Global Health Care and Lost Productivity Costs of Dengue. Vector-Borne Zoonotic Dis. 2014;14: 824–826. doi:10.1089/vbz.2013.1528

5. Kraemer MU, Sinka ME, Duda KA, Mylne AQ, Shearer FM, Barker CM, et al. The global distribution of the arbovirus vectors Aedes aegypti and Ae. albopictus. eLife. 2015. doi:10.7554/eLife.08347

6. Brady OJ, Gething PW, Bhatt S, Messina JP, Brownstein JS, Hoen AG, et al. Refining the Global Spatial Limits of Dengue Virus Transmission by Evidence-Based Consensus. PLoS Negl Trop Dis. 2012;6: e1760. doi:10.1371/journal.pntd.0001760

7. Rosenberger KD, Lum L, Alexander N, Junghanss T, Wills B, Jaenisch T. Vascular leakage in dengue – clinical spectrum and influence of parenteral fluid therapy. Trop Med Int Health. 2016;21: 445–453. doi:10.1111/tmi.12666

8. Guzman MG, Gubler DJ, Izquierdo A, Martinez E, Halstead SB. Dengue infection. Nat Rev Dis Primer. 2016;2: 16055. doi:10.1038/nrdp.2016.55

9. WHO. Dengue: Guidelines for Diagnosis, Treatment, Prevention and Control: New Edition. Geneva: World Health Organization; 2009.

10. Montoya M, Gresh L, Mercado JC, Williams KL, Vargas MJ, Gutierrez G, et al. Symptomatic Versus Inapparent Outcome in Repeat Dengue Virus Infections Is Influenced by the Time Interval between Infections and Study Year. PLoS Negl Trop Dis. 2013;7. doi:10.1371/journal.pntd.0002357

11. Guzman MG, Alvarez M, Halstead SB. Secondary infection as a risk factor for dengue hemorrhagic fever/dengue shock syndrome: an historical perspective and role of antibody-dependent enhancement of infection. Arch Virol. 2013;158: 1445–1459. doi:10.1007/s00705-013-1645-3

12. Ong EZ, Zhang SL, Tan HC, Gan ES, Chan KR, Ooi EE. Dengue virus compartmentalization during antibody-enhanced infection. Sci Rep. 2017;7: 1–9. doi:10.1038/srep40923

13. Powell JR, Tabachnick WJ. History of domestication and spread of Aedes aegypti - A Review. Mem Inst Oswaldo Cruz. 2013;108: 11–17. doi:10.1590/0074-0276130395

14. Delatte H, Dehecq J s., Thiria J, Domerg C, Paupy C, Fontenille D. Geographic Distribution and Developmental Sites of Aedes albopictus (Diptera: Culicidae) During a Chikungunya Epidemic Event. Vector-Borne Zoonotic Dis. 2008;8: 25–34. doi:10.1089/vbz.2007.0649

15. Murray NEA, Quam MB, Wilder-Smith A. Epidemiology of dengue: past, present and future prospects. Clin Epidemiol. 2013;5: 299–309. doi:10.2147/CLEP.S34440

16. Struchiner CJ, Rocklöv J, Wilder-Smith A, Massad E. Increasing Dengue Incidence in Singapore over the Past 40 Years: Population Growth, Climate and Mobility. PLOS ONE. 2015;10: e0136286. doi:10.1371/journal.pone.0136286

17. Scott TW, Clark GG, Lorenz LH, Amerasinghe PH, Reiter P, Edman JD. Detection of Multiple Blood Feeding in Aedes aegypti (Diptera: Culicidae) During a Single Gonotrophic Cycle Using a Histologic Technique. J Med Entomol. 1993;30: 94–99. doi:10.1093/jmedent/30.1.94

18. Li Y, Kamara F, Zhou G, Puthiyakunnon S, Li C, Liu Y, et al. Urbanization Increases Aedes albopictus Larval Habitats and Accelerates Mosquito Development and Survivorship. PLoS Negl Trop Dis. 2014;8: e3301. doi:10.1371/journal.pntd.0003301

19. Gubler DJ. Dengue, Urbanization and Globalization: The Unholy Trinity of the 21st Century. Trop Med Health. 2011;39: 3–11. doi:10.2149/tmh.2011-S05

20. Wilder-Smith A, Gubler DJ. Geographic Expansion of Dengue: The Impact of International Travel. Med Clin North Am. 2008;92: 1377–1390. doi:10.1016/j.mcna.2008.07.002

21. Ebi KL, Nealon J. Dengue in a changing climate. Environ Res. 2016;151: 115–123. doi:10.1016/j.envres.2016.07.026

22. Valentine MJ, Murdock CC, Kelly PJ. Sylvatic cycles of arboviruses in non-human primates. Parasit Vectors. 2019;12. doi:10.1186/s13071-019-3732-0

23. Vasilakis N, Cardosa J, Hanley KA, Holmes EC, Weaver SC. Fever from the forest: prospects for the continued emergence of sylvatic dengue virus and its impact on public health. Nat Rev Microbiol. 2011;9: 532–541. doi:10.1038/nrmicro2595

24. Thoisy B de, Lacoste V, Germain A, Muñoz-Jordán J, Colón C, Mauffrey J-F, et al. Dengue Infection in Neotropical Forest Mammals. Vector-Borne Zoonotic Dis. 2008;9: 157–170. doi:10.1089/vbz.2007.0280

25. Salazar MI, Richardson JH, Sánchez-Vargas I, Olson KE, Beaty BJ. Dengue virus type 2: replication and tropisms in orally infected Aedes aegypti mosquitoes. BMC Microbiol. 2007;7: 9. doi:10.1186/1471-2180-7-9

26. Franz AWE, Kantor AM, Passarelli AL, Clem RJ. Tissue Barriers to Arbovirus Infection in Mosquitoes. Viruses. 2015;7: 3741–3767. doi:10.3390/v7072795

27. Parikh GR, Oliver JD, Bartholomay LC. A haemocyte tropism for an arbovirus. J Gen Virol. 2009;90: 292–296. doi:10.1099/vir.0.005116-0

28. Schneider BS, Higgs S. The enhancement of arbovirus transmission and disease by mosquito saliva is associated with modulation of the host immune response. Trans R Soc Trop Med Hyg. 2008;102: 400–408. doi:10.1016/j.trstmh.2008.01.024

29. Hardy JL, Houk EJ, Kramer LD, Reeves WC. Intrinsic factors affecting vector competence of mosquitoes for arboviruses. Annu Rev Entomol. 1983;28: 229–262. doi:10.1146/annurev.en.28.010183.001305

30. Khoo CC, Piper J, Sanchez-Vargas I, Olson KE, Franz AW. The RNA interference pathway affects midgut infection- and escape barriers for Sindbis virus in Aedes aegypti. BMC Microbiol. 2010;10: 130. doi:10.1186/1471-2180-10-130

31. Franz AWE, Sanchez-Vargas I, Raban RR, Black WC, James AA, Olson KE. Fitness impact and stability of a transgene conferring resistance to dengue-2 virus following introgression into a genetically diverse Aedes aegypti strain. PLoS Negl Trop Dis. 2014;8: e2833. doi:10.1371/journal.pntd.0002833

32. Lambrechts L, Quillery E, Noël V, Richardson JH, Jarman RG, Scott TW, et al. Specificity of resistance to dengue virus isolates is associated with genotypes of the mosquito antiviral gene Dicer-2. Proc R Soc B Biol Sci. 2013;280. doi:10.1098/rspb.2012.2437

33. Mercado-Curiel RF, Black WC, Muñoz M de L. A dengue receptor as possible genetic marker of vector competence in Aedes aegypti. BMC Microbiol. 2008;8: 118. doi:10.1186/1471-2180-8-118

34. Mercado-Curiel RF, Esquinca-Avilés HA, Tovar R, Díaz-Badillo Á, Camacho-Nuez M, Muñoz M de L. The four serotypes of dengue recognize the same putative receptors in Aedes aegypti midgut and Ae. albopictus cells. BMC Microbiol. 2006;6: 85. doi:10.1186/1471-2180-6-85

35. Forrester NL, Coffey LL, Weaver SC. Arboviral Bottlenecks and Challenges to Maintaining Diversity and Fitness during Mosquito Transmission. Viruses. 2014;6: 3991–4004. doi:10.3390/v6103991

36. Vaidyanathan R, Fleisher AE, Minnick SL, Simmons KA, Scott TW. Nutritional stress affects mosquito survival and vector competence for West Nile virus. Vector Borne Zoonotic Dis Larchmt N. 2008;8: 727–732. doi:10.1089/vbz.2007.0189

37. Gubler DJ. Dengue and Dengue Hemorrhagic Fever. Clin Microbiol Rev. 1998;11: 480–496. doi:10.1128/CMR.11.3.480

38. Weaver SC, Vasilakis N. Molecular Evolution of Dengue Viruses: Contributions of Phylogenetics to Understanding the History and Epidemiology of the Preeminent Arboviral Disease. Infect Genet Evol J Mol Epidemiol Evol Genet Infect Dis. 2009;9: 523–540. doi:10.1016/j.meegid.2009.02.003

39. Lazear HM, Diamond MS. Zika Virus: New Clinical Syndromes and Its Emergence in the Western Hemisphere. J Virol. 2016;90: 4864–4875. doi:10.1128/JVI.00252-16

40. Zhang Y, Zhang W, Ogata S, Clements D, Strauss JH, Baker TS, et al. Conformational Changes of the Flavivirus E Glycoprotein. Struct Lond Engl 1993. 2004;12: 1607–1618. doi:10.1016/j.str.2004.06.019

41. Smit JM, Moesker B, Rodenhuis-Zybert I, Wilschut J. Flavivirus Cell Entry and Membrane Fusion. Viruses. 2011;3: 160–171. doi:10.3390/v3020160

42. Fibriansah G, Ng T-S, Kostyuchenko VA, Lee J, Lee S, Wang J, et al. Structural Changes in Dengue Virus When Exposed to a Temperature of 37°C. J Virol. 2013;87: 7585–7592. doi:10.1128/JVI.00757-13

43. Lewis JK, Bothner B, Smith TJ, Siuzdak G. Antiviral agent blocks breathing of the common cold virus. Proc Natl Acad Sci. 1998;95: 6774–6778. doi:10.1073/pnas.95.12.6774

44. Kuhn RJ, Dowd KA, Beth Post C, Pierson TC. Shake, rattle, and roll: Impact of the dynamics of flavivirus particles on their interactions with the host. Virology. 2015;479–480: 508–517. doi:10.1016/j.virol.2015.03.025

45. Mackenzie JM, Jones MK, Young PR. Immunolocalization of the Dengue Virus Nonstructural Glycoprotein NS1 Suggests a Role in Viral RNA Replication. Virology. 1996;220: 232–240. doi:10.1006/viro.1996.0307

46. Muller DA, Young PR. The flavivirus NS1 protein: Molecular and structural biology, immunology, role in pathogenesis and application as a diagnostic biomarker. Antiviral Res. 2013;98: 192–208. doi:10.1016/j.antiviral.2013.03.008

47. Xie X, Zou J, Puttikhunt C, Yuan Z, Shi P-Y. Two Distinct Sets of NS2A Molecules Are Responsible for Dengue Virus RNA Synthesis and Virion Assembly. J Virol. 2014;89: 1298–1313. doi:10.1128/JVI.02882-14

48. Muñoz-Jordán JL, Laurent-Rolle M, Ashour J, Martínez-Sobrido L, Ashok M, Lipkin WI, et al. Inhibition of Alpha/Beta Interferon Signaling by the NS4B Protein of Flaviviruses. J Virol. 2005;79: 8004–8013. doi:10.1128/JVI.79.13.8004-8013.2005

49. Gebhard LG, Filomatori CV, Gamarnik AV. Functional RNA Elements in the Dengue Virus Genome. Viruses. 2011;3: 1739–1756. doi:10.3390/v3091739

50. Hidari KIPJ, Suzuki T. Dengue virus receptor. Trop Med Health. 2011;39: 37–43. doi:10.2149/tmh.2011-S03

51. Cruz-Oliveira C, Freire JM, Conceição TM, Higa LM, Castanho MARB, Da Poian AT. Receptors and routes of dengue virus entry into the host cells. FEMS Microbiol Rev. 2015;39: 155–170. doi:10.1093/femsre/fuu004

52. Kuadkitkan A, Wikan N, Fongsaran C, Smith DR. Identification and characterization of prohibitin as a receptor protein mediating DENV-2 entry into insect cells. Virology. 2010;406: 149–161. doi:10.1016/j.virol.2010.07.015

53. van der Schaar HM, Rust MJ, Chen C, van der Ende-Metselaar H, Wilschut J, Zhuang X, et al. Dissecting the Cell Entry Pathway of Dengue Virus by Single-Particle Tracking in Living Cells. PLoS Pathog. 2008;4. doi:10.1371/journal.ppat.1000244

54. Acosta EG, Castilla V, Damonte EB. Alternative infectious entry pathways for dengue virus serotypes into mammalian cells. Cell Microbiol. 2009;11: 1533–1549. doi:10.1111/j.1462-5822.2009.01345.x

55. Mosso C, Galván-Mendoza IJ, Ludert JE, del Angel RM. Endocytic pathway followed by dengue virus to infect the mosquito cell line C6/36 HT. Virology. 2008;378: 193–199. doi:10.1016/j.virol.2008.05.012

56. Acosta EG, Castilla V, Damonte EB. Infectious dengue-1 virus entry into mosquito C6/36 cells. Virus Res. 2011;160: 173–179. doi:10.1016/j.virusres.2011.06.008

57. Acosta EG, Castilla V, Damonte EB. Functional entry of dengue virus into Aedes albopictus mosquito cells is dependent on clathrin-mediated endocytosis. J Gen Virol. 2008;89: 474–484. doi:10.1099/vir.0.83357-0

58. Nicholas J. Barrows, Mariano A. Garcia-Blanco. Biochemistry and Molecular Biology of Flaviviruses. Chem Rev. 2018;118: 4448–4482. doi:10.1021/acs.chemrev.7b00719

59. Forgac M. Vacuolar ATPases: rotary proton pumps in physiology and pathophysiology. Nat Rev Mol Cell Biol. 2007;8: 917–929. doi:10.1038/nrm2272

60. Schwartz M, Chen J, Janda M, Sullivan M, den Boon J, Ahlquist P. A Positive-Strand RNA Virus Replication Complex Parallels Form and Function of Retrovirus Capsids. Mol Cell. 2002;9: 505–514. doi:10.1016/S1097-2765(02)00474-4

61. den Boon JA, Ahlquist P. Organelle-Like Membrane Compartmentalization of Positive-Strand RNA Virus Replication Factories. Annu Rev Microbiol. 2010;64: 241–256. doi:10.1146/annurev.micro.112408.134012

62. Junjhon J, Pennington JG, Edwards TJ, Perera R, Lanman J, Kuhn RJ. Ultrastructural Characterization and Three-Dimensional Architecture of Replication Sites in Dengue Virus-Infected Mosquito Cells. J Virol. 2014;88: 4687–4697. doi:10.1128/JVI.00118-14

63. Welsch S, Miller S, Romero-Brey I, Merz A, Bleck CKE, Walther P, et al. Composition and three-dimensional architecture of the dengue virus replication

and assembly sites. Cell Host Microbe. 2009;5: 365–375. doi:10.1016/j.chom.2009.03.007

64. Miller S, Kastner S, Krijnse-Locker J, Bühler S, Bartenschlager R. The Non-structural Protein 4A of Dengue Virus Is an Integral Membrane Protein Inducing Membrane Alterations in a 2K-regulated Manner. J Biol Chem. 2007;282: 8873–8882. doi:10.1074/jbc.M609919200

65. Roosendaal J, Westaway EG, Khromykh A, Mackenzie JM. Regulated Cleavages at the West Nile Virus NS4A-2K-NS4B Junctions Play a Major Role in Rearranging Cytoplasmic Membranes and Golgi Trafficking of the NS4A Protein. J Virol. 2006;80: 4623–4632. doi:10.1128/JVI.80.9.4623-4632.2006

66. Lescar J, Soh S, Lee LT, Vasudevan SG, Kang C, Lim SP. The Dengue Virus Replication Complex: From RNA Replication to Protein-Protein Interactions to Evasion of Innate Immunity. In: Hilgenfeld R, Vasudevan SG, editors. Dengue and Zika: Control and Antiviral Treatment Strategies. Singapore: Springer Singapore; 2018. pp. 115–129. doi:10.1007/978-981-10-8727-1_9

67. Teo CSH, Chu JJH. Cellular vimentin regulates construction of dengue virus replication complexes through interaction with NS4A protein. J Virol. 2014;88: 1897–1913. doi:10.1128/JVI.01249-13

68. Youn S, Li T, McCune BT, Edeling MA, Fremont DH, Cristea IM, et al. Evidence for a Genetic and Physical Interaction between Nonstructural Proteins NS1 and NS4B That Modulates Replication of West Nile Virus. J Virol. 2012;86: 7360–7371. doi:10.1128/JVI.00157-12

69. Patkar CG, Kuhn RJ. Yellow Fever Virus NS3 Plays an Essential Role in Virus Assembly Independent of Its Known Enzymatic Functions. J Virol. 2008;82: 3342–3352. doi:10.1128/JVI.02447-07

70. Pijlman GP, Kondratieva N, Khromykh AA. Translation of the Flavivirus Kunjin NS3 Gene in cis but Not Its RNA Sequence or Secondary Structure Is Essential for Efficient RNA Packaging. J Virol. 2006;80: 11255–11264. doi:10.1128/JVI.01559-06

71. Pong W-L, Huang Z-S, Teoh P-G, Wang C-C, Wu H-N. RNA binding property and RNA chaperone activity of dengue virus core protein and other viral RNA-interacting proteins. FEBS Lett. 2011;585: 2575–2581. doi:10.1016/j.febslet.2011.06.038

72. Zhang Y, Corver J, Chipman PR, Zhang W, Pletnev SV, Sedlak D, et al. Structures of immature flavivirus particles. EMBO J. 2003;22: 2604–2613. doi:10.1093/emboj/cdg270

73. Oliveira ERA, de Alencastro RB, Horta BAC. New insights into flavivirus biology: the influence of pH over interactions between prM and E proteins. J Comput Aided Mol Des. 2017;31: 1009–1019. doi:10.1007/s10822-017-0076-8

74. Malina Jasamai, Boon YW, Aurapa S, Jaleel A. Current prevention and potential treatment options for dengue infection | Journal of Pharmacy & Pharmaceutical Sciences. J Pharm Pharm Sci. 2019;22: 440–456.

75. Lye DC, Archuleta S, Syed-Omar SF, Low JG, Oh HM, Wei Y, et al. Prophylactic platelet transfusion plus supportive care versus supportive care alone in adults with dengue and thrombocytopenia: a multicentre, open-label, randomised, superiority trial. The Lancet. 2017;389: 1611–1618. doi:10.1016/S0140-6736(17)30269-6

76. Wilder-Smith A, Ooi E-E, Horstick O, Wills B. Dengue. The Lancet. 2019;393: 350–363. doi:10.1016/S0140-6736(18)32560-1

77. Xu T-L, Han Y, Liu W, Pang X-Y, Zheng B, Zhang Y, et al. Antivirus effectiveness of ivermectin on dengue virus type 2 in Aedes albopictus. PLoS Negl Trop Dis. 2018;12: e0006934. doi:10.1371/journal.pntd.0006934

78. Mastrangelo E, Pezzullo M, De Burghgraeve T, Kaptein S, Pastorino B, Dallmeier K, et al. Ivermectin is a potent inhibitor of flavivirus replication specifically targeting NS3 helicase activity: new prospects for an old drug. J Antimicrob Chemother. 2012;67: 1884–1894. doi:10.1093/jac/dks147

79. Crump A, Omura S. Ivermectin, 'Wonder drug' from Japan: the human use perspective. Proc Jpn Acad Ser B. 2011;87: 13–28. doi:10.2183/pjab.87.13

80. Kobylinski KC, Sylla M, Chapman PL, Sarr MD, Foy BD. Ivermectin Mass Drug Administration to Humans Disrupts Malaria Parasite Transmission in Senegalese Villages. Am J Trop Med Hyg. 2011;85: 3–5. doi:10.4269/ajtmh.2011.11-0160

81. Luo D, Vasudevan SG, Lescar J. The flavivirus NS2B–NS3 protease–helicase as a target for antiviral drug development. Antiviral Res. 2015;118: 148–158. doi:10.1016/j.antiviral.2015.03.014

82. Hernandez-Morales I, Geluykens P, Clynhens M, Strijbos R, Goethals O, Megens S, et al. Characterization of a dengue NS4B inhibitor originating from an HCV small molecule library. Antiviral Res. 2017;147: 149–158. doi:10.1016/j.antiviral.2017.10.011

83. Sun H, Chen Q, Lai H. Development of Antibody Therapeutics against Flaviviruses. Int J Mol Sci. 2017;19. doi:10.3390/ijms19010054

84. Gómez-Calderón C, Mesa-Castro C, Robledo S, Gómez S, Bolivar-Avila S, Diaz-Castillo F, et al. Antiviral effect of compounds derived from the seeds of Mammea americana and Tabernaemontana cymosa on Dengue and Chikungunya virus infections. BMC Complement Altern Med. 2017;17. doi:10.1186/s12906-017-1562-1

85. Yao X, Ling Y, Guo S, Wu W, He S, Zhang Q, et al. Tatanan A from the Acorus calamus L. root inhibited dengue virus proliferation and infections. Phytomedicine. 2018;42: 258–267. doi:10.1016/j.phymed.2018.03.018

86. Kiat TS, Pippen R, Yusof R, Ibrahim H, Khalid N, Rahman NA. Inhibitory activity of cyclohexenyl chalcone derivatives and flavonoids of fingerroot, Boesenbergia rotunda (L.), towards dengue-2 virus NS3 protease. Bioorg Med Chem Lett. 2006;16: 3337–3340. doi:10.1016/j.bmcl.2005.12.075

87. Sabin AB, Schlesinger RW. Production of Immunity to Dengue with Virus Modified by Propagation in Mice. Science. 1945;101: 640–642. doi:10.1126/science.101.2634.640

88. Prutzman K. Summary Basis for Regulatory Action - Dengvaxia. : 32.

89. Thomas SJ, Yoon I-K. A review of Dengvaxia®: development to deployment. Hum Vaccines Immunother. 2019;0: 1–20. doi:10.1080/21645515.2019.1658503

79. Villar L, Dayan GH, Arredondo-García JL, Rivera DM, Cunha R, Deseda C, et al. Efficacy of a Tetravalent Dengue Vaccine in Children in Latin America. 2015 The New England Journal of Medicine. doi:10.1056/NEJMoa1411037

91. Capeding MR, Tran NH, Hadinegoro SRS, Ismail HIHM, Chotpitayasunondh T, Chua MN, et al. Clinical efficacy and safety of a novel tetravalent dengue vaccine in healthy children in Asia: a phase 3, randomised, observer-masked, placebo-controlled trial. The Lancet. 2014;384: 1358–1365. doi:10.1016/S0140-6736(14)61060-6

92. Sabchareon A, Wallace D, Sirivichayakul C, Limkittikul K, Chanthavanich P, Suvannadabba S, et al. Protective efficacy of the recombinant, live-attenuated, CYD tetravalent dengue vaccine in Thai schoolchildren: a randomised, controlled phase 2b trial. The Lancet. 2012;380: 1559–1567. doi:10.1016/S0140-6736(12)61428-7

93. WHO. Weekly Epidemiological Record, 2018, vol. 93, 36. Wkly Epidemiol Rec. 2018;93: 457–476.

83. FDA. First FDA-approved vaccine for the prevention of dengue disease in endemic regions. FDA 9 Nov 2019. Available: http://www.fda.gov/news-events/press-announcements/first-fda-approved-vaccine-prevention-dengue-disease-endemic-regions

95. Whitehead SS. Development of TV003/TV005, a single dose, highly immunogenic live attenuated dengue vaccine; what makes this vaccine different from the Sanofi-Pasteur CYD^{TM} vaccine? Expert Rev Vaccines. 2016;15: 509–517. doi:10.1586/14760584.2016.1115727

96. Boo CS. Legislation for Control of Dengue in Singapore. 2001;25: 5.

97. Serbus LR, Casper-Lindley C, Landmann F, Sullivan W. The Genetics and Cell Biology of Wolbachia-Host Interactions. Annu Rev Genet. 2008;42: 683–707. doi:10.1146/annurev.genet.41.110306.130354

98. Baldini F, Segata N, Pompon J, Marcenac P, Robert Shaw W, Dabiré RK, et al. Evidence of natural Wolbachia infections in field populations of Anopheles gambiae. Nat Commun. 2014;5: 1–7. doi:10.1038/ncomms4985

99. Rašić G, Endersby NM, Williams C, Hoffmann AA. Using Wolbachia-based release for suppression of Aedes mosquitoes: insights from genetic data and population simulations. Ecol Appl. 2014;24: 1226–1234. doi:10.1890/13-1305.1

89. NEA. Wolbachia-Aedes Small-Scale Field Study. Available: https://www.nea.gov.sg/corporate-functions/resources/research/wolbachia-aedes-mosquito-suppression-strategy/project-wolbachia-singapore/wolbachia-aedes-small-scale-field-study

101. Ye YH, Carrasco AM, Frentiu FD, Chenoweth SF, Beebe NW, van den Hurk AF, et al. Wolbachia Reduces the Transmission Potential of Dengue-Infected Aedes aegypti. PLoS Negl Trop Dis. 2015;9. doi:10.1371/journal.pntd.0003894

91. Callaway E. Rio fights Zika with biggest release yet of bacteria-infected mosquitoes. In: Nature 26 Oct 2016. doi:10.1038/nature.2016.20878

103. Anders KL, Indriani C, Ahmad RA, Tantowijoyo W, Arguni E, Andari B, et al. The AWED trial (Applying Wolbachia to Eliminate Dengue) to assess the efficacy of Wolbachia-infected mosquito deployments to reduce dengue incidence in Yogyakarta, Indonesia: study protocol for a cluster randomised controlled trial. Trials. 2018;19. doi:10.1186/s13063-018-2670-z

104. Alphey L, Alphey N. Five Things to Know about Genetically Modified (GM) Insects for Vector Control. PLoS Pathog. 2014;10. doi:10.1371/journal.ppat.1003909

105. Phuc HK, Andreasen MH, Burton RS, Vass C, Epton MJ, Pape G, et al. Late-acting dominant lethal genetic systems and mosquito control. BMC Biol. 2007;5: 11. doi:10.1186/1741-7007-5-11

106. Harris AF, McKemey AR, Nimmo D, Curtis Z, Black I, Morgan SA, et al. Successful suppression of a field mosquito population by sustained release of engineered male mosquitoes. Nat Biotechnol. 2012;30: 828–830. doi:10.1038/nbt.2350

107. Sriwimol W, Aroonkesorn A, Sakdee S, Kanchanawarin C, Uchihashi T, Ando T, et al. Potential Prepore Trimer Formation by the Bacillus thuringiensis Mosquito-specific Toxin. J Biol Chem. 2015;290: 20793–20803. doi:10.1074/jbc.M114.627554

108. Alto BW, Lord CC. Transstadial Effects of Bti on Traits of Aedes aegypti and Infection with Dengue Virus. PLoS Negl Trop Dis. 2016;10: e0004370. doi:10.1371/journal.pntd.0004370

109. Soonwera M, Phasomkusolsil S. Efficacy of Thai herbal essential oils as green repellent against mosquito vectors. Acta Trop. 2015;142: 127–130. doi:10.1016/j.actatropica.2014.11.010

110. Vontas J, Kioulos E, Pavlidi N, Morou E, della Torre A, Ranson H. Insecticide resistance in the major dengue vectors Aedes albopictus and Aedes aegypti. Pestic Biochem Physiol. 2012;104: 126–131. doi:10.1016/j.pestbp.2012.05.008

111. Polson KA, Rawlins SC, Brogdon WG, Chadee DD. Characterisation of DDT and Pyrethroid Resistance in Trinidad and Tobago populations of Aedes aegypti. Bull Entomol Res. 2011;101: 435–441. doi:10.1017/S0007485310000702

112. Harris AF, Rajatileka S, Ranson H. Pyrethroid Resistance in Aedes aegypti from Grand Cayman. Am J Trop Med Hyg. 2010;83: 277–284. doi:10.4269/ajtmh.2010.09-0623

113. Koou S-Y, Chong C-S, Vythilingam I, Lee C-Y, Ng L-C. Insecticide resistance and its underlying mechanisms in field populations of Aedes aegypti adults (Diptera: Culicidae) in Singapore. Parasit Vectors. 2014;7. doi:10.1186/s13071-014-0471-0

114. Moyes CL, Vontas J, Martins AJ, Ng LC, Koou SY, Dusfour I, et al. Contemporary status of insecticide resistance in the major Aedes vectors of arboviruses infecting humans. PLoS Negl Trop Dis. 2017;11: e0005625. doi:10.1371/journal.pntd.0005625

104. WHO | Global report on insecticide resistance in malaria vectors: 2010–2016. WHO. Available: http://www.who.int/malaria/publications/atoz/9789241514057/en/

116. Liu N. Insecticide Resistance in Mosquitoes: Impact, Mechanisms, and Research Directions. Annu Rev Entomol. 2015;60: 537–559. doi:10.1146/annurev-ento-010814-020828

117. Marcombe S, Poupardin R, Darriet F, Reynaud S, Bonnet J, Strode C, et al. Exploring the molecular basis of insecticide resistance in the dengue vector Aedes aegypti: a case study in Martinique Island (French West Indies). BMC Genomics. 2009;10: 494. doi:10.1186/1471-2164-10-494

118. Dusfour I, Vontas J, David J-P, Weetman D, Fonseca DM, Corbel V, et al. Management of insecticide resistance in the major Aedes vectors of arboviruses: Advances and challenges. PLoS Negl Trop Dis. 2019;13: e0007615. doi:10.1371/journal.pntd.0007615

119. Shaw DK, Tate AT, Schneider DS, Levashina EA, Kagan JC, Pal U, et al. Vector Immunity and Evolutionary Ecology: The Harmonious Dissonance. Trends Immunol. 2018;39: 862–873. doi:10.1016/j.it.2018.09.003

120. Ciota AT, Styer LM, Meola MA, Kramer LD. The costs of infection and resistance as determinants of West Nile virus susceptibility in Culex mosquitoes. BMC Ecol. 2011;11: 23. doi:10.1186/1472-6785-11-23

121. Lambrechts L, Saleh M-C. Manipulating Mosquito Tolerance for Arbovirus Control. Cell Host Microbe. 2019;26: 309–313. doi:10.1016/j.chom.2019.08.005

122. Oliveira JH, Bahia AC, Vale PF. How are arbovirus vectors able to tolerate infection? Dev Comp Immunol. 2020;103: 103514. doi:10.1016/j.dci.2019.103514

123. Cole L, Kramer PR. Chapter 1.3 - Sugars, Fatty Acids, and Energy Biochemistry. In: Cole L, Kramer PR, editors. Human Physiology, Biochemistry and Basic Medicine. Boston: Academic Press; 2016. pp. 17–30. doi:10.1016/B978-0-12-803699-0.00019-0

124. Kumari A. Chapter 2 - Citric Acid Cycle. In: Kumari A, editor. Sweet Biochemistry. Academic Press; 2018. pp. 7–11. doi:10.1016/B978-0-12-814453-4.00002-9

125. Sud M, Fahy E, Cotter D, Brown A, Dennis EA, Glass CK, et al. LMSD: LIPID MAPS structure database. Nucleic Acids Res. 2007;35: D527–D532. doi:10.1093/nar/gkl838

126. Fahy E, Subramaniam S, Brown HA, Glass CK, Merrill AH, Murphy RC, et al. A comprehensive classification system for lipids. Eur J Lipid Sci Technol. 2005;107: 337–364. doi:10.1002/ejlt.200405001

127. Rangan VS, Smith S. Chapter 6 Fatty acid synthesis in eukaryotes. New Comprehensive Biochemistry. Elsevier; 2002. pp. 151–179. doi:10.1016/S0167-7306(02)36008-3

128. Cook HW, McMaster CR. Fatty acid desaturation and chain elongation in eukaryotes. Biochem Lipid Lipoproteins Membr 4th Edn. 2002;Chapter 7: 24.

129. Schulz H. Oxidation of fatty acids in eukaryotes. Biochem Lipid Lipoproteins Membr 4th Edn. 2002;Chapter 5: 24.

130. Vance JE. Phospholipid Synthesis and Transport in Mammalian Cells. Traffic. 2015;16: 1–18. doi:10.1111/tra.12230

131. van Meer G, Voelker DR, Feigenson GW. Membrane lipids: where they are and how they behave. Nat Rev Mol Cell Biol. 2008;9: 112–124. doi:10.1038/nrm2330

132. Dawaliby R, Trubbia C, Delporte C, Noyon C, Ruysschaert J-M, Antwerpen PV, et al. Phosphatidylethanolamine Is a Key Regulator of Membrane Fluidity in Eukaryotic Cells. J Biol Chem. 2016;291: 3658–3667. doi:10.1074/jbc.M115.706523

133. Luukkonen A, Brummer-Korvenkontio M, Renkonen O. Lipids of cultured mosquito cells (Aedes albopictus): Comparison with cultured mammalian fibroblasts (BHK 21 cells). Biochim Biophys Acta BBA - Lipids Lipid Metab. 1973;326: 256–261. doi:10.1016/0005-2760(73)90251-8

134. Jenkin HM, McMeans E, Anderson LE, Yang T-K. Comparison of phospholipid composition ofAedes aegypti andAedes albopictus cells obtained from logarithmic and stationary phases of growth. Lipids. 10: 686–694. doi:10.1007/BF02532762

135. Gault C, Obeid L, Hannun Y. An overview of sphingolipid metabolism: from synthesis to breakdown. Adv Exp Med Biol. 2010;688: 1–23.

136. Bell RM, Ballas LM, Coleman RA. Lipid topogenesis. J Lipid Res. 1981;22: 391–403.

137. Rusiñol AE, Cui Z, Chen MH, Vance JE. A unique mitochondria-associated membrane fraction from rat liver has a high capacity for lipid synthesis and contains pre-Golgi secretory proteins including nascent lipoproteins. J Biol Chem. 1994;269: 27494–27502.

138. Daum G. Lipids of mitochondria. Biochim Biophys Acta BBA - Rev Biomembr. 1985;822: 1–42. doi:10.1016/0304-4157(85)90002-4

139. Henneberry AL, Wright MM, McMaster CR. The Major Sites of Cellular Phospholipid Synthesis and Molecular Determinants of Fatty Acid and Lipid Head Group Specificity. Mol Biol Cell. 2002;13: 3148–3161. doi:10.1091/mbc.01-11-0540

140. Di Paolo G, De Camilli P. Phosphoinositides in cell regulation and membrane dynamics. Nature. 2006;443: 651–657. doi:10.1038/nature05185

141. Mechanisms of phosphatidylserine exposure, a phagocyte recognition signal, on apoptotic T lymphocytes. J Exp Med. 1995;182: 1597–1601.

142. Kobayashi T, Beuchat M-H, Chevallier J, Makino A, Mayran N, Escola J-M, et al. Separation and Characterization of Late Endosomal Membrane Domains. J Biol Chem. 2002;277: 32157–32164. doi:10.1074/jbc.M202838200

143. Kolter T, Sandhoff K. PRINCIPLES OF LYSOSOMAL MEMBRANE DIGESTION: Stimulation of Sphingolipid Degradation by Sphingolipid Activator Proteins and Anionic Lysosomal Lipids. Annu Rev Cell Dev Biol. 2005;21: 81–103. doi:10.1146/annurev.cellbio.21.122303.120013

144. Fagone P, Jackowski S. Membrane phospholipid synthesis and endoplasmic reticulum function. J Lipid Res. 2009;50: S311–S316. doi:10.1194/jlr.R800049-JLR200

145. Takeuchi K, Reue K. Biochemistry, physiology, and genetics of GPAT, AGPAT, and lipin enzymes in triglyceride synthesis., Biochemistry, physiology, and genetics of GPAT, AGPAT, and lipin enzymes in triglyceride synthesis. Am J Physiol Endocrinol Metab Am J Physiol - Endocrinol Metab. 2009;296, 296: E1195, E1195-209. doi:10.1152/ajpendo.90958.2008

146. Athenstaedt K, Daum G. Phosphatidic acid, a key intermediate in lipid metabolism. Eur J Biochem. 1999;266: 1–16. doi:10.1046/j.1432-1327.1999.00822.x

147. Gibellini F, Smith TK. The Kennedy pathway—De novo synthesis of phosphatidylethanolamine and phosphatidylcholine. IUBMB Life. 2010;62: 414–428. doi:10.1002/iub.337

148. Yamashita S, Nikawa J. Phosphatidylserine synthase from yeast1This article is dedicated to Prof. Eugene Kennedy to honor his pioneering research in

phospholipid biosynthesis.1. Biochim Biophys Acta BBA - Lipids Lipid Metab. 1997;1348: 228–235. doi:10.1016/S0005-2760(97)00102-1

149. Tamura Y, Onguka O, Itoh K, Endo T, Iijima M, Claypool SM, et al. Phosphatidylethanolamine biosynthesis in mitochondria: phosphatidylserine (PS) trafficking is independent of a PS decarboxylase and intermembrane space proteins UPS1P and UPS2P. J Biol Chem. 2012;287: 43961–43971. doi:10.1074/jbc.M112.390997

150. Horvath SE, Böttinger L, Vögtle F-N, Wiedemann N, Meisinger C, Becker T, et al. Processing and Topology of the Yeast Mitochondrial Phosphatidylserine Decarboxylase 1. J Biol Chem. 2012;287: 36744–36755. doi:10.1074/jbc.M112.398107

151. Vance DE, Vance JE. CHAPTER 8 - Phospholipid biosynthesis in eukaryotes. In: Vance DE, Vance JE, editors. Biochemistry of Lipids, Lipoproteins and Membranes (Fifth Edition). San Diego: Elsevier; 2008. pp. 213–244. doi:10.1016/B978-044453219-0.50010-6

152. Gottlieb D, Heideman W, Saba JD. TheDPL1Gene Is Involved in Mediating the Response to Nutrient Deprivation inSaccharomyces cerevisiae. Mol Cell Biol Res Commun. 1999;1: 66–71. doi:10.1006/mcbr.1999.0109

153. Patel D, Witt SN. Ethanolamine and Phosphatidylethanolamine: Partners in Health and Disease. Oxid Med Cell Longev. 2017;2017. doi:10.1155/2017/4829180

154. Wang B, Tontonoz P. Phospholipid Remodeling in Physiology and Disease. Annu Rev Physiol. 2019;81: 165–188. doi:10.1146/annurev-physiol-020518-114444

155. O'Donnell VB, Rossjohn J, Wakelam MJO. Phospholipid signaling in innate immune cells. J Clin Invest. 128: 2670–2679. doi:10.1172/JCI97944

156. Moessinger C, Klizaite K, Steinhagen A, Philippou-Massier J, Shevchenko A, Hoch M, et al. Two different pathways of phosphatidylcholine synthesis, the Kennedy Pathway and the Lands Cycle, differentially regulate cellular triacylglycerol storage. BMC Cell Biol. 2014;15: 43. doi:10.1186/s12860-014-0043-3

157. Burke JE, Dennis EA. Phospholipase A2 structure/function, mechanism, and signaling. J Lipid Res. 2009;50: S237–S242. doi:10.1194/jlr.R800033-JLR200

158. Nor Aliza AR, Stanley DW. A digestive phospholipase A2 in larval mosquitoes, Aedes aegypti. Insect Biochem Mol Biol. 1998;28: 561–569. doi:10.1016/S0965-1748(98)00050-2

159. Abdul Rahim NA, Othman M, Sabri M, Stanley DW. A Midgut Digestive Phospholipase A2 in Larval Mosquitoes, Aedes albopictus and Culex quinquefasciatus. Enzyme Res. 2018;2018. doi:10.1155/2018/9703413

160. Aloulou A, Rahier R, Arhab Y, Noiriel A, Abousalham A. Phospholipases: An Overview. In: Sandoval G, editor. Lipases and Phospholipases: Methods and Protocols. New York, NY: Springer; 2018. pp. 69–105. doi:10.1007/978-1-4939-8672-9_3

161. Morgan CP, Insall R, Haynes L, Cockcroft S. Identification of phospholipase B from Dictyostelium discoideum reveals a new lipase family present in mammals, flies and nematodes, but not yeast. Biochem J. 2004;382: 441–449. doi:10.1042/BJ20040110

162. McMahon HT, Boucrot E. Membrane curvature at a glance. J Cell Sci. 2015;128: 1065. doi:10.1242/jcs.114454

163. Ali MR, Cheng KH, Huang J. Assess the nature of cholesterol-lipid interactions through the chemical potential of cholesterol in phosphatidylcholine bilayers. Proc Natl Acad Sci. 2007;104: 5372–5377. doi:10.1073/pnas.0611450104

164. Ali MR, Cheng KH, Huang J. Ceramide Drives Cholesterol Out of the Ordered Lipid Bilayer Phase into the Crystal Phase in 1-Palmitoyl-2-oleoyl-sn-glycero-3-phosphocholine/Cholesterol/Ceramide Ternary Mixtures. Biochemistry. 2006;45: 12629–12638. doi:10.1021/bi060610x

165. Marsh D. Lateral Pressure Profile, Spontaneous Curvature Frustration, and the Incorporation and Conformation of Proteins in Membranes. Biophys J. 2007;93: 3884–3899. doi:10.1529/biophysj.107.107938

166. Marquardt D, Geier B, Pabst G. Asymmetric Lipid Membranes: Towards More Realistic Model Systems. Membranes. 2015;5: 180–196. doi:10.3390/membranes5020180

167. Fadeel B, Xue D. The ins and outs of phospholipid asymmetry in the plasma membrane: roles in health and disease. Crit Rev Biochem Mol Biol. 2009;44: 264–277. doi:10.1080/10409230903193307

168. Leventis PA, Grinstein S. The Distribution and Function of Phosphatidylserine in Cellular Membranes. Annu Rev Biophys. 2010;39: 407–427. doi:10.1146/annurev.biophys.093008.131234

169. Holthuis JCM, Levine TP. Lipid traffic: floppy drives and a superhighway. Nat Rev Mol Cell Biol. 2005;6: 209–220. doi:10.1038/nrm1591

170. Li J, Wang X, Zhang T, Wang C, Huang Z, Luo X, et al. A review on phospholipids and their main applications in drug delivery systems. Asian J Pharm Sci. 2015;10: 81–98. doi:10.1016/j.ajps.2014.09.004

171. Hope MJ, Cullis PR. Lipid asymmetry induced by transmembrane pH gradients in large unilamellar vesicles. J Biol Chem. 1987;262: 4360–4366.

172. Janmey PA, Kinnunen PKJ. Biophysical properties of lipids and dynamic membranes. Trends Cell Biol. 2006;16: 538–546. doi:10.1016/j.tcb.2006.08.009

173. Radhakrishnan A, Goldstein JL, McDonald JG, Brown MS. Switch-like control of SREBP-2 transport triggered by small changes in ER cholesterol: a delicate balance. Cell Metab. 2008;8: 512–521. doi:10.1016/j.cmet.2008.10.008

174. Feigenson GW. Phase Boundaries and Biological Membranes. Annu Rev Biophys Biomol Struct. 2007;36: 63–77. doi:10.1146/annurev.biophys.36.040306.132721

175. Jouhet J. Importance of the hexagonal lipid phase in biological membrane organization. Front Plant Sci. 2013;4. doi:10.3389/fpls.2013.00494

176. Bigay J, Antonny B. Curvature, Lipid Packing, and Electrostatics of Membrane Organelles: Defining Cellular Territories in Determining Specificity. Dev Cell. 2012;23: 886–895. doi:10.1016/j.devcel.2012.10.009

177. Bartz R, Li W-H, Venables B, Zehmer JK, Roth MR, Welti R, et al. Lipidomics reveals that adiposomes store ether lipids and mediate phospholipid traffic,. J Lipid Res. 2007;48: 837–847. doi:10.1194/jlr.M600413-JLR200

178. Fairn GD, Schieber NL, Ariotti N, Murphy S, Kuerschner L, Webb RI, et al. High-resolution mapping reveals topologically distinct cellular pools of phosphatidylserine. J Cell Biol. 2011;194: 257–275. doi:10.1083/jcb.201012028

179. Ducharme NA, Bickel PE. Minireview: Lipid Droplets in Lipogenesis and Lipolysis. Endocrinology. 2008;149: 942–949. doi:10.1210/en.2007-1713

180. Penno A, Hackenbroich G, Thiele C. Phospholipids and lipid droplets. Biochim Biophys Acta BBA - Mol Cell Biol Lipids. 2013;1831: 589–594. doi:10.1016/j.bbalip.2012.12.001

181. Canavoso LE, Jouni ZE, Karnas KJ, Pennington JE, Wells MA. Fat metabolism in insects. Annu Rev Nutr. 2001;21: 23–46. doi:10.1146/annurev.nutr.21.1.23

182. Gondim KC, Atella GC, Pontes EG, Majerowicz D. Lipid metabolism in insect disease vectors. Insect Biochem Mol Biol. 2018;101: 108–123. doi:10.1016/j.ibmb.2018.08.005

183. Cheon H-M, Shin SW, Bian G, Park J-H, Raikhel AS. Regulation of Lipid Metabolism Genes, Lipid Carrier Protein Lipophorin, and Its Receptor during Immune Challenge in the Mosquito Aedes aegypti. J Biol Chem. 2006;281: 8426–8435. doi:10.1074/jbc.M510957200

184. Stanley-Samuelson DW, Jurenka RA, Cripps C, Blomquist GJ, de Renobales M. Fatty acids in insects: Composition, metabolism, and biological significance. Arch Insect Biochem Physiol. 1988;9: 1–33. doi:10.1002/arch.940090102

185. Townsend D, Jenkin HM, Tze-Ken Y. Lipid analysis of Aedes aegypti cells cultivated in vitro. Biochim Biophys Acta BBA - Lipids Lipid Metab. 1972;260: 20–25. doi:10.1016/0005-2760(72)90069-0

186. Butters TD, Hughes RC. Phospholipids and glycolipids in subcellular fractions of mosquito Aedes aegypti cells. In Vitro. 1981;17: 831–838. doi:10.1007/BF02618451

187. Sim S, Jupatanakul N, Dimopoulos G. Mosquito Immunity against Arboviruses. Viruses. 2014;6: 4479–4504. doi:10.3390/v6114479

188. Kingsolver MB, Huang Z, Hardy RW. Insect antiviral innate immunity: pathways, effectors, and connections. J Mol Biol. 2013;425: 4921–4936. doi:10.1016/j.jmb.2013.10.006

189. Chowdhury A, Modahl CM, Tan ST, Xiang BWW, Missé D, Vial T, et al. JNK pathway restricts DENV2, ZIKV and CHIKV infection by activating complement and apoptosis in mosquito salivary glands. PLOS Pathog. 2020;16: e1008754. doi:10.1371/journal.ppat.1008754

190. Sanchez-Vargas I, Travanty EA, Keene KM, Franz AWE, Beaty BJ, Blair CD, et al. RNA interference, arthropod-borne viruses, and mosquitoes. Virus Res. 2004;102: 65–74. doi:10.1016/j.virusres.2004.01.017

191. Sánchez-Vargas I, Scott JC, Poole-Smith BK, Franz AWE, Barbosa-Solomieu V, Wilusz J, et al. Dengue Virus Type 2 Infections of Aedes aegypti Are Modulated by the Mosquito's RNA Interference Pathway. PLoS Pathog. 2009;5. doi:10.1371/journal.ppat.1000299

192. Luplertlop N, Surasombatpattana P, Patramool S, Dumas E, Wasinpiyamongkol L, Saune L, et al. Induction of a Peptide with Activity against a Broad Spectrum of Pathogens in the Aedes aegypti Salivary Gland, following Infection with Dengue Virus. PLOS Pathog. 2011;7: e1001252. doi:10.1371/journal.ppat.1001252

193. Sim S, Jupatanakul N, Ramirez JL, Kang S, Romero-Vivas CM, Mohammed H, et al. Transcriptomic Profiling of Diverse Aedes aegypti Strains Reveals Increased Basal-level Immune Activation in Dengue Virus-refractory Populations and Identifies Novel Virus-vector Molecular Interactions. PLoS Negl Trop Dis. 2013;7. doi:10.1371/journal.pntd.0002295

194. Xi Z, Ramirez JL, Dimopoulos G. The Aedes aegypti Toll Pathway Controls Dengue Virus Infection. PLOS Pathog. 2008;4: e1000098. doi:10.1371/journal.ppat.1000098

195. Ramirez JL, Dimopoulos G. The Toll immune signaling pathway control conserved anti-dengue defenses across diverse Ae. aegypti strains and against multiple dengue virus serotypes. Dev Comp Immunol. 2010;34: 625–629. doi:10.1016/j.dci.2010.01.006

196. Souza-Neto JA, Sim S, Dimopoulos G. An evolutionary conserved function of the JAK-STAT pathway in anti-dengue defense. Proc Natl Acad Sci. 2009;106: 17841–17846. doi:10.1073/pnas.0905006106

197. Kakumani PK, Ponia SS, S RK, Sood V, Chinnappan M, Banerjea AC, et al. Role of RNA Interference (RNAi) in Dengue Virus Replication and Identification

of NS4B as an RNAi Suppressor. J Virol. 2013;87: 8870–8883. doi:10.1128/JVI.02774-12

198. Ashour J, Laurent-Rolle M, Shi P-Y, García-Sastre A. NS5 of Dengue Virus Mediates STAT2 Binding and Degradation. J Virol. 2009;83: 5408–5418. doi:10.1128/JVI.02188-08

199. Barletta ABF, Alves LR, Nascimento Silva MCL, Sim S, Dimopoulos G, Liechocki S, et al. Emerging role of lipid droplets in Aedes aegypti immune response against bacteria and Dengue virus. Sci Rep. 2016;6. doi:10.1038/srep19928

200. Chotiwan N, Andre BG, Sanchez-Vargas I, Islam MN, Grabowski JM, Hopf-Jannasch A, et al. Dynamic remodeling of lipids coincides with dengue virus replication in the midgut of Aedes aegypti mosquitoes. PLoS Pathog. 2018;14. doi:10.1371/journal.ppat.1006853

201. Harris SG, Padilla J, Koumas L, Ray D, Phipps RP. Prostaglandins as modulators of immunity. Trends Immunol. 2002;23: 144–150. doi:10.1016/s1471-4906(01)02154-8

202. Muñoz FLGG de, Martínez-Barnetche J, Lanz-Mendoza H, Rodríguez MH, Hernández-Hernández FC. Prostaglandin E2 modulates the expression of antimicrobial peptides in the fat body and midgut of Anopheles albimanus. Arch Insect Biochem Physiol. 2008;68: 14–25. doi:10.1002/arch.20232

203. Ricciotti E, FitzGerald GA. Prostaglandins and Inflammation. Arterioscler Thromb Vasc Biol. 2011;31: 986–1000. doi:10.1161/ATVBAHA.110.207449

204. Huang Y, Morales-Rosado J, Ray J, Myers TG, Kho T, Lu M, et al. Toll-like Receptor Agonists Promote Prolonged Triglyceride Storage in Macrophages. J Biol Chem. 2014;289: 3001–3012. doi:10.1074/jbc.M113.524587

205. Saitoh T, Satoh T, Yamamoto N, Uematsu S, Takeuchi O, Kawai T, et al. Antiviral Protein Viperin Promotes Toll-like Receptor 7- and Toll-like Receptor 9-Mediated Type I Interferon Production in Plasmacytoid Dendritic Cells. Immunity. 2011;34: 352–363. doi:10.1016/j.immuni.2011.03.010

206. Voelker DR, Numata M. Phospholipid regulation of innate immunity and respiratory viral infection. J Biol Chem. 2019;294: 4282–4289. doi:10.1074/jbc.AW118.003229

207. West J, Tompkins CK, Balantac N, Nudelman E, Meengs B, White T, et al. Cloning and expression of two human lysophosphatidic acid acyltransferase cDNAs that enhance cytokine-induced signaling responses in cells. DNA Cell Biol. 1997;16: 691–701. doi:10.1089/dna.1997.16.691

208. Schrimpe-Rutledge AC, Codreanu SG, Sherrod SD, McLean JA. Untargeted metabolomics strategies – Challenges and Emerging Directions. J Am Soc Mass Spectrom. 2016;27: 1897–1905. doi:10.1007/s13361-016-1469-y

209. Manchester M, Anand A. Chapter Two - Metabolomics: Strategies to Define the Role of Metabolism in Virus Infection and Pathogenesis. In: Kielian M, Mettenleiter TC, Roossinck MJ, editors. Advances in Virus Research. Academic Press; 2017. pp. 57–81. doi:10.1016/bs.aivir.2017.02.001

210. Vinayavekhin N, Homan EA, Saghatelian A. Exploring Disease through Metabolomics. ACS Chem Biol. 2010;5: 91–103. doi:10.1021/cb900271r

211. Noto A, Dessi A, Puddu M, Mussap M, Fanos V. Metabolomics technology and their application to the study of the viral infection. J Matern Fetal Neonatal Med. 2014;27: 53–57. doi:10.3109/14767058.2014.955963

212. Roberts LD, Souza AL, Gerszten RE, Clish CB. Targeted Metabolomics. Curr Protoc Mol Biol. 2012;CHAPTER: Unit30.2. doi:10.1002/0471142727.mb3002s98

213. Patejko M, Jacyna J, Markuszewski MJ. Sample preparation procedures utilized in microbial metabolomics: An overview. J Chromatogr B. 2017;1043: 150–157. doi:10.1016/j.jchromb.2016.09.029

214. Mushtaq MY, Choi YH, Verpoorte R, Wilson EG. Extraction for Metabolomics: Access to The Metabolome. Phytochem Anal. 2014;25: 291–306. doi:10.1002/pca.2505

215. Cajka T, Fiehn O. Toward Merging Untargeted and Targeted Methods in Mass Spectrometry-Based Metabolomics and Lipidomics. Anal Chem. 2016;88: 524–545. doi:10.1021/acs.analchem.5b04491

216. Bothwell JHF, Griffin JL. An introduction to biological nuclear magnetic resonance spectroscopy. Biol Rev. 2011;86: 493–510. doi:10.1111/j.1469-185X.2010.00157.x

217. Emwas A-HM. The Strengths and Weaknesses of NMR Spectroscopy and Mass Spectrometry with Particular Focus on Metabolomics Research. In: Bjerrum JT, editor. Metabonomics: Methods and Protocols. New York, NY: Springer; 2015. pp. 161–193. doi:10.1007/978-1-4939-2377-9_13

218. Riekeberg E, Powers R. New frontiers in metabolomics: from measurement to insight. F1000Research. 2017;6. doi:10.12688/f1000research.11495.1

219. Xiao JF, Zhou B, Ressom HW. Metabolite identification and quantitation in LC-MS/MS-based metabolomics. Trends Anal Chem TRAC. 2012;32: 1–14. doi:10.1016/j.trac.2011.08.009

220. Bajad SU, Lu W, Kimball EH, Yuan J, Peterson C, Rabinowitz JD. Separation and quantitation of water soluble cellular metabolites by hydrophilic interaction chromatography-tandem mass spectrometry. J Chromatogr A. 2006;1125: 76–88. doi:10.1016/j.chroma.2006.05.019

221. McLafferty FW. Tandem mass spectrometry. Science. 1981;214: 280–287. doi:10.1126/science.7280693

222. Ren S, Hinzman AA, Kang EL, Szczesniak RD, Lu LJ. Computational and statistical analysis of metabolomics data. Metabolomics. 2015;11: 1492–1513. doi:10.1007/s11306-015-0823-6

223. Van den Berg RA, Hoefsloot HC, Westerhuis JA, Smilde AK, van der Werf MJ. Centering, scaling, and transformations: improving the biological information content of metabolomics data. BMC Genomics. 2006;7: 142. doi:10.1186/1471-2164-7-142

224. Worley B, Powers R. Multivariate Analysis in Metabolomics. Curr Metabolomics. 2013;1: 92–107. doi:10.2174/2213235X11301010092

225. Sumner LW, Amberg A, Barrett D, Beale MH, Beger R, Daykin CA, et al. Proposed minimum reporting standards for chemical analysis Chemical Analysis Working Group (CAWG) Metabolomics Standards Initiative (MSI). Metabolomics Off J Metabolomic Soc. 2007;3: 211–221. doi:10.1007/s11306-007-0082-2

226. Godzien J, Gil de la Fuente A, Otero A, Barbas C. Chapter Fifteen - Metabolite Annotation and Identification. In: Jaumot J, Bedia C, Tauler R, editors. Comprehensive Analytical Chemistry. Elsevier; 2018. pp. 415–445. doi:10.1016/bs.coac.2018.07.004

227. Wishart DS, Feunang YD, Marcu A, Guo AC, Liang K, Vázquez-Fresno R, et al. HMDB 4.0: the human metabolome database for 2018. Nucleic Acids Res. 2018;46: D608–D617. doi:10.1093/nar/gkx1089

228. Smith C, Maille G, Want E, Qin C, Trauger S, Brandon T, et al. METLIN: A Metabolite Mass Spectral Database. Ther Drug Monit. 2005;27: 747–751. doi:10.1097/01.ftd.0000179845.53213.39

229. Hastings J, Owen G, Dekker A, Ennis M, Kale N, Muthukrishnan V, et al. ChEBI in 2016: Improved services and an expanding collection of metabolites. Nucleic Acids Res. 2016;44: D1214–D1219. doi:10.1093/nar/gkv1031

230. Kim S, Chen J, Cheng T, Gindulyte A, He J, He S, et al. PubChem 2019 update: improved access to chemical data. Nucleic Acids Res. 2019;47: D1102–D1109. doi:10.1093/nar/gky1033

231. Horai H, Arita M, Kanaya S, Nihei Y, Ikeda T, Suwa K, et al. MassBank: a public repository for sharing mass spectral data for life sciences. J Mass Spectrom. 2010;45: 703–714. doi:10.1002/jms.1777

232. Fahy E, Sud M, Cotter D, Subramaniam S. LIPID MAPS online tools for lipid research. Nucleic Acids Res. 2007;35: W606–W612. doi:10.1093/nar/gkm324

233. Kind T, Liu K-H, Lee DY, DeFelice B, Meissen JK, Fiehn O. LipidBlast in silico tandem mass spectrometry database for lipid identification. Nat Methods. 2013;10: 755–758. doi:10.1038/nmeth.2551

234. Wang M, Carver JJ, Phelan VV, Sanchez LM, Garg N, Peng Y, et al. Sharing and community curation of mass spectrometry data with Global Natural Products

Social Molecular Networking. Nat Biotechnol. 2016;34: 828–837. doi:10.1038/nbt.3597

235. Pando-Robles V, Oses-Prieto JA, Rodríguez-Gandarilla M, Meneses-Romero E, Burlingame AL, Batista CVF. Quantitative proteomic analysis of Huh-7 cells infected with Dengue virus by label-free LC–MS. J Proteomics. 2014;111: 16–29. doi:10.1016/j.jprot.2014.06.029

236. El-Bacha T, Midlej V, Pereira da Silva AP, Silva da Costa L, Benchimol M, Galina A, et al. Mitochondrial and bioenergetic dysfunction in human hepatic cells infected with dengue 2 virus. Biochim Biophys Acta BBA - Mol Basis Dis. 2007;1772: 1158–1166. doi:10.1016/j.bbadis.2007.08.003

237. Fontaine KA, Sanchez EL, Camarda R, Lagunoff M. Dengue Virus Induces and Requires Glycolysis for Optimal Replication. Sandri-Goldin RM, editor. J Virol. 2015;89: 2358–2366. doi:10.1128/JVI.02309-14

238. Allonso D, Andrade IS, Conde JN, Coelho DR, Rocha DCP, da Silva ML, et al. Dengue Virus NS1 Protein Modulates Cellular Energy Metabolism by Increasing Glyceraldehyde-3-Phosphate Dehydrogenase Activity. Diamond MS, editor. J Virol. 2015;89: 11871–11883. doi:10.1128/JVI.01342-15

239. Zhang M, Zheng X, Wu Y, Gan M, He A, Li Z, et al. Differential proteomics of Aedes albopictus salivary gland, midgut and C6/36 cell induced by dengue virus infection. Virology. 2013;444: 109–118. doi:10.1016/j.virol.2013.06.001

240. Tchankouo-Nguetcheu S, Khun H, Pincet L, Roux P, Bahut M, Huerre M, et al. Differential Protein Modulation in Midguts of Aedes aegypti Infected with Chikungunya and Dengue 2 Viruses. Fooks AR, editor. PLoS ONE. 2010;5: e13149. doi:10.1371/journal.pone.0013149

241. Birungi G, Chen SM, Loy BP, Ng ML, Li SFY. Metabolomics Approach for Investigation of Effects of Dengue Virus Infection Using the EA.hy926 Cell Line. J Proteome Res. 2010;9: 6523–6534. doi:10.1021/pr100727m

242. Cui L, Lee YH, Kumar Y, Xu F, Lu K, Ooi EE, et al. Serum Metabolome and Lipidome Changes in Adult Patients with Primary Dengue Infection. Michael SF, editor. PLoS Negl Trop Dis. 2013;7: e2373. doi:10.1371/journal.pntd.0002373

243. Voge NV, Perera R, Mahapatra S, Gresh L, Balmaseda A, Loroño-Pino MA, et al. Metabolomics-based discovery of small molecule biomarkers in serum associated with dengue virus infections and disease outcomes. PLoS Negl Trop Dis. 2016;10: e0004449.

244. Khedr A, Hegazy MA, Kammoun AK, Shehata MA. Phospholipidomic identification of potential serum biomarkers in dengue fever, hepatitis B and hepatitis C using liquid chromatography-electrospray ionization-tandem mass spectrometry. J Chromatogr B. 2016;1009–1010: 44–54. doi:10.1016/j.jchromb.2015.12.011

245. Cui L, Lee YH, Thein TL, Fang J, Pang J, Ooi EE, et al. Serum Metabolomics Reveals Serotonin as a Predictor of Severe Dengue in the Early Phase of Dengue Fever. PLoS Negl Trop Dis. 2016;10. doi:10.1371/journal.pntd.0004607

246. Melo CFOR, Delafiori J, Dabaja MZ, Oliveira DN de, Guerreiro TM, Colombo TE, et al. The role of lipids in the inception, maintenance and complications of dengue virus infection. Sci Rep. 2018;8: 11826. doi:10.1038/s41598-018-30385-x

247. Serum phospholipase A2 in dengue. J Infect. 1997;35: 251–252. doi:10.1016/S0163-4453(97)92966-2

248. Villamor E, Villar LA, Lozano A, Herrera VM, Herrán OF. Serum fatty acids and progression from dengue fever to dengue hemorrhagic fever / dengue shock syndrome. Br J Nutr. 2018;120: 787–796. doi:10.1017/S0007114518002039

249. Cui L, Pang J, Lee YH, Ooi EE, Ong CN, Leo YS, et al. Serum metabolome changes in adult patients with severe dengue in the critical and recovery phases of dengue infection. PLoS Negl Trop Dis. 2018;12. doi:10.1371/journal.pntd.0006217

250. El-Bacha T, Struchiner CJ, Cordeiro MT, Almeida FCL, Marques ET, Da Poian AT. 1H Nuclear Magnetic Resonance Metabolomics of Plasma Unveils Liver Dysfunction in Dengue Patients. J Virol. 2016;90: 7429–7443. doi:10.1128/JVI.00187-16

251. Heaton NS, Perera R, Berger KL, Khadka S, LaCount DJ, Kuhn RJ, et al. Dengue virus nonstructural protein 3 redistributes fatty acid synthase to sites of viral replication and increases cellular fatty acid synthesis. Proc Natl Acad Sci. 2010;107: 17345–17350. doi:10.1073/pnas.1010811107

252. Heaton NS, Randall G. Dengue Virus-Induced Autophagy Regulates Lipid Metabolism. Cell Host Microbe. 2010;8: 422–432. doi:10.1016/j.chom.2010.10.006

253. Wanders RJA, Komen J, Kemp S. Fatty acid omega-oxidation as a rescue pathway for fatty acid oxidation disorders in humans: Fatty acid oxidation disorders. FEBS J. 2011;278: 182–194. doi:10.1111/j.1742-4658.2010.07947.x

254. Cui L, Hou J, Fang J, Lee YH, Costa VV, Wong LH, et al. Serum Metabolomics Investigation of Humanized Mouse Model of Dengue Virus Infection. J Virol. 2017;91. doi:10.1128/JVI.00386-17

255. Lima WG, Souza NA, Fernandes SOA, Cardoso VN, Godói IP. Serum lipid profile as a predictor of dengue severity: A systematic review and meta-analysis. Rev Med Virol. 2019;29. doi:10.1002/rmv.2056

256. Perera R, Riley C, Isaac G, Hopf-Jannasch AS, Moore RJ, Weitz KW, et al. Dengue Virus Infection Perturbs Lipid Homeostasis in Infected Mosquito Cells. PLoS Pathog. 2012;8. doi:10.1371/journal.ppat.1002584

257. Chotiwan N, Andre BG, Sanchez-Vargas I, Islam MN, Grabowski JM, Hopf-Jannasch A, et al. Dynamic remodeling of lipids coincides with dengue virus replication in the midgut of Aedes aegypti mosquitoes. PLOS Pathog. 2018;14: e1006853. doi:10.1371/journal.ppat.1006853

258. Martín-Acebes MA, Merino-Ramos T, Blázquez A-B, Casas J, Escribano-Romero E, Sobrino F, et al. The Composition of West Nile Virus Lipid Envelope Unveils a Role of Sphingolipid Metabolism in Flavivirus Biogenesis. J Virol. 2014;88: 12041–12054. doi:10.1128/JVI.02061-14

259. Ma L, Jones CT, Groesch TD, Kuhn RJ, Post CB. Solution structure of dengue virus capsid protein reveals another fold. Proc Natl Acad Sci. 2004;101: 3414–3419. doi:10.1073/pnas.0305892101

260. Samsa MM, Mondotte JA, Iglesias NG, Assunção-Miranda I, Barbosa-Lima G, Da Poian AT, et al. Dengue Virus Capsid Protein Usurps Lipid Droplets for Viral Particle Formation. PLoS Pathog. 2009;5. doi:10.1371/journal.ppat.1000632

261. Meertens L, Carnec X, Lecoin MP, Ramdasi R, Guivel-Benhassine F, Lew E, et al. The TIM and TAM Families of Phosphatidylserine Receptors Mediate Dengue Virus Entry. Cell Host Microbe. 2012;12: 544–557. doi:10.1016/j.chom.2012.08.009

262. Richard AS, Zhang A, Park S-J, Farzan M, Zong M, Choe H. Virion-associated phosphatidylethanolamine promotes TIM1-mediated infection by Ebola, dengue, and West Nile viruses. Proc Natl Acad Sci U S A. 2015;112: 14682–14687. doi:10.1073/pnas.1508095112

263. Carnec X, Meertens L, Dejarnac O, Perera-Lecoin M, Hafirassou ML, Kitaura J, et al. The Phosphatidylserine and Phosphatidylethanolamine Receptor CD300a Binds Dengue Virus and Enhances Infection. J Virol. 2016;90: 92–102. doi:10.1128/JVI.01849-15

264. Lee C-J, Lin H-R, Liao C-L, Lin Y-L. Cholesterol Effectively Blocks Entry of Flavivirus. J Virol. 2008;82: 6470–6480. doi:10.1128/JVI.00117-08

265. Carro AC, Damonte EB. Requirement of cholesterol in the viral envelope for dengue virus infection. Virus Res. 2013;174: 78–87. doi:10.1016/j.virusres.2013.03.005

266. Zaitseva E, Yang S-T, Melikov K, Pourmal S, Chernomordik LV. Dengue Virus Ensures Its Fusion in Late Endosomes Using Compartment-Specific Lipids. PLoS Pathog. 2010;6. doi:10.1371/journal.ppat.1001131

267. García Cordero J, León Juárez M, González-Y-Merchand JA, Cedillo Barrón L, Gutiérrez Castañeda B. Caveolin-1 in Lipid Rafts Interacts with Dengue Virus NS3 during Polyprotein Processing and Replication in HMEC-1 Cells. PLoS ONE. 2014;9. doi:10.1371/journal.pone.0090704

268. Ngo AM, Shurtleff MJ, Popova KD, Kulsuptrakul J, Weissman JS, Puschnik AS. The ER membrane protein complex is required to ensure correct topology

and stable expression of flavivirus polyproteins. eLife. 8. doi:10.7554/eLife.48469

269. Lin DL, Inoue T, Chen Y-J, Chang A, Tsai B, Tai AW. The ER Membrane Protein Complex Promotes Biogenesis of Dengue and Zika Virus Non-structural Multi-pass Transmembrane Proteins to Support Infection. Cell Rep. 2019;27: 1666-1674.e4. doi:10.1016/j.celrep.2019.04.051

270. Yi Z, Yuan Z, Rice CM, MacDonald MR. Flavivirus Replication Complex Assembly Revealed by DNAJC14 Functional Mapping. J Virol. 2012;86: 11815. doi:10.1128/JVI.01022-12

271. Aktepe TE, Liebscher S, Prier JE, Simmons CP, Mackenzie JM. The Host Protein Reticulon 3.1A Is Utilized by Flaviviruses to Facilitate Membrane Remodelling. Cell Rep. 2017;21: 1639–1654. doi:10.1016/j.celrep.2017.10.055

272. Liebscher S, Ambrose RL, Aktepe TE, Mikulasova A, Prier JE, Gillespie LK, et al. Phospholipase A2 activity during the replication cycle of the flavivirus West Nile virus. PLoS Pathog. 2018;14. doi:10.1371/journal.ppat.1007029

273. Heaton NS, Perera R, Berger KL, Khadka S, LaCount DJ, Kuhn RJ, et al. Dengue virus nonstructural protein 3 redistributes fatty acid synthase to sites of viral replication and increases cellular fatty acid synthesis. Proc Natl Acad Sci U S A. 2010;107: 17345–17350. doi:10.1073/pnas.1010811107

274. Tang W-C, Lin R-J, Liao C-L, Lin Y-L. Rab18 Facilitates Dengue Virus Infection by Targeting Fatty Acid Synthase to Sites of Viral Replication. J Virol. 2014;88: 6793–6804. doi:10.1128/JVI.00045-14

275. McLean JE, Wudzinska A, Datan E, Quaglino D, Zakeri Z. Flavivirus NS4A-induced Autophagy Protects Cells against Death and Enhances Virus Replication. J Biol Chem. 2011;286: 22147–22159. doi:10.1074/jbc.M110.192500

276. Heaton NS, Randall G. Dengue Virus-Induced Autophagy Regulates Lipid Metabolism. Cell Host Microbe. 2010;8: 422–432. doi:10.1016/j.chom.2010.10.006

277. Zhang J, Lan Y, Li MY, Lamers MM, Fusade-Boyer M, Klemm E, et al. Flaviviruses Exploit the Lipid Droplet Protein AUP1 to Trigger Lipophagy and Drive Virus Production. Cell Host Microbe. 2018;23: 819-831.e5. doi:10.1016/j.chom.2018.05.005

278. Oya NJ de, Esler WP, Huard K, El-Kattan AF, Karamanlidis G, Blázquez A-B, et al. Targeting host metabolism by inhibition of acetyl-Coenzyme A carboxylase reduces flavivirus infection in mouse models. Emerg Microbes Infect. 2019;8: 624–636. doi:10.1080/22221751.2019.1604084

279. Soto-Acosta R, Bautista-Carbajal P, Cervantes-Salazar M, Angel-Ambrocio AH, Angel RM del. DENV up-regulates the HMG-CoA reductase activity through the impairment of AMPK phosphorylation: A potential antiviral target. PLOS Pathog. 2017;13: e1006257. doi:10.1371/journal.ppat.1006257

280. Martín-Acebes MA, Jiménez de Oya N, Saiz J-C. Lipid Metabolism as a Source of Druggable Targets for Antiviral Discovery against Zika and Other Flaviviruses. Pharmaceuticals. 2019;12. doi:10.3390/ph12020097

281. Soto-Acosta R, Bautista-Carbajal P, Syed GH, Siddiqui A, Del Angel RM. Nordihydroguaiaretic acid (NDGA) inhibits replication and viral morphogenesis of dengue virus. Antiviral Res. 2014;109: 132–140. doi:10.1016/j.antiviral.2014.07.002

282. Merino-Ramos T, Jiménez de Oya N, Saiz J-C, Martín-Acebes MA. Antiviral Activity of Nordihydroguaiaretic Acid and Its Derivative Tetra-O-Methyl Nordihydroguaiaretic Acid against West Nile Virus and Zika Virus. Antimicrob Agents Chemother. 2017;61. doi:10.1128/AAC.00376-17

283. Kraemer MU, Sinka ME, Duda KA, Mylne A, Shearer FM, Brady OJ, et al. The global compendium of Aedes aegypti and Ae. albopictus occurrence., The global compendium of Aedes aegypti and Ae. albopictus occurrence. Sci Data Sci Data. 2015;2, 2: 150035–150035. doi:10.1038/sdata.2015.35, 10.1038/sdata.2015.35

284. McMaster CR. From yeast to humans – roles of the Kennedy pathway for phosphatidylcholine synthesis. FEBS Lett. 2018;592: 1256–1272. doi:10.1002/1873-3468.12919

285. Davidsen J, Mouritsen OG, Jørgensen K. Synergistic permeability enhancing effect of lysophospholipids and fatty acids on lipid membranes. Biochim Biophys Acta BBA - Biomembr. 2002;1564: 256–262. doi:10.1016/S0005-2736(02)00461-3

286. Vial T, Tan W-L, Xiang BWW, Missé D, Deharo E, Marti G, et al. Dengue virus reduces AGPAT1 expression to alter phospholipids and enhance infection in Aedes aegypti. PLOS Pathog. 2019;15: e1008199. doi:10.1371/journal.ppat.1008199

287. Cui L, Lee YH, Kumar Y, Xu F, Lu K, Ooi EE, et al. Serum Metabolome and Lipidome Changes in Adult Patients with Primary Dengue Infection. Michael SF, editor. PLoS Negl Trop Dis. 2013;7: e2373. doi:10.1371/journal.pntd.0002373

288. Henneberry AL, Wistow G, McMaster CR. Cloning, Genomic Organization, and Characterization of a Human Cholinephosphotransferase. J Biol Chem. 2000;275: 29808–29815. doi:10.1074/jbc.M005786200

289. Henneberry AL, McMaster CR. Cloning and expression of a human choline/ethanolaminephosphotransferase: synthesis of phosphatidylcholine and phosphatidylethanolamine. Biochem J. 1999;339: 291–298.

290. Marti G, Joulia P, Amiel A, Fabre B, David B, Fabre N, et al. Comparison of the Phytochemical Composition of Serenoa repens Extracts by a Multiplexed Metabolomic Approach. Molecules. 2019;24: 2208. doi:10.3390/molecules24122208

291. Lin Z, Zhang Q, Dai S, Gao X. Discovering Temporal Patterns in Longitudinal Nontargeted Metabolomics Data via Group and Nuclear Norm Regularized Multivariate Regression. Metabolites. 2020;10: 33. doi:10.3390/metabo10010033

292. Bakovic M, Fullerton MD, Michel V. Metabolic and molecular aspects of ethanolamine phospholipid biosynthesis: the role of CTP:phosphoethanolamine cytidylyltransferase (Pcyt2). Biochem Cell Biol. 2007;85: 283–300. doi:10.1139/O07-006

293. Li Z, Vance DE. Thematic Review Series: Glycerolipids. Phosphatidylcholine and choline homeostasis. J Lipid Res. 2008;49: 1187–1194. doi:10.1194/jlr.R700019-JLR200

294. Butler PL, Mallampalli RK. Cross-talk between Remodeling and de Novo Pathways Maintains Phospholipid Balance through Ubiquitination. J Biol Chem. 2010;285: 6246–6258. doi:10.1074/jbc.M109.017350

295. Yamashita A, Hayashi Y, Nemoto-Sasaki Y, Ito M, Oka S, Tanikawa T, et al. Acyltransferases and transacylases that determine the fatty acid composition of glycerolipids and the metabolism of bioactive lipid mediators in mammalian cells and model organisms. Prog Lipid Res. 2014;53: 18–81. doi:10.1016/j.plipres.2013.10.001

296. Bobenchik AM, Augagneur Y, Hao B, Hoch JC, Ben Mamoun C. Phosphoethanolamine methyltransferases in phosphocholine biosynthesis: functions and potential for antiparasite therapy. FEMS Microbiol Rev. 2011;35: 609–619. doi:10.1111/j.1574-6976.2011.00267.x

297. Liebscher S, Ambrose RL, Aktepe TE, Mikulasova A, Prier JE, Gillespie LK, et al. Phospholipase A2 activity during the replication cycle of the flavivirus West Nile virus. PLoS Pathog. 2018;14. doi:10.1371/journal.ppat.1007029

298. Neufeldt CJ, Cortese M, Acosta EG, Bartenschlager R. Rewiring cellular networks by members of the Flaviviridae family. Nat Rev Microbiol. 2018;16: 125–142. doi:10.1038/nrmicro.2017.170

299. Sriburi R, Jackowski S, Mori K, Brewer JW. XBP1 a link between the unfolded protein response, lipid biosynthesis, and biogenesis of the endoplasmic reticulum. J Cell Biol. 2004;167: 35–41. doi:10.1083/jcb.200406136

300. Perera N, Miller JL, Zitzmann N. The role of the unfolded protein response in dengue virus pathogenesis. Cell Microbiol. 2017;19: e12734. doi:10.1111/cmi.12734

301. Barletta ABF, Silva MCLN, Sorgine MHF. Validation of Aedes aegypti Aag-2 cells as a model for insect immune studies. Parasit Vectors. 2012;5: 148. doi:10.1186/1756-3305-5-148

302. Schreiber MJ, Holmes EC, Ong SH, Soh HSH, Liu W, Tanner L, et al. Genomic Epidemiology of a Dengue Virus Epidemic in Urban Singapore. J Virol. 2009;83: 4163–4173. doi:10.1128/JVI.02445-08

303. Fraiture M, Baxter RHG, Steinert S, Chelliah Y, Frolet C, Quispe-Tintaya W, et al. Two Mosquito LRR Proteins Function as Complement Control Factors in the TEP1-Mediated Killing of Plasmodium. Cell Host Microbe. 2009;5: 273–284. doi:10.1016/j.chom.2009.01.005

304. Johnson BW, Russell BJ, Lanciotti RS. Serotype-Specific Detection of Dengue Viruses in a Fourplex Real-Time Reverse Transcriptase PCR Assay. J Clin Microbiol. 2005;43: 4977–4983. doi:10.1128/JCM.43.10.4977-4983.2005

305. Manokaran G, Finol E, Wang C, Gunaratne J, Bahl J, Ong EZ, et al. Dengue subgenomic RNA binds TRIM25 to inhibit interferon expression for epidemiological fitness. Science. 2015;350: 217. doi:10.1126/science.aab3369

306. Tsugawa H, Cajka T, Kind T, Ma Y, Higgins B, Ikeda K, et al. MS-DIAL: data-independent MS/MS deconvolution for comprehensive metabolome analysis. Nat Methods. 2015;12: 523–526. doi:10.1038/nmeth.3393

307. Tsugawa H, Kind T, Nakabayashi R, Yukihira D, Tanaka W, Cajka T, et al. Hydrogen Rearrangement Rules: Computational MS/MS Fragmentation and Structure Elucidation Using MS-FINDER Software. Anal Chem. 2016;88: 7946–7958. doi:10.1021/acs.analchem.6b00770

308. Tsugawa H, Nakabayashi R, Mori T, Yamada Y, Takahashi M, Rai A, et al. A cheminformatics approach to characterize metabolomes in stable-isotope-labeled organisms. Nat Methods. 2019;16: 295. doi:10.1038/s41592-019-0358-2

309. Chong J, Soufan O, Li C, Caraus I, Li S, Bourque G, et al. MetaboAnalyst 4.0: towards more transparent and integrative metabolomics analysis. Nucleic Acids Res. 2018;46: W486–W494. doi:10.1093/nar/gky310

310. Coleman RA, Lee DP. Enzymes of triacylglycerol synthesis and their regulation. Prog Lipid Res. 2004;43: 134–176. doi:10.1016/S0163-7827(03)00051-1

311. Yamashita A, Hayashi Y, Matsumoto N, Nemoto-Sasaki Y, Oka S, Tanikawa T, et al. Glycerophosphate/Acylglycerophosphate Acyltransferases. Biology. 2014;3: 801–830. doi:10.3390/biology3040801

312. Dircks LK, Ke J, Sul HS. A Conserved Seven Amino Acid Stretch Important for Murine Mitochondrial Glycerol-3-phosphate Acyltransferase Activity. J Biol Chem. 1999;274: 34728–34734. doi:10.1074/jbc.274.49.34728

313. Yamashita A, Nakanishi H, Suzuki H, Kamata R, Tanaka K, Waku K, et al. Topology of acyltransferase motifs and substrate specificity and accessibility in 1-acyl-sn-glycero-3-phosphate acyltransferase 1. Biochim Biophys Acta BBA - Mol Cell Biol Lipids. 2007;1771: 1202–1215. doi:10.1016/j.bbalip.2007.07.002

314. Colpitts TM, Cox J, Vanlandingham DL, Feitosa FM, Cheng G, Kurscheid S, et al. Alterations in the Aedes aegypti Transcriptome during Infection with West Nile, Dengue and Yellow Fever Viruses. Rice CM, editor. PLoS Pathog. 2011;7: e1002189. doi:10.1371/journal.ppat.1002189

315. Gillespie LK, Hoenen A, Morgan G, Mackenzie JM. The Endoplasmic Reticulum Provides the Membrane Platform for Biogenesis of the Flavivirus Replication Complex. J Virol. 2010;84: 10438–10447. doi:10.1128/JVI.00986-10

316. Fajardo-Sánchez E, Galiano V, Villalaín J. Spontaneous membrane insertion of a dengue virus NS2A peptide. Arch Biochem Biophys. 2017;627: 56–66. doi:10.1016/j.abb.2017.06.016

317. Shyu P, Ng BSH, Ho N, Chaw R, Seah YL, Marvalim C, et al. Membrane phospholipid alteration causes chronic ER stress through early degradation of homeostatic ER-resident proteins. Sci Rep. 2019;9: 1–15. doi:10.1038/s41598-019-45020-6

318. Gentile CL, Frye M, Pagliassotti MJ. Endoplasmic Reticulum Stress and the Unfolded Protein Response in Nonalcoholic Fatty Liver Disease. Antioxid Redox Signal. 2010;15: 505–521. doi:10.1089/ars.2010.3790

319. Werstuck GH, Lentz SR, Dayal S, Hossain GS, Sood SK, Shi YY, et al. Homocysteine-induced endoplasmic reticulum stress causes dysregulation of the cholesterol and triglyceride biosynthetic pathways. J Clin Invest. 2001;107: 1263–1273. doi:10.1172/JCI11596

320. Fu S, Yang L, Li P, Hofmann O, Dicker L, Hide W, et al. Aberrant lipid metabolism disrupts calcium homeostasis causing liver endoplasmic reticulum stress in obesity. Nature. 2011;473: 528–531. doi:10.1038/nature09968

321. Guo W, Wong S, Xie W, Lei T, Luo Z. Palmitate modulates intracellular signaling, induces endoplasmic reticulum stress, and causes apoptosis in mouse 3T3-L1 and rat primary preadipocytes. Am J Physiol-Endocrinol Metab. 2007;293: E576–E586. doi:10.1152/ajpendo.00523.2006

322. Wei Y, Wang D, Topczewski F, Pagliassotti MJ. Saturated fatty acids induce endoplasmic reticulum stress and apoptosis independently of ceramide in liver cells. Am J Physiol-Endocrinol Metab. 2006;291: E275–E281. doi:10.1152/ajpendo.00644.2005

323. Karasawa K, Tanigawa K, Harada A, Yamashita A. Transcriptional Regulation of Acyl-CoA:Glycerol-sn-3-Phosphate Acyltransferases. Int J Mol Sci. 2019;20. doi:10.3390/ijms20040964

324. Peña J, Harris E. Early Dengue Virus Protein Synthesis Induces Extensive Rearrangement of the Endoplasmic Reticulum Independent of the UPR and SREBP-2 Pathway. PLoS ONE. 2012;7. doi:10.1371/journal.pone.0038202

325. Leung DW. The structure and functions of human lysophosphatidic acid acyltransferases. Front Biosci. 2001; 12.

326. Allonso D, Andrade IS, Conde JN, Coelho DR, Rocha DCP, da Silva ML, et al. Dengue Virus NS1 Protein Modulates Cellular Energy Metabolism by Increasing Glyceraldehyde-3-Phosphate Dehydrogenase Activity. J Virol. 2015;89: 11871–11883. doi:10.1128/JVI.01342-15

327. Sirover MA. New insights into an old protein: the functional diversity of mammalian glyceraldehyde-3-phosphate dehydrogenase. Biochim Biophys Acta BBA - Protein Struct Mol Enzymol. 1999;1432: 159–184. doi:10.1016/S0167-4838(99)00119-3

328. El-Bacha T, Midlej V, Pereira da Silva AP, Silva da Costa L, Benchimol M, Galina A, et al. Mitochondrial and bioenergetic dysfunction in human hepatic cells infected with dengue 2 virus. Biochim Biophys Acta BBA - Mol Basis Dis. 2007;1772: 1158–1166. doi:10.1016/j.bbadis.2007.08.003

329. Fontaine KA, Sanchez EL, Camarda R, Lagunoff M. Dengue Virus Induces and Requires Glycolysis for Optimal Replication. J Virol. 2015;89: 2358–2366. doi:10.1128/JVI.02309-14

330. Abrantes JL, Alves CM, Costa J, Almeida FCL, Sola-Penna M, Fontes CFL, et al. Herpes simplex type 1 activates glycolysis through engagement of the enzyme 6-phosphofructo-1-kinase (PFK-1). Biochim Biophys Acta BBA - Mol Basis Dis. 2012;1822: 1198–1206. doi:10.1016/j.bbadis.2012.04.011

331. Ramière C, Rodriguez J, Enache LS, Lotteau V, André P, Diaz O. Activity of Hexokinase Is Increased by Its Interaction with Hepatitis C Virus Protein NS5A. J Virol. 2014;88: 3246–3254. doi:10.1128/JVI.02862-13

332. Sanaki T, Wakabayashi M, Yoshioka T, Yoshida R, Shishido T, Hall WW, et al. Inhibition of dengue virus infection by 1-stearoyl-2-arachidonoyl-phosphatidylinositol in vitro. FASEB J. 2019;33: 13866–13881. doi:10.1096/fj.201901095RR

333. Morita M, Kuba K, Ichikawa A, Nakayama M, Katahira J, Iwamoto R, et al. The Lipid Mediator Protectin D1 Inhibits Influenza Virus Replication and Improves Severe Influenza. Cell. 2013;153: 112–125. doi:10.1016/j.cell.2013.02.027

334. Numata M, Nagashima Y, Moore ML, Berry KZ, Chan M, Kandasamy P, et al. Phosphatidylglycerol provides short-term prophylaxis against respiratory syncytial virus infection. J Lipid Res. 2013;54: 2133–2143. doi:10.1194/jlr.M037077

335. Numata M, Kandasamy P, Nagashima Y, Posey J, Hartshorn K, Woodland D, et al. Phosphatidylglycerol Suppresses Influenza A Virus Infection. Am J Respir Cell Mol Biol. 2012;46: 479–487. doi:10.1165/rcmb.2011-0194OC

336. Numata M, Kandasamy P, Nagashima Y, Fickes R, Murphy RC, Voelker DR. Phosphatidylinositol inhibits respiratory syncytial virus infection. J Lipid Res. 2015;56: 578–587. doi:10.1194/jlr.M055723

337. Soares MM, King SW, Thorpe PE. Targeting Inside-Out Phosphatidylserine as a Therapeutic Strategy For Viral Diseases. Nat Med. 2008;14: 1357–1362. doi:10.1038/nm.1885

338. Moody MA, Liao H-X, Alam SM, Scearce RM, Plonk MK, Kozink DM, et al. Anti-phospholipid human monoclonal antibodies inhibit CCR5-tropic HIV-1 and

induce β-chemokines. J Exp Med. 2010;207: 763–776. doi:10.1084/jem.20091281

339. Martín-Acebes MA, Gabandé-Rodríguez E, García-Cabrero AM, Sánchez MP, Ledesma MD, Sobrino F, et al. Host sphingomyelin increases West Nile virus infection in vivo. J Lipid Res. 2016;57: 422–432. doi:10.1194/jlr.M064212

340. Wang K, Wang J, Sun T, Bian G, Pan W, Feng T, et al. Glycosphingolipid GM3 is Indispensable for Dengue Virus Genome Replication. Int J Biol Sci. 2016;12: 872–883. doi:10.7150/ijbs.15641

341. Poh MK, Shui G, Xie X, Shi P-Y, Wenk MR, Gu F. U18666A, an intra-cellular cholesterol transport inhibitor, inhibits dengue virus entry and replication. Antiviral Res. 2012;93: 191–198. doi:10.1016/j.antiviral.2011.11.014

342. Takano T, Tsukiyama-Kohara K, Hayashi M, Hirata Y, Satoh M, Tokunaga Y, et al. Augmentation of DHCR24 expression by hepatitis C virus infection facilitates viral replication in hepatocytes. J Hepatol. 2011;55: 512–521. doi:10.1016/j.jhep.2010.12.011

343. Zhu Y, Zhang R, Zhang B, Zhao T, Wang P, Liang G, et al. Blood meal acquisition enhances arbovirus replication in mosquitoes through activation of the GABAergic system. Nat Commun. 2017;8. doi:10.1038/s41467-017-01244-6

344. Hodson L, Skeaff CM, Fielding BA. Fatty acid composition of adipose tissue and blood in humans and its use as a biomarker of dietary intake. Prog Lipid Res. 2008;47: 348–380. doi:10.1016/j.plipres.2008.03.003

345. Marangoni F, Colombo C, Galli C. A method for the direct evaluation of the fatty acid status in a drop of blood from a fingertip in humans: applicability to nutritional and epidemiological studies. Anal Biochem. 2004;326: 267–272. doi:10.1016/j.ab.2003.12.016

346. Baylin A, Kim MK, Donovan-Palmer A, Siles X, Dougherty L, Tocco P, et al. Fasting Whole Blood as a Biomarker of Essential Fatty Acid Intake in Epidemiologic Studies: Comparison with Adipose Tissue and Plasma. Am J Epidemiol. 2005;162: 373–381. doi:10.1093/aje/kwi213

347. Farjana T, Tuno N. Multiple Blood Feeding and Host-Seeking Behavior in Aedes aegypti and Aedes albopictus (Diptera: Culicidae). J Med Entomol. 2013;50: 838–846. doi:10.1603/ME12146

348. Caragata EP, Tikhe CV, Dimopoulos G. Curious entanglements: interactions between mosquitoes, their microbiota, and arboviruses. Curr Opin Virol. 2019;37: 26–36. doi:10.1016/j.coviro.2019.05.005

349. Dong Y, Manfredini F, Dimopoulos G. Implication of the Mosquito Midgut Microbiota in the Defense against Malaria Parasites. PLoS Pathog. 2009;5. doi:10.1371/journal.ppat.1000423

350. Rodrigues J, Brayner FA, Alves LC, Dixit R, Barillas-Mury C. Hemocyte Differentiation Mediates Innate Immune Memory in Anopheles gambiae Mosquitoes. Science. 2010;329: 1353–1355. doi:10.1126/science.1190689

351. Gusmão DS, Santos AV, Marini DC, Russo É de S, Peixoto AMD, Bacci Júnior M, et al. First isolation of microorganisms from the gut diverticulum of Aedes aegypti (Diptera: Culicidae): new perspectives for an insect-bacteria association. Mem Inst Oswaldo Cruz. 2007;102: 919–924. doi:10.1590/S0074-02762007000800005

352. Gaio A de O, Gusmão DS, Santos AV, Berbert-Molina MA, Pimenta PF, Lemos FJ. Contribution of midgut bacteria to blood digestion and egg production in Aedes aegypti (diptera: culicidae) (L.). Parasit Vectors. 2011;4: 105. doi:10.1186/1756-3305-4-105

353. Coatsworth H, Caicedo PA, Van Rossum T, Ocampo CB, Lowenberger C. The Composition of Midgut Bacteria in Aedes aegypti (Diptera: Culicidae) That Are Naturally Susceptible or Refractory to Dengue Viruses. J Insect Sci. 2018;18. doi:10.1093/jisesa/iey118

354. Audsley MD, Ye YH, McGraw EA. The microbiome composition of Aedes aegypti is not critical for Wolbachia-mediated inhibition of dengue virus. PLoS Negl Trop Dis. 2017;11. doi:10.1371/journal.pntd.0005426

355. Hoxmeier JC, Thompson BD, Broeckling CD, Small P, Foy BD, Prenni J, et al. Analysis of the metabolome of Anopheles gambiae mosquito after exposure to Mycobacterium ulcerans. Sci Rep. 2015;5. doi:10.1038/srep09242

356. Anopheles gambiae: Metabolomic Profiles in Sugar-Fed, Blood-Fed, and Plasmodium falciparum-Infected Midgut. [cited 28 Jan 2020]. Available: https://www.hindawi.com/journals/dpis/2017/8091749/